Novel linkers for prostate-specific prodrug systems

Miller, Christian Karl

Award date:
2006

Awarding institution:
University of Bath

Novel Linkers for Prostate-Specific Prodrug Systems

Submitted by

Christian Karl Miller

for the degree of PhD

of the University of Bath

2006

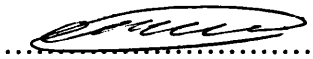

16/2/06

ProQuest LLC
789 East Eisenhower Parkway
P.O. Box 1346
Ann Arbor, MI 48106-1346

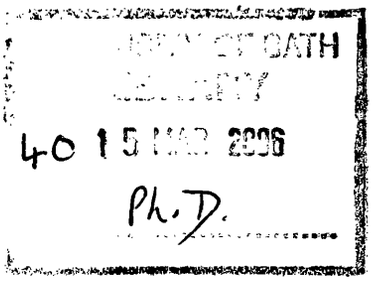
OATH
40 15 MAR 2006
Ph.D.

ABSTRACT

Prostate carcinoma is an increasing cause of male mortality in the West. Doxorubicin is the most effective treatment for hormone-independent prostate cancer but many patients relapse. A prodrug system to deliver doxorubicin selectively to the prostate would improve treatment. Polymeric prodrugs are selectively retained in solid tumours by the EPR-effect. Prostate specific antigen (PSA) is a serine protease, which is catalytically active only in the prostate. Thus, a water-soluble polymeric prodrug system in which the doxorubicin is linked to the polymer through a PSA-cleavable peptide was designed. This prodrug system would have binary selectivity: the EPR effect and the PSA localisation.

Since PSA is reported to release arylamines but not alkylamines from its specific substrate sequence SSKLQ, it was necessary to interpose a self-immolative molecular clip between the peptide and the drug. Aminobenzyloxycarbonyl and aminophenylpropargyloxycarbonyl clips were studied. Initial synthetic approaches to clip-less constructs were severely hampered by the insolubility of tripeptide derivatives containing glutamine.

Attempts to prepare the constructs containing the peptide and a model drug (2-[4-nitrophenyl]ethylamine (NPEA)) linked by the aminobenzyloxycarbonyl clip foundered on very poor coupling yields of glutamine derivatives with appropriate anilines and, again, on the insolubility of glutamine derivatives. Model experiments on assembly of aminophenylpropargyloxycarbonyl clips were not encouraging, as simple 4-amidophenylpropargyl alcohols failed to form the corresponding N-nitrophenylethyl carbamates. However, using an alternative retrosynthetic disconnection, a Sonogashira coupling of Bocglutamine-4-iodoanilide with propargyl N-2-(4-nitrophenyl)ethyl carbamate successfully formed Bocglutamine-alkyne(*CLIP*)-NPEA. The utility of this material in further elaboration of the peptide, was demonstrated by deprotection and coupling with a Bocleucine-active ester. Thus, a potential route to the target peptide-*CLIP*-model drug construct has been established.

ACKNOWLEDGEMENTS

I would like to show my deepest appreciation to:

My supervisor, Dr Mike Threadgill, to whom I feel indebted to for his expert guidance, continual encouragement and interminable enthusiasm throughout the course of my PhD. Howzat!?

Dr Steve Black for his valuable help and training in NMR; Chris Cryer for the provision of mass spectra and Alan Carver for elemental analysis; Kevin Smith and Charles Stuart for their technical assistance.

Dr Adrian P. Neal and Dr Cédric Chauvignac for all of their valuable advice and many useful discussions on many aspects of my chemistry.

The Medical Research Council (MRC) for funding *(Priority Area Studentship)*.

All those I have worked with over the years, for their friendship and assistance: Anna, Christophe, Claire, Esther, Ghadeer, Joey, Mervat, Victoria, Charles B and Steve H.

Special thanks also go out to Mrs Chapman and to the Flying Boots for all of their continual entertainment and for making my time in Bath an enjoyable one.

Finally, I would like to pay special thanks to my family and closest friends, in particular, my grandma, mum, dad, sister, Connie, Petros, Justin and Rob, for all of their love and support and for being there for me through the hard times.

This thesis is dedicated to Ozzy Miller.

The only way to discover the limits of the possible
- is to go beyond them into the impossible.

- Arthur C. Clarke

CONTENTS

ABBREVIATIONS

AcOH	acetic acid
ADEPT	antibody-directed enzyme prodrug therapy
AMC	7-amino-4-methylcoumarin
Aq	aqueous
BNH	benign nodular hyperplasia
Boc	*tert*-butoxycarbonyl
Boc_2O	di-*t*-butyl dicarbonate
Bp	boiling point
Cbz	benzyloxycarbonyl
COSY	correlation spectroscopy
DCC	N,N'-dicyclohexylcarbodiimide
DCM	dichloromethane
DCU	N,N'-dicyclohexylurea
DMAP	4-(dimethylamino)-pyridine
DMF	dimethylformamide
DMSO d_6	dimethylsulfoxide (deuterated)
DNA	deoxyribonucleic acid
Dox	doxorubicin
EC_{50}	concentration producing 50% of maximal response
EDC	1-(3-dimethylamino propyl)-3-ethylcarbodi imide hydrochloride
EEDQ	N-ethoxycarbonyl-2-ethoxy-1,2-dihydro quinoline
EI	electron impact
EPR	enhanced permeability and retention
Eq	equivalent
ES	electrospray
Et_3N	triethylamine
EtOAc	ethyl acetate
Et_2O	diethyl ether
FAB	fast atom bombardment
Fmoc	fluoren-9-ylmethoxy-carbonyl
GDEPT	gene directed enzyme prodrug therapy
h	hour
HMBC	heteronuclear multiple bond correlation
HMQC	heteronuclear multiple quantum correlation
HOBt	1-hydroxybenzotriazole
HONSu	N-hydroxysuccinimide
HPLC	high performance liquid chromatography
HPMA	hydroxypropylmethacryl-amide
IC_{50}	concentration causing 50% inhibition
IR	infra-red
MeOH	methanol

min	minute(s)
mmol	millimole
mp	melting point
MS	mass spectrometry
m/z	mass-to-charge ratio (mass spectrometry)
NMR	nuclear magnetic resonance
NOESY	nuclear overhauser enhancement spectroscopy
ONP	*para*-nitrophenyl
PEG	poly(ethylene glycol)
PFP	pentafluorophenyl
ppm	parts per million
PSA	prostate specific antigen
PSMA	prostate specific membrane antigen
RES	reticuloendothelial system
RT	room (ambient) temperature
TBAF	tetrabutyl ammonium fluoride
TBDMS	*tert*-butyldimethylsilyl chloride
TFA	trifluoroacetic acid
THF	tetrahydrofuran
TLC	thin layer chromatography
UV	ultra-violet
VDEPT	virally directed enzyme prodrug therapy

Amino acids

Ala	alanine	**A**
Arg	arginine	**R**
Asn	asparagine	**N**
Asp	aspartic acid	**D**
Chg	cyclohexylglycine	
Cys	cysteine	**C**
Gln	glutamine	**Q**
Glu	glutamic acid	**E**
Gly	glycine	**G**
His	histidine	**H**
Hyp	*trans*-4-hydroxyproline	
Ile	*iso*leucine	**I**
Leu	leucine	**L**
Lys	lysine	**K**
Met	methionine	**M**
Phe	phenylalanine	**F**
Pro	proline	**P**
Pyg	pyroglutamine	
Ser	serine	**S**
Thr	threonine	**T**
Trp	tryptophan	**W**
Tyr	tyrosine	**Y**
Val	valine	**V**

LIST OF FIGURES, SCHEMES & TABLES

Figures

Schemes

Tables

Prostate cancer is one of the most common malignant diseases for which health-care intervention is sought worldwide, and in many developed countries it is the most common non-cutaneous malignant disease[7].

Prostate cancer is the sixth most common cancer in the world (in the number of new cases), the third most common cancer in men, and the most common cancer in men in Europe, North America, and some parts of Africa[9].

[The Lancet 2003]

The term "cancer" refers to a condition in which the regulation of cell growth is lost and cells grow uncontrollably. Prostate cancer occurs when cells within the prostate grow uncontrollably, creating a small malignant growth or tumour.

Most cells in the body are constantly under going cell division, thus dividing, maturing and then dying in a tightly intricate controlled process. Unlike normal cells, the growth of cancer cells is no longer well regulated. Instead of dying as they should, cancer cells outlive normal cells and continue to form new, abnormal cells.

[prostatecancerfoundation.org]

Chapter 1

Introduction

1.1 Prostate Cancer

1.1.1 What is the prostate (*anatomy & function*)?

The prostate is a gland that surrounds the neck of the bladder and proximal urethra (Figure **1**). The prostate gland consists of five lobes (zones), separated by the ejaculatory ducts and by the urethra. Two lateral lobes and an anterior lobe enclose the urethra, with the two lateral lobes being marked by a posterior midline groove (Figure **2**), palpable on rectal examination[1].

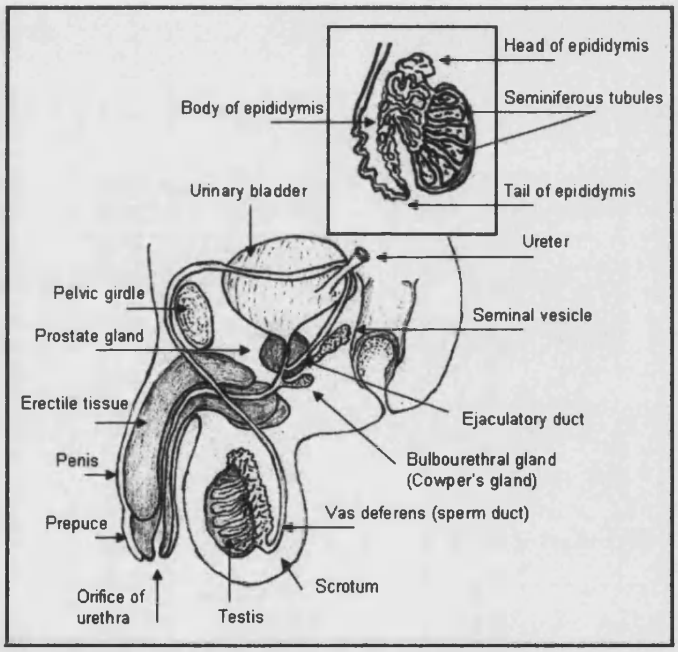

Figure 1. *A sagittal section of the male reproductive system*

The two lateral lobes are also known as the pre-prostatic tissue lobe and the transition lobe, respectively. The pre-prostatic tissue lobe contains muscles that are responsible for preventing semen from flowing backward into the bladder during ejaculation. The transition lobe can be highly susceptible towards 'Benign Prostatic Hyperplasia' (BPH),

and can enlarge upon the formation of a non-cancerous over-growth of the glandular tissue (see section **1.1.5.2**)[2]. This is also prominent in the middle lobe as well, which lies between the ejaculatory ducts and the urethra and is involved in the connection of the seminal vesicles to the prostate. The middle lobe also contains approximately 25% of the organ's glands in total. The peripheral lobe, known also as the posterior lobe, is located at the rear of the prostate behind the ejaculatory ducts, contains roughly 75% of the glands in the prostate and is where most prostate cancer occurs. The anterior lobe, which is primarily smooth muscle tissue, is situated near the front of the prostate.

A normal prostate gland weighs about 20 g and is enclosed in a fibrous capsule[1]. It is a single, doughnut-shaped gland about the size of a golf ball[3]. Within the prostate, there are three main groups of glands arranged concentrically around the urethra, the inner peri-urethral group, the submucosal gland and the external group or main prostatic glands. The ducts of all three groups, all their ducts converge and open into the prostatic urethra[1]. The blood supply to the prostate comes from the main iliac artery and prostatic veins drain to the prostate plexus around the gland and then to the internal iliac veins[1].

The function of the prostate is to secrete a thin, milky, alkaline substance that constitutes to about 31% of the seminal fluid volume[4]. It contains calcium, citrate ion, phosphate ion, a clotting enzyme, and a profibrinolysin (plasminogen)[5]. During emission, the capsule (a layer of cells covering the prostate) contracts simultaneously with that of the vas deferens, so that the thin, milky fluid of the prostate adds further bulk to the semen[5]. Its alkalinity helps protect the sperm from the acidity in the male urethra and that of the female vagina, which is very important for successful fertilization[4,5]. The acidity of vaginal secretions are at a pH of 3.5 – 4.0 and, for optimum sperm motility, the conditions have to be at least that at of pH 6.0 – 6.5. It is probable that the slightly alkaline prostatic fluid helps neutralise the acidity of the other seminal fluids during ejaculation and thus enhances the fertility of sperm[5]. If the acidity is too great, it can depress or, if strong enough, kill the sperm altogether[4].

1.1.2 Bulbourethral glands (*Cowper's glands*)

The paired bulbourethral glands, also known as Cowper's glands, resemble peas in both size and shape[4]. As shown in (Figure **1**), the location of these tubuloalveolar glands are inferior to the prostate on either side of the membranous urethra within the genital diaphragm and their ducts (approximately 2.5 cm long) connect and open into the spongy, penile portion of the urethra[3]. Like the prostate, these glands secrete an alkaline fluid (approximately 5% of the total seminal fluid volume)[4] into the urethra for counteracting the acidic environments from both the male urethra and the vagina (as mentioned in section **1.1**) [3,4]. These glands are also responsible for secreting a mucus that lines the urethra and the end of the penis for limiting the number of sperm damaged mechanically during ejaculation[4,5].

1.1.3 Seminal vesicles

There are two seminal vesicles, one located on each side of the prostate. Each vesicle is a convoluted, loculated tube lined with a secretory epithelium that secretes a mucous containing of an abundance of fructose, citric acid and other nutrient substances, as well as large quantities of fibrinogen and prostaglandins[5]. It is believed that prostaglandins are responsible towards aiding fertilisation in two ways:

1. by reacting with the female cervical mucus, triggering a more receptive response to sperm movement.

2. by causing reverse peristaltic contractions in the uterus and fallopian tubes to help move the sperm towards the ovaries.

During the process of emission and ejaculation, each vesicle empties its contents into the prostatic end of the ampulla (the part of the vas deferens that joins to the seminal vesicles) and the contents of the ampulla then pass into an ejaculatory duct; this occurs shortly after the vas deferens empties the sperm carried from the testes. All the contents are then carried through the body of the prostate gland, where they are released into the internal prostatic urethra for emission to the exterior[2,5].

1.1.4 Testes

The testes are two small oval-shaped organs, that are somewhat flattened from side to side, measuring at an average length of 4-5 cm, with a weight of approximately 10 – 15 g. They are both located below the penis in a suspended pouch of skin called the scrotum (Figure **1**), where usually, the left testicle is located about 1 cm lower to that of the right[4]. Each testis is composed of up to 900 tightly coiled seminiferous tubules, each averaging more than half a metre long, in which sperm are formed[5]. This process is otherwise known as spermatogenesis.

The collecting tubules inside the testicle join together to form a tube called the epididymis, which itself is another coiled tube of about 6 metres long[5]. Sperm then empty into the epididymis to where the tube (known as the vas deferens) carries on to the outside of the testis where it widens. It can be felt as a soft swelling at the back of the testis. The vas deferens (also known as the spermatic cord) then enlarges into the ampulla and it is here where the sperm meets the contents of the seminal vesicles (section **1.1.3**), and continues to form a short tube called the ejaculatory duct. This duct immediately opens into the urethra (the tube from the bladder to the penis) as it enters the body of prostate gland[4,5] (Figure **1**).

1.1.4.1 Male sex hormones

The testes are not only responsible for the development of sperm in the aid of reproduction but also for the production of male sex hormones, collectively known as androgens. All androgens are steroid-type compounds (*e.g.* testosterone (**1**) and its metabolite, dihydrotestosterone (**2**), see (Scheme **1**)) and can be synthesised either from cholesterol or directly from acetyl coenzyme A[5]. Testosterone is largely responsible for initiating and maintaining the sex drive (libido) in men[4,5] and is the main cause of the development of male characteristics such as a deep voice, beard growth, muscle development and the growth of vital sex organs. Testosterone is significantly more abundant than other male sex hormones, such that one can consider it to be the primary testicular hormone, even though most of it is converted to dihydrotestosterone in target tissues such as the prostate gland[3]. The proportion of testosterone that does

not become fixed to the tissues is rapidly converted and metabolised, mainly by the liver, into androsterone (Scheme **1**) and subsequently conjugated as either glucuronides or sulphates, which are secreted into the gut by way of liver or into the urine *via* the kidneys[5].

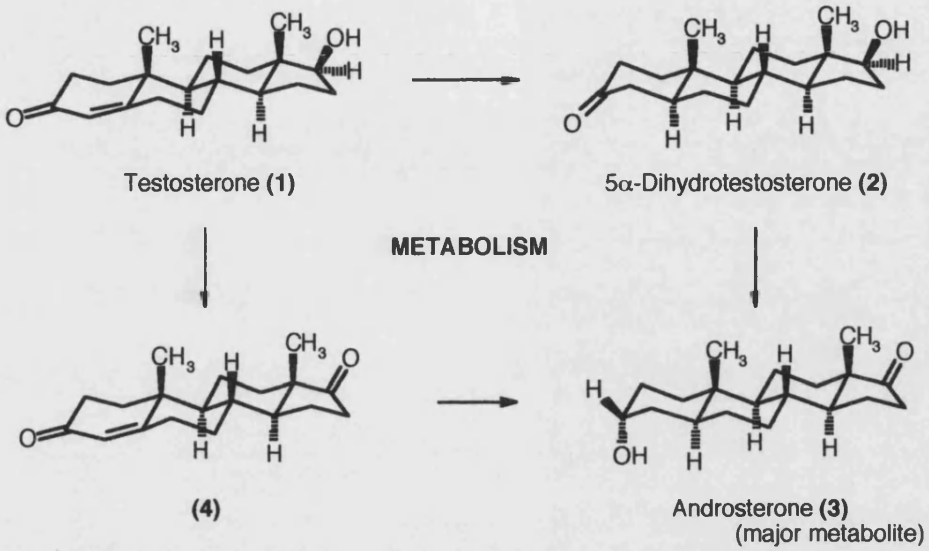

Scheme 1. *Chemical structures of the male sex hormones testosterone, dihydrotestosterone and androsterone*

1.1.4.1.1 Intracellular mechanism of action of testosterone

The prostate gland is one of the organs most affected by testosterone and other androgens[5]. Almost all of the effects of testosterone result in an increased rate of protein formation in the target prostatic cells. However, the rate at which testosterone is formed and thus secreted to the prostate gland is dependent on the controlled secretion of the gonadotropin-releasing hormone (GnRH)[6]. This hormone is secreted by the hypothalamus[†(p7)] and in conjunction it stimulates the pituitary gland[††(p7)] which releases two more very important hormones (glycoproteins), namely follicle-stimulating hormone (FSH) and luteinizing hormone (LH)[5,6]. The former is the hormone responsible for the stimulation of spermatogenesis, while the latter is the primary stimulus in the secretion of testosterone by the interstitial cells of Leydig[2,6]. Therefore,

it is important to mention that, in the absence of GnRH production from the hypothalamus, the gonadotropes within the pituitary gland secrete almost no LH or FSH[6] and, thus a decrease in the secretion of testosterone occurs. Once testosterone enters the prostatic cells within the prostate gland, it encounters an intracellular enzyme, 5α-reductase, and is converted to dihydrotestosterone. This now-active androgen then binds to a cytoplasmic receptor protein and this complex translocates to the cell nucleus, where it binds with nuclear proteins and induces DNA-RNA transcription[5]. Furthermore, this promotes prostatic cell proliferation. Testosterone stimulates production of proteins not only in the prostate and other target organs but virtually everywhere in the body by this mechanism[3,5].

1.1.5 Benign prostate disease

While the prostate gland remains relatively small throughout childhood, it begins to grow at puberty under the stimulus of testosterone. The prostate gland reaches an almost stationary size at the age of 20 years and generally remains at this size until the age of 50 years. Generally, in men over the age of 50 years, the prostate tends to involute with a decreased production of testosterone by the testes[5].

It is beyond the age of 50 years that men generally become susceptible to prostatic diseases[1], such as chronic urinary problems and benign prostatic fibroadenoma. This condition can be characterised as hypertrophy, or enlargement of the prostate[5]. This hypertrophy is an abnormal, non-testosterone dependent overgrowth of prostate tissue itself. It can be this hypertrophy that obstructs the urinary duct (prostatic urethra) pushing against it, narrowing the urethra. The incidence of these problems generally increase with age[1].

---

†(p6) The hypothalamus is a central area on the underside of the brain, controlling involuntary functions such as body temperature and the release of hormones.

††(p6) The pituitary is a small oval gland at the base of the brain producing hormones that control other glands and influence growth of bone structure, sexual maturing, and general metabolism.

1.1.5.1 Prostatitis

Prostatitis implies a prominent inflammatory lesion of the prostate gland that causes narrowing of the urethra and, consequently, urinary problems (as mentioned above in **1.1.5**). Prostatitis is often associated with a specific infective cause (*e.g.* a bacterial infection)[1]. Prostatitis is usually split into four types, these are discussed in more detail below:

1.1.5.1.1 Acute suppurative prostatitis

This usually results from the spread of infection along the prostatic ducts secondary to urethritis or cystitis[1]. It is normally a bacterial infection that spreads, leading to acute inflammation of the prostate. Acute infection of both the bladder and the urethra usually follow. Common causative micro-organisms include coliforms (such as *E. coli*), *staphylococci* and *gonococci*[1,2]. Acute prostatitis may occasionally follow urethral catheterisation or endoscopy, although a more rare case is when the infection has gone blood-borne[2]. With inevitable urinary problems due to the enlarged prostate pushing against the urethra, the lesion can usually be characterised by difficulty in micturition (urination), or by its degree of rectal pain[1]. There may even be necrosis (from the damaged epithelial cells) with formation of an abscess, which may eventually discharge into the urethra[1,2].

1.1.5.1.2 Chronic non-specific prostatits

Chronic non-specific prostatitis may develop from recurrent episodes of acute infective prostatitis[1]. The prostate is initially enlarged and tender but may eventually become fibrosed and shrunken[2]. Urethral obstruction, like that in acute prostatitis, may occur and the lesion may be mistaken clinically for prostatic carcinoma[2]. Tuberculosis of the prostate can also occur, showing characteristic caseating lesions that may involve the whole gland[2].

1.1.5.1.3 Granulomatous prostatitis

Granulomatous prostatitis is a rare condition and consists of a heterogeneous group of lesions, all of which may cause enlargement of the prostate gland and urethral

obstruction[1]. The inflammatory component and associated fibrosis produce a firm, indurated gland (rather than a soft/tender gland as in the acute prostatitis) on rectal examination, which, like the chronic prostatitis, may mimic a neoplasm clinically[1,2]. For this reason, the importance of the correct diagnosis for this type of prostatitis is critical.

1.1.5.1.4 Allergic (eosinophilic) prostatitis

This is probably the most rare of all benign prostatic diseases and most certainly of the different types of prostatitis that can occur. These types of lesions occur usually in men who are prone to allergic conditions, particularly bronchial asthma[1]. The gland contains granulomas (a small mass of granulation tissue caused by a chronic infection) with areas of fibroinoid necrosis, giant enlarged cells and numerous eosinophils[1,2].

1.1.5.2 Benign nodular hyperplasia (BNH)

Benign nodular hyperplasia is a common non-neoplastic process. It represents an overgrowth of prostatic glandular tissue and smooth muscle and is comparable to conditions such as cystic hyperplasia of the breast[2]. The incidence of BNH certainly increases with age and, by the age of 75 years, over 75% of males are affected to some degree, although only 5% have significant symptoms[1,2]. The process normally starts in the peri-urethral prostatic glands and the growth occurs mainly on each side of the urethra (in the two lateral lobes of the prostate, see Figure **2**). It is not unusual for the hyperplasia to project itself in the median lobe as well, by which these areas are susceptible to inflammation and can suffer abscesses[2].

1.1.5.2.1 Aetiology of BNH

Unlike with different forms of prostatitis, which are causally related to infections from bacteria, BNH is a different type of disease. Although the exact mechanism of the process towards BNH is uncertain, it is thought to be related to a hormonal imbalance. With increasing age, androgen levels fall, with a relative rise in oestrogens, which are notably responsible for an increase in prostatic tissue sensitivity, thus with the central

(peri-urethral) group of prostatic glands being highly oestrogen-responsive, they undergo consequent hyperplasia[1].

1.1.6 Malignant prostate disease (*prostate cancer*)

Cancer of the prostate gland is a different problem to that of benign prostatic disease and is a common cause of death, accounting for about 2-3% of all male deaths[5]. It is one of the most common cancers of an internal organ in males in the developed countries, its mortality rate being exceeded only by carcinomas of the bronchus, stomach and large intestine[2].

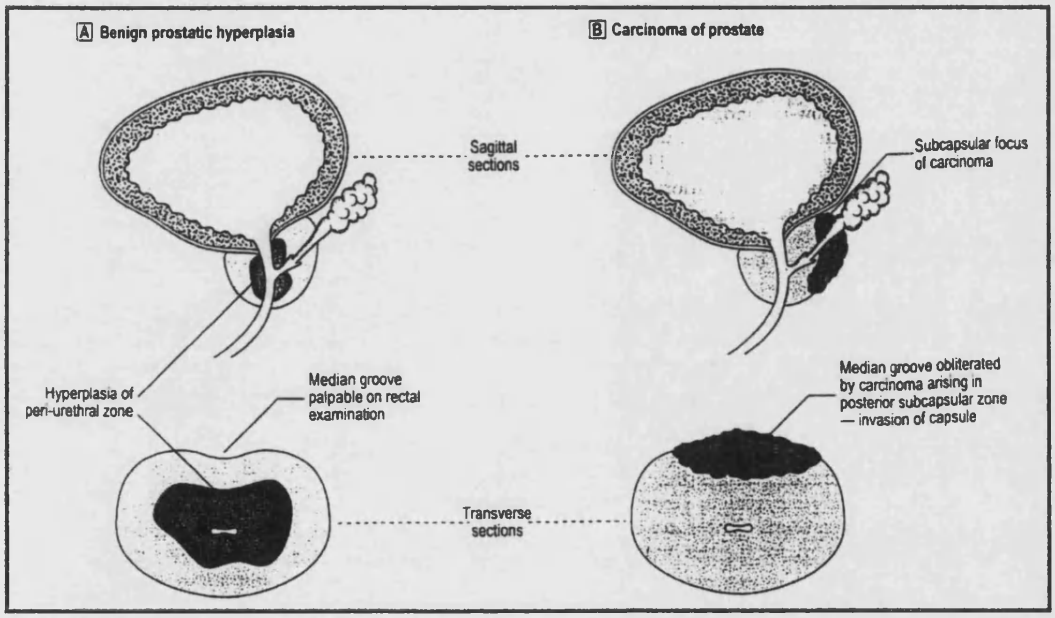

Figure 2. *A diagram that shows the difference between benign prostatic hyperplasia and malignant prostatic disease (carcinoma of the prostate)*[1]

Once cancer of the prostate does occur, the cancerous cells are usually stimulated to more rapid growth by testosterone and are inhibited by removal of both testes (castration). This way, testosterone cannot be formed[5]. The aetiology of this disease is unknown, although it is probable that a hormonal imbalance, like that for BNH, may initiate such carcinomas. Since these lesions for prostatic carcinoma coexist with those

for BNH, there is virtually no evidence that BNH is causally related to that in the development of malignancy[2].

1.1.6.1 Epidemiology of prostate cancer

With more and more men being diagnosed with prostate cancer worldwide, the knowledge and understanding of the disease is becoming increasingly more important. Prostate cancer is diagnosed in very few people younger than 50 years, < 0.1% of all patients in total. It is said that about 85% of patients are diagnosed after the age of 65 years, with the mean age for the disorder being approximately 72-75 years[8,9]. As discussed in great detail by *Henrik Grönberg* in *The Lancet*[9], the incidence of prostate cancer varies widely between ethnic populations and countries, and rates of the disease can vary as much as 90-fold between populations. The lowest rates tend to favour those in the far eastern countries, such as in Asia and especially Chinese people (1.9 per 100,000 per year). The highest rates for this disease tend to prevail in more westernised populations, with the highest being in North America, Scandinavia and especially African-American people in the USA (137 per 100,000 per year)[8,9]. These global differences are poorly understood and its said that they may be caused by a combination of genetic susceptibility, exposure to unknown external risk factors, dietary components or artifactual reasons, such as cancer registration and differences in health care[9,10]. In 15 years time, prostate cancer is predicted to be the most common cancer in men[12].

1.1.6.1.1 Genetic factors

Genetic susceptibility by the clustering of prostate cancer in families can be a large factor. This may be due to exposure to common environmental factors or simply by chance alone since prevalence of this cancer is so high[9]. It is stated that 10-15% of patients with prostate cancer (white, African or Asian) have at least one relative who is also affected[13]. It is also suggested that the disease is recessive or linked to the X-chromosome; it is believed that men who have a brother are more likely to obtain the disease than those who have a father who is affected[9].

1.1.6.1.2 Dietary factors

This is a controversial area, though results from ecological studies[9] suggest that prostate cancer is associated with a western lifestyle. Despite many dietary studies being conflicting, some components are consistently associated with prostate cancer, *e.g.* high intakes of α-linolenic acid (a polyunsaturated fatty acid found in vegetables and dairy products), fats, red meats and calcium[9]. Some studies have put forward that it may not be the intake of red meat that is causally related but the way it is cooked and prepared (*e.g.* cooking at high temperatures, charcoal grilling or frying which results in the formation of carcinogens such as heterocyclic amines)[9]. One area of interest towards reducing the risk of prostate carcinogenesis is that of the consumption of tomato products with a high lycopene content[14]. Lycopene is the principal carotenoid found in tomatoes and it is proposed that a high intake of this active lycopene component may reduce the risk of prostate cancer.

1.1.6.2 Clinicopathological types of prostatic carcinoma

There are currently two major clinicopathological types of prostatic carcinoma. There are the clinical carcinoma type, which are mainly symptomatic, and the latent carcinoma type, which are more incidental (Table **1**).

Condition	Incidence	Location of gland	Morphology	Metastasis
BNH	75% of men over 70 years	Peri-urethral zone	Nodular hyperplasia of glands and stoma	None
Clinical (*symptomatic*) carcinoma	Common tumour; peak 60-85 years	Posterior subcapsular zone	Infiltrating adeno-carcinoma	Bone Lymph node Lung Liver
Latent (*incidental*) carcinoma	Commoner than clinical carcinoma; 80% of glands over 75 years	Any site	Microscopic focus of adenocarcinoma	Rare

Table 1. *Differences between the three most common types of prostatic pathology*

1.1.6.2.1 Clinical (symptomatic) carcinoma

This type of tumour usually arises on the posterior part of the prostate and at the periphery of the gland (Figure **2**), with a large majority being adenocarcinomas (a malignant tumour with cells arranged in patterns similar to those of the prostate gland)[2]. These types of adenocarcinoma are usually well differentiated and the convoluted outline of the gland is lost and neoplastic acini are formed from a single layer of cells, unlike the glands in BNH, which have a double-layered epithelium[1]. Clinical carcinomas are very much symptomatic with their symptoms being similar to that of BNH. As with BNH and most prostatic diseases, compression of the intraprostatic portion of the urethra due to enlargement of the prostate leads to impaired urine flow and an increased risk of urinary infections[1]. However, because these tumours arise from the periphery of the gland, they are extremely susceptible to spreading within the prostate gland, causing urethral obstruction. They soon can spread to adjacent tissues and may metastasise widely and silently before urinary symptoms appear[2].

1.1.6.2.2 Mode of spread

Spread via the lymphatic system

The lymphatic system provides an important route of dissemination of prostatic carcinoma, producing metastases in the iliac and para-aortic lymph nodes. These may result in lymphatic obstruction and oedema† of the legs[1,2].

Spread via blood

Vascular invasion by the tumour results in blood-borne metastases, most commonly to bone, lungs and liver (Table **1**). The most frequent sites of bone metastases are the pelvis, the lumbar spine and the proximal femur, less frequently the ribs and skull. Bone metastases are usually osteosclerotic[2], with proliferation of osteoblasts and areas of new bone formation occurring in association with the neoplastic cells[1].

---

† Oedema is an abnormal build-up of excess serous fluid between tissue cells and thus can lead to abnormal swelling

1.1.6.2.3 Latent (incidental) carcinoma

Latent carcinoma is slightly different in comparison to clinical carcinoma (see Table **1**). Unlike clinical carcinomas which are symptomatic, latent carcinomas are generally found incidentally on histological examination of prostatectomy specimens removed for BNH, or in the prostate at autopsy[1,2]. These types of carcinoma are microscopic foci of carcinoma and the microscopical appearances are indistinguishable from those clinically overt well-differentiated prostatic carcinoma[2]. Like the clinical carcinoma, these tumours are generally adenocarcinomas and are thought not to produce clinical manifestations[1].

The aetiology of these minute tumours is uncertain and the concept of the latent carcinoma has been questioned with the recognition that some of them eventually progress and metastasise[1]. However, these forms of carcinoma are much more common than the clinically active symptomatic form of the disease. As such, minute foci are found in about 30% of prostates over 50 years old, with the incidence rising to about 80% over the age of 75 years (Table **1**)[1].

1.1.6.3 Diagnosis of adenocarcinoma of the prostate

Diagnosing prostate cancer in its early stages can be somewhat difficult. Not only being able to distinguish such carcinomas from other potential prostatic diseases that could be present (*i.e.* BNH), but choosing the right technique in determining what type of carcinoma is present, and its stage of malignancy, is critical. There are various techniques that can be adopted in the investigation of prostate cancer. The preferred method is that of a biopsy (*e.g.* transurethral resection, fine needle aspiration cytology and needle biopsy)[15], with the latter being the most common technique. Normally, such techniques are used in combination with diagnostic imaging (*i.e.* ultrasound and skeletal X-rays)[1]. This normally minimises false positives and negatives during diagnosis and aids selection of sites for such biopsies[15]. However, the difficulties with needle biopsy not only stem from the small amount of tissue available for histological examination but also arise because biopsies often identify only a few malignant glands among many benign glands[15].

Monitoring serum prostate specific antigen (PSA) is another way of diagnosing prostatic carcinoma. It is produced in prostatic epithelium and has a physiological role in the liquefaction of semen. It is also secreted in large amounts by malignant prostatic epithelial cells; thus makes it a very good diagnostic marker for the disease[15]. Also, patients with associated bone metastases have a raised level of serum acid phosphatase[16], an enzyme produced by the neoplastic cells which is also a useful diagnostic marker of prostate cancers[1,15].

1.1.6.4 Prognosis and the Gleason grading system

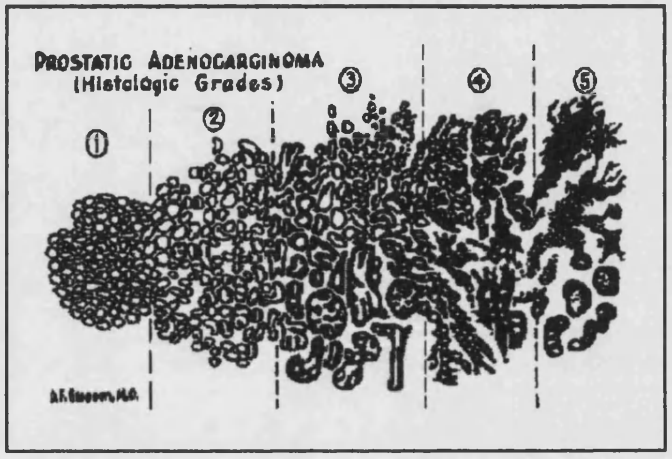

Figure 3. *A modified illustration of Dr Gleason's simplified drawing representing the five Gleason grades in determining the severity of prostatic carcinomas*[17]

Following the diagnosis, the next important clinical step is the prognosis and prognostic factors include stage of disease and grade of malignancy[11]. The degree of differentiation of the tumour is an important prognostic indicator. In the Gleason classification (Figure **3**)[17], tumours are graded on a scale of 1-5, with a grade 1 tumour being the most differentiated and grade 5 being the least differentiated, usually showing that tumours are anaplastic with a high mitotic rate[2,15,17]. More than one pattern of differentiation may be present in a surgical specimen and thus the two predominant ones are graded individually and then added together to give a final

Gleason grade (*e.g.* 3 + 5 = 8). Gleason grades 2-6 are associated with better prognosis[11,17].

1.1.6.5 Treatments

There are four main types of treatment with the aim of alleviating the prostatic disease. These treatments consist of: surgical methods (radical prostatectomy), radiation therapy (external-beam radiotherapy and brachytherapy), hormone therapy and chemotherapy.

1.1.6.5.1 Radical prostatectomy (*surgery*)

Radical prostatectomy is a surgical method for removal of all, or part of, the prostate gland[18]. If the cancer is localised within the gland and the prostate is completely removed, the likelihood of the cancer being cured is extremely high. This type of surgery has been the standard against which other local treatments are compared[7]. This procedure has been refined resulting in high cure rates with decreased morbidity[8]. Radical prostatectomy is a collective term for a family of procedures and can be separated into retropubic and transperineal approaches[19]. The retropubic approach has the advantage over the perineal method in that the lymph nodes can be dissected and the prostate gland removed in a single incision[7]. In contrast radical perineal prostatectomy requires separate incisions for the lymph-node dissection and prostatectomy[7]. The advantage of such surgery over radiation and hormone therapy (see sections **1.1.6.5.2** and **1.1.6.5.3**, respectively) is that the biochemical follow-up is far less ambiguous with respect to the diagnostic marker, PSA. Prostate specific antigen is expected to be undetectable after prostatectomy; this contrasts with the radiation/hormone approaches in which the prostate remains in place and by which the prostate continues to secrete some PSA[7,19].

1.1.6.5.2 External-beam radiotherapy & brachytherapy (*radiation*)

External-beam radiotherapy involves daily treatment for about 7-8 weeks. As with radical prostatectomy, this procedure has been refined and undergone a technological revolution with results leading to survival rates comparable to that of surgery[7,8]. Like

general radiotherapy, it offers a reasonably precise delivery of an external beam to the prostate, allowing increased doses to the gland with minimal complications. Unlike surgery, this type of radiation therapy is non-invasive[7] and has no anaesthetic risk (which could pose many problems in elderly patients). It can also be offered to patients that would not be able to tolerate either prostatectomy or brachytherapy[7]. However, one important disadvantage in external-beam radiotherapy is possible rectal complications (see Table **2** for a comparison in complication rates between the different treatments available). Since the prostate gland is close to the rectum, a therapeutic dose cannot be delivered to the prostate without some dose passing to the rectum[7]. Rectal bleeding can be the result from such therapy.

Site	**Prostatectomy**	**External-beam radiotherapy**	**Brachytherapy**	**External-beam radiotherapy + brachytherapy**
Rectal	*	* * *	*	* *
Sexual (impotence)	* * *	* *	*	* *
Urinary incontinence	* * *	*	*	*
Urinary retention	*	*	* * *	* * *

Increasing number of (*s) indicates increasing complication rates.

Table 2. *Relative complication rates from local control treatments for prostate cancer*[7]

Brachytherapy is a very effective treatment for the early stages of prostate cancer. It is said to achieve disease-free survival rates comparable to those of both prostatectomy and external-beam radiotherapy but with a different side-effect profile (Table **2**)[7]. Brachytherapy works by direct placement of radioactive sources in the area of interest. The advantage of using this technique is that it is a more precise, localised method of treatment that is less likely to affect surrounding structures (*i.e.* the rectum)[7]. However, dealing with radioactive sources and specifically in an area such as the prostate, this can lead to urinary toxic effects, like prostate oedema and urinary hesitancy. The latter may require to the need for a temporary catheter to alleviate such a problem.

In addition to the follow-up uncertainties, it is well documented that brachytherapy leads to a PSA rebound effect (the cause of which is unknown); this takes place 1-2 years after the procedure, also making follow-up PSAs difficult to interpret[7].

1.1.6.5.3 Hormone therapy

The prostate gland is a hormone-responsive organ[7] and the growth of most malignant prostatic cancer cells thrives on these male hormones, such as testosterone and other androgens. Hormonal therapy (or rather, hormone-suppression therapy) was previously accomplished mainly by the direct method of bilateral orchiectomy. Although the surgical removal of the testes eliminates the production of testosterone and is a relatively quick, painless and inexpensive process, the psychological side-effects can be highly significant, with the loss of the male libido. The latest method towards hormonal therapy is that of chemical castration[7]. Many hormonal agents are said to work along the hormone axis to inhibit and reduce the production of serum testosterone or to block the actions of this hormone altogether [16,20]. These methods are not just psychological and aesthetically more pleasing but they are said to be very effective in 75-80% of patients with prostate cancer[9]. Such chemical castration methods include the use of injectable drugs known as LHRH/GNRH agonists, the use of oral oestrogen drugs and the use of non-steroidal anti-androgen treatment.

1.1.6.5.3.1 LHRH (analogues/agonists) therapy & oestrogen therapy

Luteninizing Hormone-Releasing Hormone (LHRH) is responsible for the secretion of testosterone (see section **1.1.4.1.1**). Thus the most common way to suppress the production of such male androgens is to use LHRH agonists (such as progestogens – see Appendix Figure **24**)[21]. LHRH agonists stimulate and shut down signals from the pituitary gland in the brain, suppressing the release of the LH hormone and thus reducing the amounts of testosterone being produced. In conjunction with the LH hormone therapy, the use of Gonadotropin-Releasing Hormone (GnRH) agonists (which can also down-regulate the pituitary receptors) can also be used. This type of hormonal agonist type therapy is also known as steroidal anti-androgen therapy[21]. Oral oestrogen drugs (*e.g.* diethylstilbestrol – see Appendix Figure **24**) can be used as

an alternative therapy and can also reduce testosterone to castrate levels by blocking and suppressing the hypothalamic production of GnRH and in turn, LH secretion. Since the availability of LHRH/GnRH agonists, oestrogen type drugs are used less frequently because of their potential fatal side effects (such as heart attacks and blood clots)[21,22].

1.1.6.5.3.2 Non-steroidal anti-androgen therapy

This type of therapy is different to that of steroidal LHRH/GnRH therapy, in that these types of anti-androgens (*e.g.* flutamide – see Appendix Figure **25**), or androgen receptor antagonists, work by actually inhibiting and blocking testosterone from binding to its cellular target. These types of antagonists work without effecting the LH secretion, thus preserving the male sexual libido. Although this type of monotherapy is said to be less effective to that of steroidal hormonal therapy, a common regimen is the combination of a non-steroidal anti-androgen with an LHRH/GnRH analogue to provide total blockade of androgens[7]. Other successful combinations that have been shown to improve survival rates dramatically are the use of hormonal therapy combined with radiotherapy[7,23]. This is probably because of their different mechanisms of action and the fact that they can independently destroy prostate cancer and sensitise the tumour to radiation[7].

In general, most hormonal therapies have common side effects, such as hot flushes, loss of libido, erectile dysfunction, weight gain, gynaecomastia, liver inflammation and osteoporosis[20]. These side-effects are usually short-lived and mild in short-course hormone therapy (typically used for early-stage prostate cancer) and the balance of such benefits against the possibility of having the opposing long-course hormonal treatment, need to be recognised early on and taken in to careful consideration[7,20]. Although, at first, hormonal ablation therapy seems like the easiest choice in treating prostate cancer, certainly in its early stages, problems can occur after a brief period of time when patients start to suffer from a relapse of the prostatic disease. Hormonal therapy starts to become limited when such relapses involve androgen-independent tumours[24-25].

In a number of experimental and clinical prostate cancers, MacNeal[26] identified what is regarded as premalignant change in these cancers. These observations have led to the introduction of a new concept for the development of clinical prostate cancer that is significantly different to the established carcinogenic principles[25]. It is believed that prostatic cells do not die as normally and, although the proliferation of cells at this stage may not be faster than normal, the lack of cell death results in a greater number of cells and, thus, to an apparent new tumour growth[26]. It is said that these cells which do not age normally, escape the normal control mechanisms exerted by hormones and other growth factors and an increasing number of these cells at a given stage of growth will become relatively hormone-independent[25-26].

Aiding these observations by MacNeal, Coffey and Isaacs[27] have shown that there may be three different mechanisms for the development of hormone-independent cells:

1. The direct mutation of DNA.
2. Cells may adapt to a changing environment, in which, as androgens are suppressed by hormonal therapy, cells adapt to survive in a low-androgen environment.
3. Endogenous hormone-independent cells are present from the very start albeit in comparatively small numbers. They become prevalent only after the remainder of the initial cancerous tumour(s) has been controlled by hormone manipulation or some other therapeutic modality.

This third concept is said to fit well with the observed natural history of prostate cancer and certainly with the timing of apparent hormone relapse[26].

Usually in the latter stages of the prostatic disease and almost always in relapse metastatic prostate cancer, the treatment of hormone-resistant cells may be accomplished only by immunotherapy and by chemotherapy. Since the number of these cells is then comparatively large, the former treatment is most unlikely to be successful and thus chemotherapy takes precedence[26-27].

1.1.6.5.4 Chemotherapy (*of hormone-independent prostate cancer*)

Chemotherapy refers to the use of cytotoxic drugs that inhibit or kill off rapidly dividing cells such as prostatic cancer cells. Since 1975, a number of chemotherapeutic agents have been discovered and tested in relapsed prostate cancer[25].

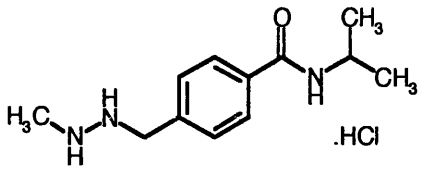

Procarbazine (5)

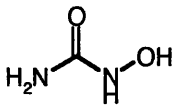

Hydroxyurea (6)

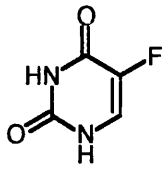

5-Fluorouracil (7)

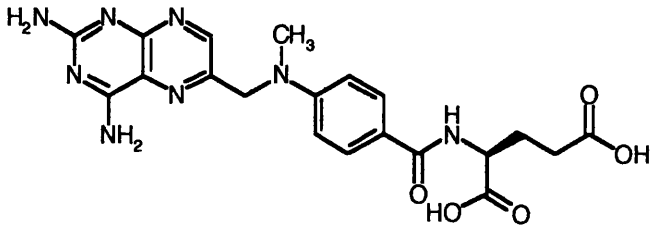

Methotrexate (8)

Figure 4. *A series of antimetabolites; procarbazine, hydroxyurea, 5-fluorouracil & methotrexate*

Early examples, such as procarbazine (**5**), hydroxyurea (**6**) and methotrexate (**8**) (see Figure **4**), failed to produce a significant response and were shown to be largely ineffective against relapsed prostate cancer, although, as a single-agent treatment, the antimetabolite, 5-fluorouracil (**7**) (Figure **4**) appeared to offer some benefit[25]. Most antimetabolites such as those shown above have a similar mode of action, where they prevent the biosynthesis of cellular metabolites by acting as enzyme inhibitors[28-29].

In contrast to these antimetabolites came the discovery of alkylating agents, such as melphalan (**9**) and cyclophosphamide (**10**). These types of alkylating agents, also known as nitrogen mustards[30], are highly reactive N,N-bis(2-chloroethyl)amines and form covalent links with biomolecules containing SH, NH_2 and OH nucleophiles, such

as nucleic acids and proteins[28]. These types of interactions can be responsible for causing various types of DNA damage, such as the alkylation of a single base leading to loss of DNA functionality. Also, the alkylation of two bases that are cross linked together, can lead to faulty DNA transcription and, further more, it can lead to single or double strand breaks in highly alkylated and cross linked regions[29]. As single agents, nitrogen mustards have proved to be reasonably effective, though at higher doses in combination with the oestrogen estramustine, they have shown to be more effective. However, they almost always produce significant systemic toxicity leading to severe side-effects[25].

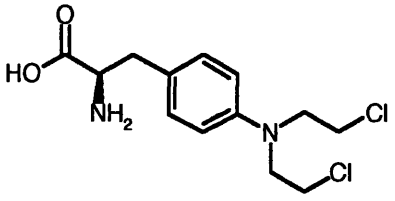

Melphalan (9)

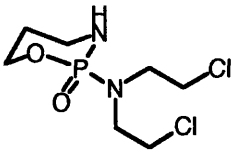

Cyclophosphamide (10)

Figure 5. *A series of nitrogen mustard alkylating agents; melphalan & cyclophosphamide*

1.1.6.5.4.1 Anthracyclines & their derivatives

Antitumour cytotoxic agents such as anthracycline antibiotics are becoming of increasing intersest in the aid of tackling hormone-refractory prostate cancer[31]. Doxorubicin (*Adriamycin* (**13**))[32] and other anthracyclines are amongst the most effective cytotoxic agents used in cancer chemotherapy. In particular, doxorubicin, daunorubicin (**14**) and epirubicin (**12**) (Figure **6**) are amongst the more effective cytotoxic agents in advanced hormone-independent prostate cancer (Table **4**)[24].

1	At the cell membrane
2	DNA intercalation
3	DNA-protein link breakage
4	Topoisomerase inhibition

Table 3. *Actions of anthracyclines*

At least one main reason suggested for the efficacy of anthracyclines, is the large number of mechanisms (Table **3**) by which they can induce potentially lethal damage to dividing malignant cells[25]. As a single agent, doxorubicin is the most commonly and widely used anthracycline antibiotic in clinical therapy[34]. It has been reported to induce a 33% response rate against the disease when administered weekly, and has been incorporated in many active combination chemotherapy regimens[32,33]. Such combination regimens that have resulted in significant synergistic cytotoxic activity at subtoxic concentrations, are that of doxorubicin and a recent cytotoxic drug of interest, doxazosin (**11**) (a quinazoline compound that is a selective inhibitor of the alpha$_1$ subtype of alpha adrenergic receptors) (Figure **6**)[31].

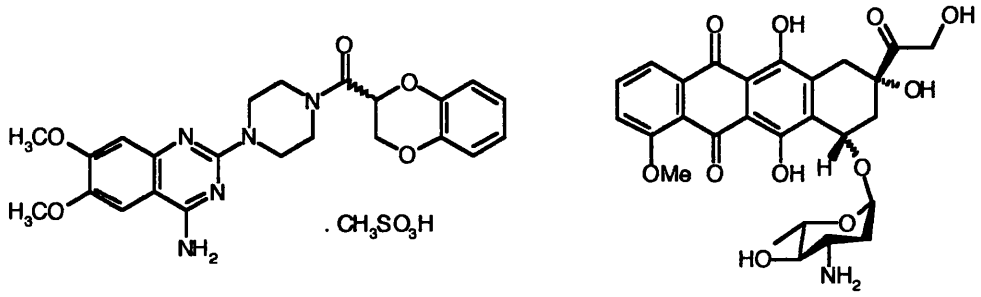

Doxazosin (11) Epirubicin (12)

Figure 6. *Structures of doxazosin & epirubicin*

Anthracyclines are said to interfere with the topoisomerase II enzyme, which is fundamentally responsible for the regulation of DNA topology[35]. More so, these anthracyclines interrupt the functions of the enzyme by stabilizing a transient DNA-topoisomerase II complex, in which DNA strands are cut and covalently linked to tyrosine residues of the enzyme[34-35]. Furthermore, it is proposed that such anthracyclines have three distinct functional domains, which are responsible for their activity towards apoptosis (Figure **7**)[36]. These have been defined from its ternary **DNA---enzyme---drug** complex, which consists of an amine-sugar moiety domain responsible for interactions with the phosphate backbone in nucleic acid, a planar ring system domain, which also is said to interact with DNA, and a substituted cyclohexane

ring (**A**) domain, which is said to be responsible in interacting with the enzyme along with the OH functional group represented at position (**C-9**)[36].

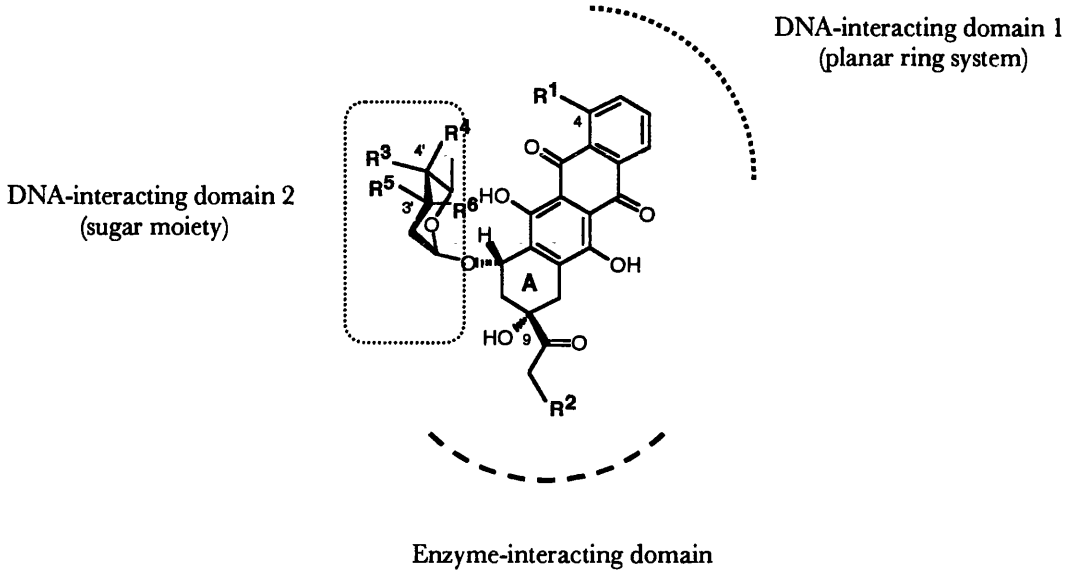

Figure 7. *Putative functional domains of the anthracycline molecule*

Although there are many types of chemotherapeutic drugs available for the treatment of hormonally resistant prostate cancer, treatments still remain palliative in patients, with the median survival duration being approximately 6 months[37].

	Compound	R^1	R^2	R^3	R^4	R^5	R^6
13	**Doxorubicin**	**OCH_3**	**OH**	**OH**	**H**	**NH_2**	**H**
14	Daunorubicin	OCH_3	H	OH	H	NH_2	H
15	Idarubicin	H	H	OH	H	NH_2	H
16	4-Demethoxy-3'-deamino-3'-hydroxy-4'-epi-doxorubicin	H	OH	H	OH	OH	H
17	3'-Deamino-4'-deoxy-4'-epi-amino-idarubicin	H	H	H	NH_2	H	H
18	3'-Epi-daunorubicin	OCH_3	H	OH	H	H	NH_2
19	3'-Deamino-3'-epi-hydroxy-4'-deoxy-4'-amino-daunorubicin	OCH_3	H	NH_2	H	H	OH

Table 4. *Common anthracyclines & their potential cytotoxic derivatives (compare with Figure 7)*

The fundamental reason for this is that most patients with metastatic prostate cancer are elderly and with concurrent illnesses such as compromised bone marrow disfunctionality. Thus doses required to destroy and reduce significantly the effect of the disease are usually held to a minimum[37]. The effects of chemotherapy on tumour growth must therefore be balanced against the discomfort caused from normal tissue toxicity[37]. Therefore, with elderly patients unable to tolerate aggressive chemotherapy, such treatments can only be justified if there are significant improvements in the rate or quality of survival[37]. In this setting of the disease in which treatment is unlikely to affect survival, the primary aim for chemotherapeutic treatments have therefore become to mitigate the symptoms and improve the quality of life.

This has however, driven the need for symptomatic improvements, and the search for new cytotoxic chemotherapeutics with an improved therapeutic index, lower side effects and a higher activity against resistant cancer cells. This has stimulated ongoing research for new anthracycline analogues, such as halogenated versions of doxorubicin and daunorubicin[34]. Analogue development was originally limited by a lack of information on the cellular drug target. Nevertheless, with the mechanism of action of such cytotoxins such as doxorubicin and daunorubicin revealed and DNA topoisomerase II recognised as their main molecular target, many analogues have been synthesised and tested. Binaschi and Capranico[35,36] are amongst the leading developers in the research of analogues based on the most successful anthracyclines used in hormone-independent prostate cancer (Table **4** and Figure **7**).

1.2 Drug targeting

The concept of drug targeting is the ability to target pharmacologically active molecules to specific sites in the body. Upon administration of a drug, by either an oral route or by an intravenous injection, the drug substance will distribute throughout the body as a function of its molecular structural properties[38]. Furthermore, the final amount of drug actually reaching its target site may only be, and likely to be, only a small fraction of the dose originally administered and thus accumulation at non-target sites may lead to severe adverse reactions, leading to unwanted side-effects[38]. Though

progress has been made in reducing the severity of cytotoxic-induced side-effects by methods of multiple administration schedules and dosage regimens based on pharmacokinetics principles[39], the idea of applying the drug directly to its intended site of action seems to be of great advantage, as side effects would surely be reduced and it would open up many possibilities to the use of highly potent toxins[39].

As mentioned in section (**1.1.6.5.4**), chemotherapy is an obvious example of the need for systemic drug targeting, where adverse reactions caused by cytotoxic agents are a major limiting factor[38,39]. The lack of antitumour specificity displayed by cytotoxic agents results from a low level of biochemical differentiation between normal cells and cancerous tumour cells, which together with the heterogeneous nature of tumour cell populations, limits the effectiveness and efficacy of current therapeutic approaches[38]. Systems that are currently available for achieving site-specific drug delivery range from the use of prodrugs (an inactive, metabolisable drug precursor) to the use of carriers such as macromolecules. Both systems will be discussed in more detail later in this section.

1.2.1 Target site specificity

There are three orders of classification towards the degree of specificity achieved by drug targeting, which accordingly relate to the level of selectivity of the delivery system[40]. The possibility of attaining each level of targeting can apply to various systems, though no single system exists that provides all three[38].

• ***First-order delivery:*** This order of delivery is also known as 'organ targeting,' by which the aim of delivery is to target individual organs or tissues.

• ***Second-order delivery:*** This order of delivery refers to 'cellular targeting,' where the idea is to target a specific cell type(s) within a tissue.

• ***Third-order delivery:*** This order of targeting involves the delivery to selected intracellular compartments within target cells, thus is referred to as 'subcellular targeting.'

In cancer chemotherapy, the importance of having such orders of targeting can play a significant role when designing a specific delivery system and failures to meet these may explain the lack of success in other areas of cancer chemotherapy[40]. Thus, ultimately, the need for a targeting system that has the capability of accommodating an array of drug types and that can deliver its toxic agents to a range of tumour cell subpopulations will obviously have a significant general application. Furthermore, in view of the fact that it is known that cytotoxic drugs work at a variety of subcellular sites, a degree of third-order targeting maybe useful (see section **1.2.2.2.3** on the concept of GDEPT) to ensure maximum therapeutic efficiency if the survival of drug resistant cells remains a major cause of treatment failure[38].

1.2.2 Modes of drug targeting

Site-specific drug delivery systems can be classified according to their mechanisms of achieving target site localisation. Such methods are that of passive and active targeting[38,40].

1.2.2.1 Passive targeting

Passive targeting is a function of the natural distribution pattern of the carrier *in vivo*. Factors affecting the biodistribution of such drug carrier systems can be determined largely on their physicochemical properties such as particle size and shape, and surface characteristics like hydrophobicity/hydrophilicity and particle surface charge[38]. It is, however, these properties that have been exploited[41] in the attempt to improve targeting efficiency. Such examples are passive lung targeting[42], where entrapment of large particles (>7 μm) in the capillary bed of the lungs has been exploited in radiodiagnostic imaging as well as for pulmonary delivery of anticancer agents. Another example is that of passive intra-arterial targeting[38,43], where the injection of large particles results in mechanical entrapment by the first capillary bed. This

entrapment effect could however be very useful upon the administration of cytotoxic agents into the arteries supplying a cancerous tumour site. This would probably result in drug accumulation at the tumour site before RES (reticuloendothelial system, known also as the mononuclear phagocytic system) clearance could take effect[38].

The RES is a collective name for a group of highly phagocytic mononuclear cells derived from the bone marrow. These cells can be found throughout the body, either at fixed sites (like in the liver and spleen) or free in circulation[42]. Thus RES-mediated clearance can be a major factor in determining the biodistribution of colloidal systems. Based on the aforementioned, the RES can however be exploited in the distribution of drug targeting delivery systems, or clearance of tumour cell residues. Therefore, the RES presents itself for passive targeting as well[44].

1.2.2.2 Active targeting

The term active targeting refers to a deliberate modification of a natural disposition pattern of a carrier in the aim to direct it to specific organs, tissues or cells[38]. A potential strategy in overcoming the limitations of chemotherapeutic agents where such modifications have been addressed is the introduction of the prodrug design (Figure **5**).

1.2.2.2.1 The prodrug concept *(the trigger-linker-effector concept)*

The term *prodrug* maybe defined as a chemical which is non-toxic and pharmacodynamically inert but which can be transformed *in vivo* to a pharmacologically active drug[45]. Prodrugs have a variety of uses in cancer chemotherapy, as shown in (Table **5**).

1	Selective activation in target cells
2	Improved pharmacokinetics
3	By-passing resistance
4	Altered distribution
5	Optimal route of administration
6	Increased stability

Table 5. *Uses of prodrugs in cancer chemotherapy*

There are two types of prodrugs to consider, the small-molecule prodrugs and the macromolecule (large) prodrugs. The latter will be discussed in more detail in section **1.2.2.2.4**. However, both types of prodrugs follow the same concept and are considered to be comprised of two major domains[46]: a ***trigger*** unit, which acts as the substrate for an activating enzyme or system, and an ***effector*** unit (active drug – cytotoxin) which is usually activated or released by a metabolic process[46] and is sometimes joined by a definable linker group (Scheme **2**)[47,48].

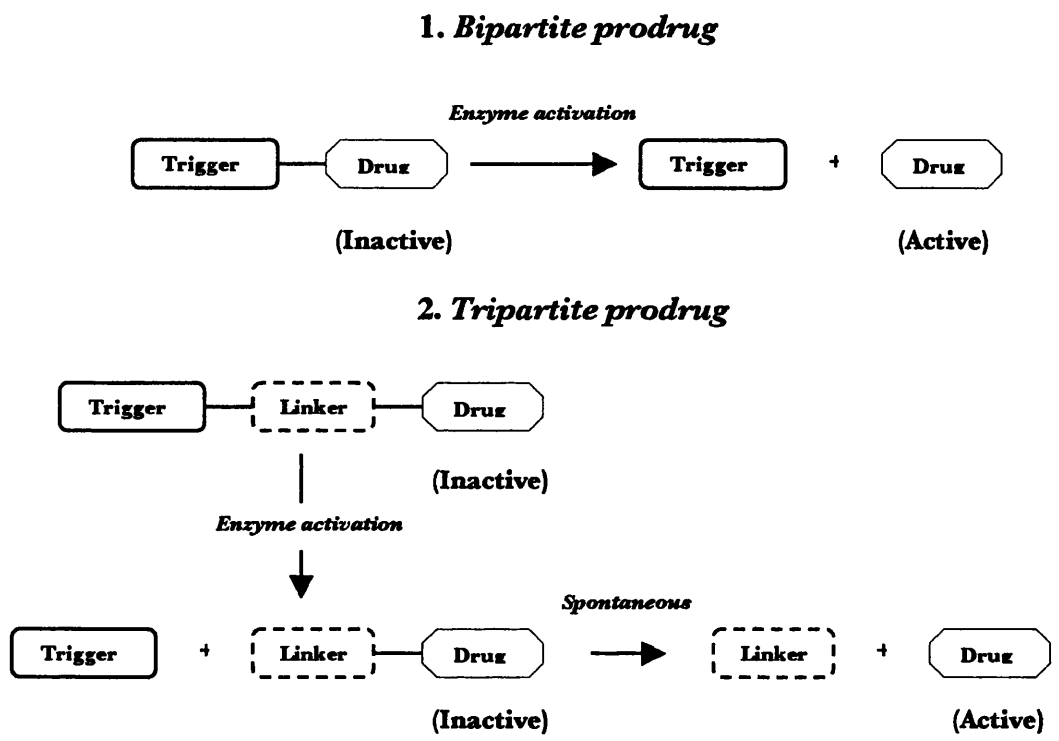

Scheme 2. *A representative schematic view of enzymatic bipartite & tripartite prodrugs for their use towards site-specific drug targeting*

Prodrugs can also be classified into being either bipartite or tripartite in design and functionality (Scheme **2**). With regard to a bipartite prodrug, this consists of a carrier or linker moiety attached directly to the drug moiety. The trigger/carrier moiety generally serves to target the drug to a particular site, while a specific bond linking the trigger to the drug is hydrolysed, releasing free active drug in the body[46,48].

In certain cases, however, this basic prodrug strategy can fail. It is possible that the inherent nature of the bipartite prodrug bond connecting the trigger to the drug maybe sometimes be too unstable. Alternatively, it may have the opposite effect and the bond maybe present itself as being quite stable. Such stability could arise from electronic or steric features of the drug and thus hinder hydrolysis of the trigger---drug bond by the desired enzyme[48]. The idea of a tripartite drug can often circumvent this problem with the addition of a linker group (sometimes expressed as a ***self-immolative molecular clip***)[49-51].

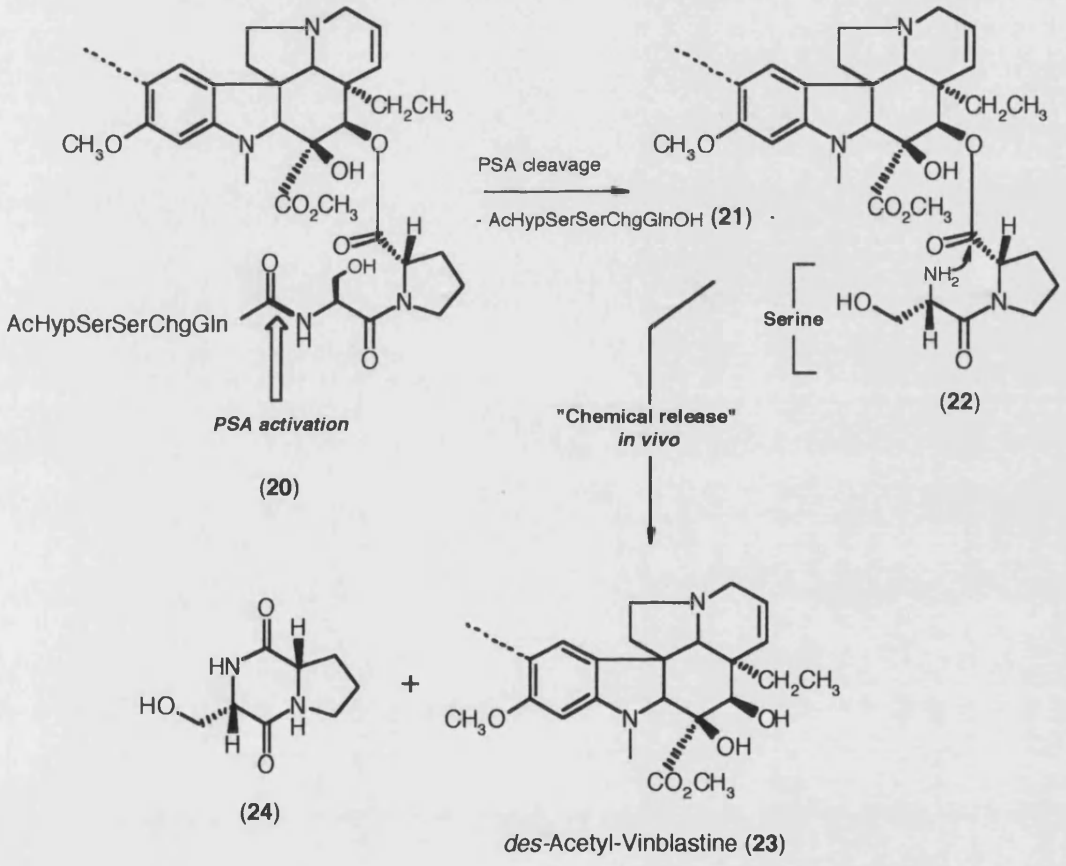

Scheme 3. *A schematic representation of the release of vinblastine from a tripartite prodrug conjugate upon activation of PSA. (for the complete structure of vinblastine - see Appendix Figure* ***26****)*

By spacing the drug away from the trigger moiety, this can allow a more viable route for enzymatic activation, where hydrolysis takes place at the trigger---linker bond

rather than at the trigger---drug bond as with the bipartite prodrug concept. However, it is rather important that the linker moiety is designed such that, following enzymatic activation, the remaining bond connecting the linker to the drug moiety spontaneously releases the active drug by means of hydrolysis (under physiological conditions) or *via* an alternative method[49].

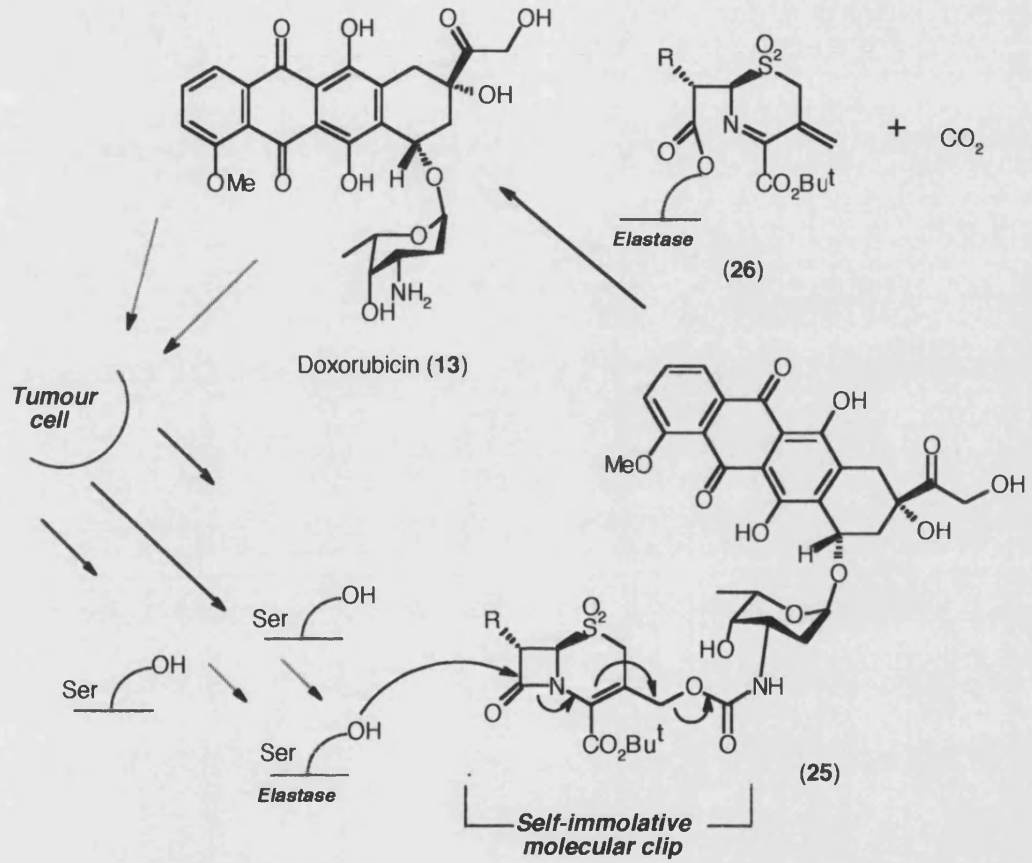

Scheme 4. *The concept of elastase mediated splitting of doxorubicin-cephalosporin prodrug*

An example of a tripartite prodrug is shown in (Scheme **3**, p30). PSA-cleavage between a serine amino-acid and glutamine residue (which occupies the P1 site)[52,53] on a sensitive peptide (trigger domain), releases a linker-drug moiety. Furthermore, upon release of the linker-drug moiety, an intramolecular cyclisation[52] between the exposed serine and proline residue leads to the spontaneous release of the drug, vinblastine (**23**) ($t_{1/2}$ ~ 12 min at 37°C)[53].

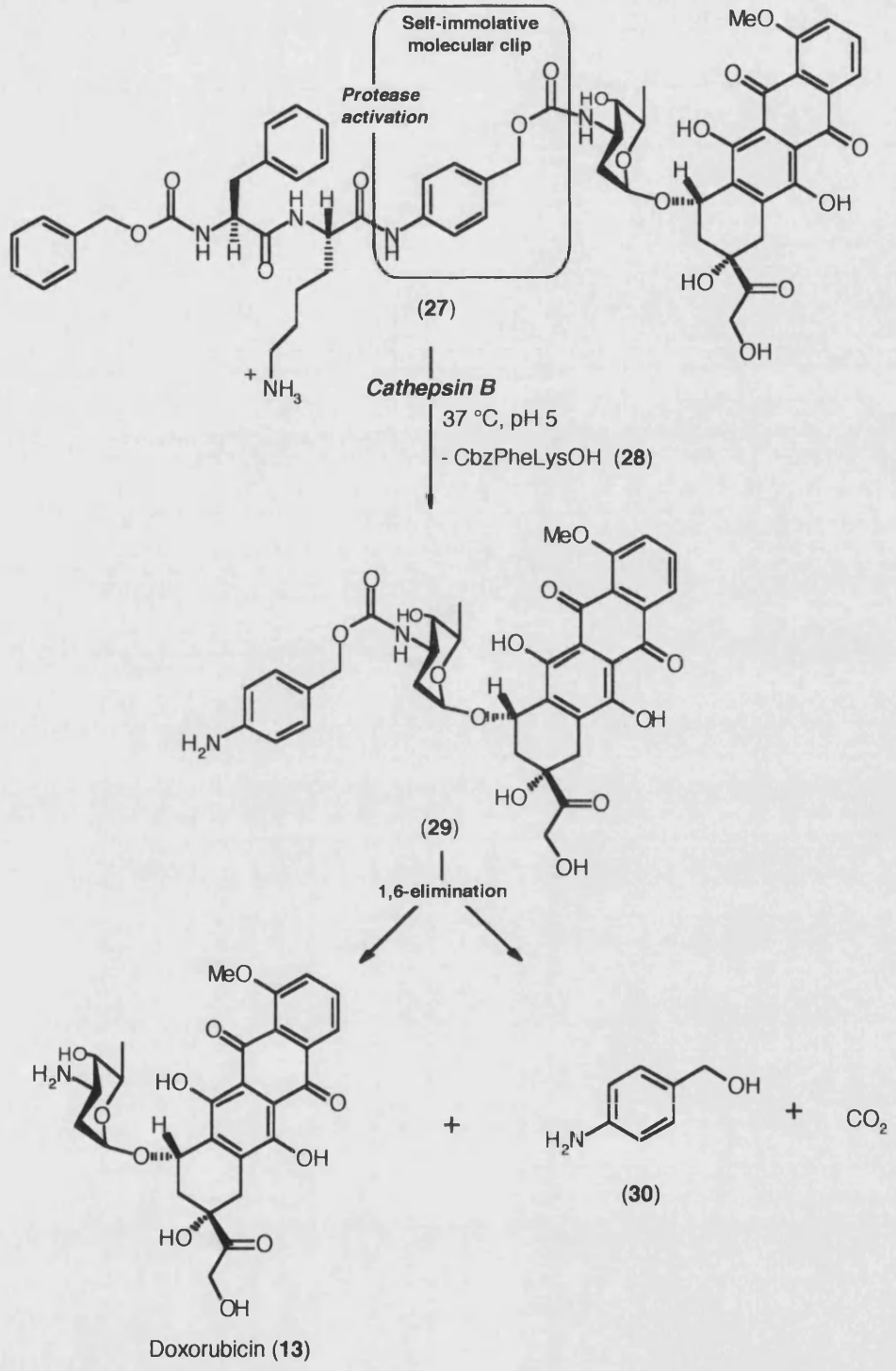

Scheme 5. *A schematic representation of the release of doxorubicin from a tripartite prodrug conjugate upon activation of the protease, cathepsin B.*

An example of a bipartite prodrug is shown in (Scheme **4,** p 31). The strategy of using cephalosporin-drug conjugates by means of selective drug targeting is a relatively new idea and was firstly introduced by Veinberg *et al*[54]. In this instance, the cephalosporin-trigger domain acts more like a linker group and is directly attached to doxorubicin. Upon enzymic cleavage of the lactam ring, causing ring opening, free doxorubicin is released spontaneously. In the final example shown in (Scheme **5**), the CbzPheLys is the trigger domain, the aminobenzyloxycarbonyl group is the linker and the doxorubicin (**13**) is the drug. In the presence of cathepsin B, this tripartite prodrug undergoes rapid 1,6-elimination, releasing doxorubicin. It is suggested that in this model, the linker group undergoes a 1,6-elimination[49] process upon activation by the enzyme ($t_{1/2}$ ~ 8 min at 25 °C)[55].

1.2.2.2.2 Antibody-drug conjugates targeting

Antibody-drug conjugate targeting involves a number of potent antitumour cytotoxins being attached to an antibody moiety with the aim for a more specific and selective targeting approach[56]. Monoclonal antibodies (often abbreviated to MoAbs) are glycoproteins of the immune system capable of distinguishing malignant cells from their normal counterparts[57] and typically have nanomolar affinities for their target[56-58]. The most commonly used chemotherapeutics towards constructing MoAb-drug conjugates are the anthracyclines doxorubicin and daunorubicin[56] and, although monoclonal antibodies are typically tolerant to the conjugation of such chemotherapeutics, the agents themselves often lose potency in their conjugated form.

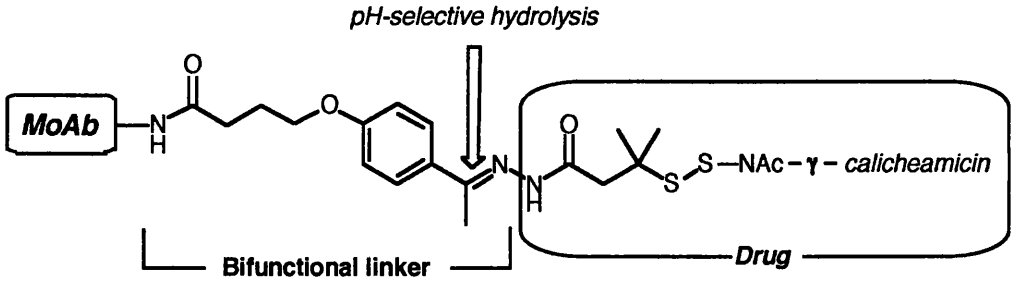

(31)

Figure 8. *Cleavable bifunctional linker for the conjugation of calicheamicin to monoclonal antibodies*

A good example of this comes from the antitumour antibiotic calicheamicin[58]. When conjugated to a tumour-targeting MoAb through an amide linkage, the conjugate is accumulated in the tumour site, but has no appreciable cytotoxicity. In contrast, when conjugated by using a pH-sensitive bifunctional linker that permits the release of calicheamicin intracellulary (see Figure **8**), the conjugate shows potent antitumour activity[58]. However, although this type of MoAb conjugate has shown reasonable potency in certain acute leukemias, immunogenicity and MoAb-drug conjugate potency towards prostate cancer still remains a problem[57,58].

1.2.2.2.2.1 Antibody-directed enzyme prodrug therapy (ADEPT)

ADEPT is one method that has been investigated in an attempt to overcome the limitations with the MoAb-drug approach. ADEPT or antibody-directed catalysis is a strategy that achieves the local activation of prodrugs by the use of enzyme immunoconjugates[59-61]. An enzyme-antibody conjugate (which is recognised by a specific extracellular antigen) is administered and allowed sufficient time to bind to the tumour cells and to be cleared from the circulation. Subsequently, a prodrug is then administered and, upon recognition of the enzyme on the enzyme-antibody conjugate, the prodrug is activated selectively at the tumour site and free drug is released extracellularly and allowed to pass into the tumour cells[59-62]. A schematic representation of ADEPT is shown in (Figure **9**).

However, certain problems can be raised with regards to ADEPT. The scarcity of tumour-selective antigens is still a limitation in the applicability of this type of therapy. Also, adverse immune effects may cause unwanted results[59]. Furthermore, the lack of effectiveness of ADEPT in humans so far is disappointing despite the high efficacy in rodent models[59,60].

1.2.2.2.3 GDEPT & VDEPT

Gene-directed enzyme prodrug therapy (GDEPT) and virally-directed enzyme prodrug therapy (VDEPT) are approaches that have been primarily designed to circumvent the limitations of ADEPT. Gene therapy may be broadly defined as a genetic technology aimed at modifying cells for therapeutic gain[63].

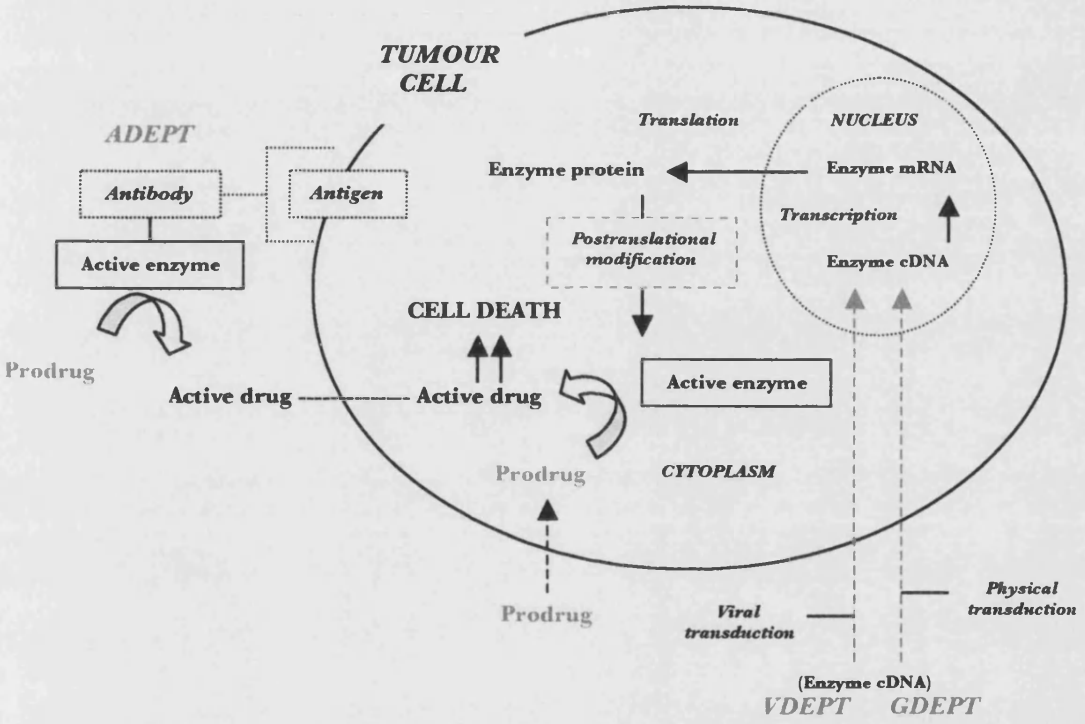

Figure 9. *A general schematic view for ADEPT, VDEPT and GDEPT strategies*

There are two main types of gene therapy, the first being that of toxin gene therapy, whereby genes are introduced directly in to malignant cells and the respective protein produced directs the killing of tumour cells[59,63]. The second is GDEPT or virally-directed enzyme prodrug therapy (VDEPT). This is where a DNA constuct containing an enzyme-encoding gene is delivered to tumour cells using nonviral (GDEPT) or viral (VDEPT) vectors[59]. The gene is then transcribed and the mRNA is translated to yield the functional enzyme. The enzyme that is subsequently expressed activates intracellularly a non-toxic prodrug into a toxic drug that causes cell death[63]. (see

Figure **9**). In GDEPT, nonviral vectors that contain gene-delivery agents, such as cationic lipids, peptides, or naked DNA, are used for gene targeting. In VDEPT, gene targeting is accomplished using viral vectors, with retroviruses and adenoviruses being the most often used viruses[59]. The process by which these vectors are taken up by the cells and expressed, is known as transduction and it is this process that has become the limiting factor in the effectiveness of both GDEPT and VDEPT[59].

An example of a recent self-immolative prodrug of interest for its use in suicide gene therapy (GDEPT) is shown below in Scheme **6**[49]. This prodrug has been designed to undergo a 1,6-elimination upon activation with the enzyme, carboxpeptidase G2 (CPG2), in the delivery of nitrogen mustards.

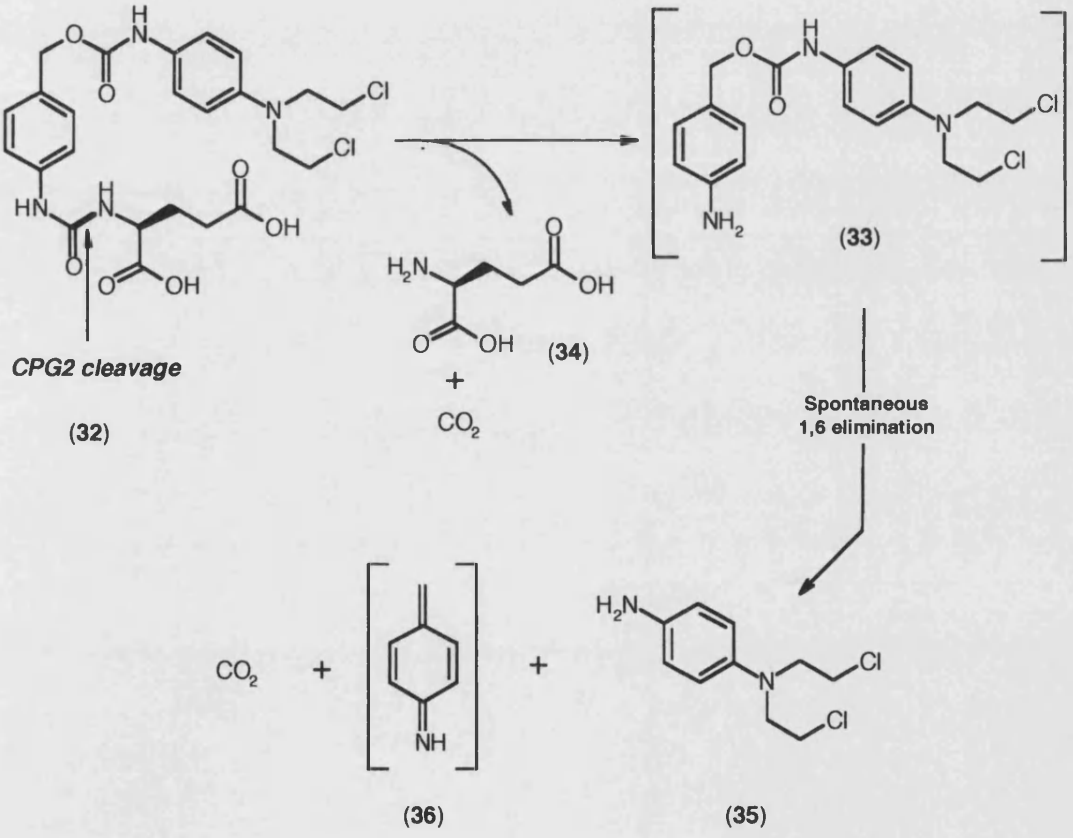

Scheme 6. *A novel nitrogen mustard tripartite prodrug used in GDEPT*

1.2.2.2.4 Polymeric prodrugs

In cancer therapy as a whole, macromolecular prodrugs are of increasing interest. The macromolecular prodrugs are thought to be selectively retained in solid tumours by the enhanced permeability and retention (EPR) effect[64-66] and are taken up into cells via pinocytosis, a process described in detail below. The most integral part to a polymeric prodrug that is responsible towards its retention in the site-specific area, is the macromolecular carrier (Figure **10**). This is the major determinant unit responsible for its pharmacokinetic property and all polymeric prodrugs contain a carrier unit (Table **6**, p38). The ideal carrier should be easily synthesised, accessible to chemical modification, water soluble, non-toxic, biodegradable and non-immunogenic[67]. However, at present, no carrier unit has been found to fulfil all these criteria[64].

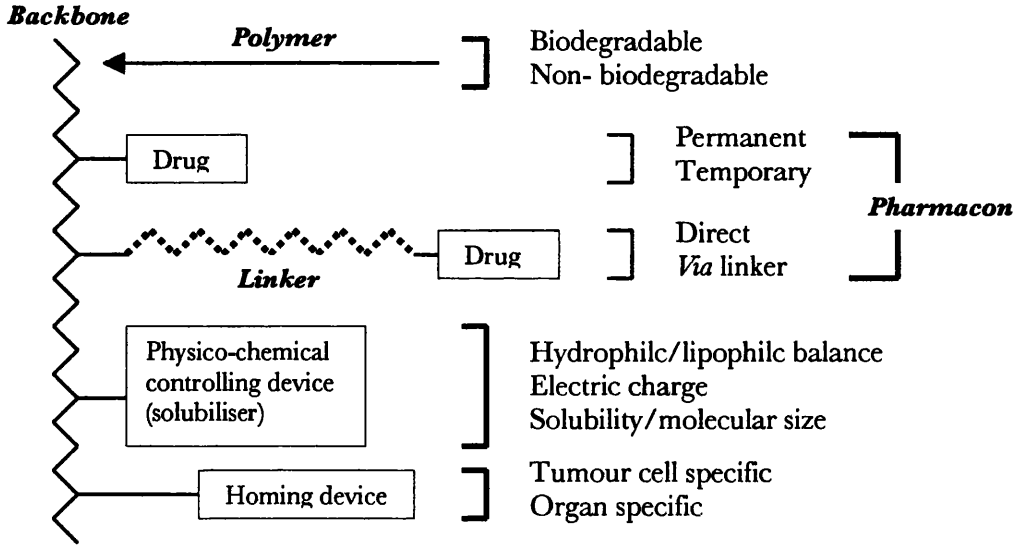

Figure 10. *Model for macromolecule-drug conjugates*

Above in Figure **10**, is a general outlined model for the design of macromolecule-drug conjugates[68]. Almost all polymeric prodrugs follow this concept in the aim to help solubility and aid retention efficacy in the required area. The model carrier consists of 3 major units of which can all be fine tuned for maximum effect. These units are represented as the, pharmacon unit, solubiliser unit and homing device. These are all

attached to the carrier (polymer unit) of which a number of naturally occurring and synthetic soluble macromolecular carriers are represented below in (Table **6**)[69].

Soluble macromolecular carriers						
Protein carriers	Antibodies	Albumin	Glycoproteins	Lipoprotein	Lectins	Hormones
Polysaccharides	Dextran	Pullulan	-			
DNA	-					
Synthetic polymers	Poly HPMA	Polyethylene glycol		Pyran copolymer	Polyamino acids	

Table 6. *The classification of soluble macromolecular carriers*

1.2.2.2.4.1 Enhanced Permeability and Retention Effect (EPR)

Within solid tumours, the vasculature is thought to be fundamentally different to that in normal tissue, as they lack any organised system of lymphatic drainage. It is this poor lymphatic drainage which allows lipophilic materials and macromolecules to accumulate selectively and be retained in the tumours[41,70]. Shown below in (Figure **11**) is a representation of extravasation and fluid drainage in normal tissue.

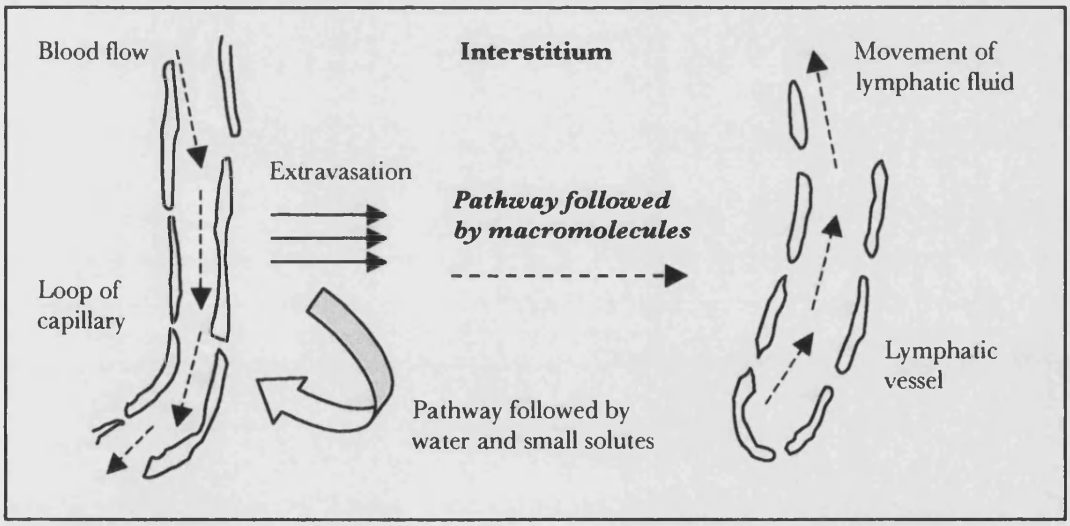

Figure 11. *A schematic representation of extravasation and fluid drainage in normal tissue*

As shown above, materials leave the bloodstream in the capillary bed by methods of diffusion, entering the interstitial space. Fluid and small solutes drain back into the bloodstream *via* postcapillary venules, while macromolecules drain into the lymphatic system, which is more freely permeable. However, in tumours, due to the absence of a lymphatic drainage system, macromolecules are denied an efficient drainage route[41], thus the EPR effect applies.

1.2.2.2.4.2 Pinocytosis

Pinocytosis is the ingestion of fluid into a cell and can also be known as fluid phase endocytosis. The initial event in pinocytosis is when the extracellular fluid is encapsulated and the cell membrane folds inwards to form a sheath that is then pinched off forming a vesicle (a pinosome) that is released into the cytoplasm. These vesicles then fuse with lysosomes (vesicles from the Golgi apparatus), forming secondary lysosomes and it is within these where degradation of macromolecules occurs, releasing small molecules into the cytoplasm[66,71].

Though macromolecule prodrugs generally follow this slow uptake process of pinocytosis, the idea of avoiding it and taking greater advantage of the EPR effect can be overcome by the interaction of an extracellular enzyme, namely Prostate Specific Antigen (PSA) (section **1.3.1.2**).

1.2.2.2.4.3 Clinically active polymeric prodrugs

As mentioned in (section **1.1.6.5.4.1**) doxorubicin (**13**) is one of the most effective cytotoxic agents used in cancer chemotherapy. With it being an amphipathic molecule, containing a hydrophobic anthraquinone moiety and a hydrophilic amino sugar moiety, it presents itself as being freely soluble in both organic and aqueous environments and thus can quite easily penetrate the cell membrane. However, it is known that chronic administration of high doses of doxorubicin can lead to severe systemic adverse effects, thus the idea of using macromolecular---doxorubicin conjugates could present a way of delivering doxorubicin more specifically and selectively to prostatic cancer cells[41].

Kopecek *et al.*[72] have reported that a water soluble polymer, PK1 (polyacrylate, namely poly(HPMA) [HPMA= (±)-N-(2-hydroxypropyl)methacrylamide]) bearing doxorubicin, is showing activity in clinical trials. It is proposed the cytotoxic drug is released intracellularly by the cleavage of the tetrapeptide linkage (GlyPheLeuGly) between the polyacrylate polymer backbone and drug by lysosomal enzymes[64,73,74], such as cathepsin B. However, this is limited by two important factors:

• The sole basis of tumour-selectivity of delivery is concentration of the prodrug by the EPR effect. Also, the (GlyPheLeuGly) sequence poses a problem because normal cells are also capable of cleaving this tetrapeptide sequence.

• The actual enzyme that is responsible in cleaving the (GlyPheLeuGly) sequence is a lysosomal enzyme, thus the whole mechanism is essentially intracellular.

This poses a problem for conventional macromolecular prodrugs, as they enter the cells *via* pinocytosis, which is a relatively slow process, thus, the release of the active drug becomes limited. An attractive way of overcoming the problem would be to find a polymeric prodrug system (see Figure **10**, p37)[68] from which the active drug could be released by the action of an endogenous enzyme that is catalytically active solely in the tumour and is located either on the outer surface of the cells or in the extracellular space. The tumour-selectivity of the drug delivery would then be binary involving:

• The EPR effect.
• Tumour-localisation of the enzyme.

Furthermore, the rate of site-selective drug release would be much greater. As mentioned previously, prostate specific antigen (PSA) satisfies these criteria for an endogenous activating enzyme (see section **1.3.1.2**).

Other examples of clinically active polymeric prodrugs that have been developed are those that incorporate the drug, 5-fluorouracil (**7**)[75-78], but in most cases, the

antitumour activity has resulted from non-specific chemical hydrolysis between the active drug and the polymer backbone[79]. Another example of a polymeric prodrug model that has showed activity in clinical trials is shown below in (Figure **12**).

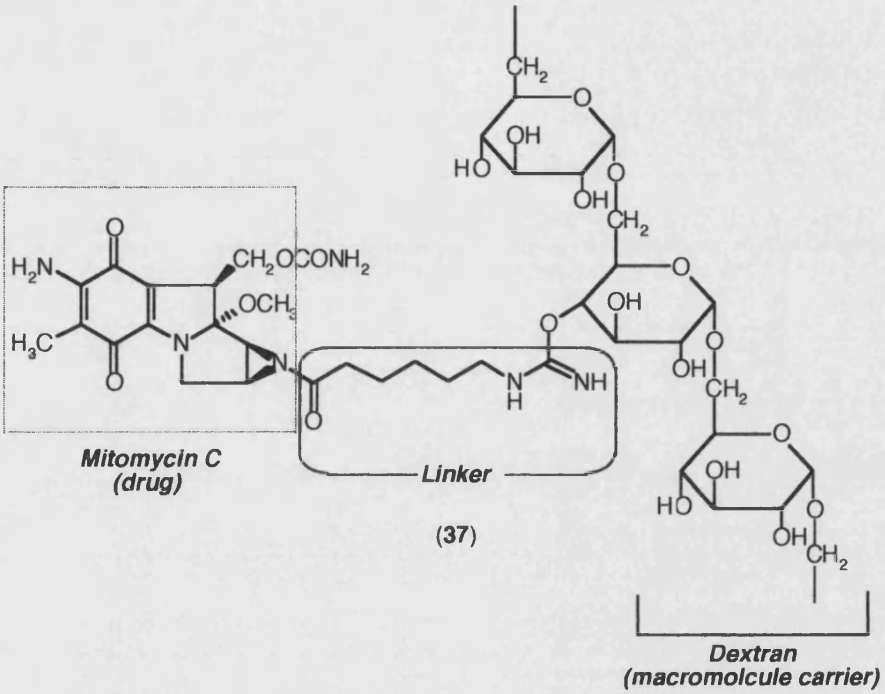

Figure 12. *A general structure of mitomycin C (MMC)-dextran conjugates*

In this polymeric prodrug, mitomycin C (drug) is attached to the dextran (macromolecule carrier) *via* the aziridine nitrogen linkage. In this case, the linker group is derived from 6-aminohexanoic acid (the length of the chain is believed to directly effect the rate of conjugate cleavage in this case). Studies on the mitomycin C-dextran conjugate (**37**)[41] of MW 70,000 Da, has shown in certain murine models (*in vivo*) to have high anti-tumour activity when compared to free mitomycin C. Furthermore, the activity of this prodrug is thought to be mediated by extracellular hydrolytic release of the drug[80].

1.3 Tumour biomarkers for prostate cancer

In recent years, considerable effort has been made to identify enzyme or antigen markers for various types of cancers with the view towards developing specific diagnostic reagents[81]. The ideal tumour marker would exhibit, amoung other characteristics, organ site or cell-type specificity and would be released into circulation or other biological milieu which is easily obtained by individuals[81]. Serum acid phosphatase enzyme (refer to section **1.1.6.3**) has been considered to be the standard diagnostic biomarker for adenocarcinoma of the prostate during the past years and has been used for the screening and staging of the disease as well as towards the monitoring of patients in response to therapy[82]. Unfortunately, as a biomarker serum acid phosphatase constitutes one major difficulty in its usage, that being its inability to report serum concentration of the *iso*enzyme produced by prostatic tissue without interference from other *iso*enzymes generated by other organs within the body[83]. This as led to the use of prostate-specific proteins as biomarkers for prostatic disease.

1.3.1 Prostate-specific proteins

Amid several prostate-specific proteins, the expression of prostate-specific membrane antigen (PSMA) and prostate-specific antigen (PSA) are sensitive biomarker proteins for prostate cancer screening, diagnosis and progression[84]. Both are well characterised and remain highly active in the hormone refractory stage of the disease.

1.3.1.1 Prostate-specific membrane antigen (PSMA)

Prostate-specific membrane antigen was discovered as a membrane antigen reactive to a monoclonal antibody (mAb), namely 7E11-C5[84]. PSMA is a putative class II transmembranous[†(p43)] glycoprotein of molecular weight (94 KDa) and is exclusively expressed in metastatic prostatic carcinoma[85]. PSMA in known to progressively cleave terminal γ-linked glutamate residues from poly-γ-glutamated folates by its carboxypeptidase activity, it is this process that is essential for γ-glutamate transport into cells[86]. Based on this, an approach to target prostate cells that over express PSMA has led to the design of a prodrug bearing the active pore-forming synthetic peptide H3 toxin (Helix-3). H3 is a 25-amino acid peptide that is capable of penetrating into

lipid bilayers by adopting a membrane pore-forming mode of action, which in turn can lead to a significant leakage of essential intracellular macromolecules or furthermore, can cause an electrolyte imbalance, resulting in cell death[87]. Unfortunately the H3-prodrug has only shown activity *in vitro*[88] and, furthermore, PMSA is also expressed in normal brain and salivary gland tissue[88] (thus PSMA is not completely prostate-specific). As a result, it is unclear whether or not it could be used for targeting therapy *in vivo*[89].

1.3.1.2 Prostate-specific antigen (PSA)

Human prostate-specific antigen (PSA)[90-95] is a glycoprotein that contains 93% amino acids and 7% carbohydrates. It is a monomer[96] with 240 amino acid residues, four carbohydrate side chains and a M_r of 33-34 kDa[91,92]. Subsequent studies have shown that one carbohydrate side chain exists at the N-side chain of amino acid 45 (asparagine) while the other remaining three exist at the O-side chain of amino acids 69 (serine), 70 (threonine) and 71 (serine) respectively. The N-terminal amino acid of the sequence is (*iso*leucine) and the C-terminal residue is (proline)[96]. PSA is synthesised in malignant prostatic epithelial cells and secreted in large amounts (0.5-2.0 gL^{-1}). It is also found at much lower levels in normal epithelial cells lining the acini and the ducts of the prostate gland[96,97]. PSA is a (chymo)trypsin-family serine protease and functions to cleave the high molecular weight proteins (semenogelins I and II) responsible for the seminal coagulum into smaller polypeptides leading to liquefaction of the coagulum. It can also be detected in the systemic serum of men with prostatic cancer, thus making it a diagnostic serological marker for the disease[98]. However, in systemic circulation, its catalytic activity is completely inhibited by complexation with inhibitory proteins, namely, α_1-antichymotrypsin and α_2-macroglobulin[99,100].

---

†(p42) The functionality of class II membrane proteins are to serve as transport or binding proteins, or possess hydrolytic activity[86]. Contrary to this, it is known that a portion of PSMA exhibits modest homology with regards to the transferrin-receptor, however, common amino acids responsible for the internalisation sequence of the receptor are absent. This suggests that PSMA does not actually operate as a transport, but rather as a binding protein or protease[85].

Thus, it is proteolytically active exclusively in the prostate[96], ***the target tissue for anti-prostate cancer therapy***, and is an ideal catalytically active enzyme for the release of drugs from polymeric prodrugs.

1.3.1.2.1 Substrate-specificity of PSA.

Based on the PSA cleavage maps for semenogelins I and II, small peptides have been synthesised containing amino acid sequences proximal to the PSA proteolytic sites[101]. Coombs *et al.*[102] are amongst those who have studied the substrate specificity of PSA in great detail. Shown in (Figure **13**) is the peptide sequence that is cleaved most efficiently by PSA.

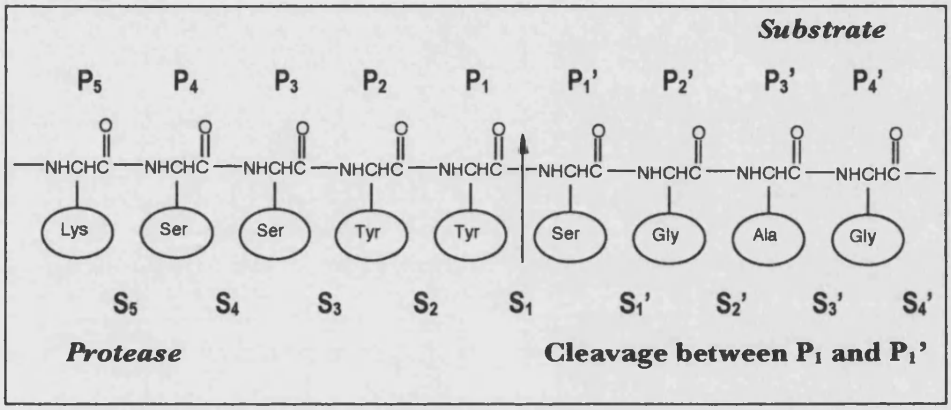

Figure 13. *Peptide sequence most efficiently cleaved by PSA.*

The consensus from this study is that the SS pair be situated at sites P_3 and P_4 respectively, and the (F/Y)Y pair at sites P_1 and P_2 respectively with Y next to the cleavage site. However, the literature suggests that these sequences have also been cleaved efficiently by chymotrypsin[102].

Based on the peptide sequence shown in (Figure **13**), Denmeade *et al.*[103] have optimised this substrate sequence for better PSA selectivity, such that it is unaffected by catalytically active enzymes in normal cells, (such as chymotrypsin). It has been shown that the substrate sequence of (HisSerSerLysLeuGln↓), where ↓ is the cleavage point of the PSA, was identified to be the most selective for PSA cleavage and proved

to be unaffected by chymotrysin, trypsin, elastase and six other proteases (see Table **7**). Denmeade *et al.*[103] also showed that, in a head-to-head study, this sequence was only cleaved some 10-20 fold less efficiently than similar sequences with Y at P_1. It has also been identified that the length of the amino acid sequence required for PSA-activation has to be at least a tetrapeptide, thus analogous to the sequence (HisSerSerLysLeuGln↓), the tetrapeptide sequence (SerLysLeuGln↓) also gave a high degree of selectivity for cleavage by PSA.

		pmol of substrate hydrolysed/min/100 pmol of indicated protease						
Substrate group	**Peptide sequence**	**PSA**	**Chymo-trypsin**	**Elastase**	**Trypsin**	**Plasmin**	**Hk1**	**Hk2**
1	**KGISSQY**	**510**	**4290**	**3068**	**658**	**ND**	**ND**	**UD**
	SRKSQQY	234	3630	2788	260	0.4	2.0	UD
	GQKGQHY	49.6	4274	922	122	UD	ND	UD
2	EHSSKLQ	31.6	UD	UD	UD	UD	UD	UD
	QNKISYQ	16.8	9.0	9.0	UD	UD	ND	UD
	ENKISYQ	14.4	3.6	2.6	1.8	0.6	UD	ND
	ATKSKQH	16	38.8	UD	UD	UD	UD	ND
	HSSKLQ	**62.7**	**UD**	**UD**	**UD**	**UD**	**UD**	**UD**
	SKLQ	**29.6**	**UD**	**UD**	**UD**	**UD**	**UD**	**ND**
	KLQ	UD	10.6	0.4	UD	ND	UD	ND
	LQ	UD	UD	UD	UD	UD	ND	ND
	Q	UD	UD	0.7	UD	UD	ND	ND
3	KGLSSQC	13.6	12.2	950	UD	UD	UD	ND
	LGGSQQL	6.0	314	94	UD	UD	ND	ND
4	QNKGHYQ	1.8	0.2	0.6	UD	UD	UD	ND
	TEERQLH	1.2	48.8	1.0	UD	3.8	UD	UD
	GSFSIQH	UD	3.6	0.4	0.4	0.2	ND	ND

Table 7. *A comparison of peptide substrates relative to their corresponding PSA activity respectively. (UD – undetectable <0.1 pmol of substrate hydrolysis/min/100 pmol of protease; ND – not done; Hk1 – human plasma kallikrein; Hk2 – human glandular kallikrein; all substrates are at a concentration of 0.2 mM in PSA assay buffer*[103]

1.3.1.2.2 PSA-activated prodrugs

In a small-molecule study, Denmeade and co-workers[103] developed a bipartite prodrug system that contained the PSA-sensitive peptide sequence, HSSKLQ and the aromatic amine drug, 7-amino-4-methyl-coumarin (AMC). The coumarin was attached to the peptide linker *via* an amide bond to the C-terminal carboxyl group on the glutamine. Interestingly, PSA had shown to cleave the Gln---AMC bond from this construct HisSerSerLysLeuGln---**AMC**, releasing free coumarin from the peptide linker. Notably, this construct was not hydrolysed by a series of other proteases (*e.g.* chymotrypsin) and was selective to PSA[104].

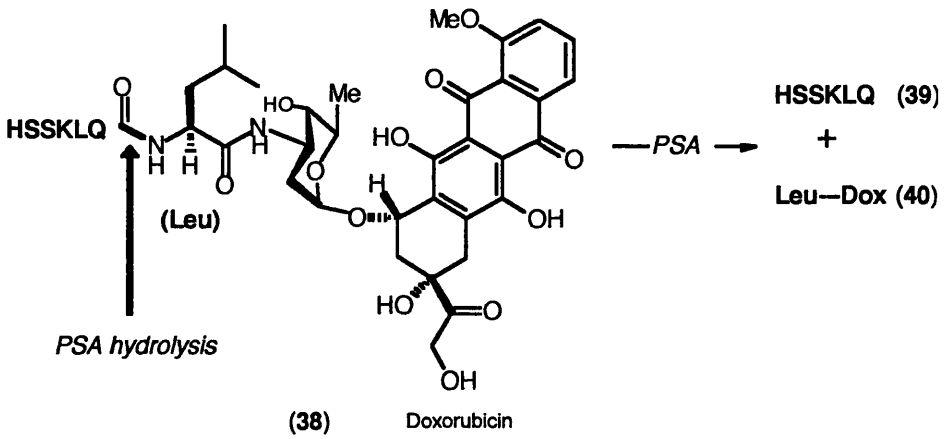

Scheme 7. *PSA-triggered release of doxorubicin from the prodrug HSSKLQL-dox.*

With the success of the HisSerSerLysLeuGln---**AMC** construct towards PSA activity, further studies by Denmeade and coworkers[103] showed a similar strategy but by incorporating an aliphatic amine drug (namely, doxorubicin) to the PSA-sensitive peptide linker. However, the consensus from these studies, showed that no cleavage by PSA had occured. What some studies had indicated though, was to achieve PSA cleavage, the construct HisSerSerLysLeuGln**Leu---doxorubicin** was needed. Moreover, it was noticed that PSA-cleavage did occur, but rather than the free cytotoxin (doxorubicin) being expelled, **Leu---doxorubicin** (**40**) was released (Scheme **7**). In conclusion to these studies, PSA is only capable of hydrolysing an amide bond directly adjacent to an aromatic ring moiety or aminoacyl group[98,104].

The specificity regarding the cytotoxic response of this prodrug had been recognised when 70 nM of the prodrug killed 50% of PSA-producing LNCaP cells, whereas no (*in vitro*) cytotoxic effect on PSA-non-producing TSU human prostate cancer cells was seen. Furthermore, based on these results, *in vivo* studies on the HSSKLQ**L-doxorubicin** prodrug (**38**) is currently in effect in LNCaP and PC-82 tumour-bearing mice[105,106].

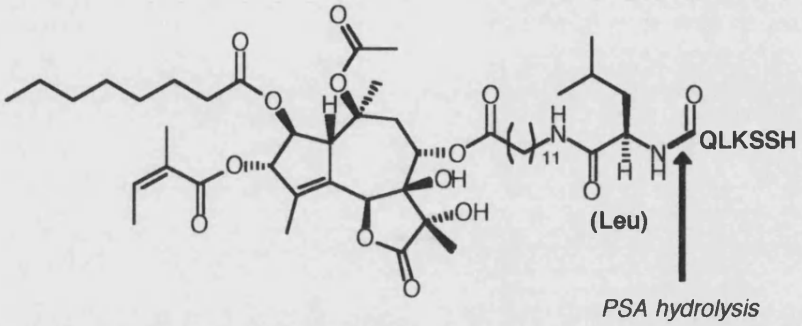

(41)

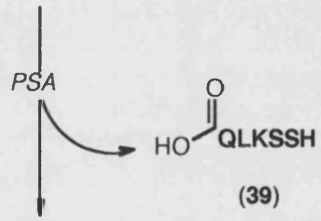

(39)

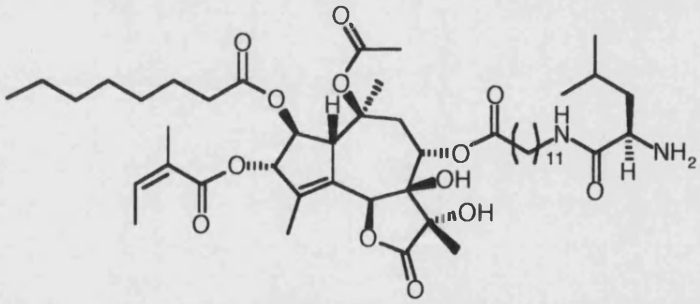

8-*O*-(12-[L-leucinoylamino]dodecanoyl)-
8-*O*-debutanoylthapsigargin (Leu-12ADT) **(42)**

Scheme 8. *PSA-triggered release of Leu12ADT from the prodrug HSSKLQ-Leu12ADT.*

With the success of the HSSKLQ**L-doxorubicin** prodrug (**38**) showing selective proteolytic activity towards PSA, other cytotoxic agents bearing this PSA-sensitive

linker (HSSKLQL) are currently in development (Scheme **8**). For example: Thapsigargin is a potent inhibitor of the Ca^{2+} dependent ATPase pump[107]. With this inhibition, the Ca^{2+} concentration rises and causes cell death[108]. Given the mechanism of action of thapsigargin, it is however, unlikely to be prostate specific (or cell-type specific for that matter) and cannot be administered systemically as a therapeutic agent without causing host toxicity. The aim of targeting thapsigargin selectively to prostatic cancer cells avoiding toxicity to normal cells, has led to the development of HisSerSerLysLeuGln**Leu-thapsigargin** (Scheme **8**). This prodrug (*in vitro*) was efficiently hydrolysed by PSA and selectively toxic to PSA-producing cancer cells[109]. Furthermore, it has been shown to cause complete growth inhibition (*in vivo*) of established PSA-producing prostate cancer xenograft tumours and, has been shown to have no effect on renal xenograft tumours (that do not produce PSA). Therefore, the use of PSA-activated thapsigargin prodrugs in prostate cancer is warranted[105].

Chapter 2

Aims & Objectives

2.1 Aim & objectives of the research

The overall aim of this research is to develop a novel polymeric prodrug that will release free doxorubicin selectively and specifically in prostate tumours *via* an innovative system.

The main objectives of the research are: **1.** to develop, compare and evaluate two self-immolative molecular clips, which after release from the polymer by action of a protease, will expel free doxorubicin. **2.** to synthesise and evaluate an advanced monomeric model comprising a peptide (which is cleavable by prostate specific antigen (PSA)) joined to doxorubicin by the molecular clip.

2.2 Research plan

2.2.1 Design of a PSA-activated polymeric prodrug system

The general features of the design for the PSA-activated polymeric prodrug system are shown in (Figure **14**).

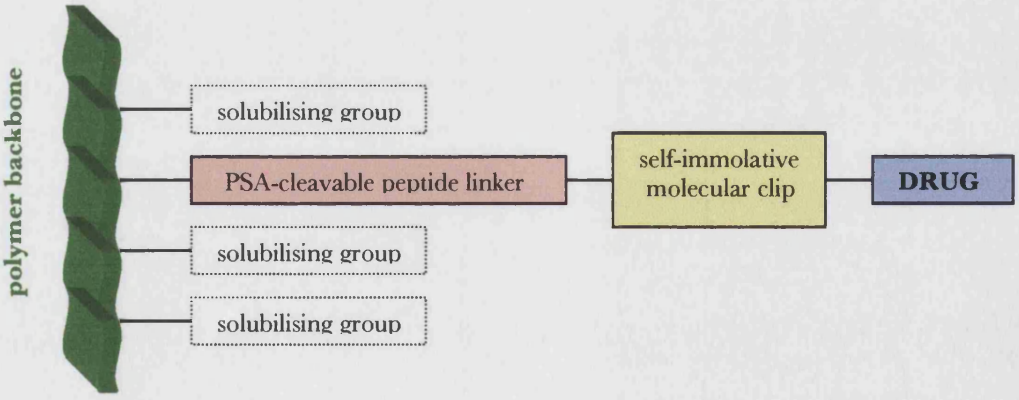

Figure 14. *Proposed structure of a polymeric prodrug for prostate-specific drug release*

The first fundamental part of the polymeric prodrug will consist of a polymer backbone which will be a polyacrylate, similar to poly(HPMA) to that of PK1 [HPMA = (±)-N-(2-hydroxypropyl)methacrylamide][72,74]. One other reason for basing the design of the prodrug on the polyacrylate backbone similar to that of PK1, is that PK1 and the homopolymer (poly(HPMA)) have both been demonstrated to be non-immunogenic[72]. Also, as in PK1, many solubilising groups are going to occupy many of the sites on the polyacrylate backbone to aid aqueous solubility.

The next key figure in the polymeric prodrug model is that of the PSA-cleavable peptide linker. Based on further work carried out by Denmeade *et al.*[103] on small-molecule prodrug studies, drugs containing amines will be conjugated to selected sites on the PSA-cleavable peptide linker. In the prodrug studies of Denmeade and co-workers[103], 7-amino-4-methyl-coumarin (AMC) was shown to have been released from the peptide linker of amino acid sequence, (HisSerSerLysLeuGln---**AMC**). However, in studies using the same peptide sequence, but with doxorubicin instead of (AMC), no sign of cleavage by PSA was shown. What some studies had shown though, was to achieve PSA cleavage, the construct of (HisSer SerLysLeuGln**Leu---doxorubicin**) was needed. It was noticed that PSA cleavage did occur, but rather than the free drug (doxorubicin) being expelled, **(Leu---doxorubicin)** was released (refer to Chapter 1, sections **1.3.1.2.1** & **1.3.1.2.2**).

These data strongly suggest and encourage the need for the innovative design and development of a ***"self-immolative molecular clip,"*** which has peptide-like character to replace that of the Leucine (Leu). The molecular clip(s) as shown in (Figures **15** and **16**) respectively, will lie between the peptide linker and the drug. It will be designed, so when the (**clip---drug**) moiety is released from the polymer by PSA-catalysed cleavage, the clip will undergo a 1,6-elimination process in becoming detached from the drug spontaneously, releasing free drug and no interfering pendant amino acid(s) or short peptide fragments. The drug for this study is, 'doxorubicin,' but this innovative design could be applied to other drugs that contain amines (*e.g.* doxazosin, a very recent drug of interest in prostate cancer[31]).

2.2.2 Design and evaluation of the self-immolative molecular clip 1

Both clips must contain a secondary amide linkage between the peptide linker and the molecular clip. The peptide-like structure of the molecular clip will strongly encourage the binding to the PSA active site, allowing PSA to cleave as shown in (Figures **15** and **16**), releasing the clip-drug moiety, followed by the rapid release of free drug, see (Scheme **9**, p53). The same system and idea also applies to the novel design of molecular clip 2 shown in (Figure **16**).

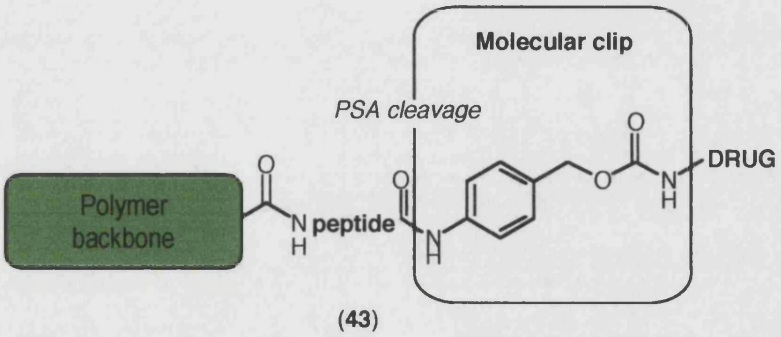

Figure 15. *Design of the tripartite prodrug, utilising molecular clip 1 and peptide sequences, HSSKLQ, SSKLQ and SKLQ respectively*

2.2.3 Design and evaluation of the self-immolative molecular clip 2

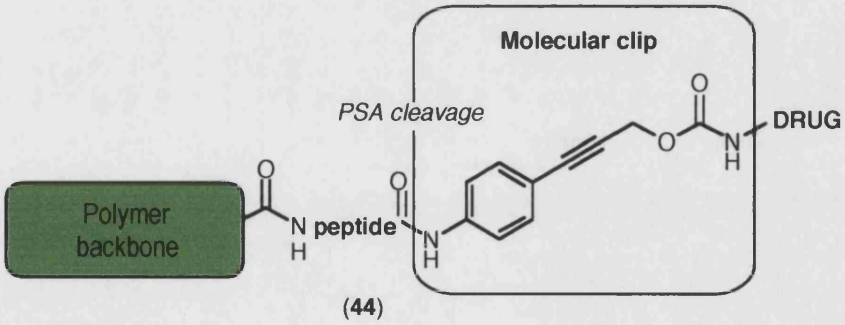

Figure 16. *A tripartite prodrug utilising molecular clip 2 and peptide sequences, HSSKLQ, SSKLQ and SKLQ respectively*

With doxorubicin being extremely expensive and toxic to work with, it is very important to establish a model for the initial stages in the synthesis and evaluation of our primary targets. 2-(4-Nitrophenyl)ethylamine (NPEA) presents itself as an excellent alternative, as it will allow us to mimic the primary aliphatic amine nature to that of doxorubicin. Not only is it significantly less toxic and less expensive than doxorubicin, it easy to work with, and it also has a signature UV chromophore, serving as a spectroscopic window for its detection during synthesis, and more importantly, its release detection in future HPLC studies.

2.2.4 Synthesis and evaluation of a monomeric model for PSA-triggered release of doxorubicin

Construct **45** (Scheme **9**) is designed as the complete monomeric model for studies of PSA-triggered release of doxorubicin from a polymeric prodrug. The first part toward this advanced prodrug model is the polymeric backbone. This will be represented by a fluorescent marker, namely dansyl, which is linked *via* a spacer group, to the N-terminus of the PSA sensitive peptide sequence. As with the NPEA (drug), its fluorophore will act as a tag and thus will be easily detected from the peptide cleavage products after the clip-drug moiety is released from the linker. (*e.g.* dansyl-HN$(CH_2)_5$CO-HSSKLQ will be detectable *via* the dansyl, and the NPEA + peptide-NPEA will be detectable through the NPEA).

Constructs containing three peptide sequences (the linker group), HSSKLQ, SSKLQ and SKLQ, will be targeted. HSSKLQ was used by Denmeade *et al.*[103] in their monomeric prodrug model, but an earlier study[104] of PSA substrate specificity showed that the histidine (His) is probably unnecessary. It may be that the synthetic difficulties occasioned by the presence of the His in the sequence, outweigh its usefulness in promoting selectivity. Therefore, based on the aforementioned, peptides SSKLQ-*CLIP*-NPEA and SKLQ-*CLIP*-NPEA will be prepared. Since these only differ in their N-termini, the synthesis will be made more efficient by the synthesis of the late common intermediate, **protected**KLQ-*CLIP*-DRUG. A careful approach will be adopted in synthesising the peptide linkers, as side chain protections will have to be

orthogonal to the respected N-termini of the exposed amino acid (this will be discussed further in Chapter 3). In the future, each of the advanced models will be evaluated for cleavage with PSA[90]. This could be achieved by incubating the advanced models with PSA and performing HPLC analysis to show the release of drug from the peptide linker and from clip-drug moiety respectively.

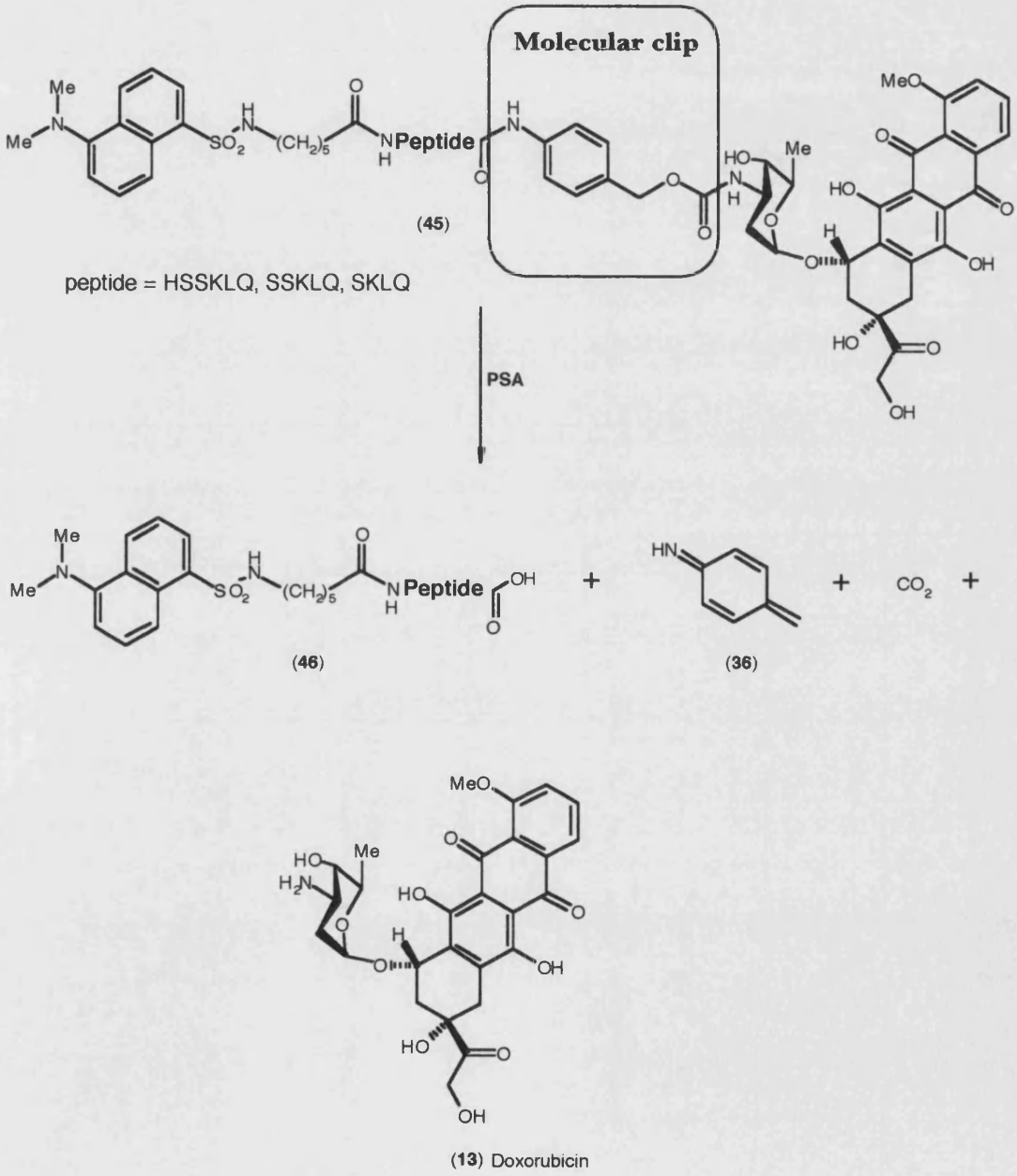

Scheme 9. *PSA-triggered release of doxorubicin from the monomeric model*

Chapter 3

Results & Discussion

3.1 Synthesis of the PSA-cleavable peptide linker

3.1.1 Negative control sequence

The key intermediate for the synthesis of the initial clip-free target is SerSerLys-LeuGlnNHCH$_2$CH$_2$Ph-*p*-NO$_2$ (**47**). This is also a critical intermediate for the synthesis of the negative control compound, SerSer**LeuLys**GlnNHCH$_2$CH$_2$Ph-*p*-NO$_2$ (**48**). In this latter compound the **Leu** and the **Lys** amino acids are transposed in the sequence, so that it should not be ***recognised*** by PSA, thus the aim of comparing these two constructs was to investigate whether the former would be cleaved by PSA and the latter would not. (NB: the NHCH$_2$CH$_2$Ph-*p*-NO$_2$ moiety can sometimes be expressed as NPEA and is often used throughout the text).

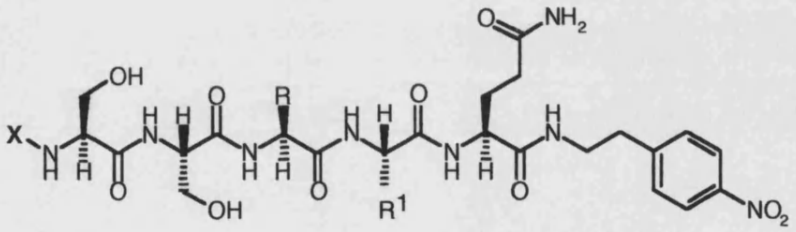

X = Fluorophore

Target intermediate (**47**): R = Lys, R^1 = Leu
(**48**): R = Leu, R^1 = Lys

Figure 17. *The structures of target intermediates (**47**) and (**48**)*

In the preparation of larger peptide sequences, there are two synthetic approaches that can be used. A convergent synthesis were units of a few amino acids are condensed in a final step, or a linear stepwise synthesis where each amino acid is added in turn to the growing peptide. Though convergent syntheses of peptides are generally more attractive, with yields being much higher than that of a linear approach, the risk of

racemisation in the final condensation step could present a major problem (Scheme **10**)[110]. A convergent synthetic approach is inappropriate in these syntheses.

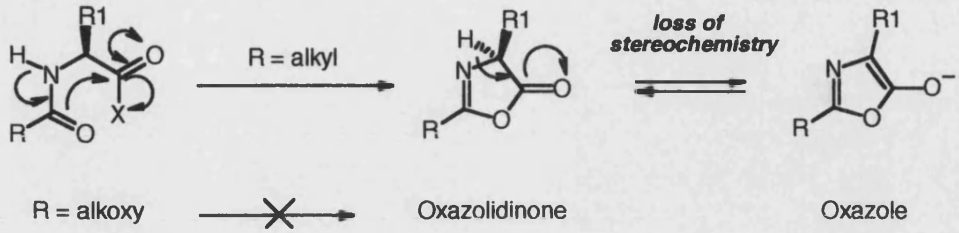

Scheme 10. *Peptide racemisation via the formation of oxazolidinones*

In developing these sequences (**47**) and (**48**), it was important to use an orthogonal protecting group strategy such that the main chain amines (alpha amines) in the growing main chain of the peptide are masked by protecting groups which can be removed efficiently while retaining the protection of amino acid side-chain functional groups, such as the ε-amine side chain of Lys. Fully orthogonal protecting groups can be defined in that protecting group A can be removed under one set of conditions leaving protecting group B untouched. And another set of conditions will remove protecting group B selectively while group A remains unscathed. When A and B are semi-orthogonal protecting groups, group A can be removed in the presence of group B, but removal of B may adversely affect group A.

In the two target sequences (**47**) and (**48**) respectively, the requirements for the protecting groups were such that the integrity of the nitro-aryl group (NPEA) of the model drug, also needs to be maintained. Thus for example, hydrogenolytic removal of Cbz would be inappropriate as nitro groups are reduced rapidly under these conditions. The Cbz (benzyloxycarbonyl) and Boc (*tert*-butoxycarbonyl) moieties are two commonly used protecting groups for primary amines, and are fully orthogonal. Thus these were the two protecting groups for these syntheses.

The Cbz group, first reported by Bergman and Zervas[111] in 1932, can be easily introduced to amino acids and other amino compounds using benzyl chloroformate

under Schotten-Baumann conditions. The Cbz protecting group is stable to mild acidic and basic conditions and can be removed on treatment with catalytic hydrogenolysis or with hydrogen bromide (HBr) in glacial acetic acid. In contrast to the Cbz group, the Boc group (*tert*-butoxycarbonyl) is unaffected by catalytic treatment with hydrogen and can be easily removed in the presence of acid, commonly HCl and trifluoroacetic acid (TFA). The Boc group can be introduced with di-*tert*-butyl dicarbonate (Boc_2O)[112] in generally fast and high yielding reactions, the byproducts being carbon dioxide and 2-methylpropene. Alternatively, 2-(*tert*-butoxycarbonyl-oxyimino)-2-phenylacetonitrile (BOC-ON)[113] can also be used, though it has been shown to be less reactive than Boc_2O.

Glutamine (**49**) was converted to the N^{α}-Cbz derivative, CbzGlnOH (**50**) by treatment with benzyl chloroformate (under Schotten-Baumann conditions) in moderate yield (45%) (Scheme **12**, p58). The side chain primary amide is not nucleophilic under these conditions. At this point the carboxylic acid needed to be activated as an electrophile, through conversion of the OH to a good leaving group.

The use of acid chlorides to achieve couplings of amino acids to peptides or other amino acids, is an attractive technique[110] as reactions *via* this method proceed very rapidly. However, the conditions required to synthesise acid chlorides are harsh and it is well known that these are prone to racemisation. For example, as shown in Scheme **11** (p57), an amino acid in the presence of a tertiary base can result in the formation of a ketene by removal of the α-proton. It is believed that going from an sp^3 chiral centre to an sp^2 centre under these conditions is more favourable. Furthermore, a nucleophile (*e.g.* another amino acid) is able to attack the highly electrophilic carbonyl of the ketene from above or below the plane, thus in turn, can give rise to a mixture of epimers upon reformation of chirality.

Although acid fluorides can be used in peptide synthesis[114], their synthesis can be difficult and yields are often modest, thus both the aforementioned and acid chlorides are inappropriate in these syntheses.

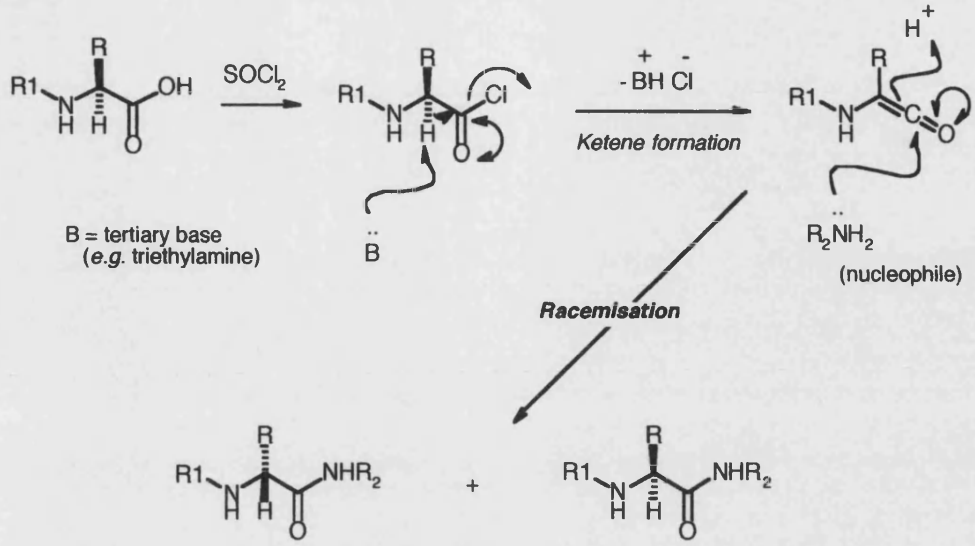

Scheme 11. *Racemisation of peptides via the use of acid chlorides*

More common is to convert the carboxylic acid into an active ester. These active esters are derived from alcohols with low pKa values (*i.e.* the conjugate base, the alkoxide or aryloxide anions) and are stabilised either by a neighbouring electron withdrawing group or by delocalisation.

Two active esters of CbzGln were prepared for their comparison in their coupling with 4-nitrophenylethylamine (NPEA) (**67**). Firstly the hydroxysuccinimide active ester (ONSu) was prepared by treatment of CbzGlnOH (**50**) with N-hydroxysuccinimide and dicyclohexylcarbodiimide (DCC) in ethyl acetate (EtOAc) under the usual conditions. DCC is a dehydrating agent, initially the proton is transferred from the carboxylic acid to the carbodiimide; this generates the nucleophilic carboxylate anion, which attacks the electrophilic carbodiimide carbon to generate an O-acyl *iso*-urea. This intermediate has electrophilic activity comparable with that of an acid anhydride, which it closely resembles in structure. The hydroxysuccinimide, which is relatively nucleophilic, then attacks the carbonyl of the intermediate expelling the *iso*-urea. The latter rapidly tautomerises to N,N'-dicyclohexylurea (DCU); thus the driving force for the formation of the active ONSu ester, is the formation of the low energy urea. This active ester was then treated with the 4-nitrophenylethylamine (NPEA) in the presence

of triethylamine as a tertiary amine base which captures the acidic N,N'-hydroxysuccinimide formed. This coupling gave the required CbzGlnNHCH$_2$CH$_2$Ph-*p*-NO$_2$ (**53**) in moderate yield (44%) (Scheme **12**). In an attempt to improve the yield an alternative active ester was investigated.

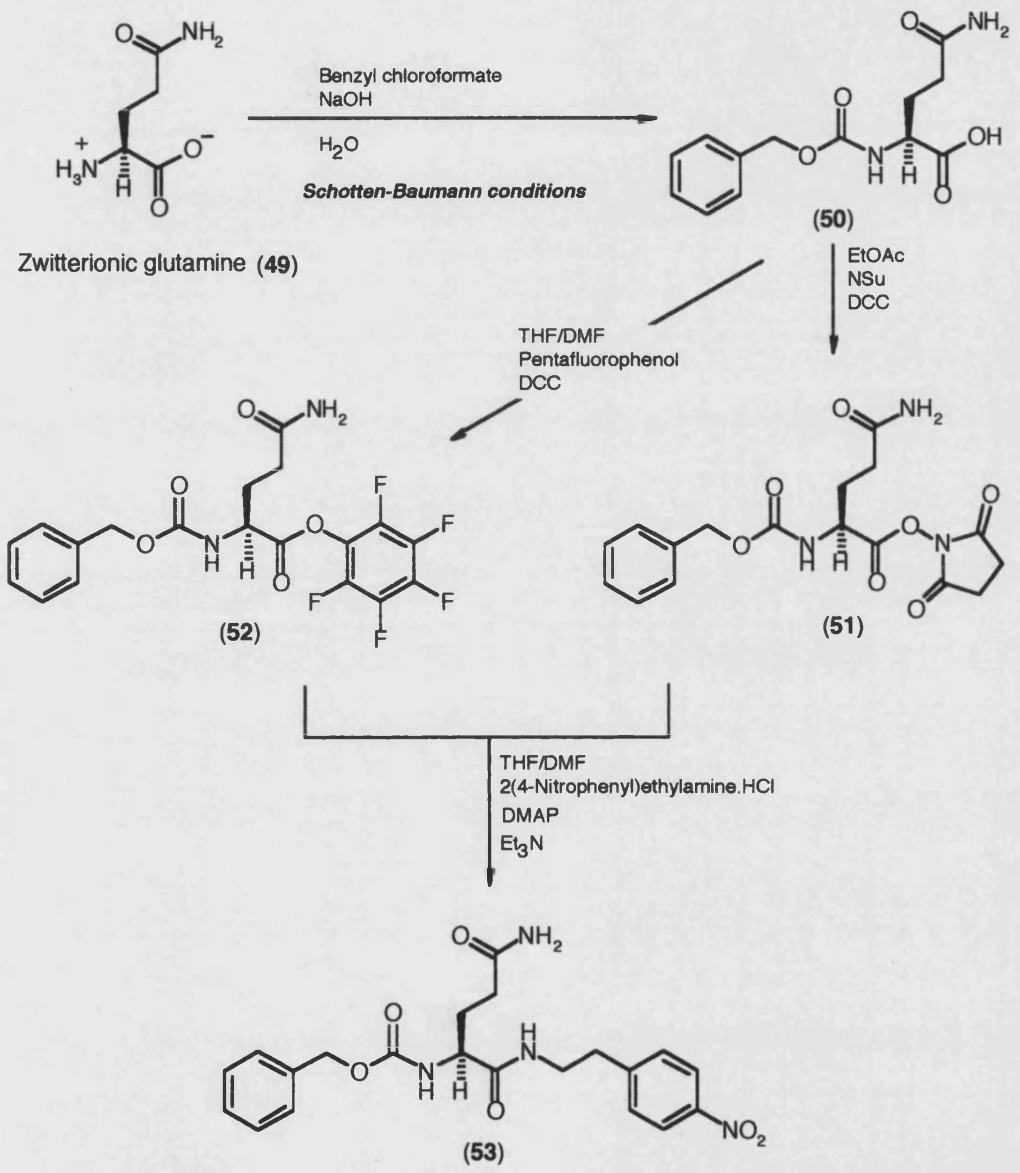

Scheme 12. *A schematic representation to the formation of compound CbzGlnNPEA (**53**) via various active ester-coupling methods*

Esters of phenols carrying electron-withdrawing substituents are often used as active esters in peptide-coupling, for example, the *para*-nitrophenyl esters were used frequently in the earlier days of solution phase peptide synthesis[110], as were 2,4,5-trichlorophenyl esters[110].

However, fluorinated phenols are now used widely in this context. Pentafluorophenyl esters (PFP-esters) are amongst the most reactive of the active esters[115], although 2,3,5,6-tetrafluorophenyl esters (TFP-esters) have found favour more recently. Although PFP-esters are considerably cheaper than TFP-esters, it has been claimed that the TFP-esters are more useful as the phenol moiety carries a proton. This proton can be observed in standard ^{1}H NMR spectroscopy to confirm the formation and structure of the active ester. Since ^{19}F NMR spectroscopy is readily available at the University of Bath, it was decided to use PFP-esters for couplings and monitor their formation by this means.

Given the limited solubility of CbzGlnOH (**50**) in EtOAc the alternative solvent mixture THF and DMF (9/1) was used for the coupling with pentafluorophenol in the presence of DCC.

The CbzGlnOPFP active ester reacted smoothly with NPEA in a 50/50 THF/DMF mixture to give the 4-nitrophenylethylamide (**53**) in a satisfactory 44% yield. This was the optimum solvent system for this coupling, a range of other single solvents and mixtures have been investigated. The need for a relatively polar solvent mixture reflects the polarity and insolubility of constructs containing glutamine (Gln) and a portent of solubility difficulties to come. This amide (**53**) was the first novel compound synthesised in this project and was fully characterised by ^{1}H NMR spectroscopy, ^{13}C spectroscopy, IR-spectroscopy, micro-analysis, mass spectrometry and polarimetry.

In the ^{1}H NMR spectrum the diastereotopic β-protons resonated as discrete multiplets centred at δ 1.66 ppm and δ 1.78 ppm. The γ-protons although also diastereotopic, are more remote from the chiral centre and resonate as overlapping multiplets around

δ 2.00 ppm. The chirality of the molecule is also reflected in the signals for the other CH_2CH_2 system adjacent to the 4-nitrophenyl group. The inequivalence of the CH_2 protons adjacent to the amide nitrogen is evident as they resonate as a complex multiplet at δ 3.28-3.40 ppm, where as the signal for the more remote CH_2 attached to the benzene ring is a straightforward triplet. Moreover, the methylene protons of the Cbz group are magnetically inequivalent in this compound and resonate as a pair of doublets at δ 5.00 ppm and δ 5.03 ppm. The coupling constant, ^2J (coupling through 2 bonds) equals 12.5 Hz, which is typical for geminal coupling[116]. Also magnetically inequivalent, but for a different reason, were the 2 protons of the side chain primary amide, the C-N bond in amides has partial double bond character since the nitrogen is sp^2 hybridised and its p-orbital, containing the lone pair, overlaps sideways with the carbonyl π-orbital. Thus one of the NH protons is held *cis* to the carbonyl oxygen and the other is held *trans*, placing them in different environments on the NMR time scale.

The signal for one of these protons appeared at δ 6.76 ppm and the other at δ 7.24 ppm. The other two NH protons in the molecule were also readily assigned though their multiplicity, the α-NH resonating as a doublet at δ 7.39 ppm and the $N\underline{H}CH_2$ proton appearing as a triplet at δ 7.99 ppm. As expected the aromatic protons *ortho* to the powerfully electron-withdrawing nitro group, resonated nearly 1 ppm downfield from the usual chemical shift of benzene (δ 8.12 ppm vs. δ 7.27 ppm). In the solid phase IR-spectrum, bands for the primary and secondary amides were observed. For example, the band at ν_{max} 1690 corresponds to the amide I band of the secondary amide whereas the broad band centred at ν_{max} 1648 represents the overlapping amide I and amide II bands of the primary amide. The nitro group gave its characteristic symmetric and anti-symmetric stretch bands at ν_{max} 1518 and 1344 cm^{-1}.

The removal of the Cbz protecting group was achieved almost quantitatively with HBr in glacial acetic acid to give $GlnNHCH_2CH_2Ph$-*p*-NO_2.HBr salt (**54**) (Scheme **13**, p61). Characterisation of this novel compound was achieved by ^1H NMR spectroscopy, mass spectrometry and elemental analysis (continued on p62).

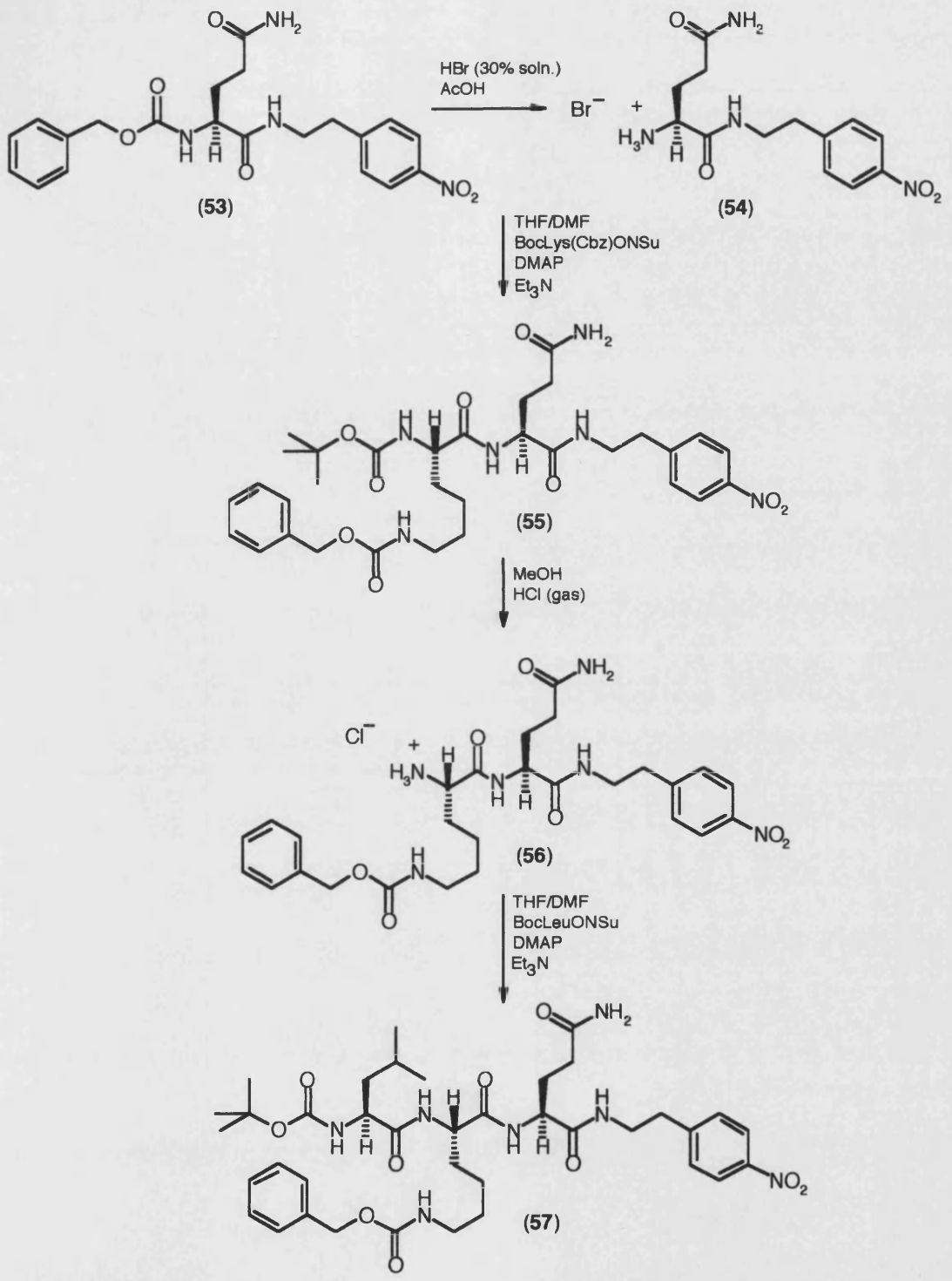

Scheme 13. *The synthetic route to the formation of tripeptide BocLeuLys(Cbz)GlnNPEA (**57**)*

The assignment of the ^{1}H NMR spectrum of (**54**) was aided by a 2D COSY (correlation spectroscopy) experiment. Notably the α-proton resonated at δ 3.72 ppm, which is significantly up-field from the corresponding signal for the Cbz precursor and reflects the removal of the electron withdrawing carbonyl from the nitrogen.

The reaction of this amine salt with commercially available N^{α}-(Boc)-N^{ε}-(Cbz)Lys N-hydroxysuccinimide ester in the presence of triethylamine afforded the dipeptide derivative BocLys(Cbz)GlnNPEA (**55**) in satisfactory 47% yield. In this case 4-dimethylaminopyridine (DMAP) was added as a nucleophilic catalyst[110].

With the orthogonality of the Cbz and Boc protecting groups proving its usefulness, treatment of the di-protected peptide derivative (**55**) with hydrogen chloride in MeOH removed only the Boc group to give a quantitative yield of the N^{α}-unmasked peptide derivative (**56**). The Cbz was not removed owing to the lesser nucleophilicity of chloride over bromide. The protecting group strategy from this point thus involved Cbz as the side chain protection and Boc as the main chain. This dipeptide was then coupled in modest yield (37%) with commercial BocLeuONSu to give the tripeptide derivative BocLeuLys(Cbz)GlnNPEA (**57**). Again, the rather complex ^{1}H NMR spectrum was assigned with the aid of a 2D COSY spectrum. A notable feature was the multiplet (actually overlaying doublets) at δ 0.77-0.90 ppm, which relate to the Leu methyl groups. This shows that these methyls are also diastereotopic in nature and thus magnetically inequivalent (resonate at different frequencies).

Unfortunately, this tripeptide proved to be too insoluble in compatible organic solvents for elaboration and further progress towards the target tetra- and penta-peptide derivatives. Further synthesis was not possible.

3.1.2 Positive control sequence

In the approach towards the putative positive control sequence SerSerLysLeuGln-$NHCH_2CH_2Ph$-*p*-NO_2 (**47**) the $GlnNHCH_2CH_2Ph$-*p*-NO_2 (**54**) was coupled with BocLeuONSu to provide $BocLeuGlnNHCH_2CH_2Ph$-*p*-NO_2 (**60**) in satisfactory yield (Scheme **15**, p64). In this sequence the removal of the Boc protecting group was with the strong organic acid TFA rather than the hydrogen chloride that had been used earlier. At this point, the observation of solubility problems from the previous sequence led to the investigation of an alternative, more lipophilic protecting group for the Lys.

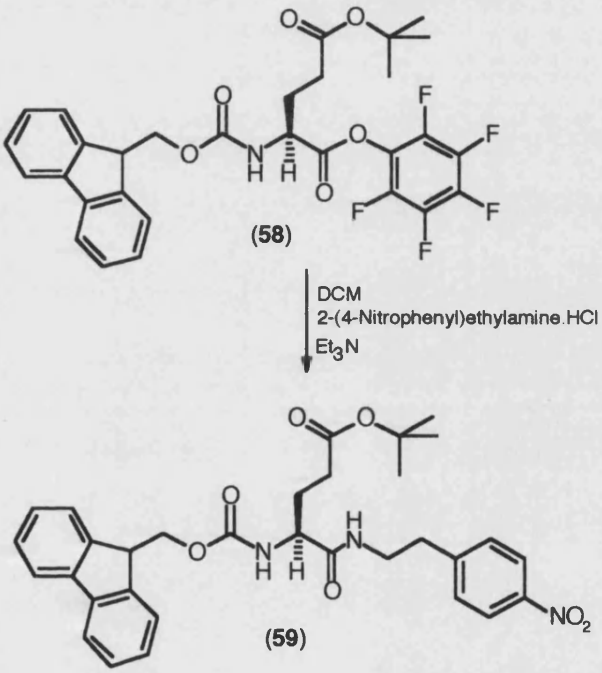

Scheme 14. *The synthesis of FmocGlu(OBu^t)NPEA as a test for the stability of the Fmoc protecting group in the presence of base*

As a model reaction to establish the stability of Fmoc-protected amino acids in peptide coupling, FmocGlu(OBu^t)OPFP active ester was treated with a primary amine (NPEA) under basic conditions (which in turn, may have affected the base labile Fmoc group). However, FmocGlu(OBu^t)NPEA (**59**) was given in excellent yield (65%) without disruption of the protecting groups (Scheme **14**).

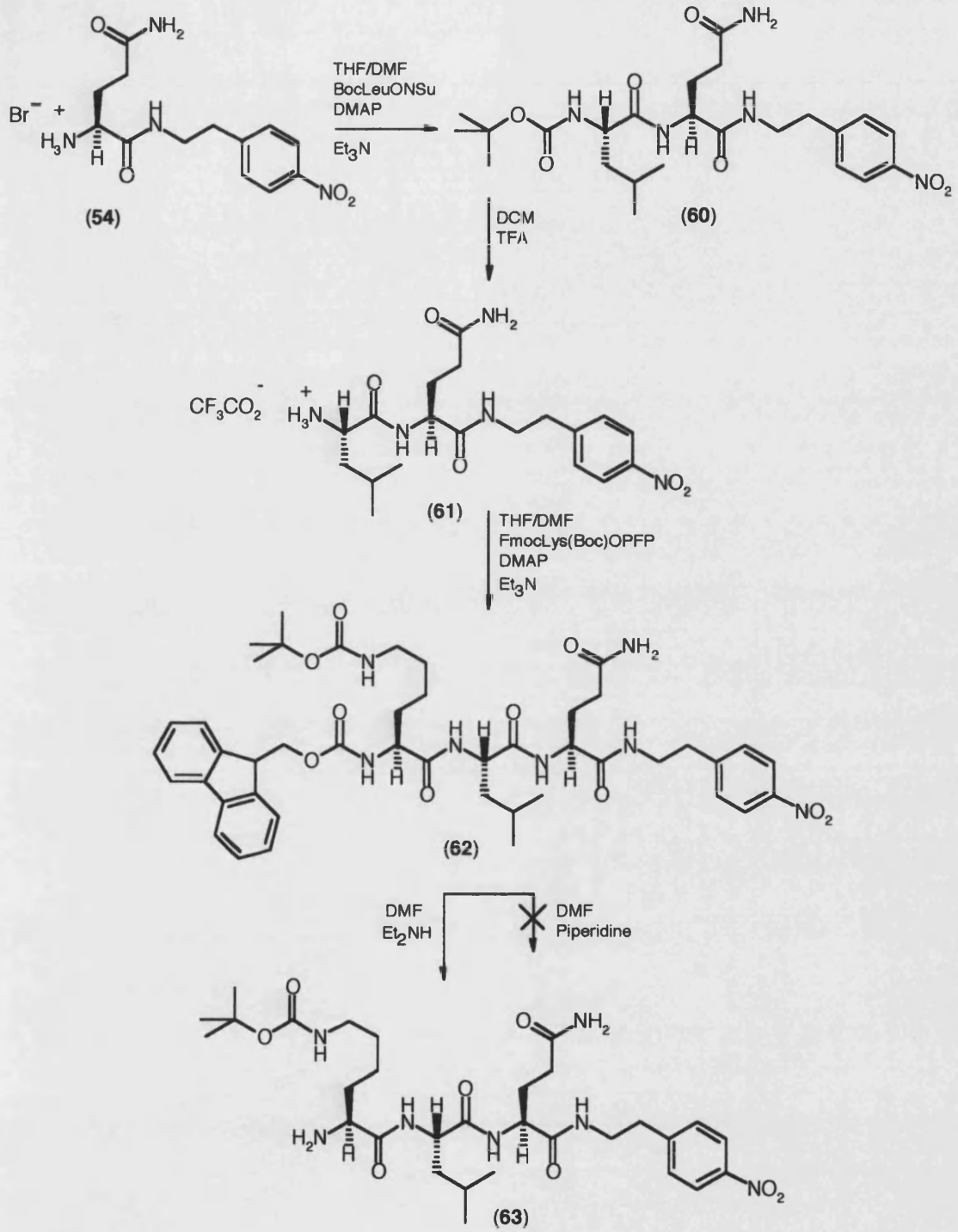

Scheme 15. *The synthesis of tripeptide Lys(Boc)LeuGlnNPEA*

Backed by the confidence of this successful model, the dipeptide derivative salt LeuGlnNHCH$_2$CH$_2$Ph-*p*-NO$_2$.TFA salt (**61**) was coupled with FmocLys(Boc)ONSu to afford the required tripeptide derivative FmocLys(Boc)LeuGlnNHCH$_2$CH$_2$Ph-*p*-NO$_2$ (**62**) in a modest yield (41%) (Scheme **15**, p64). The Fmoc and Boc protecting groups are fully orthogonal to one another, Boc being removed with acid and Fmoc, primary and secondary amines. Treatment of the tripeptide derivative (**62**) with piperidine[53] failed to affect the required cleavage of Fmoc. A convenient modification to this process was the replacement of piperidine with diethylamine, which removed the Fmoc efficiently allowing precipitation of the free amine of Lys(Boc)LeuGln NHCH$_2$CH$_2$Ph-*p*-NO$_2$ (**63**) (85%) from the reaction mixture (Scheme **15**). Regrettably this tripeptide was too insoluble for further couplings.

3.2 Synthesis of the aminobenzyloxycarbonyl clip

Where as the previous control model compounds omitted the self-immolative molecular clip, the attention was now turned to the synthesis of peptide derivatives where the PSA-sensitive peptide sequence was linked to the model drug (NPEA) through an aminobenzyloxycarbonyl linker[49,117] (self-immolative molecular clip) (Scheme **16**).

The idea of having a self-immolative clip linking the drug to the peptide has become apparent in our aims and objectives (see section **2.2**, p49). It has been stressed that having an aromatic ring directly adjacent to the PSA-sensitive amide bond shown in the monomeric model (**64**) (Scheme **16**), is essential for the cleavage of PSA. Moreover, Denmeade *et al.*[103] have shown this in their small molecule prodrug studies, where the release of 7-amino-4-methyl-coumarin (AMC) directly from the peptide constructs HisSerSerLysLeuGln, SerSerLysLeuGln and SerLysLeuGln occurred by action of the serine protease.

During cleavage of the sensitive amide bond (shown in Scheme **16**) by the action of the enzyme, the primary aromatic nitrogen on the self-immolative molecular clip is exposed. This amine has a higher electron density at the nitrogen compared with its

corresponding amide. The newly available electron pair on the exposed nitrogen can feed into the electron rich π-system of the adjacent aromatic ring and can cause 1,6-elimination of the carbamate (**66**) (very good leaving group) at the reactive *para*-benzylic position. Notably, if the amine were *ortho* to the carbamate functionality, a similar elimination would occur, but with the *ortho* being synthetically less favourable, the *para* was the obvious choice. The 1,6-elimination process could not be triggered if the amine were *meta* to the carbamate.

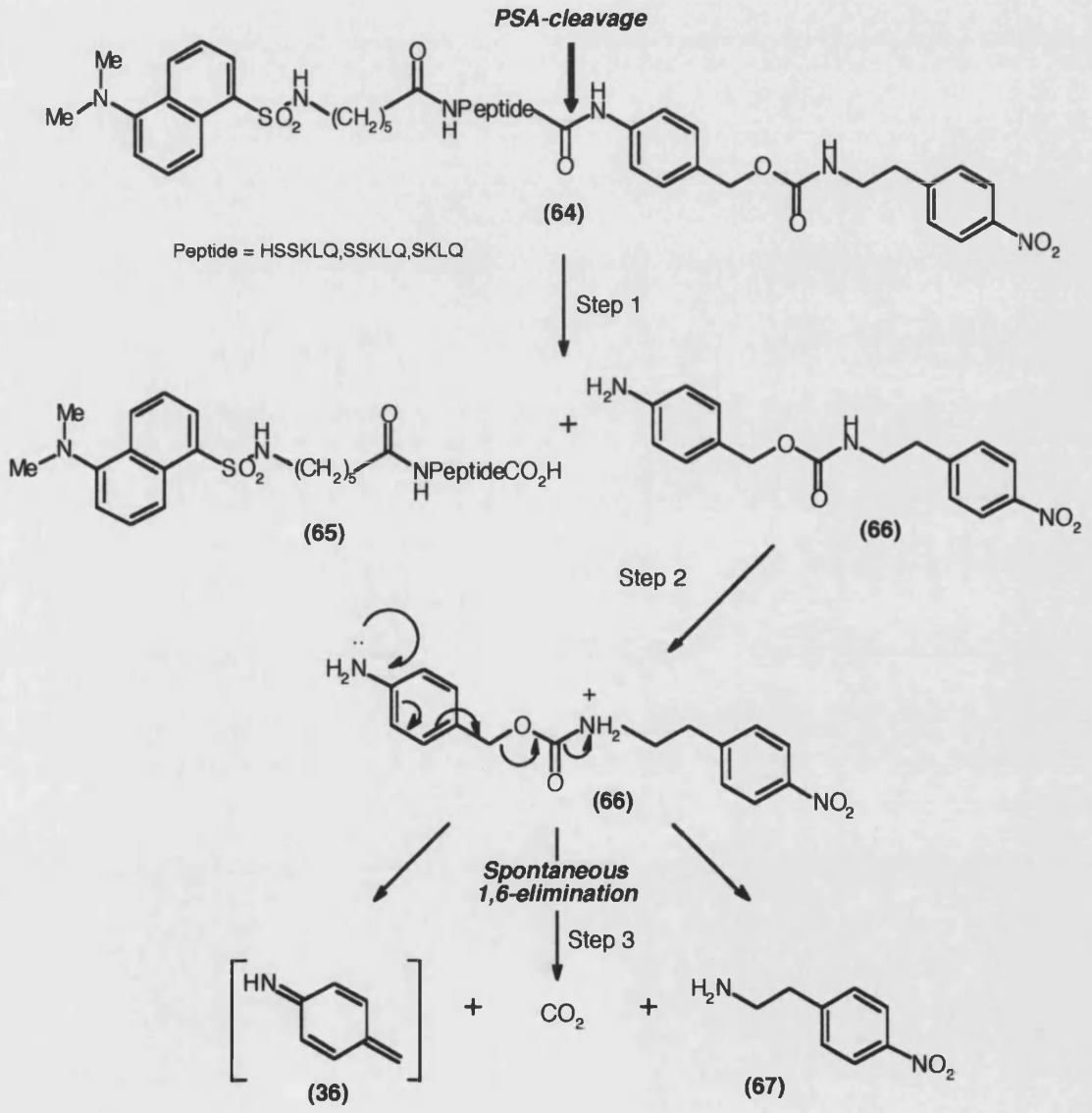

Scheme 16. *The mechanism of the PSA-triggered release of the model drug (NPEA)*

Naylor *et al.*[118] have shown the rates of a variety of leaving groups from a series of indolequinones for the use of bioreductively-activated prodrugs under both chemical and radiolytic conditions. The rate of release in the elimination step from a range of function groups, consisting of, carboxylate, phenol and thiol groups, where related to their leaving group ability. Furthermore, it is important to note that elimination would not occur if the aliphatic amine on the model drug were directly attached to the benzyl CH_2 on the anilide moiety, this is due to the amine being a poor leaving group[118].

A critical intermediate in this part of the project was BocGln-linker-NPEA (**68**). In this target, the use of Boc protection for the Gln is critical as the Cbz used in earlier studies would have been too similar to the amidobenzyloxycarbonyl linker unit (Scheme **17**): no conditions could be envisaged for selective removal of Cbz in the presence of this unit.

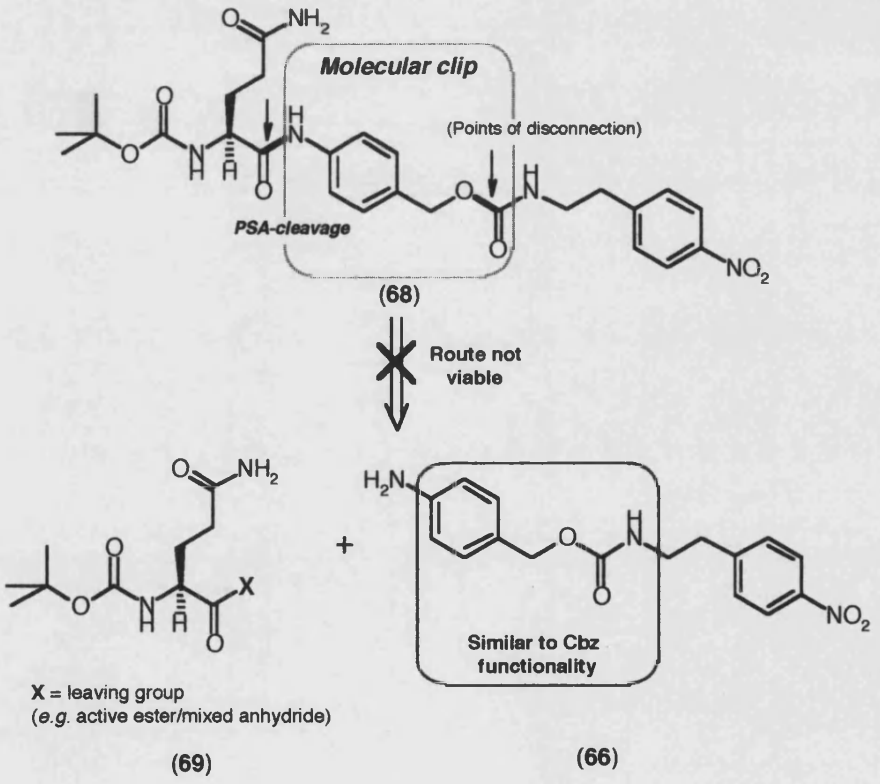

Scheme 17. *A non-viable route to the amidobenzyloxycarbonyl linker unit*

Retrosynthetically, two bonds are available in this structure for disconnection: the amide bond between the Gln and the linker and the carbonyl to oxygen bond of the carbamate joining the model drug to the linker (see Scheme **17**). Of these, the former would be more convergent in the long term but would require the synthesis of the very primary amine (**66**), which would be released by PSA-cleavage and would self-immolate. Therefore, the BocGln has to be joined to the linker (***self-immolative molecular clip***) before the linker is joined to the model drug (NPEA).

3.2.1 Synthesis of the target isocyanate intermediate (75)

In the first series of experiments on this, our primary aim was to synthesise the target intermediate, isocyanate (**75**). There are two distinct strategies available for the synthesis of isocyanates. Because isocyanates are highly electrophilic and sensitive to the presence of nucleophiles, they need to be generated under appropriate conditions. One strategy involves treating primary amines with electrophilic carbonyls carrying two leaving groups, thus the reaction of primary amines in phosgene has been used to make isocyanates, but this reagent is highly toxic and volatile and has been replaced with safer reagents such as N,N-carbonyldiimidazole (CDI), di-phosgene and tri-phosgene.

Alternatively, rearrangement reactions of acyl nitrenes or their equivalents can be used. For example, the Hoffman rearrangement in which a primary amide is treated with bromine and NaOH to give a primary amine with one less carbon, this proceeds *via* an isocyanate[119]. The Lossen rearrangement of hydroxamic acids under strongly acidic conditions is similar. In contrast, the Schmidt and Curtius rearrangements are driven by loss of molecular nitrogen, an excellent leaving group, from acyl azides. In the former, the acyl azide is generated *in situ* from the carboxylic acid and sodium azide in the presence of concentrated H_2SO_4. In the latter however, the acyl azide is synthesised under mild conditions, either by treatment of an acid chloride with sodium azide or with trimethylsilyl azide[120], or by nitrosation[121] of a hydrazide.

The initial objective was to convert phenylpropanoic acid (**71**) to its corresponding 4-nitro analogue (**72**). The first attempted nitration[122] employed concentrated H_2SO_4 and HNO_3 at room temperature for 48 h (Scheme **18**). Unfortunately, the sole isolatable product from this reaction was the di-nitro compound (**70**), which was clearly identified by ^1H NMR by a typical 1,2,4-tri-substituted benzene pattern that shows the *meta* coupling of proton **b** to proton **c** and *visa versa* (as shown in Figure **18**).

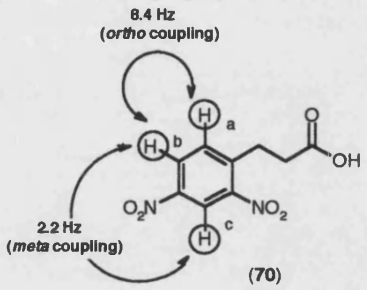

Figure 18. *Proton couplings for 3-(2,4-dinitrophenyl)propanoic acid (**70**)*

Based on the strategy adopted by Strazzolini *et al.*[123] in which more mild conditions were used (reaction time 2h at 0°C), the *para*-nitro analogue (**72**) was furnished in modest yield (34%). The next step was to convert (**72**) in to its respective target isocyanate (**75**) (Scheme **18**).

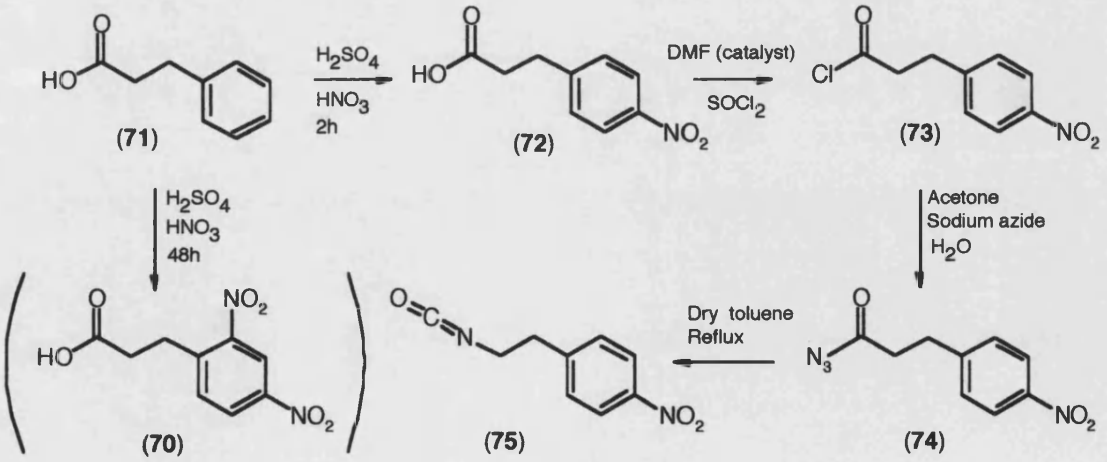

Scheme 18. *Synthesis to the formation of isocyanate (**75**)*

3-(4-Nitrophenyl)propanoic acid (**72**) reacted with thionyl chloride in the presence of catalytic DMF to afford the required acid chloride (**73**), which upon treatment of sodium azide in acetone for 2 h at RT, yielded the isocyanate precursor (**74**). Confirmation by infra-red spectroscopy clearly showed the expected N_3 peak at ν_{max} 2139 with its adjacent carbonyl peak, appearing at ν_{max} 1700. Notably, the carbonyl of the acid azide is further up-field from that of the carbonyl on the acid chloride (**73**), this is due to the available lone pair of electrons on the nitrogen of the azide shielding the carbonyl. Finally, the target isocyanate (**75**) was achieved by thermolysis of the acid azide (**74**) in toluene for approximately 2 h. Further characterisation by infra-red spectroscopy, indicated the appearance of a peak at ν_{max} 2272 which is typical for N=C=O stretching.

3.2.2 Synthesis of the target primary alcohol intermediate (83)

In the second series of experiments, the primary alcohol of the 4-aminobenzylalcohol linker was to be masked either by protection as a silyl-ether or at a higher oxidation level as the corresponding carboxylic acid and methyl ester. Taking the latter approach first, attempts were made to couple active esters of BocGln with methyl-4-aminobenzoate (**81**), however the hydroxysuccinimide and pentafluoro- phenyl esters both proved insufficiently electrophilic for a successful reaction with this weakly nucleophilic aniline which carries an electron withdrawing group *para* to the amine (see Scheme **19**, p71).

Senokuchi *et al.*[124] have reported the use of mixed aminoacyl-pivaloyl anhydrides for difficult couplings of anilines. Following this approach, BocGln was treated with triethylamine and pivaloyl chloride in a THF/DMF mixture at low temp. Attack of the Gln carboxylate on the acid chloride gave the required mixed anhydride (**79**), which was coupled *in situ* with methyl-4-aminobenzoate (**81**). The regioselective reaction of the nucleophile with the aminoacyl carbonyl is driven by steric factors (the bulk of the *tert*-butyl unit of the pivaloyl) and by electronic factors (the electronegative nitrogen makes the aminoacyl carbonyl more electrophilic) (Scheme **19**, p71).

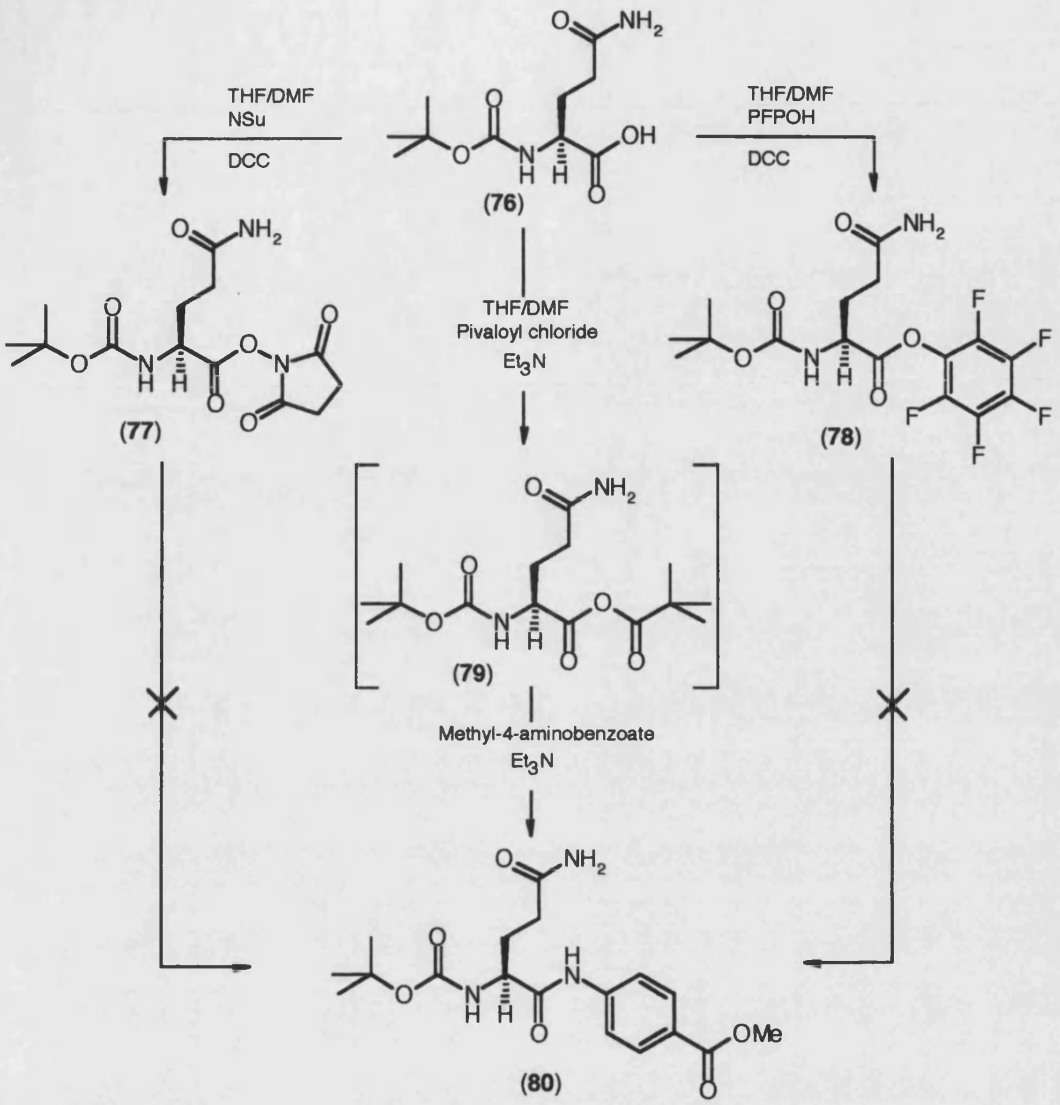

Scheme 19. *Routes to the synthesis of GlnNHPhCO₂Me (**80**)*

From here it was intended to carry out the selective reduction of the ester to the corresponding benzyl alcohol with $LiBH_4$ (Scheme **19**, p72). This reagent is selective for reduction of esters in the presence of amides[110]. However, it is incapable with hydroxylic solvents, and a suitable non-hydroxylic solvent could not be found which would dissolve (**80**), including, 1,2-dimethoxyethane and hot diglyme. The ester also could not be hydrolysed to the corresponding carboxylic acid under a variety of

conditions, due to poor solubility. Selective reduction of the carboxylic acid (**82**) with BH_3.THF would have afforded the benzyl alcohol (**83**)[125] (Scheme **20**).

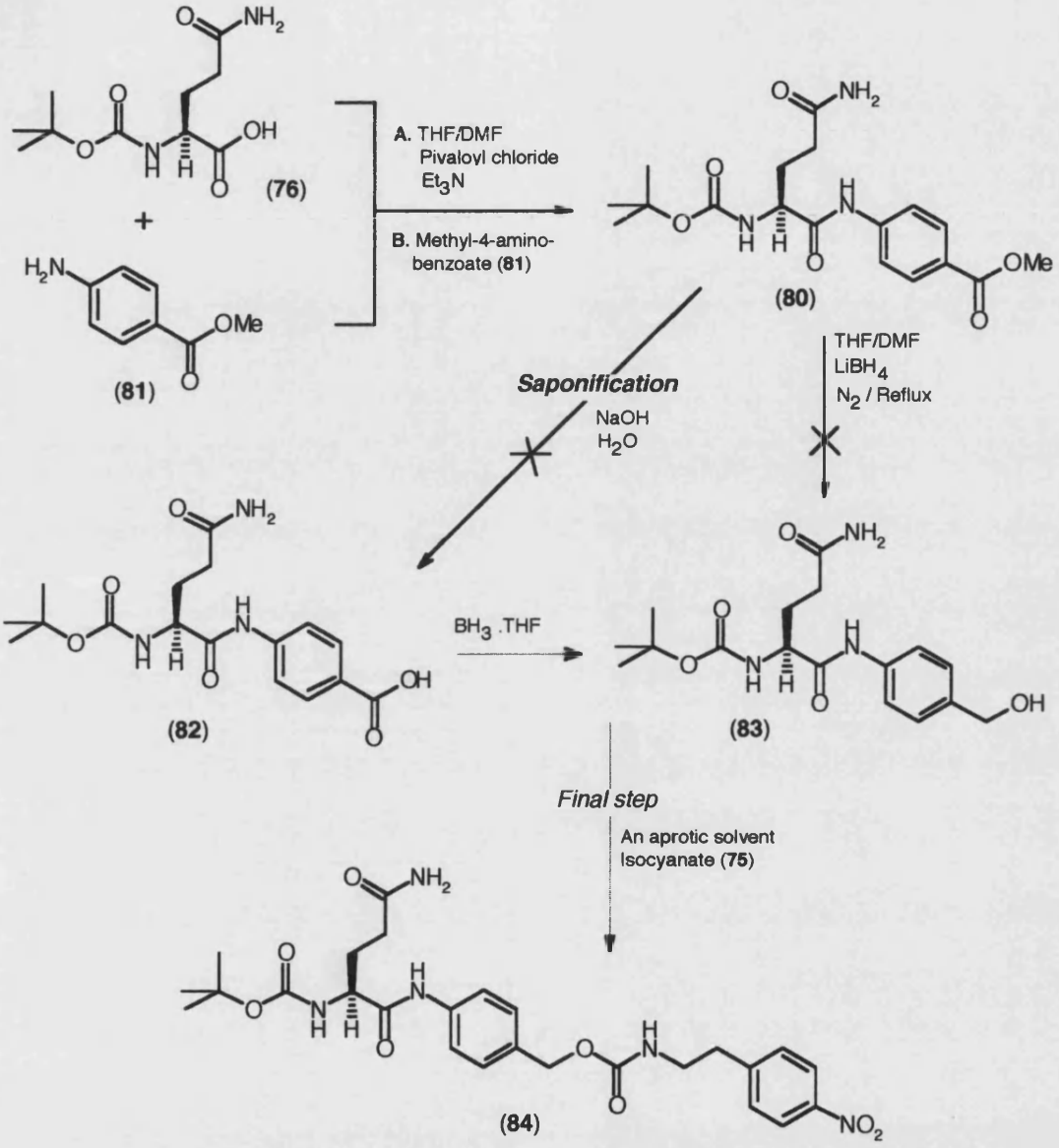

Scheme 20. *Routes to the synthesis of BocGlnCLIPNPEA (**84**)*

In an attempt to alleviate these problems of poor solubility, the use of a more lipophilic protecting group for the N^{α} of the Gln was investigated. Since insolubility was driven by the side chain primary amide, this was replaced by the corresponding *tert*-butyl ester

(**85**), which could later be converted to the amide. FmocGlu(O-*tert*-butyl)OH was converted to its pivaloyl mixed anhydride which reacted *in situ* with methyl-4-aminobenzoate to give the required 4-methoxycarbonylanilide (**87**) (Scheme **21**). Although this compound contained two esters, it was anticipated that the methyl-ester could be selectively reduced by $LiBH_4$ as the *tert*-butyl ester is considerably more bulky. This predicted selectivity could not be put to the test, as compound (**87**) was again too insoluble for reaction with $LiBH_4$.

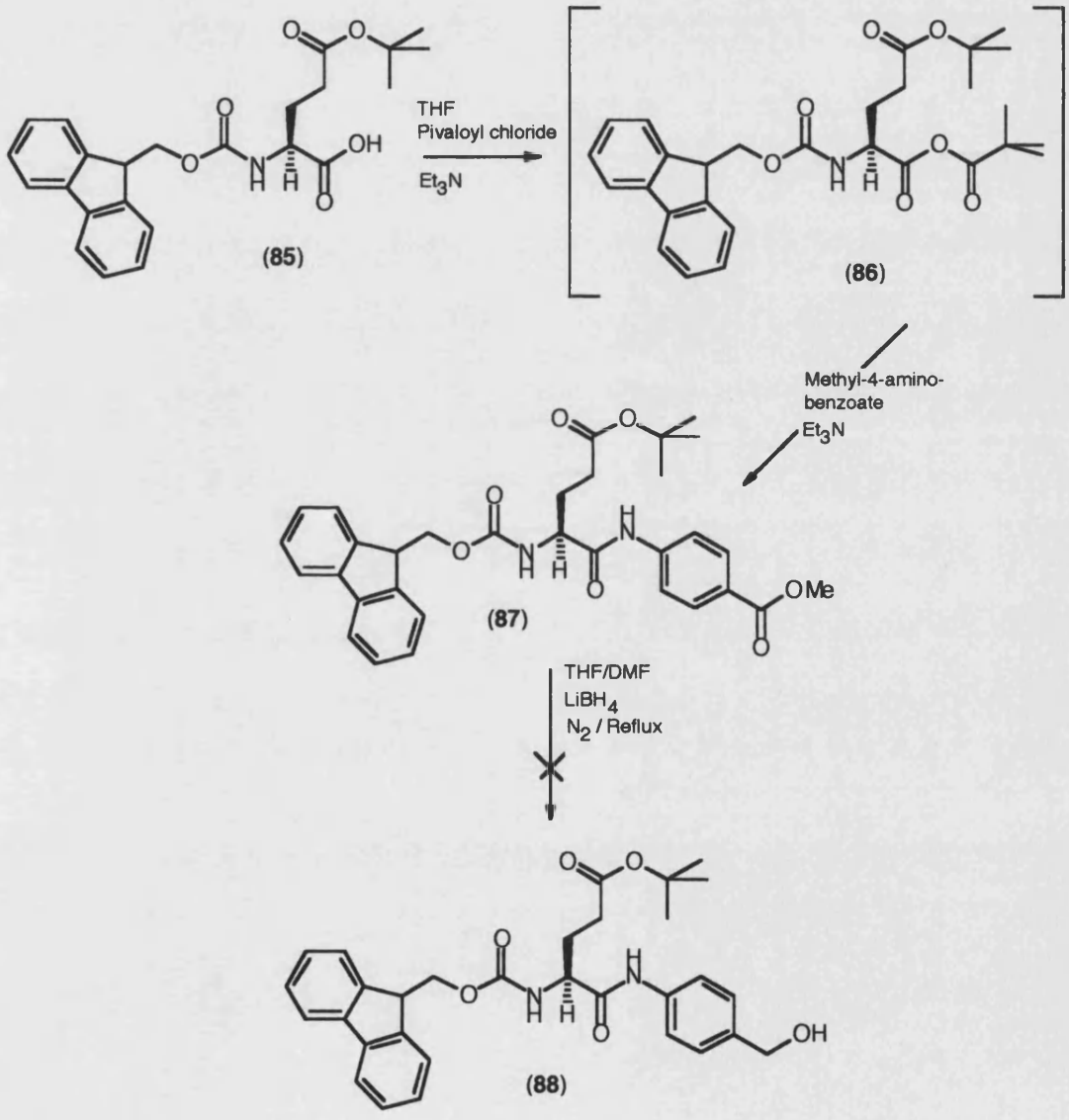

Scheme 21. *The attempted synthesis of FmocGluNHPhCH$_2$OH (**88**)*

Another strategy would be to build part, or all of the peptide before reduction of the methyl ester to the benzyl alcohol of the linker. To this end, an attempt was made to remove the N^{α} Boc protection from compound (**80**), however, treatment of (**80**) with TFA under very mild conditions followed by evaporation of the reagents, gave a material which was clearly not the deprotected Gln derivative (Scheme **22**). ^{1}H NMR analysis of the product mixture suggested that the deprotected Gln had cyclised under the reaction conditions to give Pyg-4-methoxycarboanilide (**90**) (Scheme **22**). Also evident in the ^{1}H NMR spectrum was a 1-1-1 triplet at δ 7.28 ppm integrating for 4 protons and with the very large coupling constant of $\mathcal{J}$ = 51.5 Hz. The 1-1-1 ratio of peak heights of this triplet which is different to the normal 1-2-1 ratio observed when a proton is observed to couple to 2 other protons, indicates coupling to a spin I = 1 nucleus (2 halves). ^{14}N has this spin value, although couplings to ^{14}N are usually not observed owing to rapid proton exchange and the quadrupolar nature of this nucleus, however, proton exchange is suppressed for salts in DMSO solution. Moreover, the high symmetry of the ammonium cation allows ^{14}N-^{1}H coupling to be observed despite the quadrupolar nature of the nitrogen, thus this signal is assigned to ammonium trifluoroacetate, the co-product of attack of the N^{α} amine of the Gln on the side chain carbonyl.

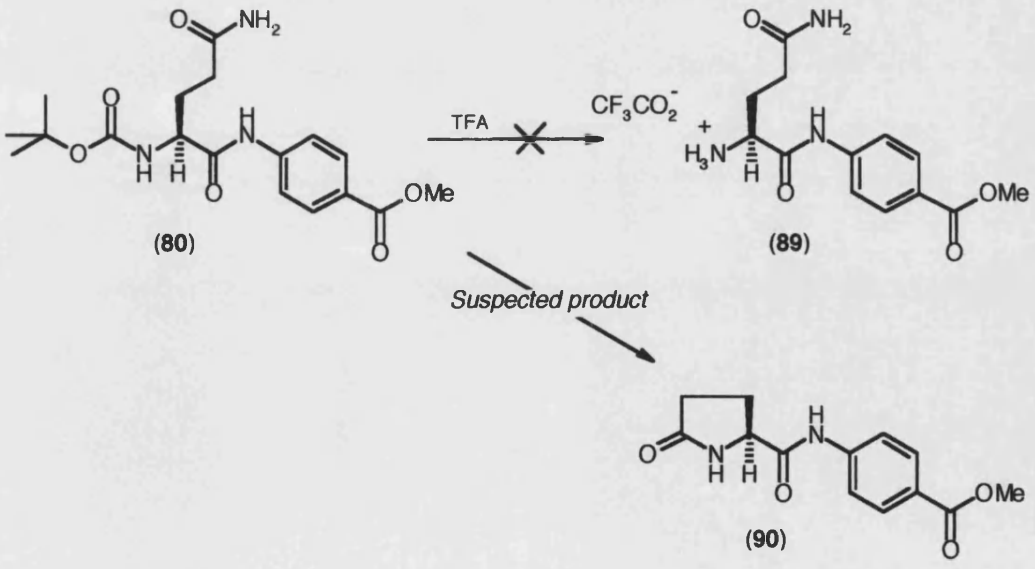

Scheme 22. *The attempted deprotection of BocGlnNHPhCO2Me (**80**) with TFA.*

In view of the lack of success regarding the strategy incorporating the benzyl alcohol as the methyl ester for later reduction, a series of experiments were conducted to study the possibility of attaching 4-aminobenzyl alcohol to glutamine derivatives, either with the primary alcohol protected or unprotected.

Firstly, 4-aminobenzyl alcohol (**30**) had to synthesised by reduction of 4-nitrobenzyl alcohol in ethanol, in the presence of palladium on activated carbon under hydrogen. Interestingly, during the purification of 4-aminobenzyl alcohol, a minor fraction was isolated and identified to be *para*-toluidine (**102**). This had showed that under these conditions above, a small amount of the amino-product (**30**) had further reduced to its arylmethyl derivative (**102**) (Scheme **27**, p80). Alternatively, other methods can be used for the reduction of nitro groups, for example, the addition of $NaBH_4$ in aqueous MeOH in the presence of palladium. This method has been claimed to be selective for reduction of nitro groups in the presence of all other functionalities, although this selectivity has recently been called into doubt[126]. 4-Aminobenzyl alcohol is commercially available but the quality of sample obtained from several sources was poor.

Studies on the coupling of BocGln to 4-aminobenzyl alcohol through a range of active esters (ONSu/ONP/OPFP) (Scheme **23**, p76) failed to give usable yields of the target amide (**83**). Although the pivaloyl mixed anhydride approach had been effective for the coupling of other anilines, it failed completely in this case. Similarly, the use of *iso*butyl chloroformate in the aim to alleviate steric compression of the mixed anhydride, failed also to be effective in this case. Furthermore, the direct coupling with the use of carbodiimide reagents (DCC/EDC[115]) failed to attach the arylamine to the protected amino acid, either in the presence, or absence of catalytic HOBt (Scheme **23**, p76).

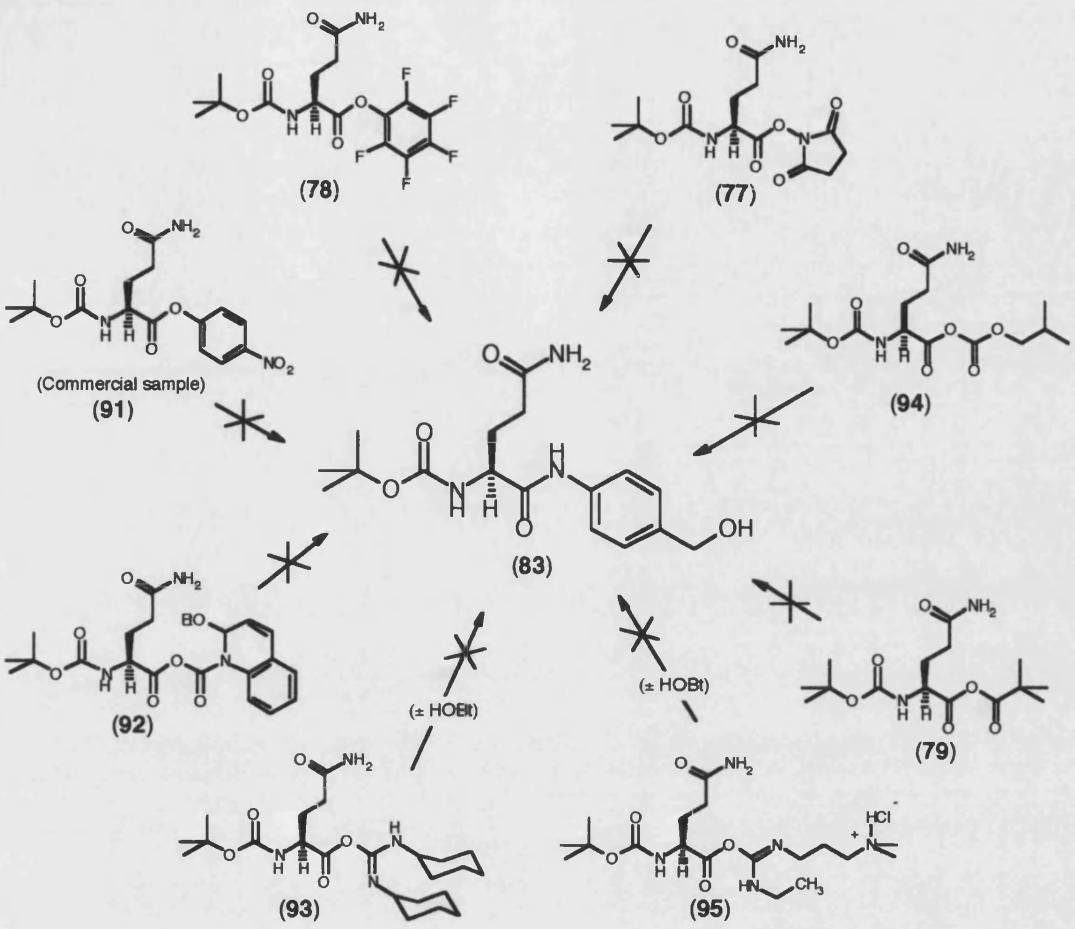

All of the glutamine derivatives shown above were reacted with 4-aminobenzyl alcohol ± DMAP (unless otherwise stated)

Scheme 23. *Attempted syntheses towards the formation of BocGln-anilide (**83**)*

Moreover, in the case of the EDC/HOBt method, a major product was isolated upon purification and characterised by ^{1}H NMR and mass spectrometry as the cyclised glutamine analogue, 2,6-piperidinedione (**96**)[127] (Scheme **24**, p77). Thus, direct carbodiimide couplings to glutamine derivatives could pose a problem in further syntheses.

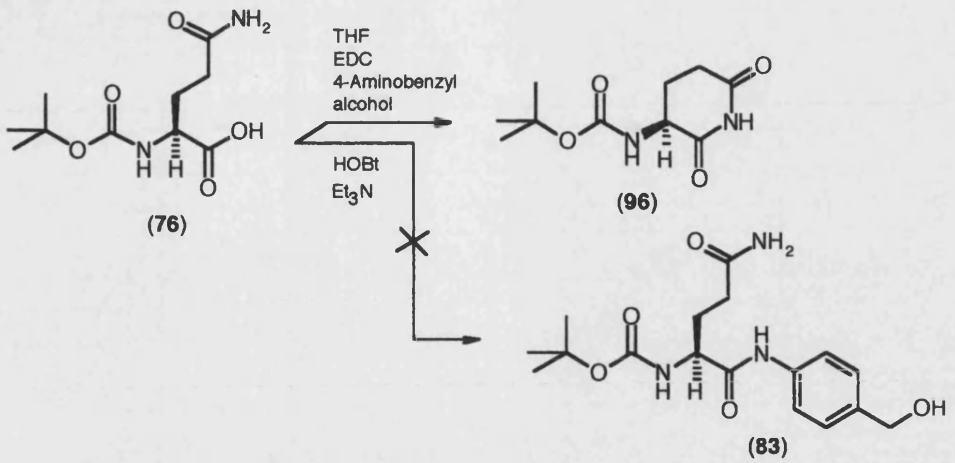

Scheme 24. *The attempted synthesis of BocGln-anilide (**83**) leading to the formation of 2,6-piperidinedione (**96**)*

Finally, Dubowchik *et al.*[128] have shown in their peptide coupling strategies, that 4-aminobenzyl alcohol can be conjugated to small peptides in the presence of EEDQ in high yields. To confirm the use of EEDQ in peptide coupling, a model run was attempted by reacting FmocLeuOH (**97**) with EEDQ followed by the addition of 4-aminobenzyl alcohol at RT. This reaction worked smoothly and yielded the anilide (**99**) in high yield (72%) (Scheme **25**).

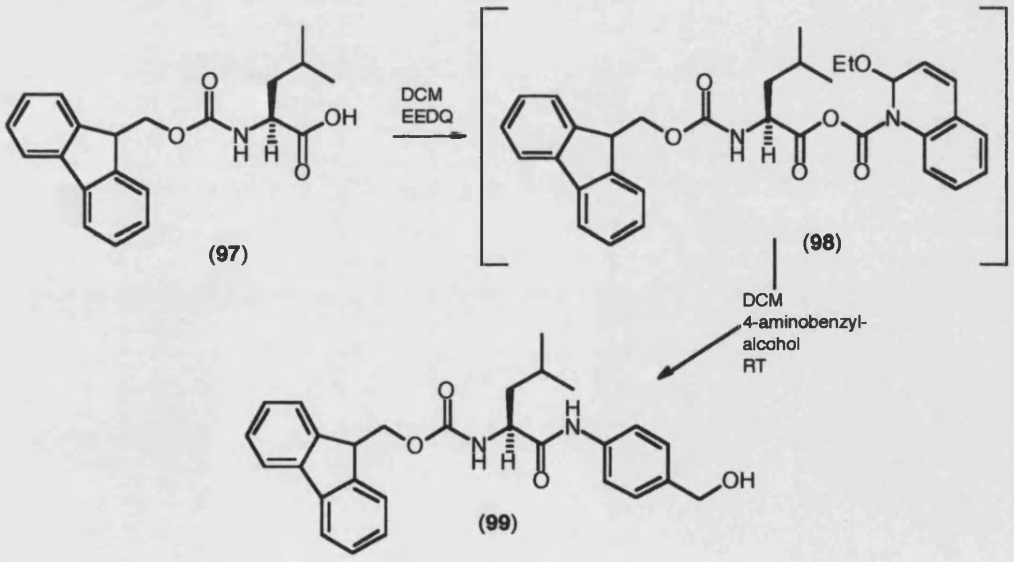

Scheme 25. *Synthesis of compound anilide (**99**)*

Based on the success of this model reaction, many attempts of coupling 4-aminobenzyl alcohol to BocGlnOH (**76**) with the newer peptide-coupling reagent EEDQ were unsuccessful. Furthermore, studies on the coupling of the more freely soluble FmocGlu(O-*tert*-butyl) (**85**) to 4-aminobenzyl alcohol *via* the EEDQ and *iso*butyl mixed anhydrides[129], all failed also to give the required anilide (**83**) (compare with Scheme **23**). The ^{1}H NMR spectra of some of the crude product mixtures suggested the presence of only a trace of the desired anilide (**83**), although its presence could not be confirmed by mass spectrometry.

With regard to the active esters of BocGln, they had been prepared in the usual way from the corresponding ONSu or phenol (PFP) with DCC. As noted above (Scheme **19**, p71), the successful synthesis of the PFP-ester[130] could be demonstrated by ^{19}F spectroscopy. Whereas the ^{19}F NMR signal for pentafluorophenol occurred in the region of δ -164-180 ppm, the additional electron-withdrawing carbonyl in the ester moves these signals downfield. Interestingly, two sets of signals were observed in an integral ratio of approximately 9:1, the *ortho*-fluorines in the major set of signals resonate as a doublet at δ -153.27 ppm, the *meta*-fluorines resonate as a double doublet at δ -162.21 ppm and the *para*-fluorine gives rise to a signal at δ 157.61 ppm. The corresponding signals for the minor component have similar multiplicity and appear at similar chemical shifts, δ -153.57, δ -157.38 and δ -162.04 ppm, respectively. Since this compound was shown by TLC to be homogenous, the presence of the two sets of signals in the fluorine NMR spectrum can be ascribed to rotamers about the carbamate carbonyl to nitrogen bond. The greater dispersion of the signals in ^{19}F NMR spectroscopy allows these rotamers to be observed as separate signals. In contrast, most of the signals of the two rotamers overlap fully in the ^{1}H NMR spectrum. The exception is the signal for the carbamate NH for which the signal from the major rotamer is at δ 7.72 ppm, and that for the minor rotamer is some 2 ppm up-field from this position at δ 5.57 ppm. Returning to the fluorine spectrum, it was also noted that the ^3J *ortho* coupling between the 2F and 3F were greater at 17.6 Hz than the corresponding ^3J between 3F and 4F which was 16.3 Hz.

These failures in the couplings may have been due to the possibility that the primary benzylic alcohol was more nucleophilic than the aromatic amine. Amines are usually much more nucleophilic than alcohols but in this case, the amine is aromatic and the alcohol is primary and unhindered. To test this, 4-aminobenzyl alcohol was treated with di-*tert*-butyl dicarbonate in the presence of base (Scheme **26**)[131]. The sole product of this reaction was the N-Boc compound (**100**) with no evidence for the formation of the carbonate at the primary alcohol.

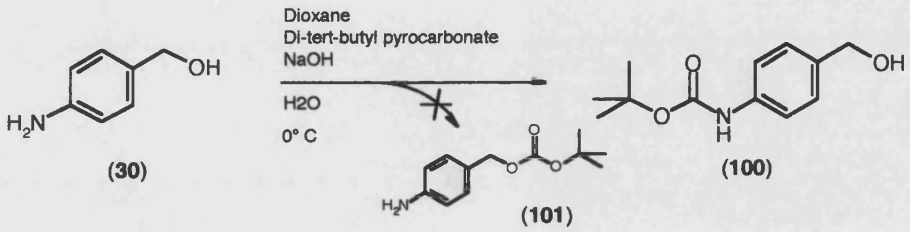

Scheme 26. *A synthetic route to 4-[N-(1,1-Dimethylethoxycarbonyl)amino]benzyl alcohol (**100**)*

The ^{1}H NMR spectrum of the product (**100**) confirmed that acylation had taken place at the nitrogen. Firstly, separate signals were seen for the OH and NH, whereas the alternative *tert*-butyl-(4-aminobenzyl) carbonate (**101**) would have shown the 2-equivalent NH_2 protons as a broad singlet. Secondly, the chemical shift of the benzylic CH_2 protons was 4.56 ppm, whereas the corresponding signal for benzyl esters comes in the region of δ 5.0-5.5 ppm. Thirdly, the protons *ortho* to the nitrogen function resonate at δ 7.22 ppm, whereas the signal of the corresponding protons in the starting material (**30**) appears up-field at δ 6.64 ppm, owing to the mesomeric electron-donating character of the primary amine.

Although this experiment on the regioselectivity of the introduction of the Boc group confirmed that the amine was significantly the most nucleophilic site in 4-aminobenzyl alcohol, masking of the hydroxyl function may avoid side reactions during coupling. A series of experiments was then conducted to prepare O-protected analogues of 4-aminobenzyl alcohol. The choice of protecting groups was critical. Esters would simply undergo acyl-migration from the corresponding 4-hydroxymethyl

anilides. Benzyl type protecting groups are clearly inappropriate, given the benzylic nature of the substrate (Scheme **17**, p67). O-*tert*-Butyl protection would have led to difficulties in orthogonality of the protecting groups late on in the synthetic sequence. Thus *tert*-butyldimethylsilyl ether (TBDMS ether) was selected as this group should not migrate from O to N. 4-Nitrobenzyl alcohol in dry DMF was treated with TBDMS chloride in the presence of imidazole under nitrogen, to give the silyl ether (**104**) (Scheme **27**) in good yield (64%).

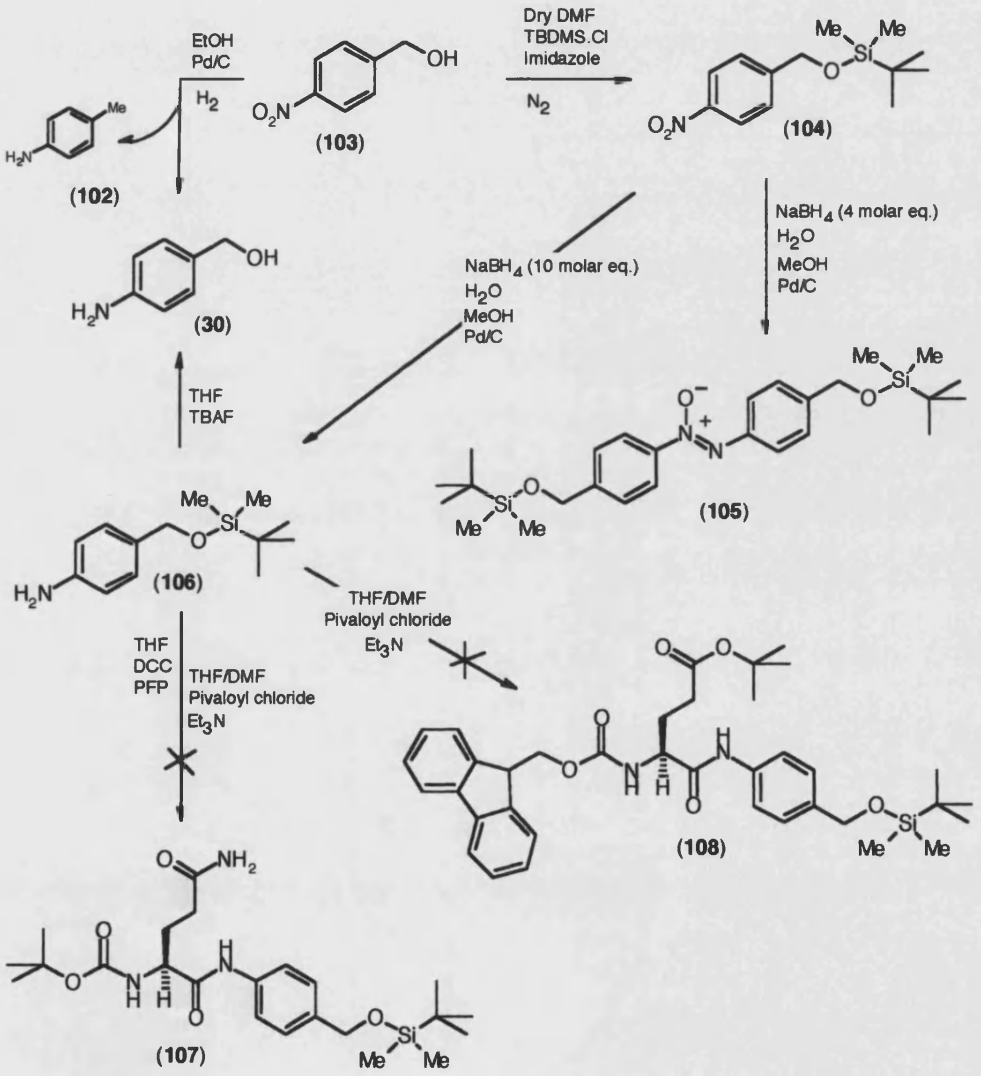

Scheme 27. *The attempted syntheses of BocGln-protected anilide (**107**) & FmocGlu(O-tert-butyl)-protected anilide (**108**)*

Now a selective reduction was required to expose the required aromatic amine (**106**) from its masked state as the nitro group. As mentioned previously, $NaBH_4$ in aqueous MeOH in the presence of palladium-on-charcoal was studied for this selective reduction. Surprisingly, use of 4 molar equivalents of $NaBH_4$, gave high yield (77%) of a very non-polar material (R_f = 0.8, 25 : 75 hexane : toluene) (**105**).

The ^1H NMR spectrum of this material indicated that it contained two inequivalent *para*-disubstituted rings, two inequivalent methylenes and two inequivalent TBDMS units. The observation of M+H ion at *m/z* 487 in the FAB+ mass spectrum pointed to the compound being an unsymmetrical dimer. Moreover, since the molecular weight is shown to be an even number, the compound must have an even number of nitrogen atoms (probably two). The aromatic portion of the ^1H NMR spectrum comprised 4 doublets, each integrating for 2 protons, these doublets were centred at δ 6.64, δ 7.11, δ 7.48 and at δ 8.19 ppm respectively. The coupling constant for each was approximately 8 Hz. A ^1H-^1H COSY spectrum (Figure **20**, p83) showed that the signal at δ 6.64 ppm was coupled to the signal at 7.11 ppm and that 7.48 ppm correlated with that at 8.19 ppm. Since the other signals in the spectrum are singlets, a 2D NOESY (Figure **19**, p82) spectrum was also required to establish through space connectivity and thus which TBDMS group was adjacent to which methylene and which methylene was adjacent to which aromatic system. This spectrum (Figure **19**) showed that the doublet at δ 7.48 ppm had through space connectivity to the methylene signal at δ 4.83 ppm. This methylene signal also showed a cross peak to the *tert*-butyl signal at δ 0.94 ppm and the $SiMe_2$ signal at δ 0.14 ppm. Similarly, the aromatic doublet at δ 7.11 ppm showed a NOE cross peak to the methylene signal at δ 4.63 ppm. In turn this methylene was shown to be close in space to the *tert*-butyl resonating at δ 0.94 ppm and to $SiMe_2$ resonating at δ 0.09 ppm. Since the chemical shifts of the methylenes correspond well with the environment of a benzyl alcohol or benzyl silyl ether, the unexpected product, therefore contains two inequivalent Ar-CH_2-OTBDMS units. The question now is what is the nature of the group linking these two units? The protons *ortho* to this linker resonate at the very different chemical shifts of δ 6.64 ppm and δ 8.19 ppm (*i.e.* some δ 1.5 ppm apart).

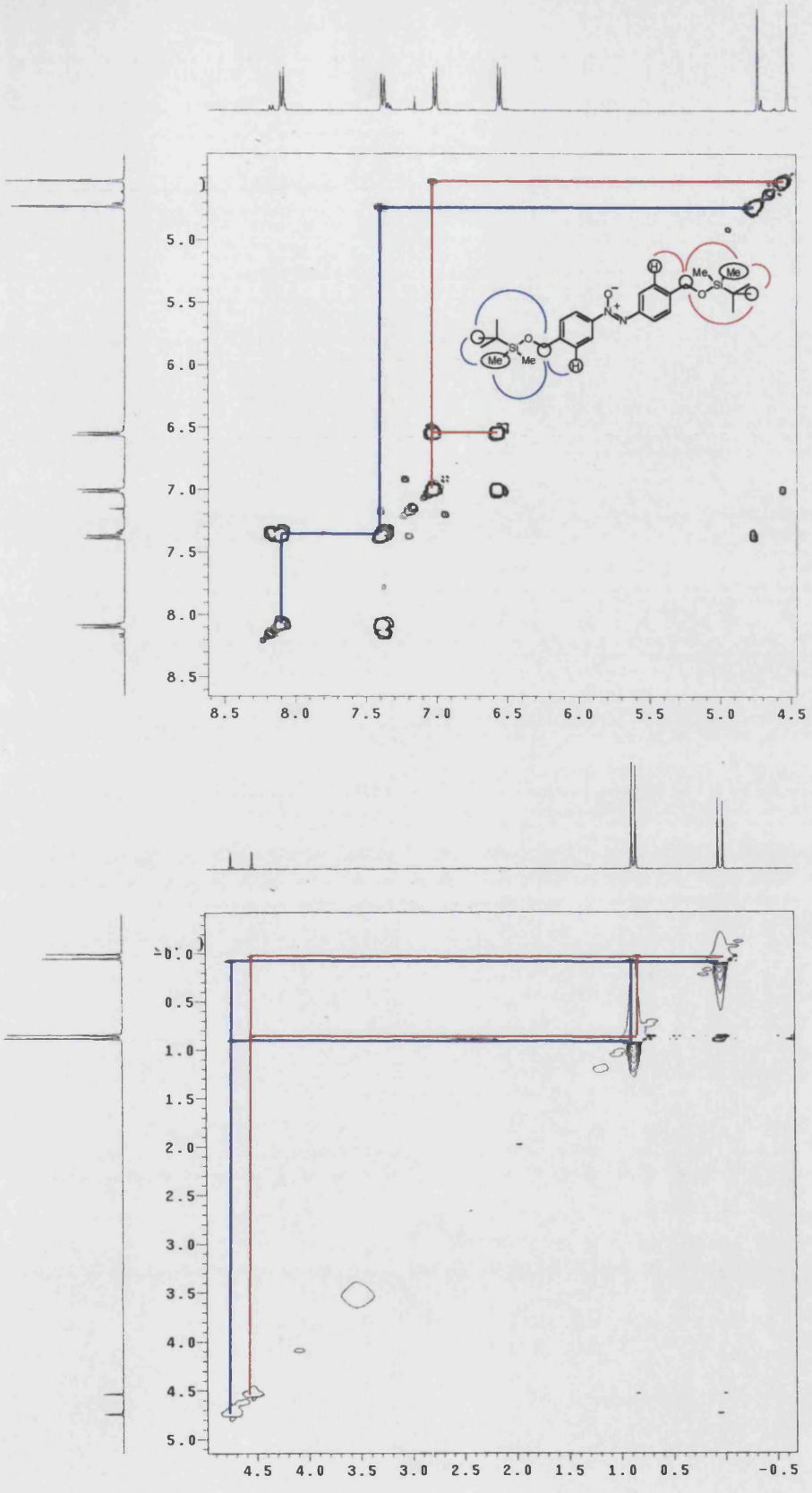

Figure 19. *NOESY expansions for azoxy compound (**105**) (All scales are in ppm represented as δ)*

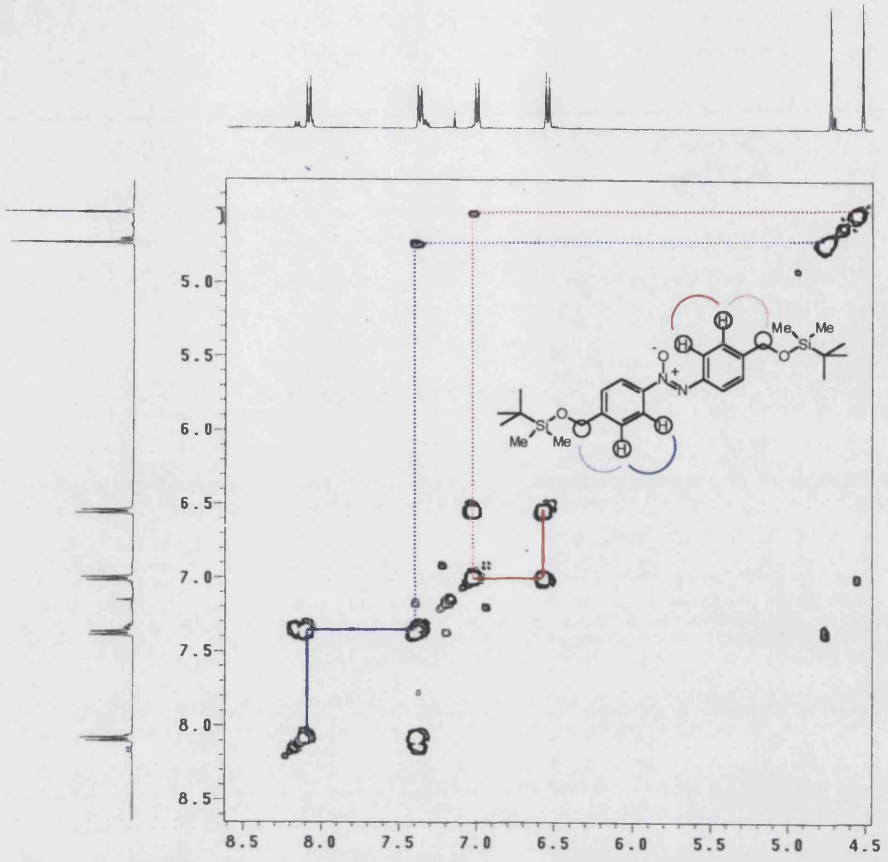

Figure 20. *A 2D COSY for azoxy compound (**105**)*

A high resolution FAB mass spectrum gave the molecular formula as $C_{26}H_{42}N_2O_3Si_2$, thus the linker contains only two nitrogens and one oxygen and the compound can be characterised as having the azoxy structure shown in (Scheme **27**, p80) (see Appendix Figure **27** for a 3D representation of azoxy compound (**105**)). The difference in the ^1H NMR chemical shifts of the 2 sets of protons *ortho* to the azoxy link is remarkable since the difference between the chemical shift of the corresponding signals for azoxybenzene is only 0.15 ppm[132,133].

Whereas the use of 4 molar equivalents of $NaBH_4$ gave the azoxy compound (**105**), reaction of the reduction with 10 molar equivalents of the reagent effected full reduction to the desired aromatic amine (**106**) (Scheme **27**). Reduction of nitro to

amino is a six-electron process; each molar equivalent of $NaBH_4$ is, in principle, an eight-electron reductant; thus it is surprising that the use of thirty two electron equivalents of reductant only reduced the nitro compound (**104**) by the equivalent of three electrons per molecule in making the azoxy compound (**105**). As a quick check to see if the TBDMS could be removed efficiently from compounds of this type, the 4-*tert*-butyl-dimethylsilyoxymethylaniline was treated with TBAF[134] in THF at 0°C to give 4-aminobenzyl alcohol (**30**) in excellent yield (65%). Unfortunately, no coupling of the OTBDMS (**106**) with BocGln derivatives could be achieved under a variety of conditions.

3.3 Synthesis of the aminophenylpropargyloxycarbonyl clip

In view of the difficulties in synthesising the aminobenzyloxycarbonyl clip derivatives, a modified aminophenylpropargyloxycarbonyl clip was designed. This latter clip is also triggered by cleavage of the amide bond, releasing electron density in the amine nitrogen to expel the (model) drug through a 1,8-elimination. Two versions of this clip were planned, the straightforward aminophenylpropargyloxycarbonyl unit and a derivative in which the propargyl CH_2 is replaced by CMe_2. It was postulated that, in the latter, expulsion of the leaving group would be speeded by relief of the steric compression between these geminal methyls as the central carbon moves from sp^3 to sp^2 hybridisation following triggering. Of course these two new clips introduce restrictions to the synthetic planning, particularly in the choice of protecting groups. The aminophenylpropargyloxycarbonyl unit will be incompatible with allyl, benzyl and Cbz-type protection, owing to the similarities in structure (Figure **21**, p86). Additionally, the aminophenyl(dimethyl)propargyloxycarbonyl unit will preclude the use of Boc and other acid-sensitive protection as it contains a tertiary carbamate. These aminophenylpropargyloxycarbonyl clips are novel and untested; therefore, a series of model compounds was designed to allow investigation of the action of the clips before incorporation into a peptide system. These models comprised simple N-protected clip-model drug systems where the protection was *e.g.* trifluoroacetyl (removed with ammonia) or Boc (removed rapidly with acid but incompatible with the dimethyl version of the aminophenylpropargyloxycarbonyl clip).

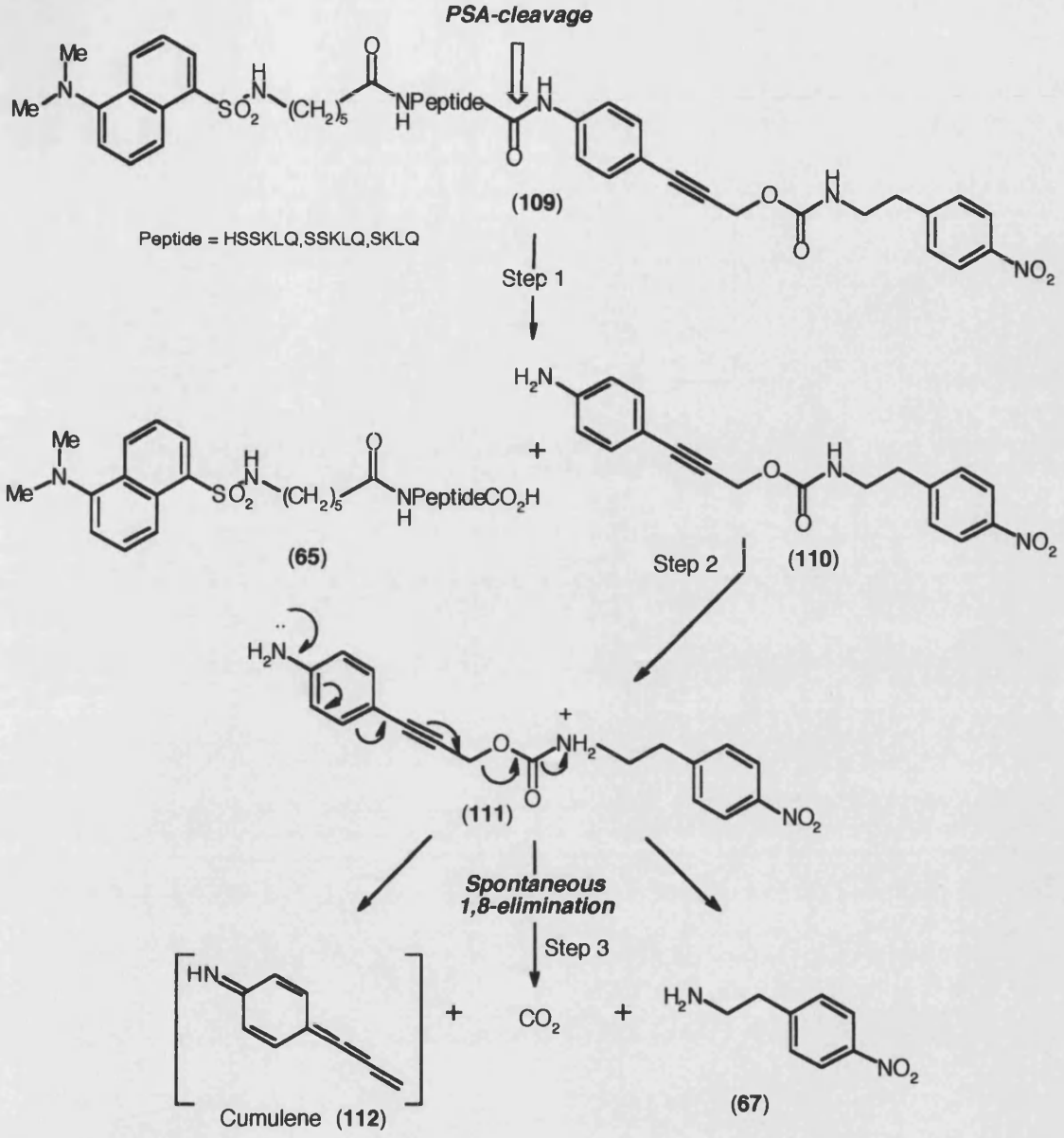

Scheme 28. *The mechanism of the PSA-triggered release of the model drug (NPEA)*

Retrosynthetic analysis of the structures of the model compounds required for testing the clip indicated several possible points of disconnection (Figure **21**, p86), firstly disconnection between the carbamate carbonyl and the nitrophenylethylamine nitrogen would require the corresponding chloroformate or equivalent to react with 4-nitrophenylethyl amine, secondly, disconnection between the carbamate carbonyl and carbamate oxygen pointed to synthesis through reaction of the aryl propargyl alcohol

with nitrophenylethyl isocyanate (**75**). Thirdly, a Sonogashira coupling of a propargyl carbamate with an iodoarene was conceivable.

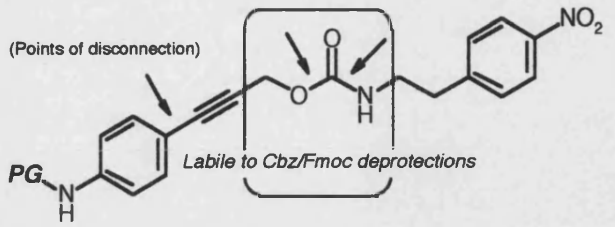

(**113**): Protecting group = Boc
(**114**): Protecting group = CF_3CO

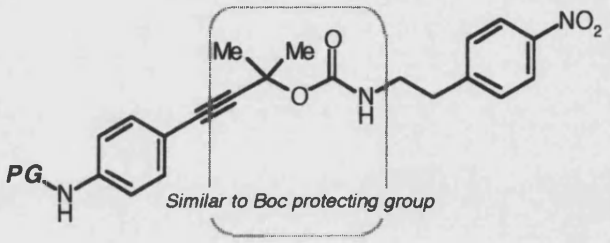

(**115**): Protecting group = Boc
(**116**): Protecting group = CF_3CO

Figure 21. *Protecting group strategies for compounds (**113-116**)*

Sonogashira cross-coupling[135] reactions are derived from the Castro-Stephens "non-palladium" coupling methods[136], where it has previously been demonstrated that a variety of aryl alkynes may be obtained by a copper-promoted cross-coupling reaction of aryl halides and copper(I) acetylides[137]. The more recent organometallic coupling strategies in aryl-alkyne coupling, are the alkyne versions of the palladium-mediated Heck reaction[138] and the (tin/zinc) metallated Negishi alkynylation[139]. Sonogashira coupling however, is considered to be more advantageous over other methods due to its versatility and high tolerance for nearly all types of functional groups. This is extremely important in our syntheses, as all of the synthetic targets contain nitro and carbonyl functional groups.

The Sonogashira reaction is responsible for cross-coupling an aryl (or vinyl) halide *(electrophile)* with a terminal alkyne *(nucleophile)* in the presence of an aliphatic amine *(base)*, a catalytic amount of a palladium-phosphine complex and copper(I) iodide in dry conditions. As presented by Sonogashira[140], the general order of reactivity of the organic halide is similar to the reactivity of the leaving group. Thus, an iodoarene generally affords quicker reaction times and higher yields compared to other halides, such as bromo and chloro. In Sonogashira reactions, there are many catalysts that can be used. It is however, more common to use Pd(II) derivatives, such as, bis(triphenylphosphine)palladium(II) chloride [$(PPh_3)_2PdCl_2$], palladium(II) acetate [$Pd(OAc)_2$] and the new catalyst of interest, tetrakis(diphenylphosphinomethyl)-cyclopentane (Tedicyp)[141], although the palladium(0) catalysts are coordinatively unsaturated and are the catalytically active species. Moreover, Pd(II) catalysts (or rather pre-catalysts) are usually more stable and less sensitive to air and generally soluble in organic solvents. Copper(I) iodide is the co-catalyst in these types of reactions and is responsible for facilitating the substitution reaction in the catalytic cycle (see Scheme **29** and **30**). Di-*iso*propylamine acts as a base during the transmetallation rate-determining step, although other bases, such as triethylamine and diethylamine can be used also.

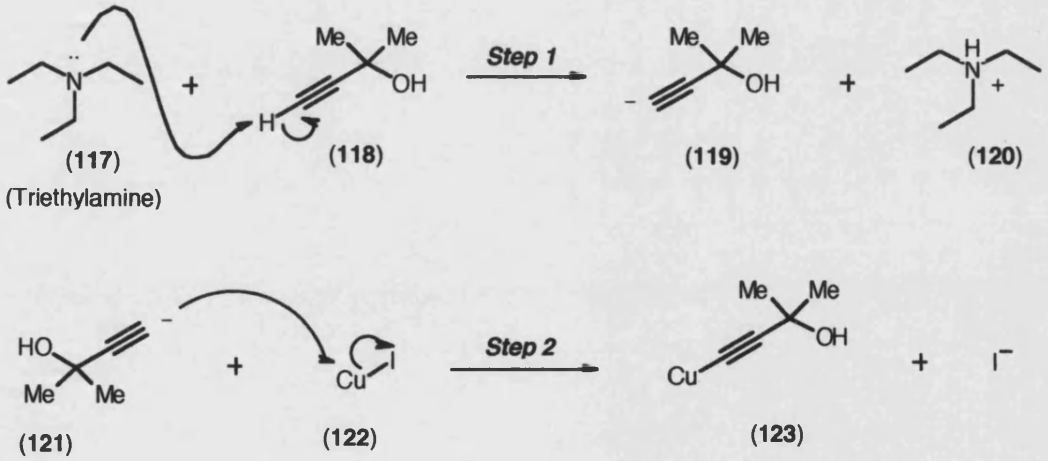

Scheme 29. *Formation of the alkynyl copper conjugate (**123**) from a reaction between 2-methyl-3-butyn-2-ol and copper(I) iodide in the presence of triethylamine*

The first model compound required was based on the trifluoroacetyl-protected type. 4-Iodoaniline (**130**) was converted to its trifluoroacetyl anilide (**129**) by treatment with the reactive ester ethyl trifluoroacetate[142] (Scheme **31**). A Sonogashira reaction of this iodo trifluoroacetyl anilide with 2-methyl-3-butyn-2-ol (dimethylpropargyl alcohol) in the presence of $[(PPh_3)_2PdCl_2]$ and copper(I) iodide under nitrogen, gave the coupled product (**126**) (Scheme **31**, p90) in good yield.

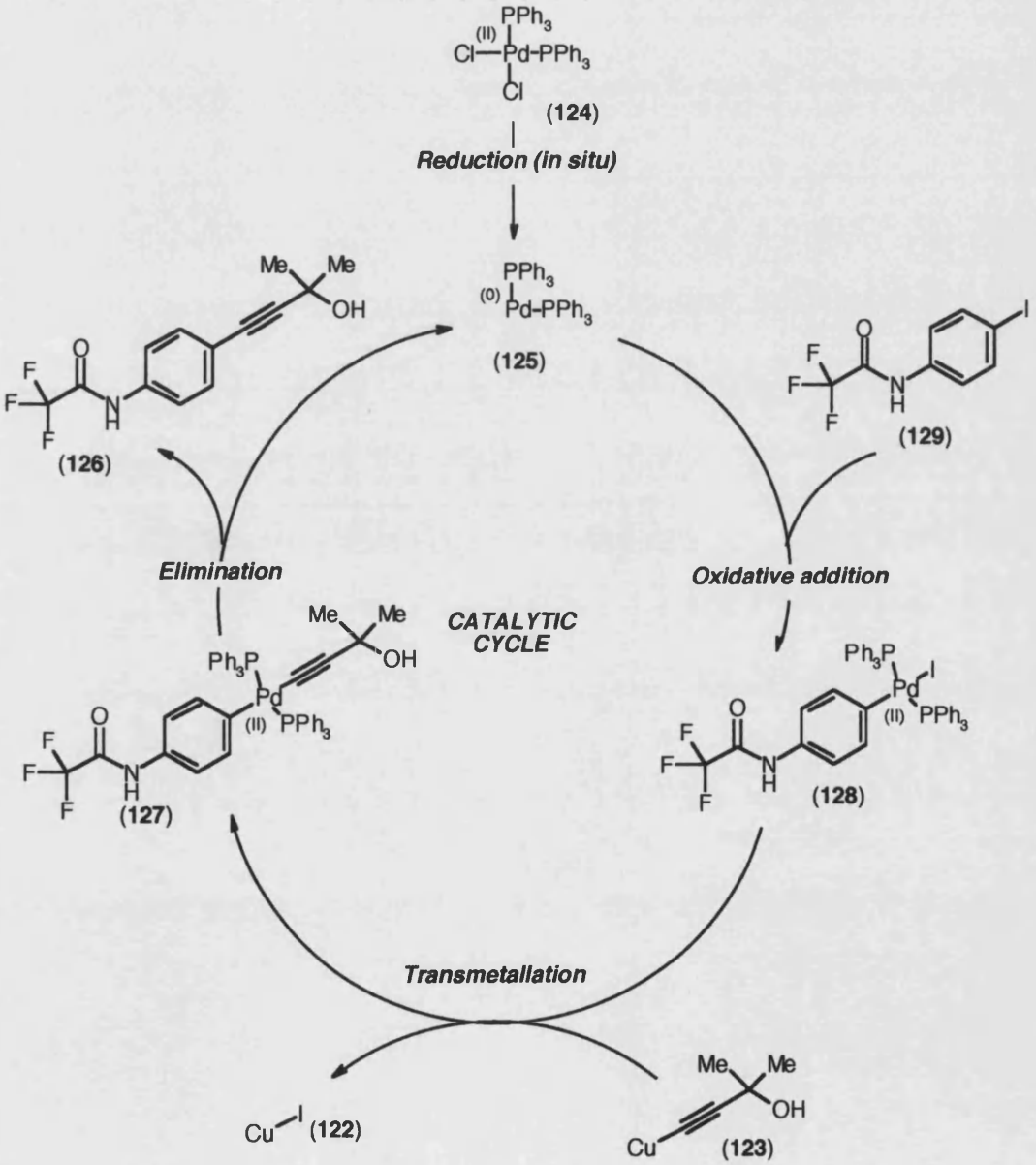

Scheme 30. *A representation of the Sonogashira catalytic cycle for compound (**126**)*

The catalyst used in the reaction was prepared separately by heating palladium(II) chloride with two equivalents of triphenylphosphine in DMF at 80°C for 24 h. Furthermore, triethylamine was the base used in this instance, as the more commonly used secondary alkyl amine (di*iso*propylamine (DIPA)) can be responsible for the removal of trifluoroacetyl-type protecting groups. In an attempt to improve the efficiency of the Sonogashira coupling reaction, effort in varying the following experimental conditions [reaction temperature, reaction time, Ar (argon) atmosphere, palladium catalyst used: tetrakis(triphenylphosphine)palladium(0) and palladium(II) acetate] were unsuccessful.

The exact detailed mechanism for Sonogashira reactions is yet to be established, though it has been proposed by Sonogashira[135,140], that the required substitution occurs *via* a catalytic cycle consisting of three stages (Scheme **30**, p88). Above is an example of these stages for formation of the required intermediate (**126**).

At this point, it was necessary to convert the tertiary alcohol of (**126**) to its corresponding chloroformate or its equivalent for reaction with 4-nitrophenylethyl amine to form the required carbamate[143,144].

Chloroformates are normally synthesised by treatment with excess phosgene, however this reagent is highly toxic and its use can be avoided by using 4-nitrophenyl chloroformate. Reaction of alcohols with 4-nitrophenyl chloroformate normally gives the corresponding 4-nitrophenyl carbonates, which are synthetic equivalents of chloroformates. The advantages of using these carbonates are the use of a solid and less toxic reagent and the opportunity to characterise and sometimes isolate the 4-nitrophenyl carbonate before the reaction with an amine. Unfortunately, the tertiary alcohol (**126**) could not be converted to its corresponding carbonate under a variety of conditions, this failure maybe attributed to the presence of a highly acidic NH in the trifluoroacetamide moiety, which is removed preferentially by the triethylamine base.

Attention was then turned to the Boc protected model in which the corresponding NH proton would be expected to be much less acidic. 4-Iodoaniline was treated with di-*tert*-butyl carbonate under the usual conditions to give the Boc protected compound (**131**) in good yield (Scheme **31**). Sonogashira coupling of 2-methyl-3-butyn-2-ol to give the Boc protected compound (**131**), was very effective in proving useful quantities of the arylalkyne alcohol to give the Boc protected compound (**132**). In this case it was possible to use DIPA as the co-solvent and base, very dry conditions was essential for all the Sonogashira couplings.

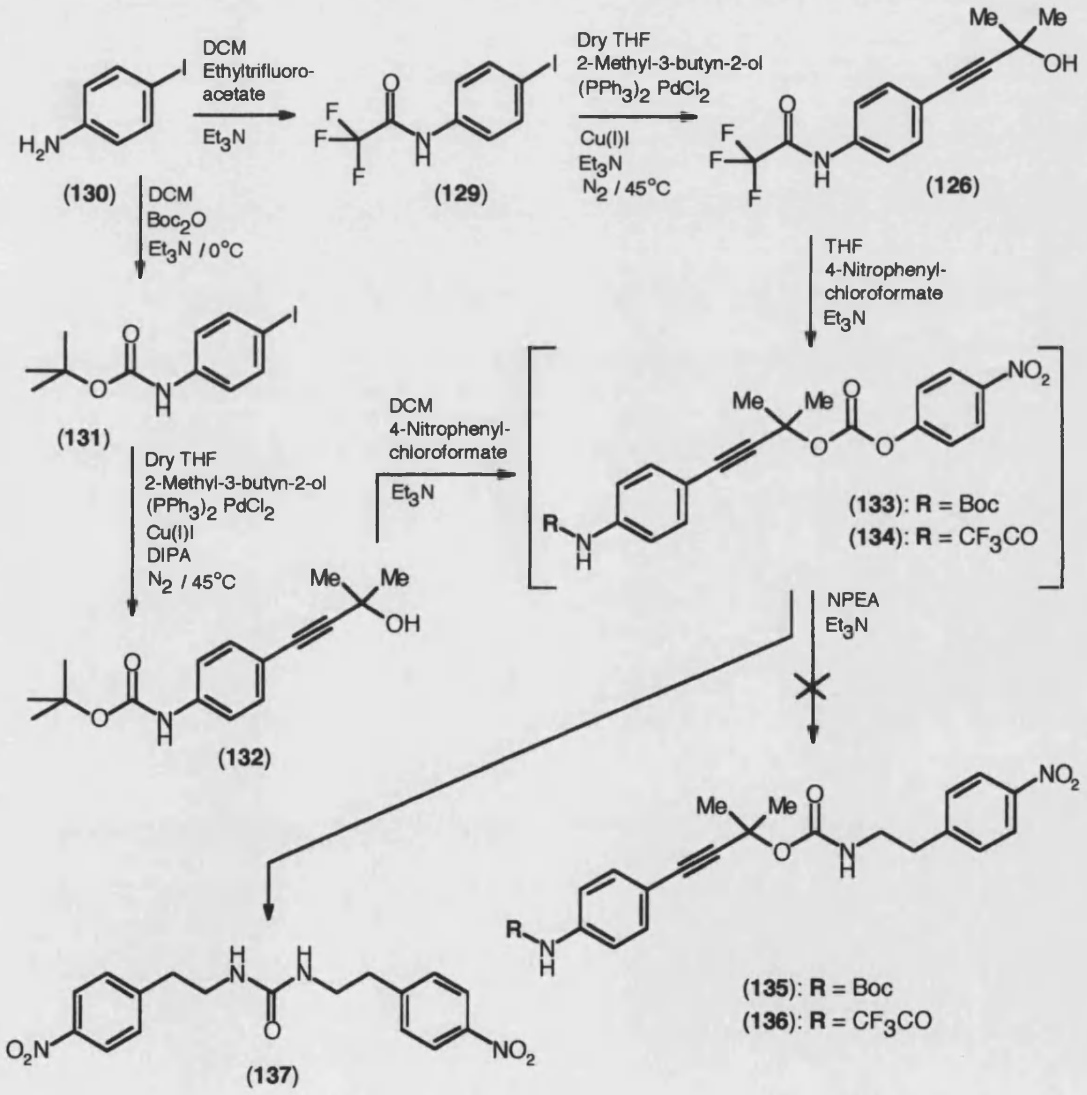

Scheme 31. *A schematic representation showing the attempted syntheses of compounds (**135,136**)*

The tertiary alcohol (**132**) was taken forward for treatment with 4-nitrophenyl chloroformate in an attempt to obtain the mixed carbonate (Scheme **31**, p90). It was anticipated that characterisation of the product carbonate by ^{1}H NMR would be challenging since it would be expected that there would be no significant change in the chemical shifts of the proton signals from the alkyne containing unit and possibly little change in the chemical shift of the nitrophenyl protons when compared to the starting materials. Since the tertiary alcohol oxygen is becoming acylated one would expect a significant downfield shift of the signal for the quaternary carbon to which this oxygen is attached. Thus, it was important to assign rigorously the ^{13}C NMR spectrum of the tertiary alcohol and, in particular to identify the signal from this quaternary carbon. The signals due to the methyl groups appear at δ 28.35 and δ 31.56 ppm, as shown by 135 DEPT spectrum. This spectrum also showed CH signals at δ 117.99 and δ 132.08 ppm. Quaternary carbon signals were observed at, δ 65.64, at δ 80.86, at δ 81.96, at δ 92.96, at δ 116.93, at δ 138.47 and δ 152.52 ppm. An HMQC (Figure **22**, p92), which shows cross peaks between directly bonded carbons and proton, showed that the up-field methyl signal at δ 28.35 ppm correlated with the Boc protons, confirming that this signal could be assigned to the Boc methyl carbons. Similarly, a cross peak linking the signals for the geminal Me_2 protons with the downfield methyl carbon signal at δ 31.56 ppm, confirmed the latter as being due to geminal Me_2 carbons. Assignment of CH tertiary carbons however was not possible by using HMQC (Figure **22**, p92), since the signals for all the aromatic protons were accidentally coincident, appearing as a 4-proton singlet at δ 7.34 ppm. The calculations of the predicted chemical shifts were made based on the formula given by Williams and Fleming[116] ($\delta_c = 128.50 + Z^i + Z^o + Z^m + Z^p$); these calculations predict δ 110.40 ppm for the carbons *ortho* to the nitrogen and δ 131.80 ppm for the carbons *ortho* to the alkyne. These values are sufficiently different from each other to assign the observed signal at δ 117.99 ppm to the carbons *ortho* to the nitrogen and δ 132.08 ppm to the carbons *ortho* to the alkyne. Similar calculations confirmed that the aromatic carbon carrying the nitrogen resonated at δ 138.47 ppm and the carbon carrying the alkyne resonated at δ 116.93 ppm. Clearly, the carbonyl gives rise to the signal at δ 152.52 ppm.

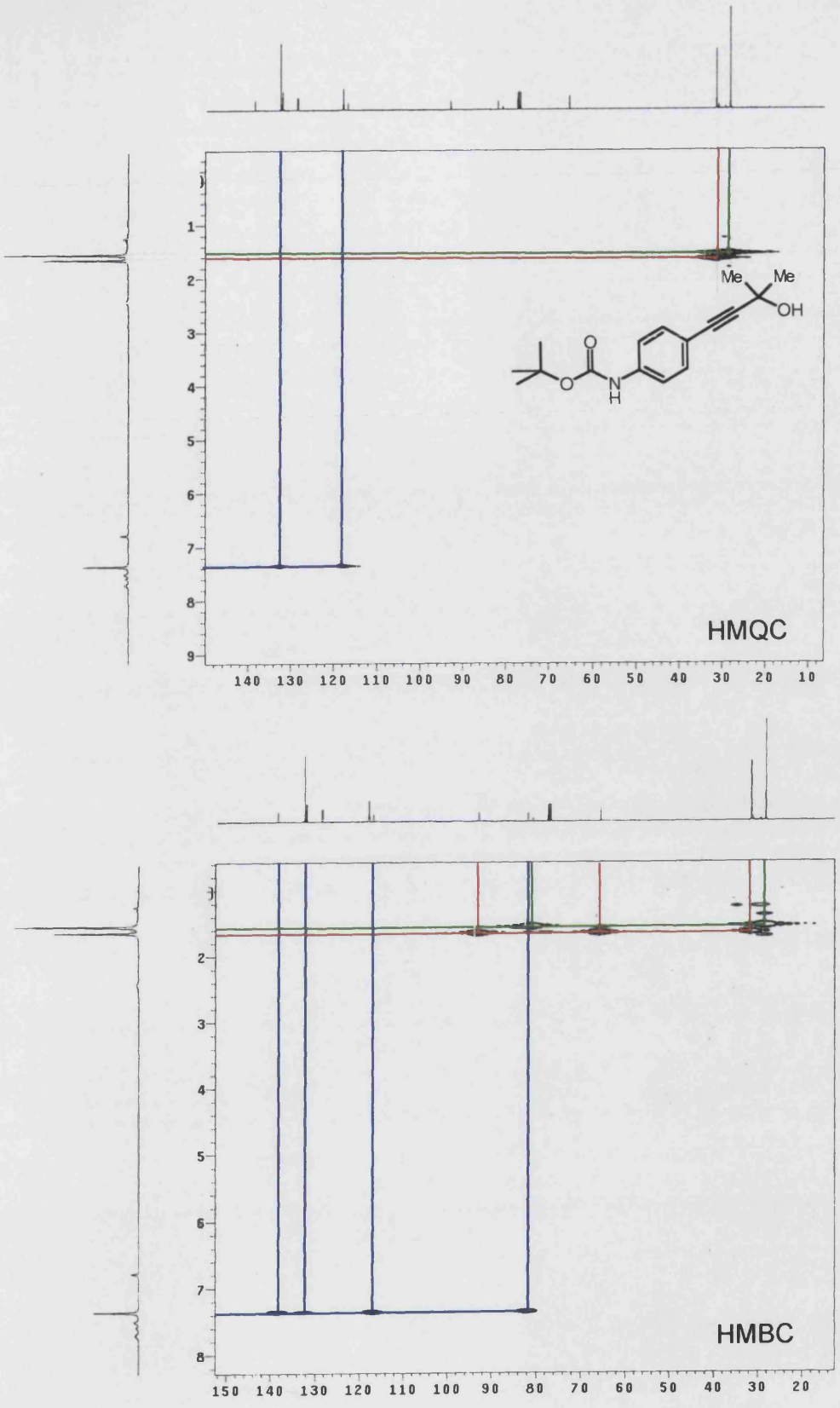

Figure 22. *HMQC & HMBC spectra for compound (**132**) (axis x = δ_C and axis y = δ_H)*

None of these methods allowed the confident assignment of the remaining 4-quarternary carbon signals. For this purpose, an HMBC was obtained. This 2D spectrum shows cross peaks between carbon and proton signals where the protons and carbons are coupled through 2 or 3 bonds. Firstly, observation of an HMBC (Figure **22**, p92) cross peak between the proton signal at δ 7.34 ppm and the carbon signal at δ 80.86 ppm confirmed the latter as being the alkyne carbon attach to the benzene ring. The Boc methyl proton signal correlated with the carbon signal at δ 81.96 ppm, thus the latter arises from the quaternary Boc carbon. However, since the geminal Me_2 proton signal gave cross peaks to both the remaining carbon signals, these could not be differentiated by HMBC spectroscopy since the alkyne carbon lies 3 bonds from these protons and the sp^3 quaternary carbon lies 2 bonds from these protons. Therefore, predicted calculations for the chemical shift were made which allowed assignment of the signal at δ 65.64 ppm to the COH carbon and of the signal at δ 92.96 ppm to the adjacent alkyne carbon (Figure **22**).

Unfortunately the reaction of the tertiary alcohol (**132**) with 4-nitrophenyl chloroformate gave materials that appeared to be a mixture of the starting alcohol and 4-nitrophenol. It maybe that the tertiary alcohol was just too sterically hindered to react effectively as a nucleophile.

In a further experiment, the reaction mixture of the tertiary alcohol and the 4-nitrophenyl chloroformate was treated *in situ* with triethylamine to test whether any mixed carbonate had been formed in the reaction. The isolation of a substantial yield of the bis(nitrophenylethyl)urea (**137**) however, demonstrated that the 4-nitrophenyl chloroformate had not reacted with the tertiary alcohol (**132**) and had therefore been available for reaction with the stronger nucleophile NPEA (**67**) (Scheme **31**).

The alternative disconnection at the arene-alkyne bond was then studied. In view of the poor nuclophilic reactivity of the tertiary alkyne alcohol noted above, this strategy was investigated using the propargyl analogue lacking the methyl substituents Scheme **32**). The critical intermediate in this sequence is the propargyl-NPEA-carbamate

(**140**), which is required for Sonogashira coupling to peptidyl iodoanilides as the final step in the assembly of the prodrugs. Sonogashira couplings are tolerant to a wide variety of functional groups including those found in anticancer drugs such as doxorubicin (**13**) and daunorubicin (**14**) (refer to Chapter 1, section **1.1.6.5.4**). Thus, this reaction is apposite for the final step in the construction of the final prodrug system. To this end, propargyl alcohol (**138**) was acylated with an equimolar amount of 4-nitrophenyl chloroformate under mild conditions to give the propargyl-NPEA-mixed carbonate (**140**).

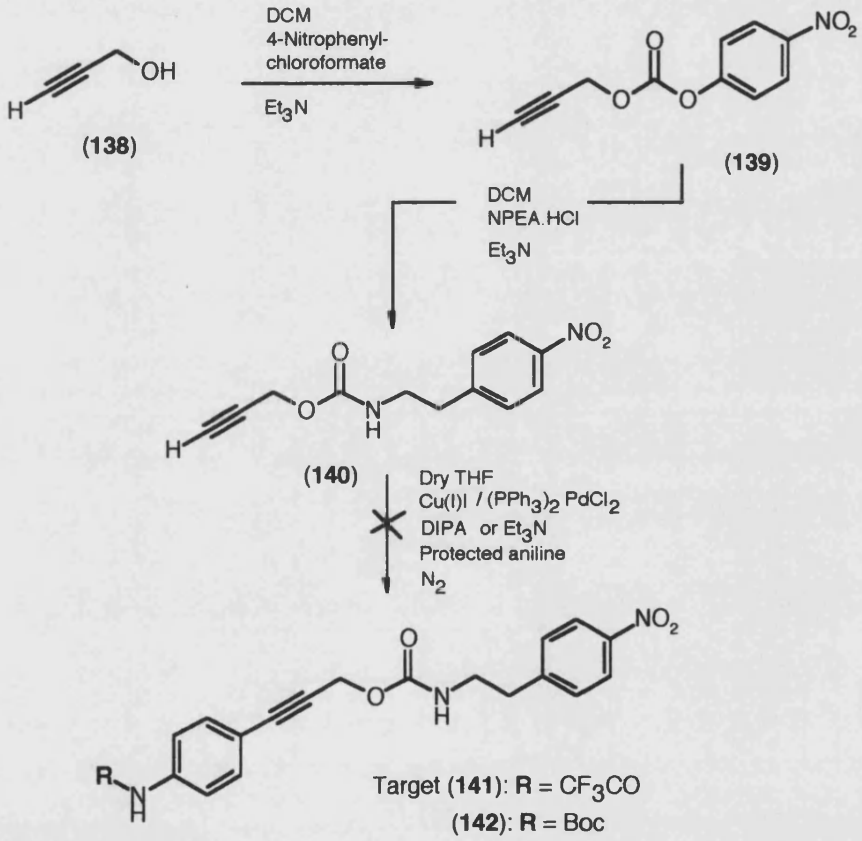

Scheme 32. *Attempted syntheses towards carbamates (**141** & **142**)*

The mild conditions were necessary to avoid nuclophilic displacement of nitrophenoxide from the product. The mixed carbonate is a good electrophile and is the synthetic equivalent of the corresponding chloroformate. Reaction with 4-

nitrophenylethylamine gave the target carbamate (**140**) in very good yield. There was no evidence for displacement of the propargyloxy group. This can be rationalised, as 4-nitrophenoxide is a much better leaving group than propargyloxide (pKa of 4-nitrophenol is 7.15 and the pKa of a typical aliphatic primary alcohol is approximately 15).

With this important carbamate (**140**) readily available, attention was turned to optimising the Sonogashira coupling of this alkyne with 4-iodoanilides. Initial experiments with model iodoanilides were discouraging in that the reaction of 4-iodotrifluoroacetyl anilide (**129**) and *tert*-butyl N-4-iodophenyl carbamate (**131**) with the alkyne (**140**) under Sonogashira conditions with a variety of palladium catalysts (as mentioned previously), failed to give significant yields of the coupled products (**141**) and (**142**) respectively.

Undaunted by these results of these model compounds, studies were initiated on Sonogashira couplings of propargyl carbamate (**140**) with amino acids and peptide 4-iodoanilides. As discussed above, formation of anilides from BocGln and 4-substitued anilines, especially those carrying electron-withdrawing groups in the 4-position, is difficult. In this case BocGlnOPFP (**78**) failed to react with 4-iodoaniline, but use of the pivaloyl mixed anhydride method, which had proven good results with other anilines, allowed the synthesis of the BocGln-iodoanilide (**145**) in 10-15% yield after optimisation. Much of the difficulty in achieving high isolated yields can be attributed to the very poor solubility of the product in most solvents. Contrary to the BocGlnOPFP (**78**) failing to react with 4-iodoaniline, a similar coupling with FmocGlu(O-*tert*-butyl)OPFP (**143**) gave the corresponding anilide (**144**) (Scheme **33**, p96) in 11% yield; this coupling was an attempt to avoid the sparingly soluble intermediate BocGln-iodoanilide (**145**), as the side chain ester could be later converted to a primary amide. However, the low coupling yields obviated this potential advantage. Since this iodoanilide was critical to this synthetic sequence, an alternative route was investigated in an attempt to improve the overall yield of this material.

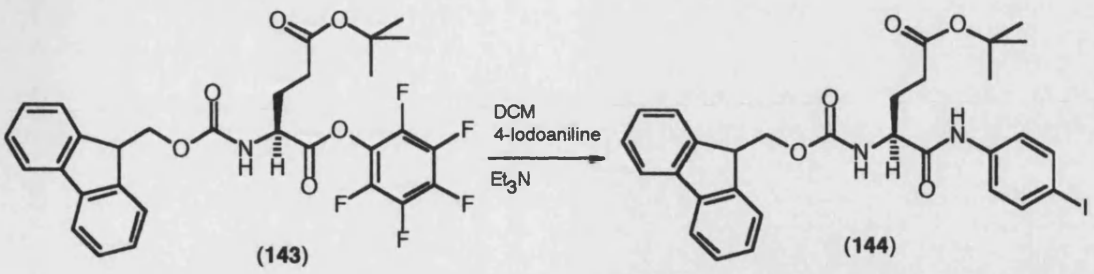

Scheme 33. *The synthesis of anilide (**144**) from its OPFP-ester*

Pyroglutamic acid (Pyg) (**146**) is an analogue of glutamic acid (Glu) where the side chain carboxylic acid has formed an amide with the alpha amine. Although ring opening of pyroglutamic acid with nucleophiles is very difficult and requires forcing conditions, as it is a gamma lactam, acylation of the nitrogen converts it to a much more electrophilic imide. Thus BocPyg (**146**) can be considered as a potential synthon for Gln and is much more lipophilic than the latter.

Pyroglutamic acid (**146**) was converted efficiently to its benzyl ester (**147**) by alkylation of the carboxylate with benzyl chloride[145] (Scheme **34**, p97). This esterification serves to mask the carboxylate nucleophile during the introduction of the N-Boc group. Treatment of the PygOBn (**147**) with an excess of di-*tert*-butyl carbonate and triethylamine, furnished BocPygOBn (**148**) in good yield. This acylation of a lactam nitrogen proceeded well despite amides normally having much lower nucleophilic reactivity than amines. The carboxylic acid was then revealed by hydrogenolysis of the benzyl ester[146] (**148**). The carboxylate was activated as its OPFP ester in the usual way. This active ester reacted slowly with the weakly nucleophilic 4-iodoaniline to give BocPyg-iodoanilide (**151**) (Scheme **34**, p97) in modest yield. It is noteworthy, that the reaction of BocPygOPFP with 4-iodoaniline was significantly more efficient than the corresponding reaction of BocGlnOPFP with this nucleophile. Also, the pivaloyl mixed anhydride coupling of BocPygOH with iodoaniline, gave BocPyg-iodoanilide (**151**) in a similar modest yield.

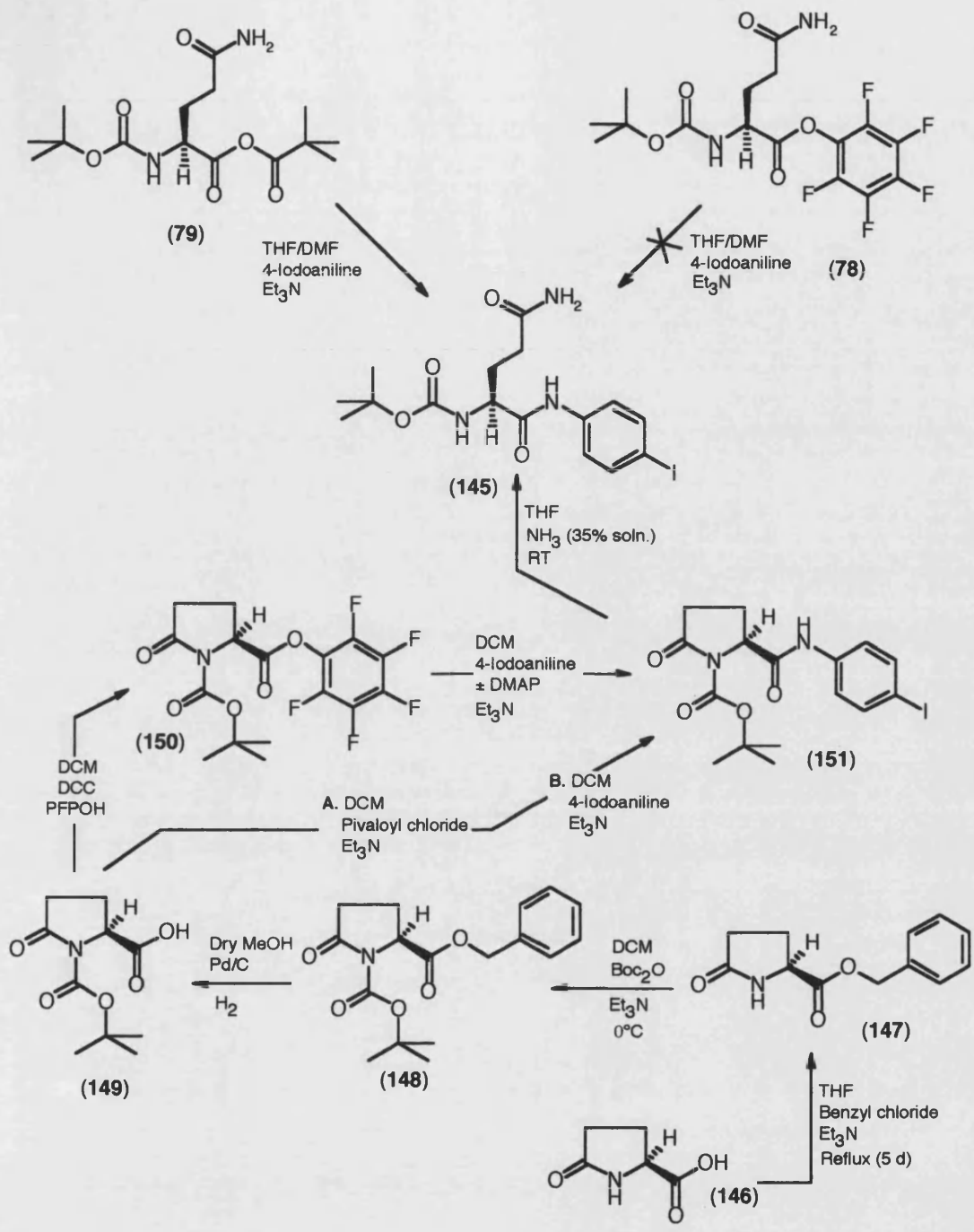

Scheme 34. *A schematic representation of multiple synthetic ways to target intermediate (**145**)*

The BocPyg-iodoanilide (**151**), lacking the primary amide of glutamine derivatives, was reasonably soluble in organic solvents and could be readily purified by column chromatography. At this point, simple treatment of ammonia in THF, gave the

BocGln-iodoanilide (**145**) in high yield. Clearly the nitrogen nucleophile has attacked the less sterically crowded of the two carbonyls of the imide, as there was no evidence of the formation of BocPyg-iodoanilide (**151**). Thus, BocPyg is shown to be a potentially useful synthetic equivalent of Gln in building peptide constructs, although its use in this context has been scarcely reported previously. Comparing the three approaches to BocGln-iodoanilide (**145**), the overall yields are similar, but the apparent advantage with solubility of the Pyg route, is balanced by the fact that is a long six-step linear sequence.

Given the success of the coupling of the BocPygOPFP (**150**) with iodoaniline, it was conjectured that this active ester may react with the amino group of 4-aminobenzyl alcohol (refer to Scheme **35** below) to give, after ring opening with ammonia, BocGln-benzyl alcohol (**83**). However, no useful coupled material was obtained. Similarly, couplings of BocPygOH (**146**) with this aniline using pivaloyl mixed anhydride couplings and EEDQ/DCC[147] also failed (Scheme **35**).

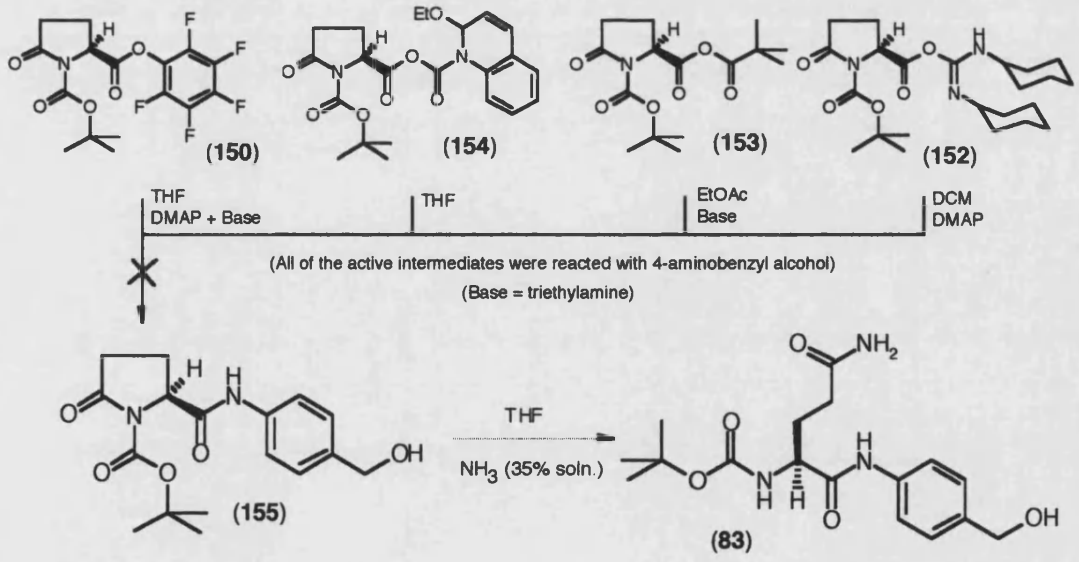

Scheme 35. *Attempted syntheses to target compound (**83**)*

At this point, there were two possible alternatives for approaching the target peptide prodrug construct (**109**). Either the required peptide could be built onto Gln-

iodoanilide (**146**), followed by Sonogashira coupling with the propargyl carbamate (**140**), or the Sonogashira coupling could precede the peptide synthesis. Clearly the former would be more synthetically efficient, particularly when doxorubicin and other anticancer drugs are used, as it is more convergent.

Removal of the Boc protecting group[148] of the BocGln-iodoanilide (**145**) was needed for coupling with amino-acid derivatives to develop the peptide. BocGln-iodoanilide was treated under mild conditions with HCl (gas) in methanol to give Gln-iodoanilide.HCl salt (**158**), which was coupled *in situ* with BocLeuONSu to give the protected dipeptide anilide (**159**). Isolation of the Gln-iodoanilide.HCl salt was not possible owing to its instability. Indeed, deprotection by dissolution of BocGln-iodoanilide in TFA[149] did remove the Boc group but also triggered cyclisation with loss of ammonia to give Pyg-iodoanilide (**156**) (Scheme **36**, p100). This material was readily purified as it was non-basic and readily soluble in organic media. Its structure was firmly characterised by ^{1}H NMR and mass spectrometry. The feature in the ^{1}H NMR spectrum, which most markedly identified the compound as the gamma lactam, was the signal for the α-proton at δ 4.14 ppm which comprised a double doublet with coupling constants, J = 4.4 and J = 8.2 Hz. These values are different from the coupling constants for open-chain Gln derivatives, but are typical for the coupling to the two β-protons in the 5-membered ring of Pyg. Interestingly, no coupling was observed between the α-proton and the lactam NH. In open-chain Gln peptides, the α-proton to NH is typically in the range of 4-8 Hz, but a chemical 3D model suggests that the dihedral angle between the α-proton and lactam NH is close to 90 degrees (see Appendix Figure **28**), suggesting a coupling constant of zero according to the Karplus relationship. From one run using trifluoroacetic acid (TFA) as the deprotecting agent for a very short contact time, the Gln-iodoaniliide.TFA salt (**157**) was obtained. Examination of the FAB+ mass spectrum of this salt and of Pyg-iodoanilide (**156**) (formed in most runs with TFA), revealed some interesting features. The base peak in the spectrum of the Pyg compound was the M+H ion of *m/z* at 331 with no abundant fragment ions. Peaks were also seen for clusters of M+H + 3-nitrobenzyl alcohol matrix at *m/z* 484 and *m/z* 637 (continued on page 101).

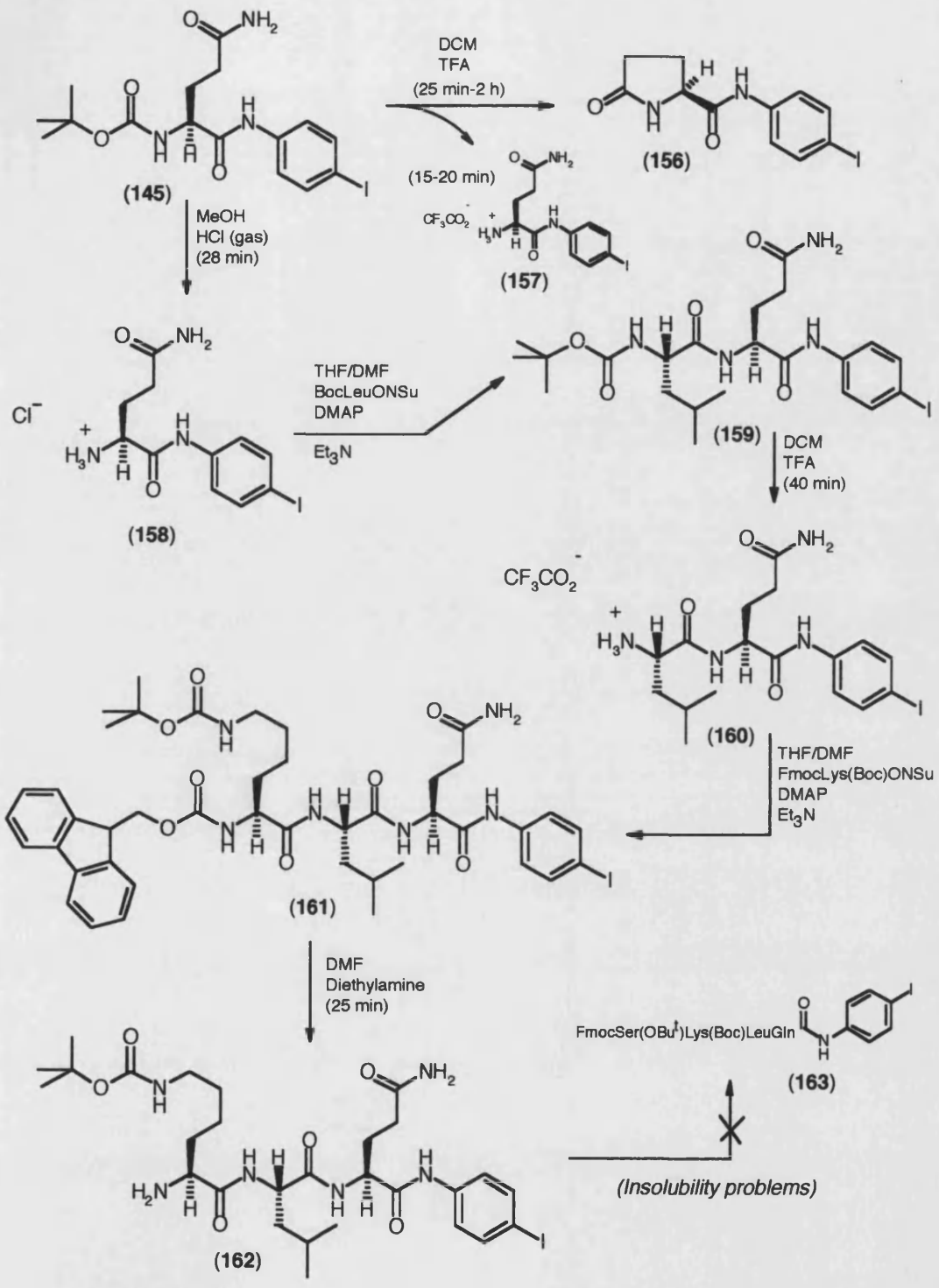

Scheme 36. *A synthetic route to the tetrapeptide target intermediate (**163**)*

The spectrum of the Gln-iodoanilide.TFA salt (**157**), showed a strong molecular ion at *m/z* 348 with a M+H + 3-nitrobenzyl alcohol at *m/z* 501. Interestingly, each spectrum obtained from the Gln-iodoanilide.TFA salt and the analogous HCl salt (**158**), showed a significant fragment ion at *m/z* 331. This indicated loss of ammonia from the parent ion and reflects the propensity of this type of salt to undergo cyclisation to the Pyg derivative.

Having observed this novel cyclisation of BocGln-iodoanilide (**145**) and BocGln-methoxycarbonylanilide (**90**) to the Pyg anilides with acids under mild conditions, one experiment was conducted to investigate whether this reaction could be extend to N-alkyl glutamine amides (Scheme **37**). BocGlnNPEA (**164**) was dissolved in TFA; the ^{1}H NMR spectrum obtained after a few minutes, revealed the characteristic signals for the Pyg-nitrophenylethylamide (**165**) (where it has been assumed that the stereochemistry has not altered) and the 1-1-1 triplet for ammonium trifluoroacetate. Pyg-NPEA (**165**) was isolated in high yield from this mixture. Thus, this cyclisation is potentially a significant problem in the deprotection of BocGln derivatives.

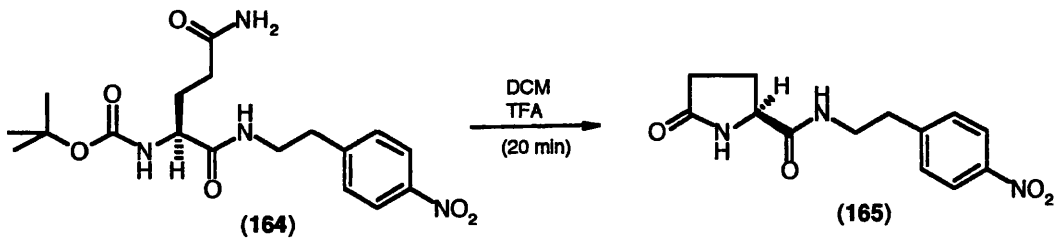

Scheme 37. *A cyclisation to compound(**165**) from the Boc deprotection of compound (**164**)*

In contrast, the removal of the Cbz group from CbzGln-nitroanilide (**166**), formed from a pivaloyl mixed anhydride coupling of CbzGlnOH (**50**) with 4-nitroaniline under highly acidic conditions (HBr (30% in acetic acid)), gave no trace of the Pyg cyclisation product (Scheme **38**, p102). Gln-nitrophenylanilide.HBr salt (**167**) was obtained in a quantitative yield and was coupled efficiently with BocLeuONSu to give the protected dipeptide nitroanilide (**168**) as a demonstration of the utility of this procedure.

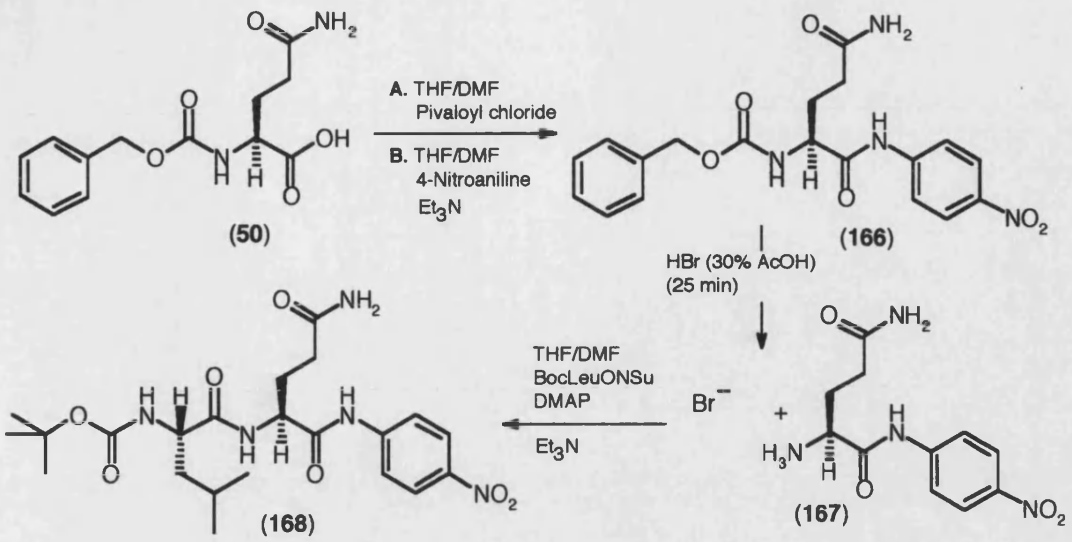

Scheme 38. *A schematic route to dipeptide (**168**)*

Returning to the main reaction sequence towards the target peptide iodoanilide reaction of Gln-iodoanilide.HCl (**158**) with BocLeuONSu, efficiently gave the protected BocLeuGln dipeptide iodoanilide (**159**) (Scheme **36**, p100). From here, the Boc protection was removed under acidic conditions, giving LeuGln-iodoanilide (**160**) to which FmocLys(Boc) was introduced using FmocLys(Boc)ONSu (Scheme **36**). As noted above, the Fmoc and Boc protecting groups are fully orthogonal and treatment of the protected tripeptide (**161**) with diethylamine, afforded Lys(Boc)LeuGln-iodoanilide (**162**). This material was sufficiently soluble in the dipolar aprotic solvent DMSO to allow a proton ^1H NMR spectrum to be attained, but it was too insoluble in solvents suitable for peptide coupling to permit further chain extension.

Since it was not possible to assemble the tetrapeptide iodoanilide (**163**) (Scheme **36**), the next series of experiments investigated Sonogashira couplings onto BocGln-iodoanilide (Scheme **39**, p103). Although propargyl alcohol has been reported to give very poor yields[150] for Sonogashira couplings, treatment of the BocGln-iodoanilide (**145**) with propargyl alcohol in DIPA and DMF in the presence of bis(triphenylphosphine) palladium(II) chloride and copper(I) iodide under very dry conditions, did give a moderate yield of the arylpropargyl alcohol (**169**).

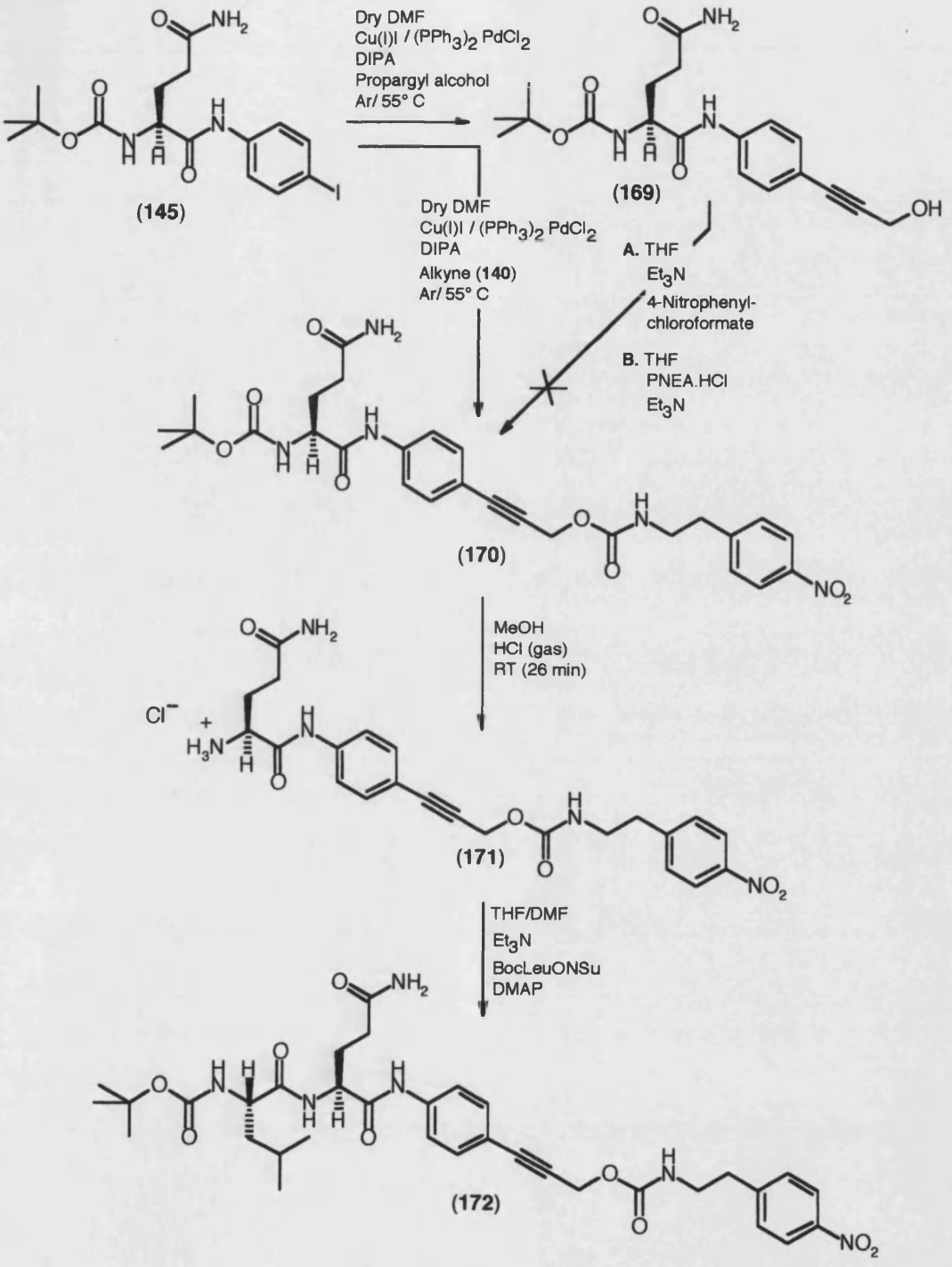

Scheme 39. *The synthesis of the target alkyne molecular clip derivative (**172**)*

However, this could not be elaborated to the carbamate (**170**) *via* the 4-nitrophenyl carbonate. In contrast, the Sonogashira coupling of the pre-assembled propargyl carbamate (**140**) with BocGln-iodoanilide (**145**) was successful in furnishing a useful quantity of the target intermediate BocGln-*CLIP*-model drug (**170**) (see ^{1}H NMR in Figure **22**). Removal of the Boc deprotection with HCl in MeOH for a very short contact time (to avoid Pyg formation), followed by coupling with BocLeuONSu in the presence of DMAP, afforded the dipeptide-*CLIP*-model drug target (**172**) in a good yield (Scheme **39**, p103). This has the potential for elongation of the peptide sequence to give the advanced target containing the PSA-sensitive sequence, a self-immolative molecular clip and the model drug.

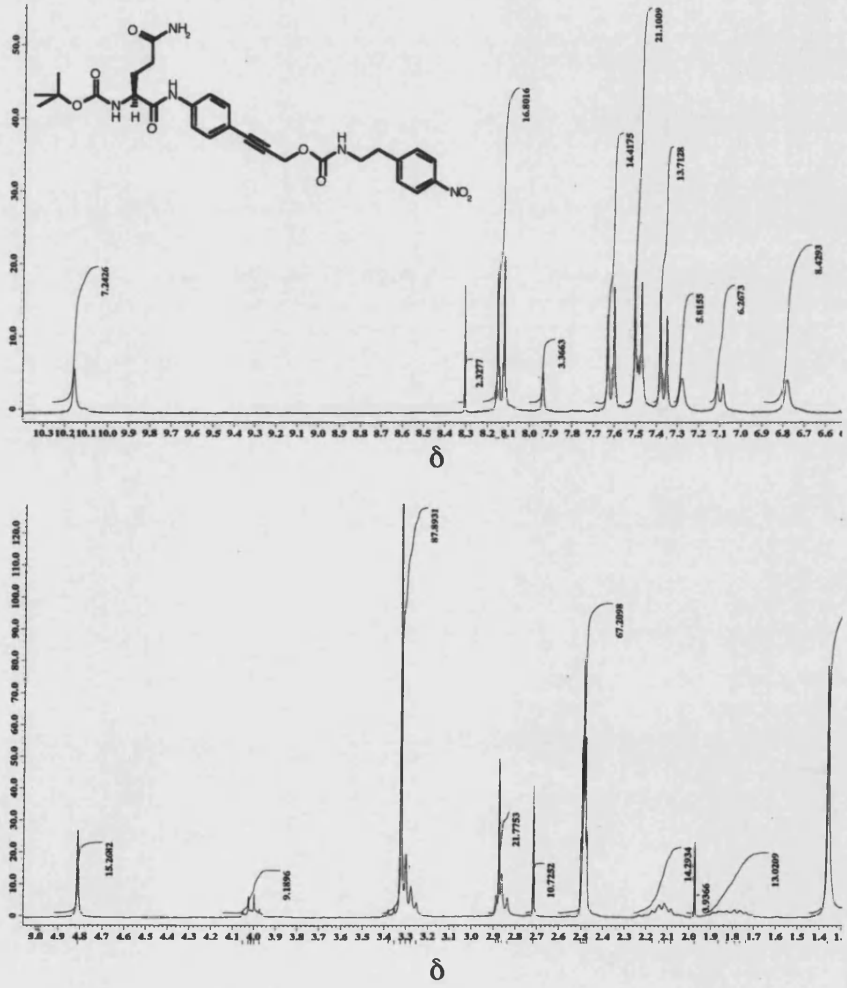

Figure 23. *A ^{1}H NMR spectrum for compound (**170**) (scales in ppm)*

3.4 Synthesis of a monomeric model for chymotrypsin-triggered release of model drug (NPEA)

In parallel with the above synthetic approaches to PSA-triggered prodrug systems, which required tetra-peptides and penta-peptides containing "difficult" amino acids, an approach towards a simpler construct designed for triggering by chymotrypsin was initiated.

Chymotrypsin is a serine protease related to PSA but with a different sequence selectivity. It normally cuts peptides at the C-terminal side of aromatic amino acids, especially phenylaniline[103]. Thus the construct AlaPhe-*CLIP*-model drug (**180**) (Scheme **40**, p106) was devised as a system in which the function of this new (alkyne) self-immolative molecular clip could be tested under enzymic conditions. The chymotrypsin, a cheap and readily available enzyme should cleave between the Phe and the aniline releasing the aminophenylpropargyl carbamate (**111**) (refer to Scheme **28**, p85).

BocPheOH (**173**) was converted to its pivaloyl mixed anhydride which reacted *in situ* with 4-iodoaniline (**130**) to give the BocPhe-iodoanilide (**175**) in modest yield. Acidolytic removal of Boc furnished Phe-iodoanilide (**176**) quantitatively for coupling with BocAlaOPFP (which was prepared in the usual way from BocAlaOH with PFP and DCC, Scheme **40**). The required protected dipeptide iodoanilide (**179**) was formed smoothly and is now available for future Sonogashira coupling with propargyl carbamate (**140**).

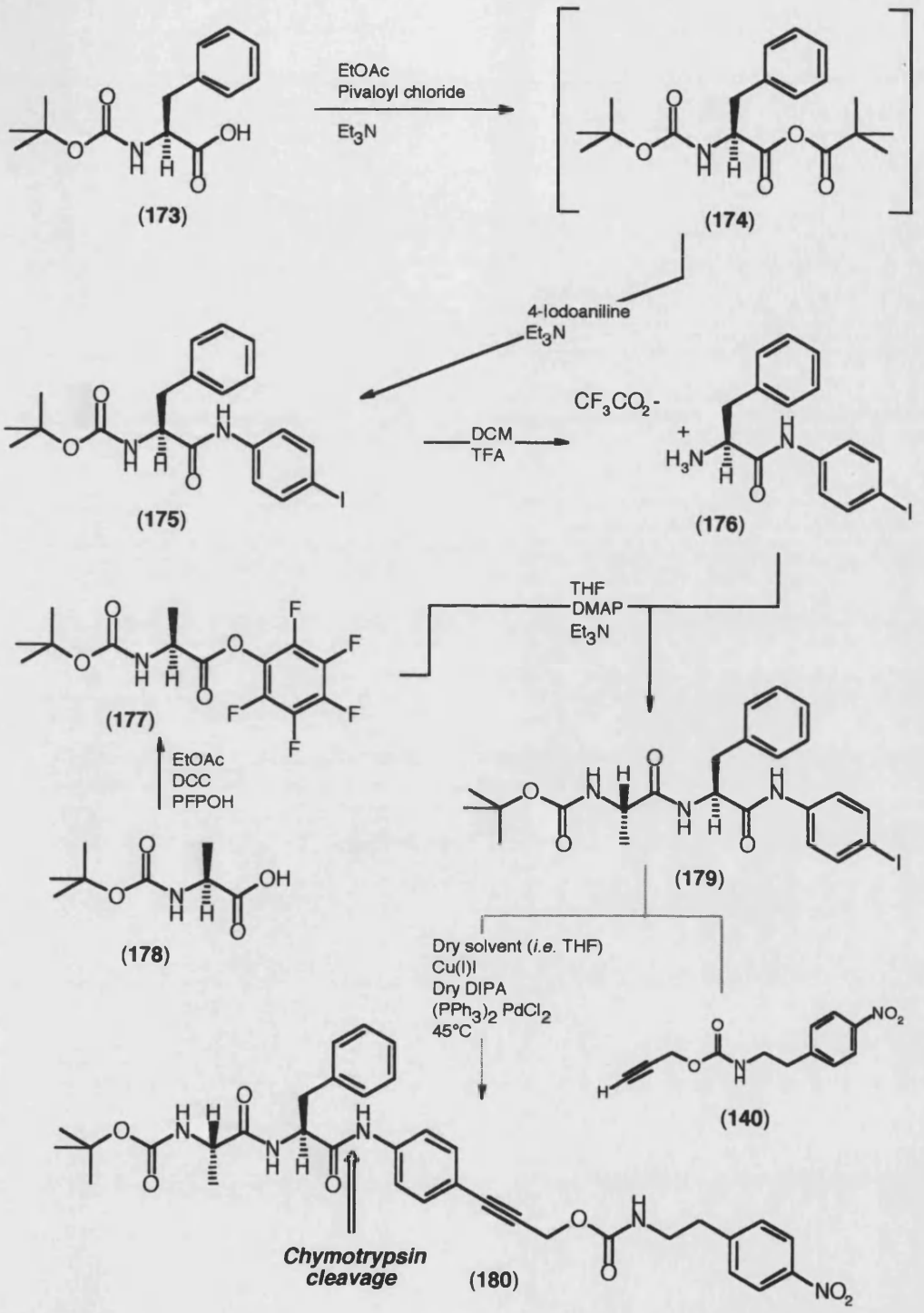

Scheme 40. *The synthesis of the chymotrypsin-sensitive monomeric model*

3.5 Synthesis of the N-terminal fluorescent marker

In the overall design of the advance model prodrug system, it was planned to incorporate a fluorescent marker at the PSA-sensitive peptide to mimic the eventual polymer backbone and to report on the fate of the peptide sequence during the enzymatic reaction with PSA (see below in Scheme **41** and refer also to Chapter 2).

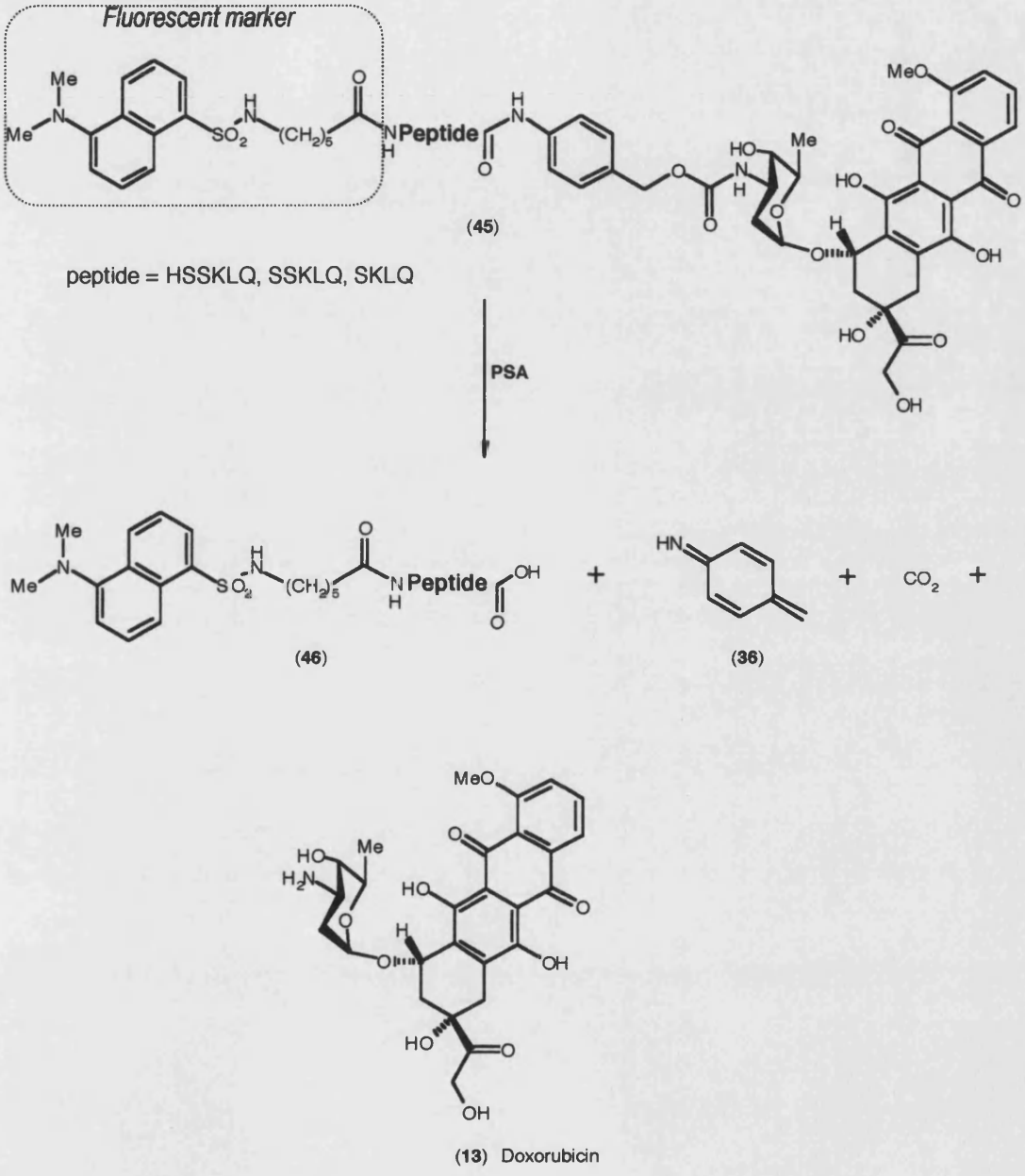

Scheme 41. *The use of the fluorescent marker in the PSA-triggered release of doxorubicin from the monomeric model (this fluorophore would be viable for either molecular clip system)*

Dansyl (5-dimethylaminonaphthalene-1-sulfonyl) is a convenient biocompatible fluorophore. To avoid any possible steric encumbrance of the dansyl group with the enzyme active site, it was proposed to link the dansyl to the N-terminals of the peptides through a simple 6- carbon linker.

6-Aminohexanoic acid was converted quantitatively to its methyl ester[151] with thionyl chloride in MeOH. This protection stops the 6-aminohexanoyl unit being zwitterionic and aids its solubility in organic solvents, correspondingly, the amine (**182**) was treated with dansyl chloride[152,153] in a THF/DMF mixture in the presence of triethylamine to give the 6-dansylaminohexanoate ester (**183**) in 72% yield.

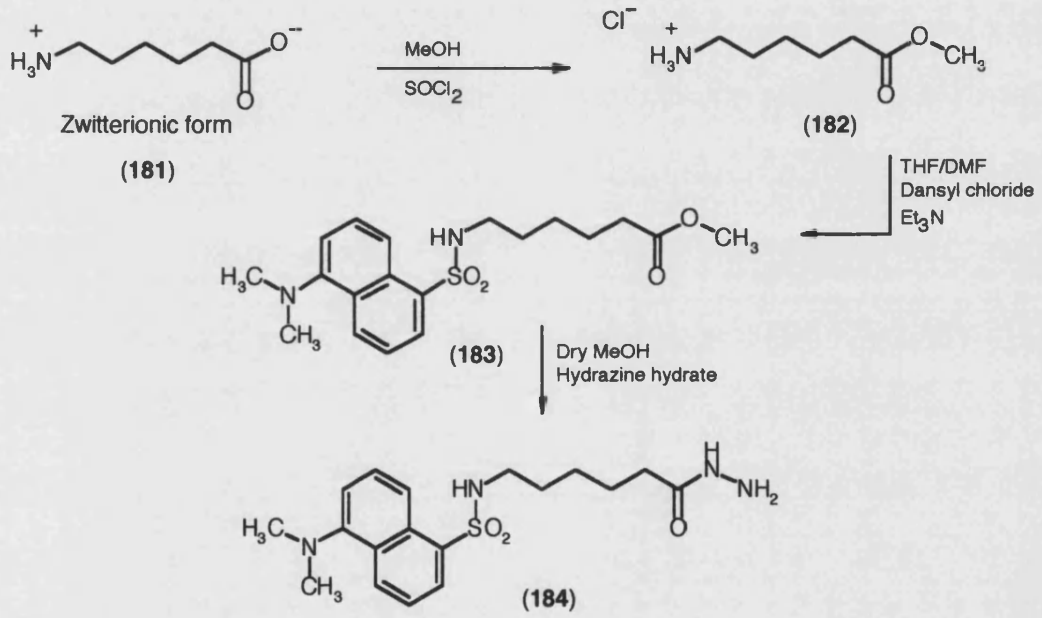

Scheme 42. *The synthetic steps to the formation of the fluorophore-hydrazide (**184**)*

Since it was necessary to activate the carbonyl as the electrophile for later coupling with the N-terminals of the peptides, the ester in dry MeOH was treated with hydrazine hydrate to afford the hydrazide (**184**) in one step. Hydrazides are readily converted[110] to the corresponding acyl azides with *tert*-butyl nitrite and HCl at very low temperatures. The low temperature is necessary to avoid accidental Curtius

rearrangements. Acyl azides such as the one derived from this azide are effective acyl electrophiles with reactivity similar to that of acid anhydrides.

Chapter 4
Conclusions

The aim of the project was to develop an advanced model for a PSA-triggered polymeric prodrug system. The specific objectives included synthesis of the PSA-sensitive peptide sequence and development of self-immolative molecular clips to link this sequence to a model drug NPEA (**67**). This molecular clip was expected to be required, as studies by other workers had shown that the aliphatic amine of doxorubicin (**13**) is not cleaved from the sequence HisSerSerLysLeuGln-dox but Leu-dox is released from HisSerSerLysLeuGln**Leu-dox**. Aromatic amines are also released by PSA-mediated cleavage of HisSerSerLysLeuGlnNHAr. Thus, PSA can release aromatic amines and amino acids, but not, apparently, conventional aliphatic amines. Synthetic approaches to peptide-*CLIP*-model drug constructs were investigated, where the clip is either a 4-aminobenzyl moiety or the extended 4-aminophenylethynyl methyl unit.

Early experiments focused on assembling peptide-model drug constructs omitting the molecular clip to test whether such a clip was indeed necessary. Active-ester peptide couplings, together with appropriate use of the orthogonal Boc, Cbz and Fmoc protecting groups led to the successful synthesis of LysBocLeuGlnNPEA (**55**) and BocLeuLys(Cbz)GlnNPEA (**57**). The latter, with the Leu and Lys reversed in the sequence, would have provided an *iso*meric construct, which should not be recognisable by PSA. Unfortunately, the very low solubility of these tripeptide derivatives in appropriate organic solvents precluded further elaboration to the target pentapeptides.

Two synthetic units were required for assembly of the full peptide-*CLIP*-model drug construct, the 4-hydroxymethyl anilide of the pentapeptide and 2-(4-nitrophenylethyl)isocyanate (**75**). The latter was conveniently prepared by Curtius rearrangement of 3-(4-nitrophenyl)propanoyl azide (**74**). However, a large number of

coupling reagents all failed to link 4-aminobenzyl alcohol to protected glutamine derivatives. Although methyl-4-aminobenzoate could be coupled to Bocglutamine, the product anilide (**80**) was too insoluble for selective reduction of the ester.

In developing suitably O-protected versions of 4-aminobenzyl alcohol, reduction of the TBDMS-ether of 4-nitrobenzyl alcohol with a large excess of $NaBH_4$ in aqueous methanol in the presence of Pd/C, gave the O-TBDMS-4-aminobenzyl alcohol (**106**) in good yield. In contrast, the use of 4 molar equivalents gave the 3-electron reduction product 4,4'-bis(TBDMSOCH_2)azoxybenzene (**105**), the structure of which was proven by COSY and NOESY 2D NMR spectra.

Synthetic approaches to a modified peptide-*CLIP*-model drug construct were more successful. In this, the molecular clip is a 4-aminophenylethynylmethyl unit. The presence of this new clip, allows a new point of retrosynthetic disconnection to be identified as a potential Sonogashira coupling of a terminal alkyne with an iodoanilide. In model experimental sequences to study viability of such Sonogashira couplings, propargyl N-nitrophenylethyl carbamate (**140**) was assembled from propargyl 4-nitrophenyl carbonate and 2-(4-nitrophenyl)ethylamine (NPEA). However, this terminal alkyne failed to couple with the model anilides 4'-iodotrifluoroacetanilide (**141**) and *tert*-butyl N-4-iodophenyl carbamate (**142**). Undaunted by the disappointing results of these model experiments, the coupling of this propargyl carbamate (**140**) with BocGln-iodo anilide (**145**) was attempted. This anilide was prepared by two distinct routes. Firstly, BocGln (**76**) was coupled directly with 4-iodoaniline in modest yield through a pivaloyl mixed anhydride. Again, solubility constraints limited the effectiveness of this procedure. To avoid these, a longer synthetic sequence was investigated in which the troublesome primary amide side chain of glutamine was masked by cyclisation as pyrogluatamine. BocPygOPFP (**150**), prepared in 4 steps from PygOH (**146**), reacted with 4-iodoaniline to give BocPyg 4-iodoanilide (**151**) in satisfactory yield. In an innovative approach, simple ring opening of this lactam with ammonia gave the BocGln iodoanilide (**145**).

Encouragingly, this iodoanilide did undergo Sonogashira coupling with propargyl N-nitrophenylethyl carbamate (**140**) to give a good yield of the phenylalkyne (**170**). Demonstration of the potential of this construct for elaboration into the target pentapeptide prodrug construct was made by removal of the Boc protection and coupling with BocLeuONSu in the usual way.

In summary, despite the major difficulties occasioned by the low solubility of the critical glutamine residue, a route has been discovered which has strong potential for synthetic access to the target pentapeptide-*CLIP*-model drug construct for biological incubation studies with recombinant human PSA.

Chapter 5
Experimental

5.1 Materials

Chemicals were purchased from Aldrich, Acros, Lancaster, Nova Biochem, Sigma chemical companies and used without further purification. All anhydrous solvents were purchased in anhydrous form, except THF which was freshly distilled from Na/benzophenone and triethylamine (Et_3N) and diethylamine (DEA) which were freshly distilled and dried from sodium hydride (NaH). All chiral amino acids are (L), unless otherwise stated.

5.2 General analytical procedures

All ^1H and ^{13}C NMR spectra were acquired on Jeol EX400 or Jeol GX270 spectrometers. All ^{19}F NMR, COSY 2D, NOESY, HMBC and HMQC spectra were recorded on a Jeol EX400 spectrometer. Chemical shifts are reported in ppm (parts per million) relative to the protons of tetramethylsilane (TMS), which was the internal standard for samples dissolved in $CDCl_3$. TMS or DMSO for samples in $(CD_3)_2SO$ and deuterated methanol for samples in CD_3OD. Multiplicities are indicated as follows: s (singlet), d (doublet), dd (doublet of doublets), t (triplet), dt (doublet of triplets), q (quartet), m (multiplet) and br (broad singlet). IR spectra were recorded on a Perkin Elmer RX 1 FTIR spectrometer in two forms, all liquid and oils were recorded as liquid films between NaCl plates and all solid materials as potassium bromide (KBr) disks. ν_{max} Values are given in cm^{-1}. Mass spectra were obtained by chemical ionisation (CI), by electrospray (ES) or by fast atom bombardment (FAB) (with *m*-nitrobenzyl alcohol as the matrix) using a Fisons VG mass spectrometer. Thin layer chromatography (TLC) was carried out on Merck Kieselgel $60F_{254}$ pre-coated aluminium plates. Purifications of all crude compounds were performed using flash chromatography on Merck Silica Gel 60 flash silica. Components were visualised using ninhydrin (for detection of amines) (ninhydrin 1.5g/100mL propan-2-ol), iodine or

UV light. Melting points were acquired on a Reichert-Jung Thermo Galen Kofler block and are uncorrected. Elemental analyses were carried out by the University of Bath microanalysis service. All $[\alpha]_D$ values were measured at 24°C (in DMF) at wavelength (λ 589 nm) using sodium light. All specific rotation values were acquired on a AA-10 polarimeter (Optical Activity Ltd).

5.3 General laboratory procedures

Unless otherwise stated, after solvent extractions, all solutions were dried using magnesium sulfate ($MgSO_4$) and all solvents were evaporated under reduced pressure. Solutions of aqueous citric acid and copper(II) sulfate were of 5% w/v concentration; brine was a saturated solution. Gaseous HCl was generated by addition of concentrated sulfuric acid to NaCl. Experiments were conducted at ambient temperature, unless otherwise stated.

Sonogashira reactions: Unless otherwise stated, the Pd catalyst, $(PPh_3)_2PdCl_2$ used in the Sonogashira reactions was prepared as follows: A mixture of PPh_3 (375 mg, 1.4 mmol) and $PdCl_2$ (130 mg, 0.7 mmol) in DMF (20 mL) was heated at 80°C for 24 h. Filtration and drying yielded $(PPh_3)_2PdCl_2$ as a bright yellow powder (469 mg, 93%).

5.4 Synthesis & analysis

4-Aminobenzyl alcohol 30

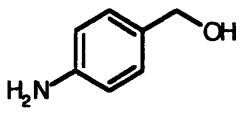

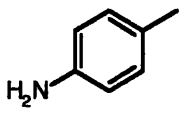

Procedure A

A solution of 4-nitrobenzyl alcohol (2.27 g, 15 mmol) and palladium (10% wt on activated carbon) (502 mg, 10 mmol) in ethanol (25 mL) was stirred for 24 h at RT under hydrogen atmosphere. The reaction mixture was filtered (Celite®) and concentrated under vacuum. Purification by column chromatography (300 : 10 : 1

DCM : MeOH : NH_4OH) yielded two main fractions, 4-methylaniline (270 mg, 17%) and 4-aminobenzyl alcohol (1.22 g, 66%) as a dark brown solid: mp 59-61°C; ^1H NMR ($CDCl_3$) δ 1.65 (brs, 1H, NH or OH), 2.15 (brs, 1H, NH or OH), 3.67 (brs, 1H, NH), 4.51 (s, 2H, CH_2), 6.64 (d, $\mathcal{J}$ = 8.4 Hz, 2H, Ar 2,6-H_2), 7.12 (d, $\mathcal{J}$ = 8.4 Hz, 2H, Ar 3,5-H_2); ^{13}C NMR ($CDCl_3$) δ 65.11 (CH_2), 115.12 (CH), 128.70 (CH), 131.04 (Cq), 145.90 (Cq). MS (FAB+) *m/z* 123 (M^+).

Side product: 4-methylaniline (para-toluidine) **102**

R_f = 0.65 (100 : 10 : 1 DCM : MeOH : NH_4OH); ^1H NMR ($CDCl_3$) δ 2.31 (s, 3H, CH_3), 3.59 (brs, 2H, NH_2), 6.63 (d, $\mathcal{J}$ = 8.1 Hz, 2H, Ar 2,6-H_2), 7.03 (d, $\mathcal{J}$ = 8.1 Hz, 2H, Ar 3,5-H_2); ^{13}C NMR ($CDCl_3$) δ 21.10 (CH_3), 115.44 (CH), 128.51 (Cq), 129.98 (CH), 145.12 (Cq). MS (EI) *m/z* 165.0790 (M^+) (C_7H_9N requires 165.0789).

Procedure B

4-(*tert*-Butyldimethylsilyloxy)aniline (500 mg, 2.1 mmol) in THF (5 mL) was stirred at 0°C for 30 min. TBAF (1.2 mL, 4.2 mmol) was then added and the whole mixture was allowed to stir for 30 min at RT. Evaporation and purification by column chromatography (10 : 1 $CHCl_3$: MeOH) yielded 4-aminobenzyl alcohol (167 mg, 65%) as a dark brown solid: R_f = 0.5 (10 : 1 $CHCl_3$: MeOH). Data as above.

N^{α}-(Benzyloxycarbonyl)glutamine 50

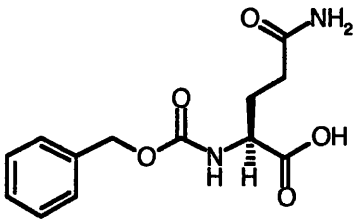

Benzyl chloroformate (95%, 11.08 g, 65 mmol) was added to L-glutamine (7.30 g, 50 mmol) and NaOH (6.0 g, 150 mmol in H_2O (100 mL)) at 0°C. The mixture was stirred for 24 h. The mixture was washed with Et_2O (4x) and the aqueous layer was

acidified to pH 2-3. The product was extracted into EtOAc (4x 25 mL) and dried. Evaporation gave N^{α}-(benzyloxycarbonyl)glutamine (6.31 g, 45%) as a fine white powder: mp 138-140°C (Lit.[154] mp 134-136.5°C): R_f = 0.2 (10 : 1 $CHCl_3$: MeOH); ^1H NMR ($CDCl_3$) δ 1.86-2.00 (m, 1H, β-H), 2.12-2.24 (m, 1H, β-H), 2.28-2.38 (m, 2H, γ-H_2), 4.16 (q, $\mathcal{J}$ = 4.7 Hz, 1H, α-H), 5.10 (s, 2H, $PhCH_2$), 7.27-7.33 (m, 3H, δ-$CONH_2$, α-NH), 7.33-7.39 (m, 5H, Ph-H_5). MS (FAB+) *m/z* 281 (M + H). $[\alpha]_D$ = - 6.8° (Lit.[154] $[\alpha]_D$ = - 6.9°).

N^{α}-(Benzyloxycarbonyl)glutamine N-hydroxysuccinimide ester 51

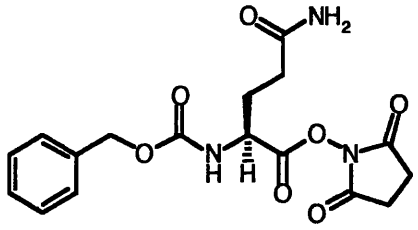

N^{α}-(Benzyloxycarbonyl)glutamine (2.39 g, 10 mmol) in EtOAc (20 mL) was cooled to 0°C. N-Hydroxysuccinimide (1.15 g, 10 mmol) in EtOAc (10 mL) was added at 0°C and the mixture were stirred for 30 min. DCC (2.16 g, 10 mmol) in EtOAc (20 mL) was added and the mixture was stirred for 2 h. The suspension was filtered (Celite®) and the filtrate was kept at 0°C for 24 h. Filtration and evaporation yielded N^{α}-(benzyloxycarbonyl)glutamine hydroxysuccinimide ester (3.91 g, quantitative) as a buff coloured gum. This was used without further purification: ^1H NMR ($(CD_3)_2SO$) δ 2.2-2.5 (m, 4H, Gln β, γ-H_2), 2.86 (s, 4H, succ-H_4), 4.78 (m, 1H, Gln α-H), 5.12 (br, 1H, α-NH), 5.49 (s, 1H, δ-CONH), 5.85 (s, 1H, δ-CONH), 5.91 (m, 2H, $PhCH_2$), 7.36 (s, 1H, Ph-H_5). MS (FAB+) *m/z* 378 (M + H).

N^{α}-(Benzyloxycarbonyl)glutamine pentafluorophenyl ester 52

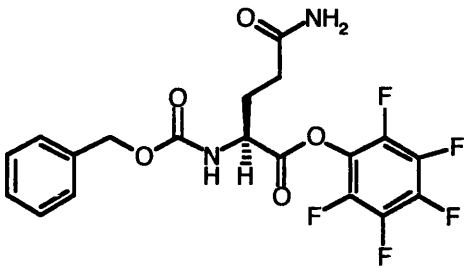

N^{α}-(Benzyloxycarbonyl)glutamine (1.12 g, 4.0 mmol) in dry THF (8 mL) and dry DMF (2 mL) was cooled to 0°C. Pentafluorophenol (0.81 g, 4.4 mmol) in dry THF (6 mL) was added at 0°C and the mixture were stirred for 25 min under N_2. DCC (0.91 g, 4.4 mmol) in dry THF (3 mL) was added and the mixture was stirred for 90 min. The suspension was filtered (Celite®) and the filtrate was kept at 0°C for 24 h. Filtration and evaporation yielded N^{α}-(benzyloxycarbonyl)glutamine pentafluorophenyl ester (2.29, quantitative) as an off-white gum. This was used without further purification. MS (FAB+) *m/z* 437 (M + H).

N^{α}-(Benzyloxycarbonyl)glutamine N-(2-(4-nitrophenyl)ethyl)amide 53

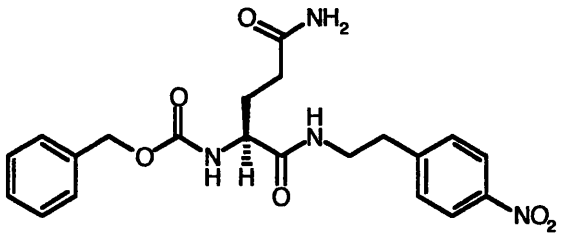

2-(4-Nitrophenyl)ethylamine hydrochloride (1.03 g, 5.1 mmol), Et_3N (2.1 mL, 15 mmol) and DMAP (5 mg) were stirred with N^{α}-(benzyloxycarbonyl)glutamine pentafluorophenyl ester (2.29 g, 5.1 mmol) in THF (10 mL) and DMF (10 mL) for 6 h. The evaporation residue, in EtOAc, was washed with H_2O (3x). Drying, evaporation and chromatography (10 : 1 $CHCl_3$: MeOH) gave N^{α}-(benzyloxycarbonyl)glutamine N-(2-(4-nitrophenyl)ethyl)amide (992 mg, 44%) as a light yellow powder: mp 162-

164°C. R_f = 0.4 (10 : 1 $CHCl_3$: MeOH); ^1H NMR ($(CD_3)_2SO$) δ 1.58-1.70 (m, 1H, β-H), 1.70-1.85 (m, 1H, β-H), 1.95-2.12 (m, 2H, γ-H_2), 2.85 (t, J = 7.0 Hz, 2H, Ar$\underline{CH_2}$ CH_2), 3.28-3.40 (m, 2H, Ar$CH_2\underline{CH_2}$), 3.83-3.92 (m, 1H, α-H), 5.00 (d, J = 12.8 Hz, 1H, Ph$\underline{CH}$O), 5.03 (d, J = 12.5 Hz, 1H, Ph$\underline{CH}$O), 6.76 (brs, 1H, δ-CONH), 7.24 (brs, 1H, δ-CONH), 7.28-7.62 (m, 5H, Ph-H_5), 7.39 (d, J = 8.2 Hz, 1H, α-NH), 7.48 (d, J = 8.6 Hz, 2H, Ar 2,6-H_2), 7.99 (t, J = 5.7 Hz, 1H, CO$\underline{NH}CH_2$), 8.12 (d, J = 8.6 Hz, 2H, Ar 3,5-H_2); ^{13}C NMR ($(CD_3)_2SO$) δ 27.72 (Ar$CH_2\underline{CH_2}$), 31.52 (β-C), 34.80 (Ar$\underline{CH_2}CH_2$), 54.61 (α-C), 65.48 (Ph$\underline{CH_2}$), 65.56 (γ-C), 123.32 (3-Ph, 5-Ph), 127.71 (4-Ph), 127.81 (2-Ar, 6-Ar), 128.37 (3-Ar, 5-Ar), 130.24 (2-Ph, 6-Ph), 137.00 (1-Ar), 146.02 (1-Ph), 147.93 (4-Ar), 155.99 (δ-C), 171.62 (CONH), 173.60 (OCONH). MS (FAB+) m/z 429.1729 (M + H) ($C_{21}H_{25}N_4O_6$ requires 429.1772). IR (KBr) ν_{max} 1690 (II-amide C=O), 1648 (I-amide C=O), 1605 (Ar), 1518, 1344 (NO_2). Anal. ($C_{21}H_{24}N_4O_6$) Calc'd C 58.88% H 5.61% N 13.08% Found C 58.70% H 5.69% N 13.01%. $[\alpha]_D$ = - 2.3°.

Glutamine N-(2-(4-nitrophenyl)ethyl)amide hydrobromide 54

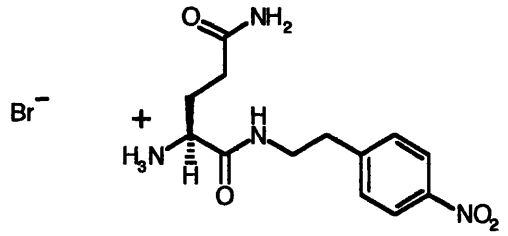

N^{α}-(Benzyloxycarbonyl)glutamine N-(2-(4-nitrophenyl)ethyl)amide (120 mg, 0.3 mmol) was stirred with AcOH (1.5 mL) and HBr (30% in AcOH) (1.5 mL) for 25 min and then concentrated. Et_2O (8 mL) was added and the suspension was stirred for 5 min. The ether layer was then decanted off and the process repeated 10 times. This solid was dried to yield glutamine N-(2-(4-nitrophenyl)ethyl)amide hydrobromide (103 mg, 96%) as a pale orange powder: mp 148-150°C. R_f = 0.2 (10 : 1 $CHCl_3$: MeOH); ^1H NMR ($(CD_3)_2SO$) (COSY 2D) δ 1.80-1.90 (m, 2H, β-H_2), 2.00-2.18 (m, 2H, γ-H_2), 2.90 (t, J = 6.6 Hz, 2H, Ar$\underline{CH_2}CH_2$), 3.26-3.46 (m, 1H, Ar$CH_2\underline{CH_2}$), 3.46-3.58 (m, 1

H, $ArCH_2C\underline{H}_2$), 3.72 (q, $\mathcal{J}$ = 5.6 Hz, 1H, α-H), 6.96 (s, 1H, δ-CONH), 7.42 (s, 1H, δ-CONH), 7.53 (d, $\mathcal{J}$ = 8.6 Hz, 2H, Ar 2,6-H_2), 8.11 (brs, 3H, $^+NH_3$), 8.16 (d, $\mathcal{J}$ = 8.6 Hz, 2H, Ar 3,5-H_2), 8.54 (t, $\mathcal{J}$ = 5.5 Hz, 1H, $CON\underline{H}CH_2$). MS (FAB+) *m/z* 295 (M + H). Anal. ($C_{13}H_{19}BrN_4O_4.2H_2O$) Calc'd C 38.00% H 4.62% N 13.60% Found C 38.20% H 4.68% N 13.40%.

N^{α}-(N^{α}-(1,1-Dimethylethoxycarbonyl)-N^{ε}-(phenylmethoxycarbonyl)lysyl) glutamine N-(2-(4-nitrophenyl)ethyl)amide 55

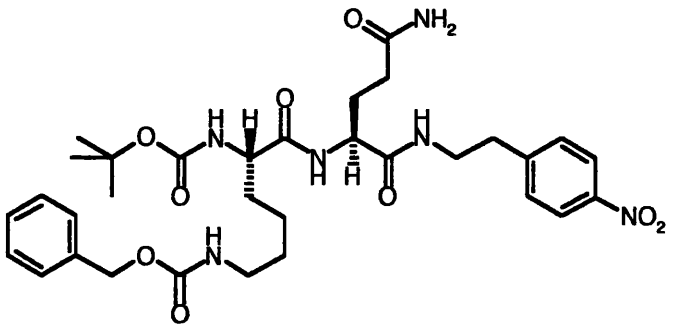

N^{α}-(1,1-Dimethylethoxycarbonyl)-N^{ε}-(phenylmethoxycarbonyl)lysine N-hydroxysuccinimide ester (62 mg, 0.13 mmol), Et_3N (50 μL, 0.4 mmol), DMAP (5 mg) and glutamine N-(2-(4-nitrophenyl)ethyl)amide hydrobromide (50 mg, 0.13 mmol) were stirred in THF (3 mL) and DMF (2 mL) for 16 h. The evaporation residue, in EtOAc, was washed with H_2O (3x). Drying, evaporation and recrystallisation (EtOAc / hexane) gave N^{α}-(N^{α}-(1,1-dimethylethoxycarbonyl)-N^{ε}-(benzyloxycarbonyl)lysyl)glutamine N-(2-(4-nitrophenyl)ethyl)amide (40 mg, 47%) as a light yellow powder: mp 148-150°C. R_f = 0.4 (10 : 1 $CHCl_3$: MeOH); ^1H NMR ($(CD_3)_2SO$) δ 1.10-1.60 (m, 8H, Lys β-H_2, Lys γ-H_2, Lys δ-H_2), 1.35 (s, 9H, $OC(CH_3)_3$), 1.60-1.85 (m, 2H, Gln β-H_2), 2.00 (t, $\mathcal{J}$ = 7.8 Hz, 2H, Gln γ-H_2), 2.85 (t, $\mathcal{J}$ = 7.0 Hz, 2H, $ArC\underline{H}_2CH_2$), 2.95 (q, $\mathcal{J}$ = 6.0 Hz, 2H, Lys ε-H_2), 3.20-3.42 (m, 2H, $ArCH_2C\underline{H}_2$), 3.75-3.90 (m, 1H, Lys α-H), 4.15 (q, $\mathcal{J}$ = 7.8 Hz, 1H, Gln α-H), 5.00 (s, 2H, $PhCH_2$), 6.76 (s, 1H, Gln δ-CONH), 6.94 (d, $\mathcal{J}$ = 7.4 Hz, 1H, Gln α-NH), 7.21 (s, 1H, Gln δ-CONH), 7.24 (t, $\mathcal{J}$ = 5.5 Hz, 1H, $PhCH_2OCON\underline{H}$), 7.26-7.39 (m, 5H, Ph-H_5), 7.48 (d, $\mathcal{J}$ = 8.6 Hz, 2H, Ar

2,6-H_2), 7.82 (d, J = 7.8 Hz, 1H, Lys α-NH), 8.00 (t, J = 5.4 Hz, 1H, CONHCH$_2$), 8.13 (d, J = 8.6 Hz, 2H, Ar 3,5-H_2). MS (FAB+) m/z 657 (M + H). $[\alpha]_D$ = - 13.3°..

N^{α}-(N^{ε}-(Benzyloxycarbonyl)lysyl)glutamine N-(2-(4-nitrophenyl)ethyl) amide hydrochloride 56

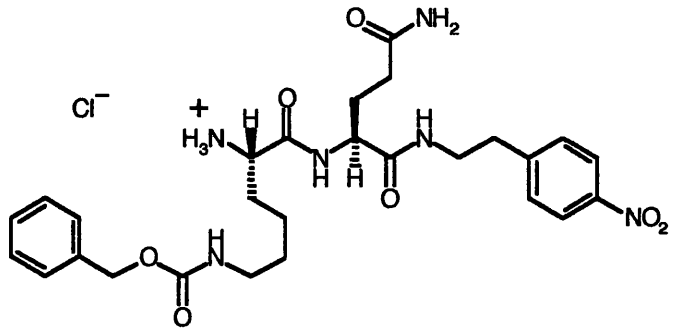

HCl was passed through a solution of N^{α}-(N^{α}-(1,1-dimethylethoxycarbonyl)-N^{ε}-(benzyloxycarbonyl)lysyl)glutamine N-(2-(4-nitrophenyl)ethyl)amide (40 mg, 0.06 mmol) in MeOH (10 mL) for 25 min and then concentrated to yield N^{α}-(N^{ε}-(benzyloxycarbonyl)lysyl)glutamine N-(2-(4-nitrophenyl)ethyl)amide hydrochloride as a buff oil (32 mg, quantitative). This was used in the next step without further purification: ^{1}H NMR ((CD$_3$)$_2$SO) δ 1.20-1.45 (m, 2H, Gln β-H_2), 1.60-2.10 (m, 6H, Lys β-H_2, Lys γ-H_2, Lys δ-H_2), 2.05 (t, J = 7.8 Hz, 2H, Gln γ-H_2) 2.85 (t, J = 7.0 Hz, 2H, ArC$\underline{H}_2$CH$_2$), 2.95 (q, J = 6.2 Hz, 2H, Lys ε-H_2), 3.09 (dt, J = 7.0 Hz, ArCH$_2$C$\underline{H}_2$), 3.70-3.80 (m, 1H, Lys α-H), 4.20 (q, J = 6.0 Hz, 1H, Gln α-H), 5.00 (s, 2H, PhCH$_2$), 6.80 (s, 1H, Gln δ-CONH), 6.90 (d, J = 7.2 Hz, 1H, CONHCH$_2$), 7.22 (t, J = 4.3 Hz, 1H, PhCH$_2$OCONH), 7.26-7.38 (m, 6H, Ph-H_5, Gln δ-CONH), 7.48 (d, J = 8.6 Hz, 2H, Ar 2.6-H_2), 8.12 (d, J = 8.6 Hz, 2H, Ar 3,5-H_2), 8.14-8.23 (m, 3H, $^+$NH$_3$), 8.60 (d, J = 7.8 Hz, 1H, Gln α-NH). MS (FAB+) m/z 558.2751 (M + H) ($C_{26}H_{37}N_6O_7$ requires 558.2757).

N^{α}-(N^{α}-(N^{α}-(1,1-Dimethylethoxycarbonyl)leucyl)-N^{ε}-(benzyloxycarbonyl) lysyl)glutamine N-(2-(4-nitrophenyl)ethyl)amide 57

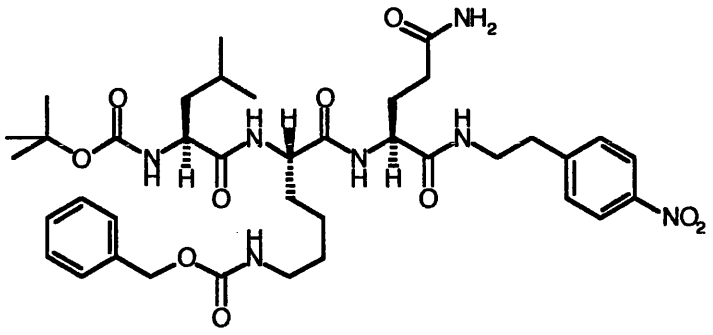

N^{α}-(1,1-Dimethylethoxycarbonyl)leucine N-hydroxysuccinimide ester (30 mg, 0.09 mmol), Et_3N (0.04 mL, 0.27 mmol), DMAP (5 mg) N-(N^{ε}-(benzyloxycarbonyl) lysyl)glutamine N-(2-(4-nitrophenyl)ethyl)amide hydrochloride (50 mg, 0.09 mmol) were stirred in THF (4 mL) and DMF (1.5 mL) for 16 h. The evaporation residue, in EtOAc, was washed with H_2O (3x). Drying, evaporation and recrystallisation (EtOAc / hexane) gave N^{α}-(N^{α}-(N^{α}-(1,1-dimethylethoxycarbonyl)leucyl)-N^{ε}-(benzyloxycarbon yl)lysyl)glutamine N-(2-(4-nitrophenyl)ethyl)amide (25 mg, 37%) as an off-white powder: mp 156-158°C; ^1H NMR ($(CD_3)_2SO$) (COSY 2D) δ 0.77-0.90 (m, 6H, Leu γ-$(CH_3)_2$), 1.35 (s, 9H, $OC(CH_3)_3$), 1.18-1.82 (m, 10H, Lys β-H_2, Lys γ-H_2, Lys δ-H_2, Leu β-H_2, Leu γ-H, Gln β-H_2), 1.94-2.00 (m, 2H, Gln γ-H_2) 2.82 (t, J = 6.6 Hz, 2H, $ArCH_2CH_2$), 2.93 (q, J = 6.6 Hz, 2H, Lys ε-H_2), 3.20-3.38 (m, 2H, $ArCH_2CH_2$), 3.92 (q, J = 6.2 Hz, 1H, Lys α-H), 4.04-4.12 (m, 1H, Glu α-H), 4.15-4.24 (m, 1H, Leu α-H), 4.98 (s, 2H, $PhCH_2$), 6.74 (brs, 1H, Gln δ-CONH), 6.96 (d, J = 7.4 Hz, 1H, $CONHCH_2$), 7.20 (brs, 1H, $PhCH_2OCONH$, Gln δ-CONH), 7.25-7.37 (m, 5H, $Ph-H_5$), 7.46 (d, J = 8.6 Hz, 2H, Ar 2,6-H_2), 7.78 (d, J = 7.8 Hz, 1H, Lys α-NH), 7.88-7.98 (m, 1H, Leu α-NH), 8.01 (m, 1H, Gln α-NH), 8.11 (d, J = 8.6 Hz, 2H, Ar 3,5-H_2). MS (FAB+) m/z 770 (M + H).

N^{α}-(Fluoren-9-ylmethoxycarbonyl)glutamic acid N-(2-(4-nitrophenyl) ethyl)amide δ-(1,1-dimethylethyl)ester 59

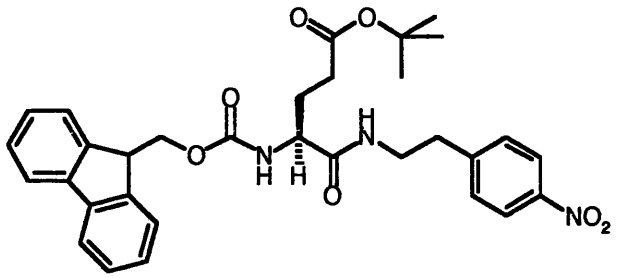

2-(4-Nitrophenyl)ethylamine hydrochloride (103 mg, 0.51 mmol) was stirred with N^{α}-(fluoren-9-ylmethoxycarbonyl)glutamic acid δ-(1,1-dimethylethyl) ester α-pentafluorophenyl ester (300 mg, 0.51 mmol) and Et_3N (0.21 mL, 1.5 mmol) in CH_2Cl_2 (5.0 mL) for 16 h. The evaporation residue, in EtOAc, was washed with H_2O (3x). Drying, evaporation and recrystallisation (EtOAc / hexanes) gave N^{α}-(fluoren-9-ylmethoxycarbonyl)glutamic acid N-(2-(4-nitrophenyl)ethyl)amide δ-(1,1-dimethyl ethyl)ester (190 mg, 65%) as a fine off-white powder: mp 138-140°C. R_f = 0.9 (10 : 1 $CHCl_3$: MeOH); ^{1}H NMR ($CDCl_3$) δ 1.40 (s, 9H, $OC(CH_3)_3$), 1.78-2.08 (m, 4H, β-H_2, γ-H_2), 2.90 (t, J = 6.6 Hz, 2H, $ArC\underline{H}_2CH_2$), 3.55 (q, J = 6.2 Hz, 2H, $ArCH_2C\underline{H}_2$), 4.02-4.12 (m, 1H, α-H), 4.19 (t, J = 7 Hz, 1H, Flu 9-H), 4.30-4.42 (m, 2H, $FluCH_2$), 5.70 (d, J = 6.2 Hz, 1H, α-NH), 6.44 (br, 1H, $CON\underline{H}CH_2$), 7.29 (t, J = 7.3 Hz, 2H, Flu 3,6-H_2), 7.32 (d, J = 8.4 Hz, 2H, Ar 2,6-H_2), 7.38 (t, J = 7.3 Hz, 2H, Flu 2,7-H_2), 7.55 (d, J = 7.3 Hz, 2H, Flu 1,8-H_2), 7.75 (d, J = 7.7 Hz, 2H, Flu 4,5-H_2), 8.12 (d, J = 8.4 Hz, 2H, Ar 3,5-H_2); ^{13}C NMR ($CDCl_3$) δ 27.91 ($OC\underline{C}(CH_3)_3$), 27.98 ($OC(\underline{C}H_3)_3$), 31.51 ($Ar\underline{C}H_2CH_2$), 35.57 (β-C), 40.12 ($ArCH_2\underline{C}H_2$), 41.14 ($FluCH_2$), 47.00 (α-C), 54.46 (9-Flu), 67.12 (γ-C), 81.22 ($\underline{C}ONHCH_2$), 119.92 (3-Ar, 5-Ar), 123.78 (2-Ar, 6-Ar), 124.90 (4-Flu, 5-Flu), 127.01 (2-Flu, 7-Flu), 127.72 (1-Flu, 8-Flu), 129.65 (3-Flu, 6-Flu), 141.24 (1-Ar), 143.60 (4-Ar), 146.44 (2x quat.-Flu), 146.74 (2x quat.-Flu), 171.40 (δ-C), 173.80 (OCONH). MS (FAB+) m/z 574 (M + H).

N^{α}-(N^{α}-(1,1-Dimethylethoxycarbonyl)leucyl)glutamine N-(2-(4-nitro phenyl)ethyl)amide 60

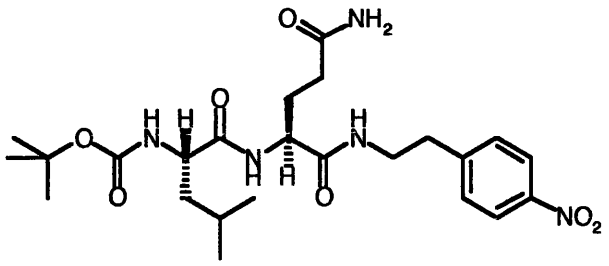

N^{α}-(1,1-Dimethylethoxycarbonyl)leucine N-hydroxysuccinimide ester (290 mg, 0.89 mmol), Et_3N (0.37 mL, 2.66 mmol) and DMAP (1 mg) were stirred with glutamine N-(2-(4-nitrophenyl)ethyl)amide hydrobromide (332 mg, 0.89 mmol) in THF (2 mL) and DMF (3 mL) for 16 h. The evaporation residue, in EtOAc, was washed with H_2O (3x). Drying, evaporation and recrystallisation (EtOAc / hexane) gave N^{α}-(N^{α}-(1,1-dimethylethoxycarbonyl)leucyl)glutamine N-(2-(4-nitrophenyl)ethyl)amide (225 mg, 50%) as a light brown powder: R_f = 0.4 (10 : 1 $CHCl_3$: MeOH); ^1H NMR ($(CD_3)_2SO$) δ 0.82 (d, J = 5.9 Hz, 3H, Leu γ-CH_3), 0.84 (d, J = 5.9 Hz, 3H, Leu γ-CH_3), 1.35 (s, 9H, $OC(CH_3)_3$), 1.38 (m, 2H, Leu β-H_2), 1.60 (m, 1H, Leu γ-H), 1.66-1.80 (m, 2H, Gln β-H_2), 1.97 (t, J = 7.2 Hz, 2H, Gln γ-H_2), 2.83 (t, J = 6.9 Hz, 2H, $ArCH_2$), 3.24-3.40 (m, 2H, $ArCH_2C\underline{H}_2$), 3.90 (m, 1H, Leu α-H), 4.12 (m, 1H, Gln α-H), 6.73 (br, 1 H, δ-CONH), 6.97 (d, J = 7.9 Hz, 1H, α-NH), 7.20 (br, 1H, δ-CONH), 7.46 (d, J = 8.7 Hz, 2H, Ar 2,6-H_2), 7.76 (d, J = 8.0 Hz, 1H, α-NH), 7.98 (t, J = 5.7 Hz, 1H, $N\underline{H}CH_2$), 8.12 (d, J = 8.9 Hz, 2H, Ar 3,5-H_2). MS (FAB+) *m/z* 508.2773 (M + H) ($C_{24}H_{38}N_5O_7$ requires 508.2771).

N^{α}-(N^{α}-(Leucyl)glutamine N-(2-(4-nitrophenyl)ethyl)amide trifluoroacetic acid salt 61

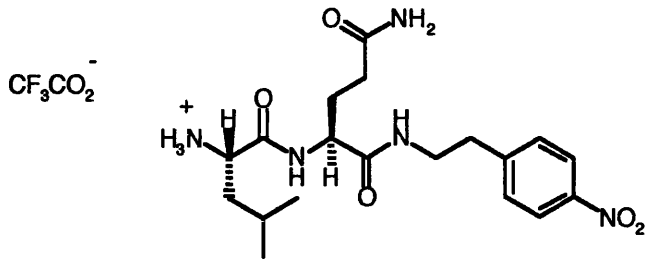

N^{α}-(N^{α}-(1,1-Dimethylethoxycarbonyl)leucyl)glutamine N-(2-(4-nitrophenyl)ethyl) amide (221 mg, 0.44 mmol) was stirred with TFA (1 mL) in DCM (2 mL) at RT for 30 min. Evaporation gave N^{α}-(N^{α}-(leucyl)glutamine N-(2-(4-nitrophenyl)ethyl)amide trifluoroacetic acid salt (352 mg, 65%) as a brown oil: ^{1}H NMR ($(CD_3)_2SO$) δ 0.84 (d, J = 5.9 Hz, 3H, Leu γ-CH_3), 0.87 (d, J = 6.2 Hz, 3H, Leu γ-CH_3), 1.45-1.83 (m, 5H, Leu β, γ-H_3 + Gln β-H_2), 1.95-2.07 (m, 2H, Gln γ-H_2), 2.85 (brt, J = 5.8 Hz, 2H, Ar CH_2), 3.35 (m, 2H, $ArCH_2C\underline{H_2}$), 3.76 (m, 1H, Leu α-H), 4.72 (m, 1H, Gln α-H), 6.78 (m, 1H, δ-CONH), 7.24 (br, 1H, δ-CONH), 7.47 (d, J = 8.9 Hz, 2H, Ar 2,6-H_2), 8.07 (m, 1H, $N\underline{H}CH_2$), 8.12 (d, J = 8.7 Hz, 2H, Ar 3,5-H_2), 8.61 (d, J = 7.9 Hz, 1H, Gln α-NH). MS (FAB+) *m/z* 409 (M).

N^{α}-(N^{α}-(N^{ε}-(1,1-Dimethylethoxycarbonyl)-N^{α}-(fluoren-9-ylmethoxy-carbonyl)lysyl)leucyl)glutamine N-(2-(4-nitrophenyl)ethyl)amide 62

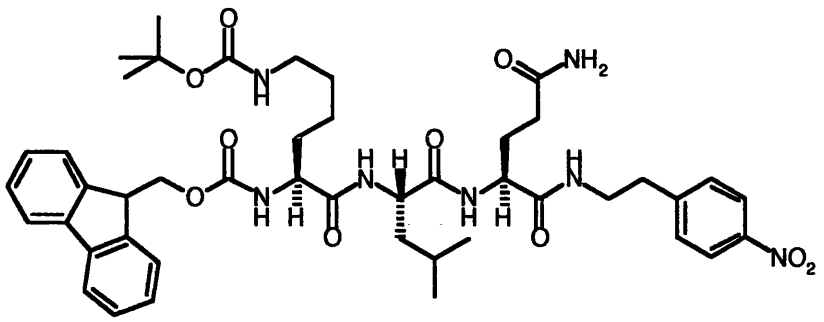

N^{ε}-(1,1-Dimethylethoxycarbonyl)-N^{α}-(fluoren-9-ylmethoxycarbonyl)lysine N-hydroxy succinimide ester (382 mg, 0.68 mmol), Et_3N (0.28 mL, 205 mg, 2.03 mmol) and DMAP (1 mg) were stirred with N^{α}-(Leucyl)glutamine N-(2-(4-nitrophenyl)ethyl)amide trifluoroacetic acid salt (352 mg, 0.68 mmol) in THF (2 mL) and DMF (3 mL) for 14 h. The evaporation residue, in EtOAc, was washed with H_2O (3x). Drying, evaporation and recrystallisation (EtOAc / hexane) gave N^{α}-(N^{α}-(N^{ε}-(1,1-dimethylethoxycarbonyl)-N^{α}-(fluoren-9-ylmethoxycarbonyl)lysyl)leucyl)glutamine N-(2-(4-nitrophenyl)ethyl) amide (243 mg, 41%) as a light brown solid: R_f = 0.5 (10 : 1 $CHCl_3$: MeOH); ^1H NMR ($(CD_3)_2SO$) δ 0.83 (m, 6H, 2x Leu γ-CH_3), 1.34 (s, 9H, $OC(CH_3)_3$), 1.20-1.80 (m, 11H, Lys β, γ, δ-H_6 + Leu β, γ-H_3 + Gln β-H_2), 1.97 (t, J = 7.2 Hz, 2H, Gln γ-H_2), 2.48 (t, J = 6.9 Hz, 2H, $ArCH_2$), 2.84 (m, 4H, 2x CH_2N), 3.72 (m, 1H, Leu α-H), 3.94 (m, 1H, Lys α-H), 4.06-4.30 (m, 4H, Gln α-H + Flu 9-H + $FluCH_2$), 6.75 (m, 3H, 2x NH + Gln δ-CONH), 7.20 (br, 1H, Gln δ-CONH), 7.30 (t, J = 7.4 Hz, 2H, Flu 2,7-H_2), 7.40 (t, J = 7.2 Hz, 2H, Flu 3,6-H_2), 7.45 (d, J = 8.7 Hz, 2H, Ar 2,6-H_2), 7.70 (d, J = 8.0 Hz, 1H, α-NH), 7.72 (d, J = 7.2 Hz, 2H, Flu 1,8-H_2), 7.87 (d, J = 7.2 Hz, 2H, Flu 4,5-H_2), 7.95 (m, 1H, $N\underline{H}CH_2$), 8.02 (m, 1H, NH), 8.13 (d, J = 8.7 Hz, 2H, Ar 3,5-H_2).

3-(2,4-Dinitrophenyl)propanoic acid 70

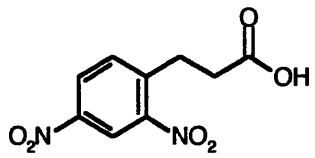

3-Phenylpropanoic acid (2.00 g, 13.3 mmol) was added at 0°C to an ice-cold stirred mixture of conc. H_2SO_4 (15 mL) and conc. HNO_3 (5 mL). The solution was stirred for a further 2 d, extracted in to EtOAc and washed with H_2O (3x). The organic layer was then dried, concentrated and purified by chromatography (9 : 1 $CHCl_3$: MeOH). Recrystallisation (EtOAc / hexane) yielded 3-(2,4-dinitrophenyl)propanoic acid (1.95 g, 61%) as fine yellow needles: mp 126-128°C. (Lit.[122] mp 125.5-126.5°C). R_f = 0.35 (9 : 1 $CHCl_3$: MeOH); ^1H NMR ($(CD_3)_2SO$) δ 2.65 (t, J = 7.4 Hz, 2H, $ArCH_2C\underline{H}_2$), 3.15 (t, J = 7.4 Hz, 2H, $ArC\underline{H}_2$), 7.86 (d, J = 8.4 Hz, 1H, 6'-H), 8.45 (dd, J = 8.4, 2.2 Hz, 1H, 5'-H), 8.69 (d, J = 2.4 Hz, 1H, 3'-H), 12.37 (brs, 1H, OH); ^{13}C NMR ($(CD_3)_2SO$) δ 27.11 ($Ar\underline{C}H_2$), 33.72 ($ArCH_2\underline{C}H_2$), 119.82 (6-Ar), 127.20 (5-Ar), 133.50 (3-Ar), 142.51 (1-Ar), 146.16 (2-Ar), 149.18 (4-Ar), 173.12 (CO_2H). MS (FAB+) *m/z* 240 (M).

3-(4-Nitrophenyl)propanoic acid 72

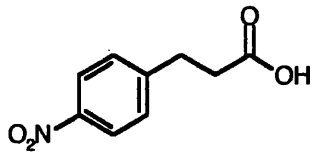

3-Phenylpropanoic acid (2.00 g, 13.3 mmol) was added at 0°C to an ice-cold stirred mixture of conc. H_2SO_4 (15 mL) and HNO_3 (5 mL). The solution was stirred for 2 h, extracted in to EtOAc and washed with H_2O (3x). The organic layer was then dried, concentrated and purified by chromatography (10 : 1 $CHCl_3$: MeOH). Re-crystallisation (EtOAc / hexane) yielded 3-(4-nitrophenyl)propanoic acid (894 mg, 34%) as fine white needles: mp 165-167°C. (Lit.[123] mp 165°C). R_f = 0.38 (10 : 1

$CHCl_3$: MeOH); ^1H NMR ($(CD_3)_2SO$) δ 2.64 (t, J = 7.4 Hz, 2H, $ArCH_2C\underline{H_2}$), 2.96 (t, J = 7.4 Hz, 2H, $ArC\underline{H_2}$), 7.54 (d, J = 7.0 Hz, 2H, 2',6'-H_2), 8.17 (d, J = 7.0 Hz, 2H, 3',5'-H_2), 12.30 (brs, 1H, OH); ^{13}C NMR ($(CD_3)_2SO$) δ 30.12 ($Ar\underline{C}H_2$), 34.40 ($ArCH_2\underline{C}H_2$), 123.46 (2-Ar, 6-Ar), 129.64 (3-Ar, 5-Ar), 145.91 (1-Ar), 149.32 (4-Ar), 173.40 (CO_2H). MS (FAB+) m/z 196 (M + H).

2-(4-Nitrophenyl)ethyl isocyanate 75

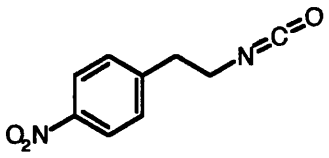

3-(4-Nitrophenyl)propanoic acid (200 mg, 1.0 mmol) was stirred with thionyl chloride (2 mL) and DMF (2 drops) at 85°C for 14 h. Evaporation gave crude 3-(4-nitrophenyl)propanoyl chloride as a yellow solid: IR (KBr) ν_{max} 1793 (C=O), 1607 (Ar), 1519, 1346 (NO_2). This material was dissolved in acetone (3 mL) and added to sodium azide (200 mg, 3 mmol) in H_2O (2 mL) and the mixture was stirred at RT for 3 h. Evaporation at 25°C gave a solid which was extracted with CH_2Cl_2 (3x 10 mL) and washed with H_2O (3x). The combined organic extracts were dried and the solvent was evaporated to give 3-(4-nitrophenyl)propanoyl azide. IR (film) ν_{max} 2139 (N_3), 1700 (C=O), 1653 (C=O), 1518, 1346 (NO_2). This material, in dry toluene (10 mL) was heated under reflux for 100 min. Evaporation afforded 2-(4-nitrophenyl)ethyl isocyanate (120 mg crude) as orange needles: mp 140-142°C. The isocyanate was used without further purification. IR (KBr) ν_{max} 2272 (N=C=O), 1518, 1346 (NO_2).

N^{α}-(1,1-Dimethyloxycarbonyl)glutamine pentafluorophenyl ester 78

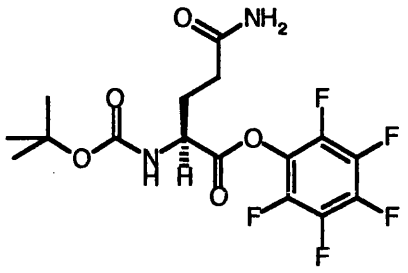

N^{α}-(1,1-Dimethyloxycarbonyl)glutamine (2.05 g, 10 mmol) in EtOAc (50 mL) was cooled to 0°C. Pentafluorophenol (0.81 g, 4.4 mmol) in EtOAc (10 mL) was added at 0°C and the mixture were stirred for 30 min. DCC (2.16 g, 10 mmol) was added and the mixture was stirred for 2 h. The suspension was filtered (Celite®) and the filtrate was kept at 0°C for 24 h. Filtration and evaporation yielded N^{α}-(1,1-dimethyloxycarbonyl)glutamine pentafluorophenyl ester (2.95 g, quantitative) as a colourless gum. This was used without further purification: ^{1}H NMR ($(CD_3)_2SO$) δ 1.40 (s, 9H, $OC(CH_3)_3$), 1.92 (m, 1H, Gln β-H), 2.09 (m, 1H, Gln β-H), 2.26 (t, J = 7.4 Hz, 2H, Gln γ-H_2), 4.32 (m, 1H, Gln α-H), 5.57 (d, J = 7.8 Hz, 0.1H, α-NH), 6.86 (s, 1H, δ-CONH), 7.35 (s, 1H, δ-CONH), 7.72 (d, J = 7.0 Hz, 0.9H, α-NH); ^{19}F NMR (DMSO) δ -162.21 (dd, J = 22.3, 18.4 Hz, 1.8F, 3,5-F_2), -162.04 (t, J = 19 Hz, 0.2F, 3,5-F_2), -157.61 (t, J = 18.0 Hz, 0.9F, 4-F), -157.38 (t, J = 17.4 Hz, 0.1F, 4-F), -153.57 (d, J = 20.3 Hz, 0.2F, 2,6-F_2), -153.27 (d, J = 21.6 Hz, 1.8F, 2,6-F_2). MS (FAB+) *m/z* 413 (M + H).

N^{α}-(1,1-Dimethylethoxycarbonyl)glutamine N-(4-methoxycarbonyl phenyl)amide 80

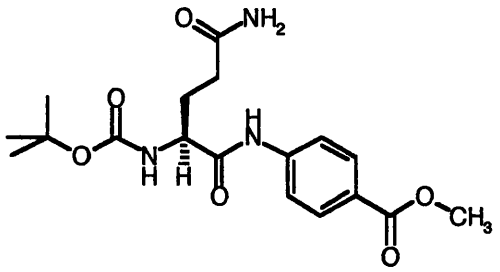

N^{α}-(1,1-Dimethylethoxycarbonyl)glutamine (0.99 g, 4.0 mmol) was stirred in dry THF (12 mL) at 0°C with pivaloyl chloride (603 mg, 5.0 mmol) and Et_3N (0.56 mL, 4.0 mmol) for 30 min. Methyl 4-aminobenzoate (760 mg, 5.0 mmol) was added and the mixture was brought to RT and stirred for 2 h. The evaporation residue, in EtOAc, was washed with H_2O (3x). Drying, evaporation and chromatography (9 : 0.5 $CHCl_3$: MeOH) gave N^{α}-(1,1-dimethylethoxycarbonyl)glutamine N-(4-methoxycarbonyl-phenyl)amide (820 mg, 54%) as a white powder: mp 190-192°C. R_f = 0.35 (10 : 1 $CHCl_3$: MeOH); ^1H NMR ($(CD_3)_2SO$) δ 1.30 (s, 9H, $OC(CH_3)_3$), 1.70-1.95 (m, 2H, β-H_2), 2.05-2.22 (m, 2H, γ-H_2), 3.80 (s, 3H, CH_3) 4.05 (q, $\mathcal{J}$ = 7.0 Hz, 1H, α-H), 6.78 (s, 1H, δ-CONH), 7.14 (d, $\mathcal{J}$ = 7.0 Hz, 1H, α-NH), 7.28 (s, 1H, δ-CONH), 7.73 (d, $\mathcal{J}$ = 7.4 Hz, 2H, Ar 2,6-H_2), 7.91 (d, $\mathcal{J}$ = 7.4 Hz, 2H, Ar 3,5-H_2), 10.28 (s, 1H, CONHAr); ^{13}C NMR ($(CD_3)_2SO$) δ 27.21 ($OC(CH_3)_3$), 28.21 ($OC(CH_3)_3$), 31.46 (β-C), 51.94 (CH_3), 54.90 (α-C), 78.20 (γ-C), 118.68 (2-Ar, 6-Ar), 123.94 (1-Ar), 130.33 (3-Ar, 5-Ar), 143.41 (4-Ar), 155.47 (δ-C), 165.82 (CONHAr), 171.70 (OCONH), 173.69 (ArCO). MS (FAB+) *m/z* 380 (M + H). $[\alpha]_D$ = + 5.2°.

N^{α}-(Fluoren-9-ylmethoxycarbonyl)-O^{γ}-(1,1-dimethylethyl)glutamic acid N-(4-methoxycarbonylphenyl)amide 87

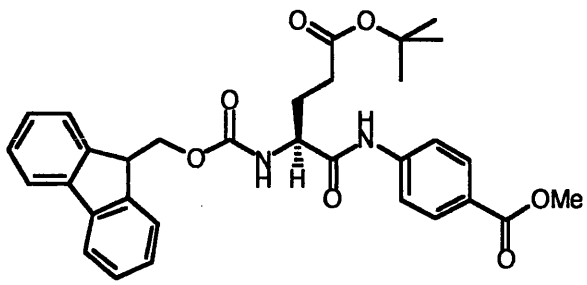

N^{α}-(Fluoren-9-ylmethoxycarbonyl)-O^{γ}-(1,1-dimethylethyl)glutamic acid (1.70 g, 4.0 mmol) was stirred in dry THF (12 mL) at 0°C with pivaloyl chloride (603 mg, 5.0 mmol) and Et_3N (0.56 mL, 4.0 mmol) for 30 min. Methyl 4-aminobenzoate (760 mg, 5.0 mmol) was added and the mixture was brought to RT and stirred for 2 h. The evaporation residue, in EtOAc, was washed with H_2O (3x). Drying, evaporation and chromatography (9 : 0.5 $CHCl_3$: MeOH) gave N^{α}-(fluoren-9-ylmethoxycarbonyl)-O^{γ}-(1,1-dimethylethyl)glutamic acid N-(4-methoxycarbonylphenyl)amide (1.42 g, 63%) as a white powder: R_f = 0.5 (9 : 0.5 $CHCl_3$: MeOH); ^1H NMR ($(CD_3)_2SO$) δ 1.44 (s, 9H, $OC(CH_3)_3$), 2.04 (m, 1H, Glu β-H), 2.13 (m, 1H, Glu β-H), 2.40 (dt, $\mathcal{J}$ = 16.6, 6.5 Hz, 1H, Glu γ-H), 2.55 (dt, $\mathcal{J}$ = 16.6, 6.4 Hz, 1H, Glu γ-H), 3.88 (s, 3H, OMe), 4.17 (t, $\mathcal{J}$ = 6.9 H, 1H, Flu 9-H), 4.36 (m, 1H, Glu α-H), 4.39 (d, $\mathcal{J}$ = 6.9 Hz, 2H, $FluCH_2$), 5.98 (d, $\mathcal{J}$ = 7.7 Hz, 1H, Glu α–NH), 7.25 (t, $\mathcal{J}$ = 7.4 Hz, 2H, Flu 2,7-H_2), 7.36 (t, $\mathcal{J}$ = 7.4 Hz, 2H, Flu 3,6-H_2), 7.52-7.60 (m, 4H, Ar 2,6-H_2 + Flu 1,8-H_2), 7.73 (d, $\mathcal{J}$ = 7.6 Hz, 2H, Flu 4,5-H_2), 7.95 (d, $\mathcal{J}$ = 8.7 Hz, 2H, Ar 3,5-H_2), 8.99 (br, 1H, NH). MS (FAB+) *m/z* 559.2432 (M + H) ($C_{32}H_{35}N_2O_7$ requires 559.2444), 503 (M – $Me_2C{=}CH_2$).

Pyroglutamic acid N-(4-methoxycarbonyl)amide 90

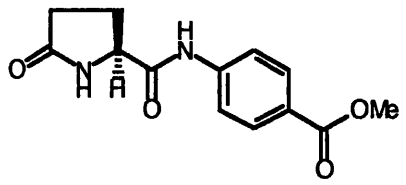

N^{α}-(1,1-Dimethylethoxycarbonyl)glutamine N-(4-methoxycarbonylphenyl)amide (25 mg, 0.06 mmol) was stirred in TFA (1.0 mL) for 20 min. Evaporation gave a mixture of pyroglutamic acid N-(4-methoxycarbonyl)amide and ammonium trifluoroacetate: ^{1}H NMR ($(CD_3)_2SO$) δ 1.80-2.20 (m, 4H, Pyg β, γ-H_4), 3.80 (s, 3H, OMe), 4.42 (m, 1H, Pyg α-H), 7.28 (t, J = 51.2 Hz, 4H, $^+NH_4$), 7.78 (m, 2H, Ar 2,6-H_2), 7.91 (m, 2H, Ar 3,5-H_2), 8.61 (br, 1H, Pyg NH), 11.43 (s, 1H, ArNH).

***S*-3-(1,1-Dimethylethoxycarbonylamino)piperidine-2,6-dione 96**

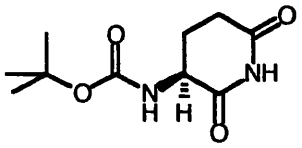

N^{α}-(1,1-Dimethyloxycarbonyl)glutamine (2.00 g, 8.12 mmol) in dry THF (15 mL) was stirred with EDC (1.71 g, 8.93 mmol) and HOBt (1.20 g, 8.93 mmol) at 0°C for 30 mins. 4-Aminobenzyl alcohol (1.00 g, 8.12 mmol) and Et_3N (1.24 mL, 904 mg, 8.12 mmol) in dry THF (10 mL) was added and the mixture was allowed to stir at RT for a further 16 h. The suspension was filtered (Celite®) and the filtrate evaporated. The evaporation residue, in EtOAc, was washed with H_2O (3x), dried and concentrated to yield *S*-3-(1,1-dimethylethoxycarbonylamino)piperidine-2,6-dione (950 mg, 51%) as a brown oil: R_f = 0.5 (EtOAc); ^{1}H NMR ($CDCl_3$) δ 1.44 (s, 9H, $OC(CH_3)_3$), 1.86 (m, 1H, 4-H), 2.47 (m, 1H, 4-H), 2.65 (ddd, J = 18.0, 10.3, 5.2 Hz, 1H, 5-H), 2.76 (ddd, J = 18.0, 5.7, 2.3 Hz, 1H, 5-H), 4.31 (m, 1H, 3-H), 5.40 (d, J = 6.0 Hz, 1H, BocNH), 8.55 (br, 1H, NH). MS (FAB-) *m/z* 227 (M - H).

N^{α}-(Fluoren-9-ylmethoxycarbonyl)leucine N-(4-hydroxymethylphenyl)-amide 99

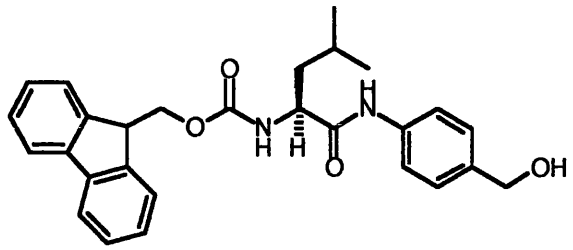

N^{α}-(Fluoren-9-ylmethoxycarbonyl)leucine (283 mg, 0.8 mmol), Et_3N (162 mg, 1.6 mmol) and DMAP (1 mg) were stirred with EEDQ (198 mg, 0.8 mmol) in DCM (4 mL) for 30 mins at 0°C. 4-Aminobenzyl alcohol (98 mg, 0.8 mmol) was then added to the mixture and allowed to stir for 16 h at RT. The evaporation residue, in EtOAc, was washed with H_2O (3x) and brine (2x). Drying, evaporation and column chromatography (9 : 1 $CHCl_3$: hexane) afforded N^{α}-(fluoren-9-ylmethoxycarbonyl) leucine N-(4-hydroxymethylphenyl)amide (270 mg, 72%) as a white powder: R_f = 0.85 (10 : 1 $CHCl_3$: MeOH); ^1H NMR ($CDCl_3$) δ 0.93 (m, 6H, 2x Leu γ-CH_3), 1.62-1.77 (m, 3H, Leu β, γ-H_3), 4.10 (t, J = 6.7 Hz, 1H, Flu 9-H), 4.25-4.45 (m, 3H, Leu α-H + FluCH_2), 4.51 (s, 2H, ArCH_2O), 5.81 (d, J = 8.2 Hz, 1H, Leu α-NH), 7.10 (t, J = 7.9 Hz, 2H, Flu 2,7-H_2), 7.23 (t, J = 7.2 Hz, 2H, Flu 3,6-H_2), 7.30-7.40 (m, 4H, Ar-H_4), 7.50 (d, J = 7.7 Hz, 2H, Flu 1,8-H_2), 7.71 (d, J = 7.4 Hz, 2H, Flu 4,5-H_2), 8.84 (s, 1H, ArNH). MS (FAB+) *m/z* 459 (M + H), 441 (M − OH).

4-(N-(1,1-Dimethylethoxycarbonyl)amino)benzyl alcohol 100

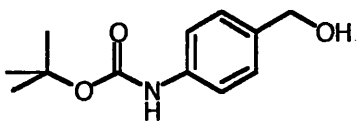

4-Aminobenzyl alcohol (2.5 g, 20 mmol) in dioxane (13 mL), water (13 mL) and NaOH (1M) (20 mL) was cooled to 0°C and allowed to stir. Di-*tert*-butyl

pyrocarbonate (6.7 g, 30 mmol) was added in one portion, and the mixture was stirred at RT for 12 h. The evaporation residue, in EtOAc, was washed with H_2O (3x). Drying, evaporation and purification by column chromatography (1 : 1 EtOAc : hexane) afforded 4-(N-(1,1-dimethylethoxycarbonyl)amino)benzyl alcohol (3.9 g, 89%) as a light brown oil. R_f = 0.4 (1 : 1 EtOAc : hexane); ^{1}H NMR ($CDCl_3$) δ 1.51 (s, 9H, $OC(CH_3)_3$), 2.35 (s, 1H, OH), 4.56 (s, 2H, CH_2), 6.71 (brs, 1H, NH), 7.22 (d, $\mathcal{J}$ = 8.3 Hz, 2H, Ar 2,6-H_2), 7.31 (d, $\mathcal{J}$ = 8.3 Hz, 2H, Ar 3,5-H_2). MS (FAB+) *m/z* 223 (M^+).

1-((1,1-Dimethylethyl)dimethylsilyloxymethyl)-4-nitrobenzene 104

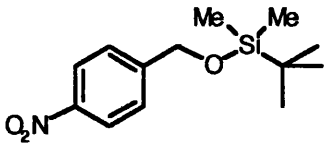

To a solution of 4-nitrobenzyl alcohol (5.65 g, 36.9 mmol) in dry DMF (15 mL), were added, TBDMS (8.84 g, 58.7 mmol) and imidazole (8.29 g, 122 mmol) and then the reaction mixture was stirred at RT for 2.5 h under nitrogen. Evaporation and purification by column chromatography (25 : 75 hexane : toluene) afforded 1-((1,1-dimethylethyl)dimethylsilyloxymethyl)-4-nitrobenzene (6.4 g, 64%) as yellow crystals: mp 30-32°C. (Lit.[156] mp 30.5-32.5°C). R_f = 0.4 (25 : 75 hexane : toluene); ^{1}H NMR ($CDCl_3$) δ 0.11 (s, 6H, $SiMe_2$), 0.94 (s, 9H, $OC(CH_3)_3$), 4.82 (s, 2H, CH_2), 7.47 (d, $\mathcal{J}$ = 8.4 Hz, 2H, Ar 2,6-H_2), 8.18 (d, $\mathcal{J}$ = 8.6 Hz, 2H, Ar 3,6-H_2). MS (FAB+) *m/z* 268 (M + H). Anal. ($C_{13}H_{23}NOSi$) Calc'd C 65.8% H 9.87% N 5.96% Found C 65.75% H 9.78% N 5.90%.

N,N'-Bis(4-(dimethyl(1,1-dimethylethyl)silyloxymethyl)azoxybenzene 105

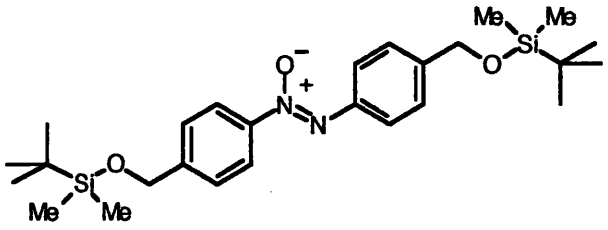

1-((1,1-Dimethylethyl)dimethylsilyloxymethyl)-4-nitrobenzene (1.07 g, 4.0 mmol) was stirred with sodium borohydride (608 mg, 16.0 mmol) in H_2O (6.0 mL) and MeOH (50 mL) in the presence of Pd/C (10%, 100 mg) for 4 h. Filtration (Celite®) and evaporation gave a semi-solid, which in EtOAc, was washed with H_2O (3x) and brine (2x). Drying and evaporation gave N,N'-bis(4-(dimethyl(1,1-dimethylethyl)silyloxy methyl)azoxybenzene (1.50 g, 77%) as a buff oil: R_f = 0.8 (25 : 75 hexane : toluene); ^{1}H NMR ($CDCl_3$) δ 0.09 (s, 6H, $SiMe_2$), 0.14 (s, 6H, $SiMe_2$), 0.94 (s, 9H, $OC(CH_3)_3$), 0.97 (s, 9H, $OC(CH_3)_3$), 4.63 (s, 2H, CH_2), 4.83 (s, 2H, CH_2), 6.64 (d, $\mathcal{J}$ = 8.2 Hz, 2H, Ar 2,6-H_2), 7.11 (d, $\mathcal{J}$ = 8.2 Hz, 2H, Ar 3,5-H_2), 7.48 (d, $\mathcal{J}$ = 8.2 Hz, 2H, Ar' 3,5-H_2), 8.19 (d $\mathcal{J}$ = 7.9 Hz, 2H, Ar' 2,6-H_2). MS (FAB+) *m/z* 487.2815 (M + H) ($C_{26}H_{43}N_2O_3Si_2$ requires 487.2812).

4-Amino-1-((1,1-dimethylethyl)dimethylsilyloxymethyl)benzene 106

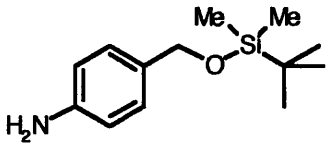

1-((1,1-Dimethylethyl)dimethylsilyloxymethyl)-4-nitrobenzene (504 mg, 2.0 mmol) was stirred with sodium borohydride (760 mg, 16.0 mmol) in H_2O (6.0 mL) and MeOH (50 mL) in the presence of Pd/C (10%, 100 mg) for 5 h at RT. Filtration (Celite®) and evaporation gave a semi-solid, which in EtOAc, was washed with H_2O (3x) and brine (3x). Drying and evaporation gave 4-amino-1-((1,1-dimethylethyl)dimethylsilyloxy-methyl)benzene (350 mg, 74%) as a brown oil: R_f = 0.77 (25 : 75 hexane : toluene); ^{1}H

NMR ($CDCl_3$) δ 0.16 (s, 6H, $SiMe_2$), 1.01 (s, 9H, $OC(CH_3)_3$), 3.60 (br, 2H, NH_2), 4.69 (s, 2H, CH_2), 6.66 (d, J = 8.6 Hz, 2H, Ar 3,6-H_2), 7.16 (d, J = 8.4 Hz, 2H, Ar 2,6-H_2). MS (FAB+) *m/z* 238 (M + H), 237 (M), 180, 106. Anal. ($C_{13}H_{21}NO_3Si$) Calc'd C 58.5% H 7.92% N 5.36% Found C 58.39% H 7.93% N 5.24%.

1,1-Dimethyl-3-(4-trifluoroacetamidophenyl)prop-2-yn-1-ol 126

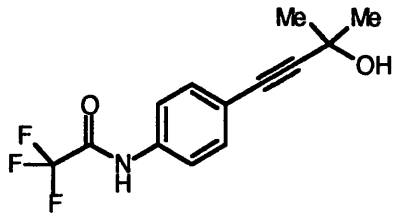

N-(4-Iodophenyl)trifluoroacetamide (700 mg, 2.2 mmol) was stirred with $(PPh_3)_2PdCl_2$ (60 mg), CuI (70 mg), 2-methyl-3-butyn-2-ol (0.33 mL, 280 mg, 3.3 mmol) in dry Et_3N (7 mL) and dry THF (17 mL) at 45°C for 2 d under nitrogen. Filtration (Celite®), evaporation and column chromatography (10 : 1 $CHCl_3$: MeOH) gave 1,1-dimethyl-3-(4-trifluoroacetamidophenyl)prop-2-yn-1-ol (230 mg, 39%) as a white crystalline solid: mp 118-120°C. (Lit.[142] mp 120-122°C). R_f = 0.4 (10 : 1 $CHCl_3$: MeOH); ^1H NMR ($CDCl_3$) δ 1.59 (s, 6H, $C(Me)_2$), 2.48 (br, 1H, OH), 7.37 (d, J = 8.6 Hz, 2H, Ar 2,6-H_2), 7.53 (d, J = 8.6 Hz, 2H, Ar 3,5-H_2), 8.83 (brs, 1H, NH). MS (FAB+) *m/z* 271.0820 (M + H) ($C_{13}H_{12}NO_2F_3$ requires 271.0820).

N-(4-Iodophenyl)trifluoroacetamide 129

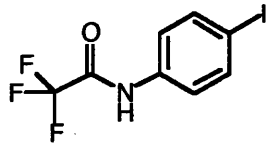

4-Iodoaniline (1.0 g, 4.6 mmol) was stirred with ethyl trifluoroacetate (5.4 mL, 6.49 g, 45.7 mmol) and Et_3N (0.63 mL, 4.6 mmol) in DCM (15 mL) for 16 h at RT. The evaporation residue, in EtOAc, was washed with H_2O (3x) and saturated sodium

bicarbonate (3x) and dried. Evaporation gave N-(4-iodophenyl)trifluoroacetamide (1.03 g, 66%) as light brown needles: mp 135-137°C. (Lit.[142] mp 136-138°C); ^{1}H NMR ($CDCl_3$) δ 7.33 (d, J = 8.9 Hz, 2H, Ar 2,6-H_2), 7.69 (d, J = 8.9 Hz, 2H, Ar 3,5-H_2), 7.91 (brs, 1H, NH); ^{13}C NMR ($CDCl_3$) δ 76.85 (Ar 4-C), 114.79 (Ar 2,6-C_2), 135.37 (Ar 3,5-C_2), 143.56 (Ar 1-C), [the F_3CCO signals were obscured by the noise]. MS (FAB+) *m/z* 315 (M + H).

1,1-Dimethylethoxycarbonyl N-(4-iodophenyl)carbamate 131

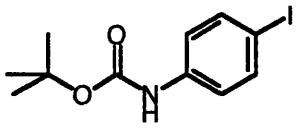

4-Iodoaniline (1.5 g, 6.9 mmol) was stirred with di-*tert*-butyl dicarbonate (2.98 g, 13.7 mmol) in DCM (30 mL) for 18 h. The evaporation residue, in EtOAc, was washed with H_2O (3x) and aq. citric acid (3x) and dried. Evaporation gave 1,1-dimethylethoxy carbonyl N-(4-iodophenyl)carbamate (2.64 g, 83%) as a colourless oil: ^{1}H NMR ($(CD_3)_2SO$) δ 1.47 (s, 9H, $OC(CH_3)_3$), 7.29 (d, J = 7.7 Hz, 2H, Ar 2,6-H_2), 7.57 (d, J = 7.4 Hz, 2H, Ar 3,5-H_2), 9.47 (brs, 1H, NH). MS (FAB+) *m/z* 319.0073 (M + H) ($C_{11}H_{14}NO_2I$ requires 319.0069).

1,1-Dimethyl-3-(4-(1,1-dimethylethoxycarbonylamino)phenyl)prop-2-yn-1-ol 132

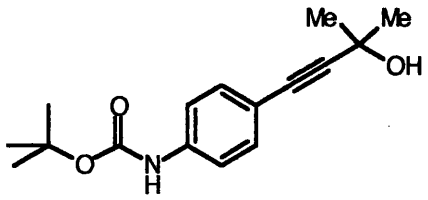

1,1-Dimethylethoxycarbonyl N-(4-iodophenyl)carbamate (180 mg, 0.56 mmol) was stirred with $(PPh_3)_2PdCl_2$ (15 mg), CuI (20 mg), 2-methyl-3-butyn-2-ol (0.08 mL, 71

mg, 0.84 mmol) in dry diisopropylamine (2 mL) and dry THF (5 mL) at 45°C for 2 d under nitrogen. Filtration (Celite®), evaporation and column chromatography (10 : 1 $CHCl_3$: MeOH) gave 1,1-dimethyl-3-(4-(1,1-dimethylethoxycarbonylamino)phenyl) prop-2-yn-1-ol (80 mg, 52%) as a cream solid: R_f = 0.5 (10 : 1 $CHCl_3$: MeOH); ^1H NMR ($CDCl_3$) δ 1.53 (s, 9H, $OC(CH_3)_3$), 1.63 (s, 6H, $C(Me)_2$), 2.41 (br, 1H, OH), 6.77 (s, 1H, NH), 7.34 (s, 4H, Ar-H_4); ^{13}C NMR ($CDCl_3$) δ 28.35 ($OC(\underline{C}H_3)_3$), 31.56 ($C(Me)_2$), 65.64 (COH), 80.86 ($C\equiv\underline{C}COH$), 81.96 ($O\underline{C}(CH_3)_3$), 92.96 ($Ar\underline{C}\equiv C$), 116.93 (4-Ar), 118 (2-Ar, 6-Ar), 132 (3-Ar, 5-Ar), 138.47 (1-Ar), 152.52 (C=O). MS (FAB+) *m/z* 275.1522 (M + H) ($C_{16}H_{21}NO_3$ requires 275.1521).

Bis(2-(4-nitrophenyl)ethyl)urea 137

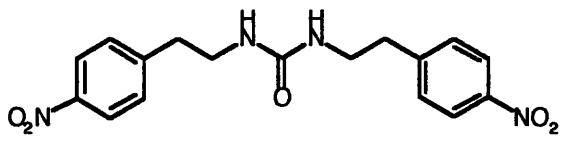

1,1-Dimethyl-3-(4-(1,1-dimethylethoxycarbonylamino)phenyl)prop-2-yn-1-ol (50 mg, 0.18 mmol) was stirred with 4-nitrophenyl chloroformate (36 mg, 0.18 mmol) and Et_3N (40 mg, 0.4 mmol) in DCM (4 mL) for 1 h. 2-(4-Nitrophenyl)ethylamine hydrochloride (37 mg, 0.18 mmol) was added and the mixture was stirred for 16 h. Evaporation and chromatography (10 : 1 $CHCl_3$: MeOH) gave bis(2-(4-nitrophenyl) ethyl)urea (17 mg, 27%) as a pale buff solid: ^1H NMR ($(CD_3)_2SO$) δ 2.81 (t, $\mathcal{J}$ = 7.0 Hz, 4H, 2x $ArCH_2$), 3.26 (dt, $\mathcal{J}$ = 5.7, 7.0 Hz, 4H, 2x NCH_2), 5.92 (t, $\mathcal{J}$ = 5.7 Hz, 2H, 2x NH), 7.47 (d, $\mathcal{J}$ = 8.6 Hz, 4H, 2x Ar 2,6-H_2), 8.15 (d, $\mathcal{J}$ = 8.2 Hz, 4H, 2x Ar 3,5-H_2); ^{13}C NMR ($(CD_3)_2SO$) δ 36.37 (CH_2), 40.67 (CH_2), 123.36 (CH), 130.06 (CH), 146.00 (Cq), 148.38 (Cq), 157.80 (CO). MS (FAB+) *m/z* 359.1362 (M + H) ($C_{17}H_{19}N_4O_5$ requires 359.1355).

Prop-2-ynyl N-(2-(4-nitrophenyl)ethyl)carbamate 140

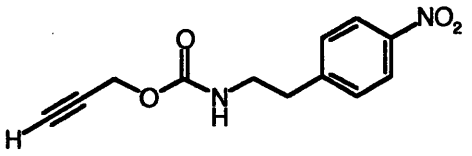

Propargyl alcohol (1.1 g, 20 mmol) was stirred with 4-nitrophenyl chloroformate (4.0 g, 20 mmol) in DCM (15 mL) in the presence of Et_3N (4.02 g, 40 mmol) for 1 h. 2-(4-Nitrophenyl)ethylamine hydrochloride (3.7 g, 20 mmol) was added and the mixture was stirred for 16 h. The evaporation residue, in EtOAc, was washed with H_2O (3x) and was dried. The evaporation residue was triturated with diethyl ether to give prop-2-ynyl N-(2-(4-nitrophenyl)ethyl)carbamate (2.0 g, 40%) as a pale yellow solid: R_f = 0.5 (10 : 1 $CHCl_3$: MeOH); ^1H NMR ($CDCl_3$) δ 2.46 (t, $\mathcal{J}$ = 2.5 Hz, 1H, C≡CH), 2.94 (t, $\mathcal{J}$ = 6.9 Hz, 2H, $ArCH_2$), 3.47 (q, $\mathcal{J}$ = 6.7 Hz, 2H, $NHC\underline{H_2}$), 4.66 (d, $\mathcal{J}$ = 2.3 Hz, 2H, OCH_2), 4.80 (brs, 1H, NH), 7.35 (d, $\mathcal{J}$ = 8.9 Hz, 2H, Ar 2,6-H_2), 8.16 (d, $\mathcal{J}$ = 8.8 Hz, 2H, 3,5-H_2). MS (FAB+) *m/z* 249.0882 (M + H) ($C_{12}H_{13}N_2O_4$ requires 249.0875).

N^{α}-(Fluoren-9-ylmethoxycarbonyl)glutamic acid N-(4-iodophenyl)amide γ-(1,1-dimethylethyl)ester 144

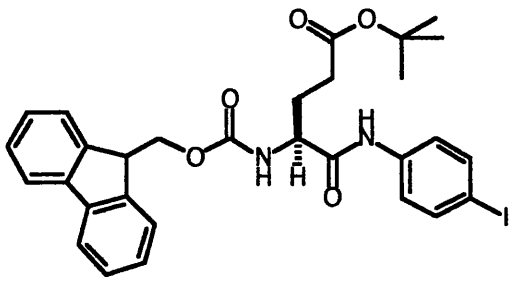

N^{α}-(Fluoren-9-ylmethoxycarbonyl)glutamic acid γ-(1,1-dimethylethyl)ester pentafluoro phenyl ester (787 mg, 1.33 mmol) was stirred with 4-iodoaniline (292 mg, 1.33 mmol) and Et_3N (270 mg, 2.7 mmol) in DCM (8 mL) for 5 h. The evaporation residue, in EtOAc, was washed with H_2O (3x) and aq. citric acid (3x). Chromatography (2 : 3 EtOAc : hexane) gave N^{α}-(fluoren-9-ylmethoxycarbonyl)glutamic acid N-(4-iodo

phenyl)amide γ-(1,1-dimethylethyl)ester (92 mg, 11%) as a white semi-solid: ^{1}H NMR ($CDCl_3$) δ 1.41 (s, 9H, $OC(CH_3)_3$), 2.00 (m, 1H, β-H_2), 2.11 (m, 1H, β-H_2), 2.38 (m, 1H, γ-H), 2.40 (m, 1H, γ-H), 4.18 (d, J = 6.9 Hz, 1H, Flu 9-H), 4.32 (m, 1H, α-H), 4.39 (d, J = 6.9 Hz, 2H, FluCH_2), 5.95 (d, J = 7.5 Hz, 1H, α-NH), 7.28 (m, 4H, Flu 2,7-H_2, Ar 2,6-H_2), 7.37 (t, J = 8.0 Hz, 2H, Flu 3,6-H_2), 7.57 (m, 4H, Flu 1,8-H_2, Ar 3,5-H_2), 7.74 (d, J = 7.7 Hz, 2H, Flu 4,5-H_2), 8.76 (brs, 1H, ArNH). MS (FAB+) *m/z* 627.1345 (M + H) ($C_{30}H_{32}N_2O_5I$ requires 627.1356).

N^{α}-(1,1-Dimethylethoxycarbonyl)glutamine N-(4-iodophenyl)amide 145

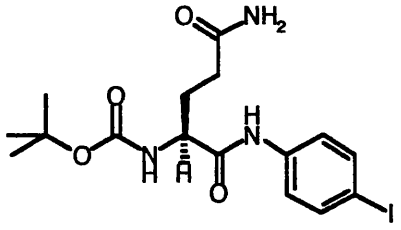

N^{α}-(1,1-Dimethylethoxycarbonyl)pyroglutamic acid N-(4-iodophenyl) amide (80 mg, 0.19 mmol) was stirred in THF (5.0 mL) with aq. ammonia (35%, 1.0 mL) for 18 h. Evaporation gave N^{α}-(1,1-dimethylethoxycarbonyl)glutamine N-(4-iodophenyl)amide as a pale buff solid: ^{1}H NMR ($(CD_3)_2SO$) δ 1.38 (s, 9H, $OC(CH_3)_3$), 2.10 (dt, J = 17, 7.0 Hz, 1H, Gln β-H), 2.16 (dt, J = 17, 7.0 Hz, 1H, Gln β-H), 2.50-2.70 (m, 2H, Gln γ-H_2), 4.00 (m, 1H, Gln α-H), 6.79 (s, 1H, δ-CONH), 7.09 (d, J = 7.4 Hz, 1H, α-NH), 7.29 (s, 1H, δ-CONH), 7.44 (d, J = 8.9 Hz, 2H, Ar 2,6-H_2), 7.64 (d, J = 8.7 Hz, 2H, Ar 3,5-H_2), 10.08 (s, 1H, ArNH). MS (FAB+) *m/z* 448 (M + H), 392 (M – $Me_2C{=}CH_2$), 348 (M – Boc).

Pyroglutamic acid benzyl ester 147

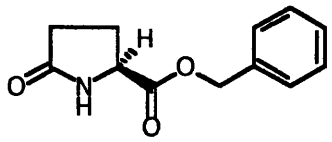

Pyroglutamic acid (25.0 g, 194 mmol) was stirred with Et_3N (19.6 g, 194 mmol) and benzyl chloride at reflux for 5 d in THF (250 mL). H_2O (200 mL) was added and the THF was evaporated. The DCM extract was washed with H_2O (3x) and aq. citric acid (3x) and was dried. Evaporation gave pyroglutamic acid benzyl ester (31.4 g, 74%) as a pale buff oil: ^1H NMR ($CDCl_3$) δ 1.98-2.39 (m, 4H, Pyg β, γ-H_4), 4.16 (dd, $\mathcal{J}$ = 7.7, 4.7 Hz, 1H, Pyg α-H), 5.06 (d, $\mathcal{J}$ = 12.4 Hz, 1H, PhCH), 5.07 (d, $\mathcal{J}$ = 12.4 Hz, 1H, PhCH), 7.25 (m, 5H, Ph-H_5), 7.49 (s, 1H, Pyg NH). MS (FAB+) *m/z* 220 (M + H), 91 (Bn).

N^{α}-(1,1-Dimethylethoxycarbonyl)pyroglutamic acid benzyl ester 148

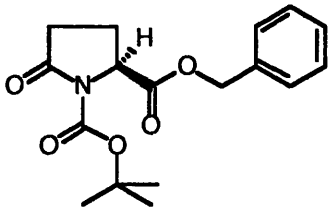

Pyroglutamic acid benzyl ester (31.3 g, 142 mmol) was stirred in DCM (250 mL) with di-*tert*-butyl dicarbonate (62 g, 285 mmol) and Et_3N (14.5 g, 142 mmol) and DMAP (2.5 g, 4 mmol) for 18 h. The evaporation residue, in EtOAc, was washed with H_2O (3x) and aq. copper(II) sulfate (2x) and dried. The evaporation residue was recrystallised (cyclohexane) to give N^{α}-(1,1-dimethylethoxycarbonyl)pyroglutamic acid benzyl ester (34 g, 75%) as pale yellow crystals: mp 60-62°C. (Lit.[145] mp 57-59°C); ^1H NMR ($CDCl_3$) δ 1.40 (s, 9H, $OC(CH_3)_3$), 2.00 (ddt, $\mathcal{J}$ = 13.1, 9.6, 3.2 Hz, 1H, Pyg β-H), 2.30 (m, 1H, Pyg β-H), 2.47 (ddd, $\mathcal{J}$ = 13.6, 8.2, 3.7 Hz, 1H, Pyg γ-H), 2.56 (dt, $\mathcal{J}$ = 13.6, 9.4 Hz, 1H, Pyg γ-H), 4.62 (dd, $\mathcal{J}$ = 9.4, 3.0 Hz, 1H, Pyg α-H), 5.18 (d, $\mathcal{J}$ =

12.3 Hz, 1H, PhCH), 5.19 (d, $\mathcal{J}$ = 12.3 Hz, 1H, PhCH), 7.34 (m, 5H, Ph-H_5). MS (FAB+) *m/z* 320 (M + H), 264 (M – $Me_2C{=}CH_2$), 220 (M – Boc), 91 (Bn).

N^{α}-(1,1-Dimethylethoxycarbonyl)pyroglutamic acid 149

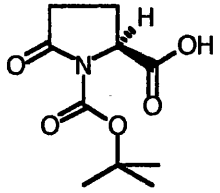

N^{α}-(1,1-Dimethylethoxycarbonyl)pyroglutamic acid benzyl ester (2.0 g, 6.2 mmol) was stirred in dry MeOH (50 mL) with Pd/C (10%, 50 mg) under hydrogen for 16 h. Filtration (Celite®) and evaporation gave N^{α}-(1,1-dimethylethoxycarbonyl)pyro glutamic acid (1.6 g, 78%) as white crystals: mp 69-72°C (Lit.[155] mp 77-80°C); ^{1}H NMR ($CDCl_3$) δ 1.36 (s, 9H, $OC(CH_3)_3$), 2.00 (m, 1H, Pyg β-H), 2.26 (m, 1H, Pyg β-H), 2.43 (m, 1H, Pyg γ-H), 2.51 (m, 1H, Pyg γ-H), 4.52 (dd, $\mathcal{J}$ = 9.4, 3.0 Hz, 1H, Pyg α-H), 10.87 (br, 1H, OH). MS (FAB+) *m/z* 230 (M + H), 174 (M – $(CH_3)_2C{=}CH_2$), 130 (M – Boc).

N^{α}-(1,1-Dimethylethoxycarbonyl)pyroglutamic acid pentafluorophenyl ester 150

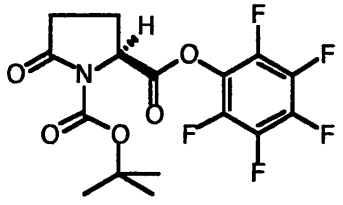

N^{α}-(1,1-Dimethylethoxycarbonyl)pyroglutamic acid (22.0 g, 100 mmol) was stirred in EtOAc (250 mL) with pentafluorophenol (37 g, 200 mmol) and DCC (22 g, 100 mmol) at 0°C for 2 h. Filtration and evaporation gave the N^{α}-(1,1-dimethylethoxy carbonyl)pyroglutamic acid pentafluorophenyl ester (10.5 g, 44%) as a colourless gum:

^{1}H NMR ($CDCl_3$) δ 1.41 (s, 9H, $OC(CH_3)_3$), 2.00 (m, 1H, Pyg β-H), 2.33 (m, 1H, Pyg β-H), 2.49 (ddd, J = 12.7, 9.3, 3.3 Hz, 1H, Pyg γ-H), 2.62 (ddd, J = 12.2, 10.2, 9.3 Hz, 1H, Pyg γ-H), 4.65 (dd, J = 9.5, 3.0 Hz, 1H, Pyg α-H); ^{19}F NMR ($CDCl_3$) δ -160.93 (dd, J = 20.1, 16.8 Hz, 2F, 3,5-F_2), -156.11 (t, J = 20.6 Hz, 1F, 4-F), -152.57 (d, J = 17.2 Hz, 2F, 2,6-F_2).

N^{α}-(1,1-Dimethylethoxycarbonyl)pyroglutamic acid N-(4-iodophenyl) amide 151

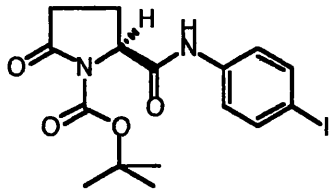

N^{α}-(1,1-Dimethylethoxycarbonyl)pyroglutamic acid pentafluorophenyl ester (3.4 g, 8.6 mmol) was stirred in DCM (10 mL) with 4-iodoaniline (1.9 g, 8.6 mmol), DMAP (20 mg) and Et_3N (2.6 g, 2.6 mmol) for 16 h. The mixture was washed with aq. citric acid (3x) and dried. Chromatography (10 : 1 $CHCl_3$: MeOH) gave N^{α}-(1,1-dimethylethoxycarbonyl)pyroglutamic acid N-(4-iodophenyl)amide (702 mg, 19%) as a pale buff solid: ^{1}H NMR ($CDCl_3$) δ 1.45 (s, 9H, $OC(CH_3)_3$), 2.22 (m, 1H, Pyg β-H), 2.36 (m, 1H, Pyg β-H), 2.53 (ddd, J = 17.6, 9.7, 5.0 Hz, 1H, Pyg γ-H), 2.56 (dt, J = 16.5, 9.0 Hz, 1H, Pyg γ-H), 4.69 (dd, J = 8.8, 4.1 Hz, 1H, Pyg α-H), 7.41 (d, J = 8.8 Hz, 2H, Ar 2,6-H_2), 7.60 (d, J = 8.8 Hz, 2H, Ar 3,5-H_2), 8.92 (s, 1H, NH); ^{13}C NMR ($CDCl_3$) δ 21.91, 28.02, 31.81, 61.22, 84.10, 87.68, 122.02, 137.56, 137.89, 169.66, 171.32. MS (FAB+) *m/z* 431.0468 (M + H) ($C_{16}H_{20}N_2O_4I$ requires 431.0468).

Pyroglutamic acid N-(4-iodophenyl)amide 156

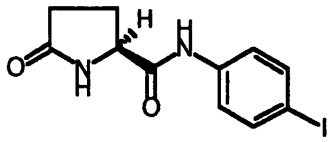

N^{α}-(1,1-Dimethylethoxycarbonyl)pyroglutamic acid N-(4-iodophenyl) amide (250 mg, 0.56 mmol) was stirred with TFA (2.0 mL) in DCM (3 mL) for 25 min. Evaporation gave Pyroglutamic acid N-(4-iodophenyl)amide (172 mg, 93%) as a light brown hydroscopic oil: R_f = 0.3 (10 : 1 $CHCl_3$: MeOH); ^1H NMR ($CDCl_3$) δ 1.99 (m, 1H), 2.16 (m, 2H), 2.34 (m, 1H) (Pyg β, γ-H_4), 4.14 (dd, $\mathcal{J}$ = 8.2, 4.4 Hz, 1H, Pyg α-H), 7.43 (d, $\mathcal{J}$ = 8.8 Hz, 2H, Ar 2,6-H_2), 7.63 (d, $\mathcal{J}$ = 8.9 Hz, 2H, Ar 3,5-H_2), 7.86 (s, 1H, Pyg NH), 10.14 (s, 1H, ArNH). MS (FAB+) *m/z* 331 (M + H), 484, 637 (M + H + nitrobenzyl alcohol clusters).

N^{α}-(N^{α}-(1,1-Dimethylethoxycarbonyl)leucyl)glutamine N-(4-iodophenyl) amide 159

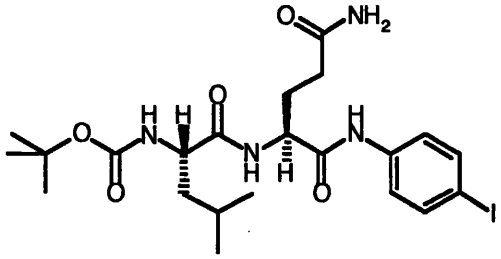

HCl was passed through a solution of N^{α}-(1,1-dimethylethoxycarbonyl)glutamine N-(4-iodophenyl)amide (300 mg, 0.67 mmol) in MeOH (30 mL) for 30 mins at RT. The mixture was then concentrated to yield glutamine N-(4-iodophenyl) amide hydrochloride (277 mg, 0.72 mmol) which was then reacted *in situ* with Et_3N (0.2 mL, 1.44 mmol), DMAP (1 mg) and N^{α}-(1,1-dimethylethoxycarbonyl)leucine N-hydroxysuccinimide ester (332 mg, 0.89 mmol) in THF (4 mL) and DMF (3 mL) for 16 h at RT. The evaporation residue, in EtOAc, was washed with H_2O (3x). Drying,

evaporation and recrystallisation (EtOAc / hexane) gave N^{α}-(N^{α}-(1,1-dimethylethoxycarbonyl)leucyl)glutamine N-(4-iodophenyl) amide (155 mg, 38%) as a buff solid: R_f = 0.4 (10 : 1 $CHCl_3$: MeOH); ^1H NMR ($(CD_3)_2SO$) δ 0.84 (d, J = 5.2 Hz, 3H, Leu γ-CH_3), 0.86 (d, J = 6.2 Hz, 3H, Leu γ-CH_3), 1.37 (s, 9H, $OC(CH_3)_3$), 1.38-1.45 (m, 2H, Leu β-H_2), 1.60 (m, 1H, Leu γ-H), 1.80-1.95 (m, 2H, Gln β-H_2), 2.08-2.16 (m, 2H, Gln γ-H_2), 3.98 (brq, J = 7.0 Hz, 1H, Leu α-H), 4.34 (m, 1H, Gln α-H), 6.79 (s, 1H, δ-CONH), 6.96 (d, J = 8.0 Hz, 1H, α-NH), 7.29 (s, 1H, δ-CONH), 7.43 (d, J = 8.9 Hz, 2H, Ar 2,6-H_2), 7.64 (d, J = 8.8 Hz, 2H, Ar 3,5-H_2), 8.03 (d, J = 8.0 Hz, 1H, α-NH), 10.12 (s, 1H, ArNH). MS (FAB+) *m/z* 560.1496 (M + H) ($C_{22}H_{33}N_4O_5I_1$ requires 560.1490).

N^{α}-(N^{α}-(Leucyl)glutamine N-(4-iodophenyl)amide trifluoroacetic acid salt 160

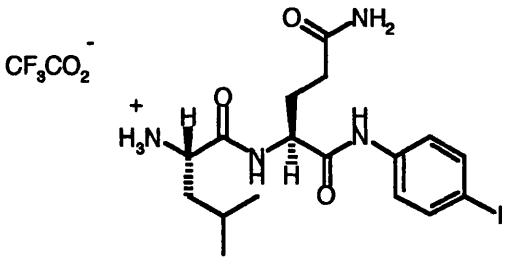

N^{α}-(N^{α}-(1,1-Dimethylethoxycarbonyl)leucyl)glutamine N-(4-iodophenyl)amide (90 mg, 16 mmol) was stirred with TFA (1 mL) in DCM (2 mL) for 30 min. Evaporation gave N^{α}-(N^{α}-(leucyl)glutamine N-(4-iodophenyl)amide trifluoroacetic acid salt (100 mg, 94%) as a light brown hydroscopic oil: ^1H NMR (CD_3OD) δ 0.88 (d, J = 5.7 Hz, 3H, Leu γ-CH_3), 0.89 (d, J = 5.4 Hz, 3H, Leu γ-CH_3), 1.64 (m, 3H, Leu β, γ-H_3), 1.99 (m, 1H, Gln β-H), 2.08 (m, 1H, Gln β-H), 2.33 (t, J = 7.2 Hz, 2H, Gln γ-H_2), 3.95 (t, J = 7.2 Hz, 1H, Leu α-H), 4.47 (dd, J = 8.9, 5.2 Hz, 1H, Gln α-H), 7.24 (d, J = 8.7 Hz, 2H, Ar 2,6-H_2), 7.48 (d, J = 8.6 Hz, 2H, Ar 3,5-H_2); ^1H NMR ($(CD_3)_2SO$) δ 0.88 (d, J = 6.2 Hz, 3H, Leu γ-CH_3), 0.90 (d, J = 5.9 Hz, 3H, Leu γ-CH_3), 1.40-1.60 (m, 3H, Leu β, γ-H_3), 1.92 (m, 2H, Gln β-H_2), 2.16 (m, 2H, Gln γ-H_2), 3.83 (m, 1H, Leu α-H), 4.42 (m, 1H, Gln α-H), 6.86 (s, 1H, δ-CONH), 7.33 (s, 1H, δ-CONH), 7.43 (d, J = 8.4

Hz, 2H, Ar 2,6-H_2), 7.66 (d, $\mathcal{J}$ = 8.4 Hz, 2H, Ar 3,5-H_2), 8.11 (br, 3H, $^+NH_3$). MS (FAB+) *m/z* 461 (M + H).

N^{α}-(N^{α}-(N^{α}-(Fluoren-9-ylmethoxycarbonyl)-N^{ε}-(1,1-dimethylethoxy carbonyl)lysyl)leucyl)glutamine N-(4-iodophenyl)amide 161

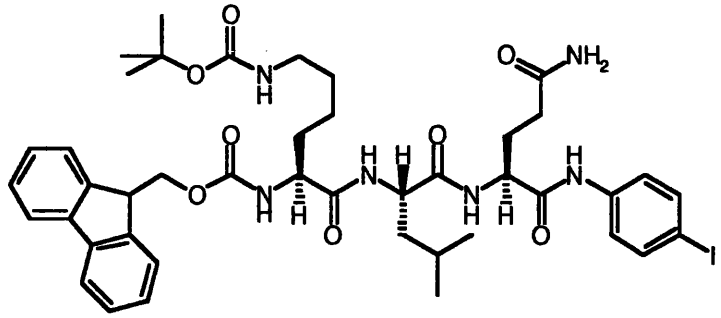

N^{α}-(Fluoren-9-ylmethoxycarbonyl)lysine N^{ε}-(1,1-dimethylethoxycarbonyl) N-hydroxy succinimide ester (382 mg, 0.68 mmol) was stirred with N^{α}-(N^{α}-(leucyl)glutamine N-(4-iodophenyl)amide trifluoroacetate salt (352 mg, 0.68 mmol), Et_3N (205 mg, 2.0 mmol) and DMAP (1 mg) in THF (2 mL) and DMF (3 mL) for 14 h. The evaporation residue, in EtOAc, was washed with H_2O (3x) and aq. citric acid (3x) and dried. Evaporation gave N^{α}-(N^{α}-(N^{α}-(fluoren-9-ylmethoxycarbonyl)-N^{ε}-(1,1-dimethylethoxycarbonyl)lysyl) leucyl)glutamine N-(4-iodophenyl)amide (243 mg, 41%) as a white solid: ^1H NMR ($(CD_3)_2SO$) δ 0.80 (d, $\mathcal{J}$ = 6.4 Hz, 3H, Leu γ-CH_3), 0.84 (d, $\mathcal{J}$ = 6.4 Hz, 3H, Leu γ-CH_3), 1.34 (s, 9H, $OC(CH_3)_3$), 1.30-1.95 (m, 11H, Lys β-H_2, Lys γ-H_2, Lys δ-H_2, Leu β-H_2, Leu γ-H, Gln β-H_2), 2.11 (m, 2H, Gln γ-H_2), 2.87 (m, 2H, Lys ε-H_2), 3.94-4.34 (m, 6H, Lys α-H, Gln α-H, Leu α-H, Flu 9-H, FluCH_2), 6.75 (brt, $\mathcal{J}$ = 6.0 Hz, 1H, CONHCH_2), 6.78 (br, 1H, Gln δ-CONH), 7.27 (br, 1H, Gln δ-CONH), 7.30 (t, $\mathcal{J}$ = 8.0 Hz, 2H, Flu 3,6-H_2), 7.40 (d, $\mathcal{J}$ = 8.7 Hz, 2H, Ar 2,6-H_2), 7.43 (t, $\mathcal{J}$ = 8.0 Hz, 2H, Flu 2,7-H_2), 7.47 (d, $\mathcal{J}$ = 7.7 Hz, 1H, α-NH), 7.62 (d, $\mathcal{J}$ = 8.7 Hz, 2H, Ar 3,5-H_2), 7.69 (d, $\mathcal{J}$ = 8.0 Hz, 1H, Flu 1-H), 7.70 (d, $\mathcal{J}$ = 8.0 Hz, 1H, Flu 8-H), 7.87 (d, $\mathcal{J}$ = 7.4 Hz, 2H, Flu 4,5-H_2), 7.93 (d, $\mathcal{J}$ = 7.9 Hz, 1H, α-NH), 8.08 (d, $\mathcal{J}$ = 7.0 Hz, 1H, α-NH), 10.07 (s, 1H, ArNH).

N^{α}-(N^{α}-(N^{ε}-(1,1-Dimethylethoxycarbonyl)lysyl)leucyl)glutamine N-(4-iodophenyl)amide 162

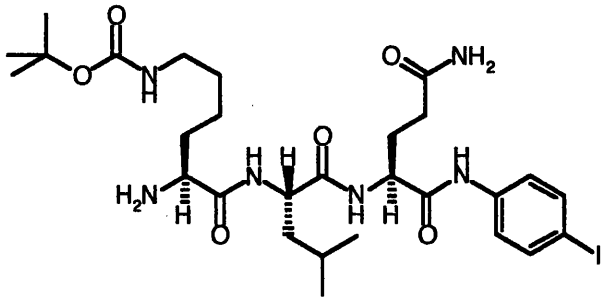

N^{α}-(N^{α}-(N^{ε}-(1,1-Dimethylethoxycarbonyl)-N^{α}-(fluoren-9-ylmethoxycarbonyl)lysyl)leucyl)glutamine N-(4-iodophenyl)amide (179 mg, 19.7 mmol) was stirred with diethylamine (0.3 mL) in DMF (2 mL) for 25 min. Evaporation and trituration with diethyl ether gave N^{α}-(N^{α}-(N^{ε}-(1,1-dimethylethoxycarbonyl)lysyl)leucyl)glutamine N-(4-iodophenyl) amide (114 mg, 84%) as white crystals: R_f = 0.2 (10 : 1 $CHCl_3$: MeOH); ^1H NMR ($(CD_3)_2SO$) δ 0.84 (d, J = 6.6 Hz, 3H, Leu γ-CH_3), 0.88 (d, J = 6.7 Hz, 3H, Leu γ-CH_3), 1.36 (s, 9H, $OC(CH_3)_3$), 1.30-1.96 (m, 11H, Lys β, γ, δ-H_6 + Leu β, γ-H_3 + Gln β-H_2), 2.12 (m, 2H, Gln γ-H_2), 2.87 (m, 2H, Lys ε-H_2), 4.25-4.37 (m, 3H, 3x α-H), 6.75 (m, 1H, Lys ε-NH), 6.81 (br, 1H, δ-CONH), 7.30 (s, 1H, δ-CONH), 7.44 (d, J = 8.6 Hz, 2H, Ar 2,6-H_2), 7.70 (d, J = 8.0 Hz, 1H, α-NH), 7.64 (d, J = 8.6 Hz, 2H, Ar 3,5-H_2) 7.95-8.13 (m, 3H, α-NH + α-NH_2), 8.25 (m, 2H, 2x NH), 10.07 (s, 1H, ArNH). MS (FAB+) *m/z* 689.2549 (M + H) ($C_{28}H_{46}N_6O_6I$ requires 689.2524).

N^{α}-(1,1-Dimethylethoxycarbonyl)glutamine N-(2-(4-nitrophenyl)ethyl) amide 164

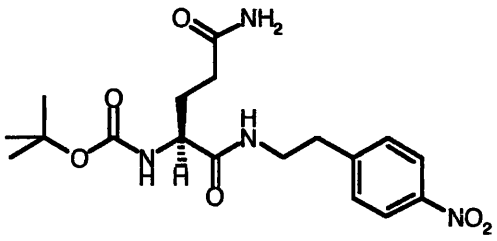

N^{α}-(1,1-Dimethyloxycarbonyl)glutamine pentafluorophenyl ester (412 mg, 1.0 mmol) was stirred with 2-(4-nitrophenyl)ethylamine hydrochloride (205 mg, 1.0 mmol) and Et_3N (202 mg, 2.0 mmol) in THF (4 mL) and DMF (0.5 mL) for 16 h. The evaporation residue, in EtOAc, was washed with H_2O (3x) and aq. citric acid (3x) and dried. Evaporation gave N^{α}-(1,1-dimethylethoxycarbonyl)glutamine N-(2-(4-nitro phenyl)ethyl)amide (190 mg, 52%) as a pale yellow solid: ^1H NMR ($(CD_3)_2SO$) δ 1.36 (s, 9H, $OC(CH_3)_3$), 1.61 (m, 1H, β-H), 1.73 (m, 1H, β-H), 2.01 (t, $\mathcal{J}$ = 6.4 Hz, 2H, γ-H_2), 2.85 (t, $\mathcal{J}$ = 6.6 Hz, 2H, $ArCH_2$), 3.25-3.45 (m, 2H, $NHCH_2$), 3.79 (m, 1H, α-H), 6.74 (brs, 1H, δ-CONH), 6.81 (d, $\mathcal{J}$ = 7.9 Hz, 1H, α-NH), 7.24 (brs, 1H, δ-CONH), 7.48 (d, $\mathcal{J}$ = 8.7 Hz, 2H, Ar 2,6-H_2), 7.88 (t, $\mathcal{J}$ = 5.7 Hz, 1H, $NHCH_2$), 8.13 (d, $\mathcal{J}$ = 8.7 Hz, 2H, Ar 3,5-H_2).

Pyroglutamic acid N-(2-(4-nitrophenyl)ethyl)amide 165

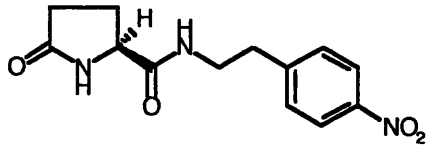

N^{α}-(1,1-Dimethylethoxycarbonyl)glutamine N-(2-(4-nitrophenyl)ethyl)amide (400 mg, 1.02 mmol) was stirred in TFA (1.0 mL) for 20 min. Evaporation gave a mixture of pyroglutamic acid N-(2-(4-nitrophenyl)ethyl)amide and ammonium trifluoroacetate (412 mg) as a brown oil: ^1H NMR ($(CD_3)_2SO$) δ 1.99 (m, 1H, Pyg β-H), 2.04-2.12 (m,

2H, Pyg β, γ-H_2), 2.18 (m, 1H, Pyg β-H), 2.87 (t, J = 6.9 Hz, 2H, $ArCH_2$), 3.32-3.45 (m, 2H, $ArCH_2\underline{CH_2}$), 3.91 (dd, J = 8.4, 4.5 Hz, 1H, Pyg α-H), 7.16 (t, J = 51.0 Hz, 4 H, $^+NH_4$), 7.49 (d, J = 8.7 Hz, 2H, Ar 2,6-H_2), 7.78 (s, 1H, Pyg NH), 8.08 (t, J = 5.7 Hz, 1H, NH), 8.15 (d, J = 8.6 Hz, 2H, Ar 3,5-H_2).

N-(Benzyloxycarbonyl)glutamine N-(4-nitrophenyl)amide 166

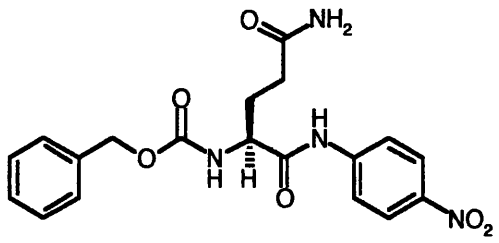

N^{α}-(Benzyloxycarbonyl)glutamine (200 mg, 0.71 mmol) was dissolved in dry THF (4 mL) and dry DMF (2 mL) at 0°C and allowed to stir for 5 min. To this mixture, pivaloyl chloride (94 mg, 0.78 mmol) and Et_3N (0.25 mL, 1.78 mmol) were added and the mixture was stirred for 30 min. 4-Nitroaniline (97 mg, 0.71 mmol) was added and the mixture was brought to RT and stirred for 3 h. The evaporation residue, in EtOAc, was washed with H_2O (3x). Drying, evaporation and chromatography ($CHCl_3$) gave N^{α}-(benzyloxycarbonyl)glutamine N-(4-nitrophenyl)amide (148 mg, 52%) as a cream-coloured powder: mp 206-208°C. R_f = 0.8 (10 : 1 $CHCl_3$: MeOH); ^1H NMR ($(CD_3)_2SO$) δ 1.76-1.88 (m, 1H, β-H), 1.80-2.00 (m, 1H, β-H), 2.08-2.28 (m, 2H, γ-H_2), 4.10-4.20 (m, 1H, α-H), 5.10 (s, 2H, $PhCH_2$), 6.82 (brs, 1H, δ-CONH), 7.32 (brs, 1H, δ-CONH), 7.34-7.41 (m, 5H, Ph-H_5), 7.74 (d, J = 7.4 Hz, 1H, α-NH), 7.85 (d, J = 7.4 Hz, 2H, Ar 2,6-H_2), 8.30 (d, J = 7.4 Hz, 2H, Ar 3,5-H_2), 10.70 (s, 1H, CONHAr). MS (FAB+) 401 (M + H). $[\alpha]_D$ = + 50.0°.

Glutamine N-(4-nitrophenyl)amide hydrobromide 167

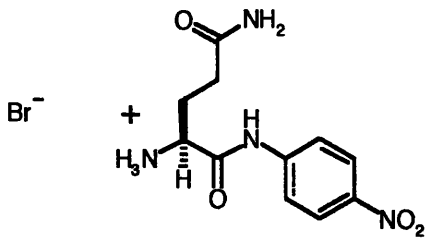

N^{α}-(Benzyloxycarbonyl)glutamine N-(4-nitrophenyl)amide (60 mg, 0.15 mmol), AcOH (1 mL) and HBr (30% in AcOH) (1 mL) were stirred for 25 min and then concentrated. Et_2O (8 mL) was added and the suspension was stirred for 5 min. The ether layer was then decanted off and the process repeated 10 times. This solid was dried to yield glutamine N-(4-nitrophenyl)amide hydrobromide (42 mg, quantitative) as a buff gum; ^1H NMR ($(CD_3)_2SO$) δ 2.00 (brs, 2H, β-H), 2.10 (brs, 2H, β-H), 2.30 (brs, 2H, γ-H_2), 4.20 (brs, 1H, α-H), 7.00 (brs, 1H, δ-CONH), 7.50 (brs, 1H, δ-CONH), 8.00 (brs, 2H, Ar 2,6-H_2), 8.40 (brs, 2H, Ar 3,5-H_2), 8.50 (brs, 3H, $^+NH_3$), 11.40 (brs, 1H, ArNH). MS (FAB+) 268 (M + H).

N^{α}-(N^{α}-(1,1-Dimethylethoxycarbonyl)leucyl)glutamine N-(4-nitrophenyl) amide 168

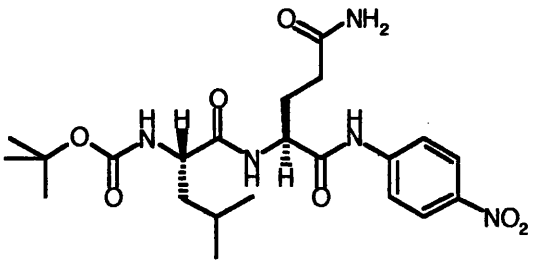

N^{α}-(1,1-Dimethylethoxycarbonyl)leucine N-hydroxysuccinimide ester (50 mg, 0.15 mmol), Et_3N (60 μL, 0.45 mmol) and DMAP (5 mg) were stirred with glutamine N-(4-nitrophenyl)amide hydrobromide (40 mg, 0.15 mmol) in CH_2Cl_2 (3 mL), THF (0.5 mL) and DMF (0.5 mL) for 16 h. The evaporation residue, in EtOAc, was washed

with H_2O (3x). Drying, evaporation and recrystallisation (EtOAc / hexane) gave N^{α}-(N^{α}-(1,1-dimethylethoxycarbonyl)leucyl)glutamine N-(4-nitrophenyl)amide (29 mg, 41%) as a light orange powder: R_f = 0.5 (10 : 1 $CHCl_3$: MeOH); ^1H NMR ($CDCl_3$) δ 0.78-0.96 (m, 6H, Leu γ-$(CH_3)_2$), 1.38 (s, 9H, $OC(CH_3)_3$), 1.44-1.58 (m, 2H, Leu β-H_2), 1.58-1.70 (m, 1H, Leu γ-H), 2.00-2.38 (m, 2H, Gln β-H_2), 2.40-2.54 (m, 2H, Gln γ -H_2), 3.90-4.05 (m, 1H, Gln α-H), 4.61-4.71 (m, 1H, Leu α-H), 5.25 (d, $\mathcal{J}$ = 5.5 Hz, 1H, Leu-NH), 6.50 (s, 1H, Gln δ-CONH), 6.65 (s, 1H, Gln δ-CONH), 7.80 (d, $\mathcal{J}$ = 9.3 Hz, 2H, Ar 2,6-H_2), 7.85 (d, $\mathcal{J}$ = 8.5 Hz, 1H, Gln α-NH), 8.10 (d, $\mathcal{J}$ = 9.3 Hz, 2H, Ar 3,5-H_2), 10.25 (brs, 1H, ArNH). MS (FAB+) 480 (M + H).

N^{α}-(1,1-Dimethylethoxycarbonyl)glutamine N-(4-(3-hydroxypropynyl) phenyl)amide 169

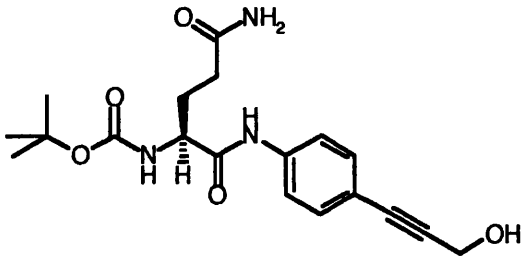

N^{α}-(1,1-Dimethylethoxycarbonyl)glutamine N-(4-iodophenyl)amide (300 mg, 0.7 mmol) was heated at 55°C for 2 d with CuI (30 mg), $(PPh_3)_2PdCl_2$ (20 mg), dry DEA (3 mL) and propargyl alcohol (101 mg, 1.0 mmol) in dry DMF (5 mL) under Argon. Filtration, evaporation and chromatography ($CHCl_3$) gave N^{α}-(1,1-dimethylethoxy carbonyl)glutamine N-(4-(3-hydroxypropynyl)phenyl)amide (116 mg, 46%) as a white solid: ^1H NMR ($(CD_3)_2SO$) δ 1.35 (s, 9H, $OC(CH_3)_3$), 1.80 (m, 1H, β-H), 2.10 (m, 1H, β-H), 3.32 (m, 2H, γ-H_2), 3.99 (m, 1H, α-H), 4.25 (d, $\mathcal{J}$ = 5.7 Hz, 2H, CH_2O), 5.28 (t, $\mathcal{J}$ = 5.7 Hz, 1H, OH), 6.77 (brs, 1H, δ-CONH), 7.09 (d, $\mathcal{J}$ = 7.0 Hz, 1H, α-NH), 7.27 (brs, 1H, δ-CONH), 7.34 (d, $\mathcal{J}$ = 8.7 Hz, 2H, Ar 2,6-H_2), 7.59 (d, $\mathcal{J}$ = 8.8 Hz, 2H, Ar 3,5-H_2), 10.12 (brs, 1H, ArNH). MS (FAB+) *m/z* 376.1801 (M + H) ($C_{19}H_{22}N_3O_5$ requires 376.1794).

N^{α}-(1,1-Dimethylethoxycarbonyl)glutamine N-(4-(3-(2-(4-nitrophenyl) ethylaminocarbonyloxy)prop-1-ynyl)phenyl)amide 170

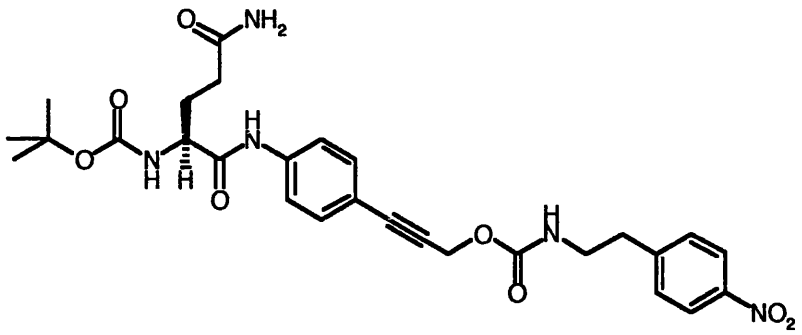

N^{α}-(1,1-Dimethylethoxycarbonyl)glutamine N-(4-iodophenyl)amide (900 mg, 2 mmol) was stirred with $(PPh_3)_2PdCl_2$ (60 mg), CuI (90 mg), propargyl N-(2-(4-nitrophenyl)ethyl)carbamate (625 mg, 2.5 mmol) in dry diisopropylamine (9 mL) and dry DMF (10 mL) at 55°C for 3 d under Argon. Filtration (Celite®), evaporation and column chromatography (10 : 1 $CHCl_3$: MeOH) gave N^{α}-(1,1-dimethylethoxy carbonyl)glutamine N-(4-(3-(2-(4-nitrophenyl)ethylaminocarbonyloxy)prop-1-ynyl) phenyl)amide (520 mg, 43%) as a brown semi-solid: R_f = 0.4 (10 : 1 $CHCl_3$: MeOH); ^1H NMR ($(CD_3)_2SO$) δ 1.37 (s, 9H, $OC(CH_3)_3$), 1.70-1.92 (m, 2H, Gln β-H_2), 2.11 (m, 1H, Gln γ-H), 2.13 (m, 1H, Gln γ-H), 2.88 (t, J = 6.9 Hz, 2H, $ArCH_2$), 3.24-3.34 (m, 2H, $ArCH_2C\underline{H_2}$), 4.01 (m, 1H, Gln α-H), 4.81 (s, 2H, CH_2O), 6.78 (s, 1H, δ-CONH), 7.09 (d, J = 7.4 Hz, 1H, α-NH), 7.28 (br, 1H, δ-CONH), 7.37 (d, J = 8.9 Hz, 2H, Ar 2,6-H_2), 7.48 (d, J = 8.7 Hz, 2H, Ar' 2,6-H_2), 7.49 (d, J = 7.0 Hz, 1H, NH), 7.62 (d, J = 8.7 Hz, 2H, Ar 3,5-H_2), 8.13 (d, J = 8.8 Hz, 2H, Ar' 3,5-H_2), 10.15 (br, 1H, ArNH). MS (FAB+) *m/z* 568 (M + H).

N^{α}-(N^{α}-(1,1-Dimethylethoxycarbonyl)leucyl)glutamine N-(4-(3-(2-(4-nitro phenyl)ethylaminocarbonyloxy)prop-1-ynyl)phenyl)amide 172

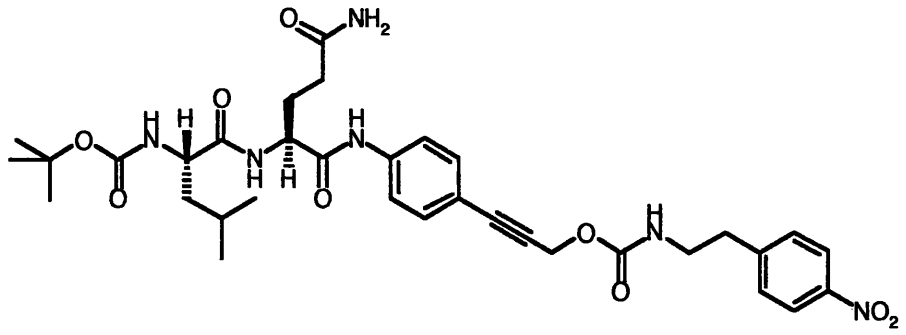

Glutamine N-(4-(3-(2-(4-nitrophenyl)ethylaminocarbonyloxy)prop-1-ynyl)phenyl) amide hydrochloride (231 mg, 0.4 mmol) was stirred with N^{α}-(1,1-dimethylethoxy carbonyl)leucine N-hydroxysuccinimide ester (151 mg, 0.4 mmol), Et_3N (122 mg, 1.2 mmol) and DMAP (1 mg) in THF (1 mL) and DMF (3 mL) for 16 h. The evaporation residue, in EtOAc, was washed with H_2O (3x) and aq. citric acid (3x) and was dried. Evaporation gave N^{α}-(N^{α}-(1,1-dimethylethoxycarbonyl)leucyl)glutamine N-(4-(3-(2-(4-nitrophenyl)ethylaminocarbonyloxy)prop-1-ynyl)phenyl) amide (85 mg, 29%) as a light brown gum: R_f = 0.5 (10 : 1 $CHCl_3$: MeOH); ^1H NMR ($(CD_3)_2SO$) δ 0.85 (d, $\mathcal{J}$ = 5.2 Hz, 3H, Leu γ-CH_3), 0.86 (d, $\mathcal{J}$ = 6.1 Hz, 3H, Leu γ-CH_3), 1.37 (s, 9H, $OC(CH_3)_3$), 1.60-2.20 (m, 7H, Leu β, γ-H_3 + Gln β, γ-H_4), 2.45 (m, 2H, $ArCH_2$), 2.85 (t, $\mathcal{J}$ = 6.5 Hz, 2H, $ArCH_2C\underline{H_2}$), 4.00 (m, 1H, Leu α-H), 4.36 (m, 1H, Gln α-H), 4.82 (s, 2H, CH_2O), 6.78 (s, 1H, δ-CONH), 6.96 (m, 2H, 2x α-NH), 7.30 (br, 1H, δ-CONH), 7.37 (d, $\mathcal{J}$ = 8.9 Hz, 2H, Ar 2,6-H_2), 7.52 (d, $\mathcal{J}$ = 8.2 Hz, 2H, Ar' 2,6-H_2), 7.67 (d, $\mathcal{J}$ = 8.6 Hz, 2H, Ar 3,5-H_2), 8.05 (m, 1H, NH), 8.14 (d, $\mathcal{J}$ = 8.6 Hz, 2H, Ar' 3,5-H_2), 8.22 (br, 1H, NH).

N^{α}-(1,1-Dimethylethoxycarbonyl)phenylalanine N-(4-iodophenyl)amide 175

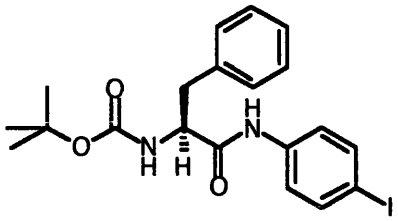

N^{α}-(1,1-Dimethylethoxycarbonyl)phenylalanine (2.5 g, 4.42 mmol) was stirred in dry EtOAc (20 mL) at 0°C with pivaloyl chloride (533 mg, 4.42 mmol) and Et_3N (0.61 mL, 4.42 mmol) for 3 h. 4-Iodoaniline (968 mg, 4.42 mmol) in EtOAc (10 mL) was added and the mixture was brought to RT and stirred for 16 h. The evaporation residue, in EtOAc, was washed with H_2O (3x). Drying, evaporation and chromatography (9 : 1 EtOAc : hexane) gave N^{α}-(1,1-dimethylethoxycarbonyl)phenylalanine N-(4-iodophenyl)amide (900 mg, 45%) as a brown oil: R_f = 0.85 (10 : 1 $CHCl_3$: MeOH); ^1H NMR ($CDCl_3$) δ 1.42 (s, 9H, $OC(CH_3)_3$), 3.13 (d, $\mathcal{J}$ = 7.2 Hz, 2H, Phe β-H_2), 4.43 (m, 1H, Phe α-H), 5.06 (br, 1H, ArNH), 7.15 (d, $\mathcal{J}$ = 8.5 Hz, 2H, Ar 2,6-H_2), 7.21-7.34 (m, 5H, Ph-H_5), 7.58 (d, $\mathcal{J}$ = 8.7 Hz, 2H, Ar 3,5-H_2), 7.77 (brd, $\mathcal{J}$ = 7.0 Hz, 1H, α-NH). MS (FAB-) *m/z* 465.0667 (M - H) ($C_{20}H_{22}N_2O_3I$ requires 465.0675).

Phenylalanine N-(4-iodophenyl)amide trifluoroacetic acid salt 176

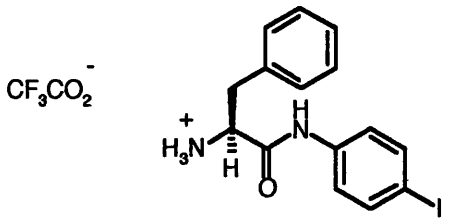

N^{α}-(1,1-Dimethylethoxycarbonyl)phenylalanine N-(4-iodophenyl)amide (125 mg, 26 mmol) was stirred with TFA (1 mL) in DCM (2 mL) at RT for 30 min. Evaporation gave phenylalanine N-(4-iodophenyl)amide trifluoroacetic acid salt (170 mg, 71%) as a

light brown oil: R_f = 0.4 (10 : 1 $CHCl_3$: MeOH); ^1H NMR (CD_3OD) δ 3.09 (dd, $\mathcal{J}$ = 13.8, 7.7 Hz, 1H, Phe β-H), 3.18 (dd, $\mathcal{J}$ = 13.8, 6.8 Hz, 1H, Phe β-H), 4.15 (dd, $\mathcal{J}$ = 7.7, 6.8 Hz, 1H, Phe α-H), 7.16-7.26 (m, 7H, Ph-H_5 + Ar 2,6-H_2), 7.53 (d, $\mathcal{J}$ = 8.7 Hz, 2H, Ar 3,5-H_2). MS (FAB+) *m/z* 734 (2x M + H), 368 (M + H).

N^{α}-(1,1-Dimethylethoxycarbonyl)alanine pentafluorophenyl ester 177

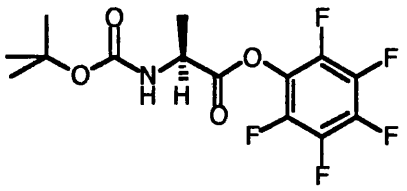

N^{α}-(1,1-Dimethylethoxycarbonyl)alanine (1.89 g, 10 mmol) in EtOAc (30 mL) was cooled to 0°C. Pentafluorophenol (1.84 g, 10 mmol) in EtOAc (10 mL) was added at 0°C and the mixture were stirred for 30 min. DCC (2.06 g, 10 mmol) was added and the mixture was stirred for 2 h. The suspension was filtered (Celite®) and the filtrate was kept at 0°C for 24 h. Filtration and evaporation yielded N^{α}-(1,1-dimethylethoxycarbonyl)alanine pentafluorophenyl ester (3.56 g, quantitative) as a colourless gum. This was used without further purification: ^1H NMR ($CDCl_3$) δ 1.47 (s, 9H, $OC(CH_3)_3$), 1.59 (d, $\mathcal{J}$ = 6.0 Hz, 3H, Ala-CH_3), 4.66 (quintet, $\mathcal{J}$ = 6.0 Hz, 1H, α-H), 5.06 (d, $\mathcal{J}$ = 6.0 Hz, 1H, α-NH); ^{19}F NMR ($CDCl_3$) δ -162.03 (dd, $\mathcal{J}$ = 21.0, 18.4 Hz, 1.8F, 3,5-F_2), -161.89 (m, 0.2F, 3,5-F_2), -157.49 (t, $\mathcal{J}$ = 21.0 Hz, 0.9F, 4-F), -157.34 (m, 0.1F, 4-F), -152.98 (d, $\mathcal{J}$ = 20.3 Hz, 0.2F, 2,6-F_2), -521.51 (d, $\mathcal{J}$ = 18.4 Hz, 1.8F, 2,6-F_2). MS (FAB+) *m/z* 356.0991 (M + H) ($C_{14}H_{15}NO_4F_5$ requires 356.0921).

N^{α}-(N^{α}-(1,1-Dimethylethoxycarbonyl)alanyl)phenylalanine N-(4-iodo phenyl)amide 179

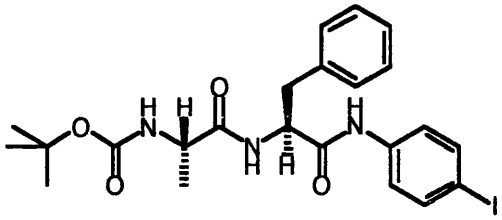

Phenylalanine N-(4-iodophenyl)amide trifluoroacetate salt (170 mg, 0.35 mmol) was stirred with N^{α}-(1,1-dimethylethoxycarbonyl)alanine pentafluorophenyl ester (120 mg, 0.35 mmol), Et_3N (107 mg, 1 mmol) and DMAP (1 mg) in THF (4 mL) for 16 h. The evaporation residue, in EtOAc, was washed with H_2O (3x) and aq. citric acid (3x) and was dried. Evaporation and chromatography (10 : 1 $CHCl_3$: hexane) gave N^{α}-(N^{α}-(1,1-dimethylethoxycarbonyl)alanyl)phenyl alanine N-(4-iodophenyl)amide (120 mg, 64%) as a white wax: R_f = 0.8 (10 : 1 $CHCl_3$: MeOH); ^1H NMR ($CDCl_3$) δ 1.36 (d, $\mathcal{J}$ = 7.2 Hz, 3H, Ala-Me), 1.42 (s, 9H, $OC(CH_3)_3$), 3.11 (dd, $\mathcal{J}$ = 13.6, 6.4 Hz, 1H, Phe β-H), 3.27 (dd, $\mathcal{J}$ = 13.3, 5.5 Hz, 1H, Phe β-H), 4.07 (dq, $\mathcal{J}$ = 5.0, 7.0 Hz, 1H, Ala α-H), 4.81 (*ca.* q, $\mathcal{J}$ = 6 Hz, 1H, Phe α-H), 5.02 (br, 1H, Ala α-NH), 6.81 (d, $\mathcal{J}$ = 7.0 Hz, 1H, Phe α-NH), 7.12-7.36 (m, 5H, Ph-H_5), 7.26 (d, $\mathcal{J}$ = 8.7 Hz, 2H, Ar 2,6-H_2), 7.52 (d, $\mathcal{J}$ = 8.7 Hz, 2H, Ar 3,5-H_2), 8.57 (s, 1H, ArNH). MS (FAB-) *m/z* 536 (M - H).

Methyl 6-aminohexanoate hydrochloride 182

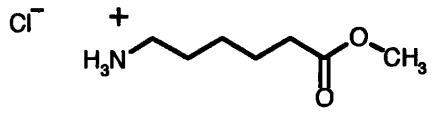

Thionyl chloride (2.0 mL) was added slowly to 6-aminohexanoic acid (4.00 g, 30.5 mmol) in MeOH (30 mL) at 0°C and the mixture stirred at RT for 4 d. Evaporation yielded methyl 6-aminohexanoate hydrochloride (5.47 g, 99%) as white crystals: mp 120-122°C. (Lit.[151] mp 120-121°C); ^1H NMR ($(CD_3)_2SO$) δ 1.22-1.34 (m, 2H, 4-H_2),

1.45-1.59 (m, 4H, 3,5-H_4), 2.28 (t, J = 7.4 Hz, 2H, 2-H_2), 2.71 (t, J = 7.4 Hz, 2H, 6-H_2), 3.60 (s, 3H, CH_3), 8.10 (brs, 3H, $^+NH_3$); ^{13}C NMR ($(CD_3)_2SO$) δ 23.02 (4-C), 25.00 (5-C), 27.01 (3-C), 34.08 (6-C), 39.08 (2-C), 52.02 (CH_3), 174.00 (Cq). MS (FAB+) *m/z* 146 (M + H).

Methyl 6-(5-dimethylaminonaphthalenesulfonamido)hexanoate 183

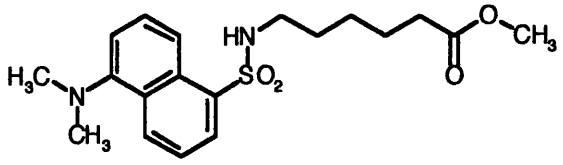

Dansyl chloride (190 mg, 0.7 mmol) was added to a solution of methyl 4-aminohexanoate hydrochloride (126 mg, 0.7 mmol) and Et_3N (0.29 mL, 2.1 mmol) in dry THF (4 mL) and DMF (1 mL). The solution was then left to stir for 16 h at RT. Evaporation and chromatography (10 : 0.5 $CHCl_3$: MeOH) yielded methyl 6-(5-dimethylaminonaphthalenesulfonamido)hexanoate (190 mg, 72%) as a light green oil: R_f = 0.76 (10 : 1 $CHCl_3$: MeOH); ^1H NMR ($CDCl_3$) δ 1.10-1.50 (m, 6H, 3,4,5-H_6), 2.15 (t, J = 7.4 Hz, 2H, 2-H_2), 2.86 (s, 6H, $N(CH_3)_2$), 2.88 (q, J = 7.4 Hz, 2H, 6-H_2), 3.62 (s, 3H, CH_3), 4.96 (t, J = 6.2 Hz, 1H, dansyl-NH), 7.18 (d, J = 7.7 Hz, 3'-H), 7.52 (t, J = 8.6 Hz, 1H, 5'-H_2), 7.56 (t, J = 8.4 Hz, 1H, 2'-H), 8.22 (dd, J = 8.4 Hz, J = 1.5 Hz, 1H, 4'-H), 8.31 (d, J = 8.8 Hz, 1H, 1'-H), 8.54 (d, J = 8.4 Hz, 1H, 6'-H). MS (FAB+) *m/z* 379 (M + H).

6-(5-Dimethylaminonaphthalenesulfonamido)hexanhydrazide 184

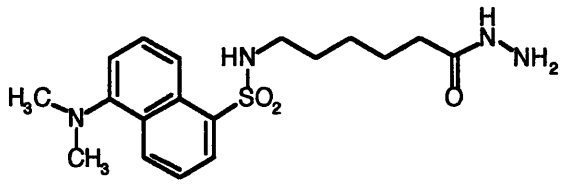

Hydrazine hydrate (355 mg, 7.08 mmol, 0.34 mL) was added to a solution of methyl 6-(5-dimethylaminonaphthalenesulfonamido)hexanoate (765 mg, 2.02 mmol) in dry methanol (10 mL) and allowed to stir for 16 h at RT. In addition, excess hydrazine hydrate (355 mg, 7.08 mmol, 0.34 mL) was added to the mixture and stirred for a further 2 d. Evaporation yielded 6-(5-dimethylaminonaphthalenesulfonamido)hexan-hydrazide (752 mg, 98%) as a light brown oil: R_f = 0.48 (10 : 1 $CHCl_3$: MeOH); ^1H NMR ($CDCl_3$) δ 1.11 (m, 2H, 4-H_2), 1.28 (m, 4H, 3,5-H_4), 1.85 (t, J = 7.4 Hz, 2H, 2-H_2), 2.74 (m, 2H, 6-H_2), 2.82 (s, 6H, $N(CH_3)_2$), 7.25 (d, J = 7.4 Hz, 1H, 3'-H), 7.58 (t, J = 8.5 Hz, 1H, 5'-H), 7.61 (m, 1H, 2'-H), 7.86 (br, 1H, dansyl-NH), 8.08 (dd, J = 7.1, 1.2 Hz, 1H, 4'-H), 8.29 (d, J = 8.6 Hz, 1H, 1'-H), 8.45 (d, J = 8.6 Hz, 1H, 6'-H), 8.87 (s, 1H, CONH); ^{13}C NMR ($CDCl_3$) δ 24.72 (CH_2), 25.67 (CH_2), 28.92 (CH_2), 33.25 (CH_2), 42.33 (CH_2), 45.10 ($N(CH_3)_2$), 115.14 (CH), 119.19 (CH), 123.63 (CH), 127.82 (CH), 128.22 (CH), 129.04 (CH), 129.35 (Cq), 136.17 (Cq), 151.36 (dansyl 5-C), 162.36 (Cq), 171.49 (C=O). MS (FAB+) m/z 379.1800 (M + H) ($^{13}C_1C_{17}H_{26}N_4O_3S_1$ requires 379.1759).

REFERENCES

1. Underwood, J. C. E.; Britton, R. eds. General and systemic pathology, **2000**, Edinburgh: Churchill Livingstone, pp 526-551. (ISBN 0443062854)

2. MacSween, R. N. M.; Whaley, K. eds. Muir's textbook of pathology, **1992**, Arnold, London: pp 1064-1071. (ISBN 0340662336)

3. Tortora, G. L.; Grabowski, S. R. eds. Principles of anatomy and physiology, **2003**, Wiley, New York: pp 1024-1026. (ISBN 0471224723)

4. Thibodeau, G. A.; Patton, K. T.; Louis, S. T. eds. Anatomy and physiology, **1999**, Mosby, London: pp 891-902. (ISBN 0323001920)

5. Guyton, A. C.; Hall, J. E. eds. Textbook of medical physiology, **2000**, Philadelphia, London: Saunders, W. A. pp 916-928. (ISBN 072168677)

6. Clegg, C. J.; Mackean, D. G. eds. Advanced biology principles and applications, **1994**, John Murray, London: pp 595-598. (ISBN 0719550785)

7. Jani, A. B.; Hellman, S. Early prostate cancer: clinical decision-making. *Lancet* **2003**, *361*, 1045-1049.

8. Frankel, S.; Smith, G. D.; Donovan, J.; Neal, D. Screening for prostate cancer. *Lancet* **2003**, *361*, 1122-1128.

9. Grönberg, H. Prostate cancer epidemiology. *Lancet* **2003**, *361*, 859-864.

10. Hayes, R. B.; Liff, J. M.; Pottern, L. M. Prostate cancer risk in US blacks and whites with a family history of cancer. *Int. J. Cancer* **1995**, *60*, 361-364.

11. Prakash, B. S. Mayo Internal Medicine Board review, Mayo Foundation for Medical Education and Research, Rochester, **1996-1997**, p. 629.

12. Parkin, D. M.; Bray F. I.; Devesa S. S. Cancer burden in the year 2000: the global picture. *Eur. J. Cancer* **2001**, *37*, 4-66.

13. Whittemore, A. S.; Wu, A. H.; Kolonel L. N. Family history and prostate cancer risk in black, white, and Asian men in the United States and Canada. *Am. J. Epidemiology* **1995**, *141*, 732-740.

14. Boileau, T. W. M.; Liao, Z.; Kim, S.; Lemeshow, S.; Erdman, J. W.; Clinton, S. K. Prostate carcinogenesis in *N*-methyl-*N*-nitrosourea(NMU)-testosterone-treated rats fed tomato powder, lycopene, or energy-restricted diets. *J. Nat. Cancer Inst.* **2003**, *95*, 1578-1585.

15. DeMazo, A. M.; Nelson, W. G.; Isaacs, W. B.; Epstein, J. I. Pathological and molecular aspects of prostate cancer. *Lancet* **2003**, *361*, 955-963.

16. Huggins, C.; Hodges, C. V. Studies on prostate cancer. 1. The effect of castration, of estrogen and of androgen injection on serum phosphatases in metastatic carcinoma of the prostate. *Cancer Res.* **1941**, *1*, 293-297.

17. Gleason, D. F.; Mellinger, G. T.; and the Veterans Administration Cooperative Urological Research Group. Prediction of prognosis for prostatic adenocarcinoma by combined histologic grading and clinical staging. *J. Urol.* **1974**, *111*, 58-64.

18. Catalona, W. J.; Carvalhal, G. F.; Mager, D. E.; Smith, D. S. Potency, continence and complication rates in 1870 consecutive radical retropubic prostatectomies. *J. Urol.* **1999**, *162*, 433-438.

19. Walsh, P. C.; Mostwin, J. L. Radical prostatectomy and cystoprostatectomy with preservation of potency: results using a new nerve-sparing technique. *Br. J. Urol.* **1984**, *156*, 694-697.

20. Zlotta, A. R.; Schulman, C. Neoadjuvant hormone therapy for prostate cancer. *World J. Urol.* **2000**, *18*, 179-182.

21. Papatsoris, A. G.; Papavassiliou, A. G. Prostate cancer: horizons in the development of novel anti-cancer strategies. *Current Medicinal Chemistry – Anti-Cancer Agents* **2001**, 47-70.

22. Odrazka, K.; Vanasek, J.; Vaculikova, M.; Stejskal, J.; Filip, S. The role of chemotherapy in prostate cancer. *Neoplasma* **2000**, *47*, 197-203.

23. Pilepich, M. V.; Asbell, S. O.; Krall, J. M.; Baerwald, W. H.; Sause, W. T.; Rubin, P.; Emami, B. N.; Pidcock, G. M. Correlation of radiotherapeutic parameters and treatment related morbidity: analysis of RTOG Study 77-06. *Int. J. Radiat. Oncol. Biol. Phys.* **1987**, *13*, 1007-1012.

24. Kyprianou, N.; Litvak, J. P.; Borkowski, A.; Alexander, R.; Jacobs, S. C. Induction of prostate apoptosis by doxazosin in benign prostatic hyperplasia. *J. Urol.* **1998**, *159*, 1810-1815.

25. Newling, D. W. W. The use of adriamycin and its derivatives in the treatment of prostate cancer. *Cancer Chemother. Pharmacol.* **1992**, *30*, S90-S94.

26. MacNeal, J. E. New morphologic findings relevant to the origin and evolution of carcinoma of the prostate and B.P.H. *UICC technical reports series* **1979**, *48*, 24-37.

27. Isaacs, J. T. New principles in the management of metastatic prostate cancer. In: Das Prostatakarzinom zwischen Hormontherapie and Zytostase. *Med. Trends* **1986**, Solingen, 5027.

28. Remers, W. A. Wilson and Gisvold's textbook of organic medicinal and pharmaceutical chemistry, eds. Delgado, J. N.; Remers, W. A, Philadelphia, **1998**, pp 343-401. (ISBN 0397515839)

29. Creasy, W. A. Cancer, an introduction. New York; Oxford: Oxford University Press, **1981**, p 195. (ISBN 0195029526)

30. Gilman, A.; Phillips, F. S. The biological actions and therapeutic applications of the β-chloroethyl amines and sulfides. *Science* **1946**, *103*, 409-415.

31. Cal, C.; Uslu, R.; Gunaydin, G.; Ozyurt, C.; Omay, S. B. Doxazosin: a new cytotoxic agent for prostate cancer? *BJU Int.* **2000**, *85*, 672-675.

32. Stella, A.; Kilbourn, R.; Amato, R.; Bui, C.; Zukiwski, A. A.; Ellerhorst, J.; Logothetis, C. J. Phase II study of ketoconazole combined with weekly doxorubicin in patients with androgen-independent prostate cancer. *J. Clin. Oncol.* **1994**, *12*, 683-688.

33. Yagoda, A.; Petrylak, D. Cytotoxic chemotherapy for advanced hormone-resistant prostate cancer. *Cancer* **1993**, *71*, 1098-1109.

34. Berettoni, M.; Cipollone, A.; Olivieri, L.; Palomba, D.; Arcamone, F.; Maggi, C. A.; Animati, F. Synthesis of 14-fluorodoxorubicin. *Tetrahedron Lett.* **2002**, *43*, 2867-2871.

35. Binaschi, M.; Capranico, G.; Bo, L. D.; Zunino, F. Relationship between lethal effects and topoisomerase II-mediated double stranded DNA breaks produced by anthracyclines with different sequence specificity. *Mol. Pharmacol.* **1997**, *51*, 1053-1059.

36. Capranico, G.; Butelli, E.; Zunino, F. Change of the sequence specificity of daunorubicin-stimulated topoisomerase II DNA cleavage by epimerization of the amino group of the sugar moiety. *Cancer Res.* **1995**, *55*, 312-317.

37. Moore, M. J.; Osoba, D.; Murphy, K.; Tannock, I. F.; Armitage, B.; Findlay, C.; Coppin, A.; Neville, P.; Venner, P.; Wilson, J. Use of palliative end points to evaluate the effects of mitoxantrone and low-dose prednisone in patients with hormonally resistant prostate cancer. *J. Clin. Oncol.* **1994**, *12*, 689-694.

38. Douglas, S. J.; Davies, S. S.; Illum, L. Nanoparticles in drug delivery. *CRC Crit. Rev. Ther. Drug Carrier Sys.* **1987**, *3*, 233-261.

39. Mhaka, A.; Denmeade, S. R.; Yao, W.; Isaacs, J. T.; Khan, I.; Khan, S. R. A 5-fluorodeoxyuridine prodrug as targeted therapy for prostate cancer. *Bioorg. Med. Chem. Lett.* **2002**, *12*, 2459-2461.

40. Poste, G.; Kirsh, R. Site-specific (targeted) drug delivery in cancer chemotherapy. *Biotechnology* **1983**, *1*, 869-878.

41. Seymour, L. W. Passive tumour targeting of soluble macromolecules and drug conjugates. *CRC Crit. Rev. Ther. Drug Carrier Sys.* **1992**, *9*, 135-187.

42. Yoshioka, T.; Hashida, M.; Muranishi, S.; Sezaki, H. Specific delivery of mitomycin C to the liver, spleen and lung: nano- and microspherical carriers of gelatin. *Int. J. Pharm.* **1981**, *8*, 131-141.

43. Russell, G. F. J. Starch microspheres as delivery systems. *Pharm. Int.* **1983**, *4*, 260-262.

44. Alving, C. R. Delivery of liposomes-encapsulated drugs to macrophages. *Pharm. Ther.* **1983**, *22*, 407-423.

45. Connors, T. A. Prodrugs in cancer chemotherapy. *Xenobiotica* **1986**, *16*, 975-988.

46. Denny, W. A. Prodrugs for gene-directed enzyme prodrug therapy. *Biomed. Biotechnol.* **2003**, *1*, 48-70.

47. Denny, W. A.; Wilson, W. R.; Hay, M. P. Recent developments in the design of bioreductive drugs. *Br. J. Cancer* **1996**, *27*, S32-S38.

48. Phillip, L. C.; Chakravarty, P. K.; Katzenellenbogen, J. A. A novel connector linkage applicable in prodrug design. *J. Med. Chem.* **1981**, *24*, 479-480.

49. Niculescu-Duvaz, D.; Niculescu-Duvaz, I.; Freidlos, F.; Martin, J.; Spooner, R.; Davies, L.; Marais, R.; Springer, C. J. Self-immolative nitrogen mustard prodrugs for suicide gene therapy. *J. Med. Chem.* **1998**, *41*, 5297-5309.

50. Amir, R. J.; Shabat, D. Self-immolative dendrimer biodegradability by multi-enzymic triggering. *Chem. Commun.* **2004**, 1614-1615.

51. Hay, M. P.; Wilson, W. R.; Denny, W. A. Design, synthesis and evaluation of imidazolylmethyl carbamate prodrugs of alkylating agents. *Tetrahedron* **2000**, *56*, 645-657.

52. Shan, D. X.; Nicolaou, M. G.; Borchardt, R. T.; Wang, B. H. Prodrug strategies based on intramolecular cyclisation reactions. *J. Pharm. Sci.* **1997**, *86*, 765-767.

53. Brady, S. F.; Pawluczyk, J. M.; Lumma, P. K.; Feng, D.; Wai, J. M.; Jones, R.; Jones, D. D.; Wong, B. K.; Stein, C. M.; Lin, J. H.; Oliff, A.; Freidinger, R. M.; Garsky, V. M. Design and synthesis of a pro-drug of vinblastine targeted at treatment of prostate cancer with enhanced efficacy and reduced systemic toxicity. *J. Med. Chem.* **2002**, *45*, 4706-4715.

54. Veinberg, G.; Shestakova, I.; Vorona. M.; Kanepe, I.; Domrachova, I.; Lukevics, E. Doxorubicin prodrug on the basis of *tert*-butyl cephalosporanate sulfones. *Bioorg. Med. Chem. Lett.* **2004**, *14*, 1007-1010.

55. Dubowchik, G. M.; Firestone, R. A. Cathepsin B-sensitive dipeptide prodrugs. 1. A model study of structural requirements for efficient release of doxorubicin. *Bioorg. Med. Chem. Lett.* **1998**, *41*, 3341-3346.

56. Upeslacis, J. Antibody-drug conjugates for cancer therapy. *J. Pharm. Ed.* **1992**, *56*, 464-467.

57. Dvorak, H. F.; Nagy, J. A.; Dvorak, A. M. Structure of solid tumours and their vasculature – implication for therapy with monoclonal antibodies. *Cancer Cells – Mon. Rev.* **1991**, *3*, 77-85.

58. Maison, W.; Frangioni, J. V. Improved chemical strategies for the targeted therapy of cancer. *Angew. Chem. Int. Ed. Engl.* **2003**, *42*, 4726-4728.

59. Rooseboom, M.; Commandeur, J. M.; Vermeulen, N. E. Enzymic-catalyzed activation of anticancer prodrugs. *Pharmacol. Rev.* **2004**, *56*, 53-102.

60. Lougerstay, R. M.; Florent, J. C.; Monneret, C. Synthesis of self-immolative glucuronide spacers based on aminomethylcarbamate. Application to 5-fluorouracil prodrugs for antibody-directed enzyme prodrug therapy. *J. Chem. Soc., Perkin Trans.* **1999**, *1*, 1369-1375.

61. Senter, P. D.; Wallace, P. M.; Svensson, H. P.; Kerr, D. E.; Hellstrom, K. E. Activation of prodrugs by antibody-enzyme conjugates. *Adv. Exp. Med. Biol.* **1991**, *303*, 97-105.

62. Jiménez, C.; Tramontano, A. Synthesis of a new hapten for generating catalytic antibodies that activate doxorubicin prodrugs. *Tetrahedron Lett.* **2002**, *42*, 7819-7822.

63. Niculescu-Duvaz, I.; Spooner, R.; Marais, R.; Springer, C. J. Gene-directed enzyme prodrug therapy. *Bioconj. Chem.* **1998**, *9*, 4-22.

64. Matthews, S.E.; Pouton, C. W.; Threadgill, M. D. Macromolecular systems for chemotherapy and magnetic resonance imaging. *Adv. Drug Deliv. Rev.* **1996**, *18*, 219-267.

65. Maeda, H. SMANCS and polymer-conjugated macromolecular drugs: advantages in cancer chemotherapy. *Adv. Drug Deliv. Rev.* **1991**, *6*, 181-202.

66. Maeda, H.; Matsumara, Y. Tumoritropic and lymphotropic principles of macromolecular drugs. *CRC Crit. Rev. Ther. Drug Carrier Sys.* **1989**, *6*, 193-201.

67. Sezaki, H.; Hashida, M. eds. Macromolecules as drug delivery systems, in directed delivery, Humana Press, Clifton N. J. **1985**, p 189. (ISBN 089603089).

68. Sezaki, H.; Hashida, M. Macromolecule-drug conjugates in targeted cancer chemotherapy. *CRC Crit. Rev. Ther. Drug Carrier Sys.* **1984**, *1*, 1-38.

69. Kálal, J.; Drobnik, J.; Kopecek, J.; Exner, J. Synthetic polymer in chemotherapy: general problems, in polymeric prodrugs, eds, Donaruma, L. G.; Vogl, O. Academic Press, New York, **1978**, 131.

70. Dvorak, H. F.; Nagy, J. A.; Dvorak, J. T.; Dvorak, A. M. Identification and characterization of the blood vessels of solid tumours that are leaky to circulating macromolecules. *Am. J. Pathol.* **1988**, *133*, 95-109.

71. Kopecek, J.; Duncan, R. Targetable polymeric prodrugs. *J. Controlled Release* **1987**, *6*, 315-327.

72. Kopecek, J. The potential of water-soluble polymeric carriers in targeted and site-specific drug delivery. *J. Controlled Release* **1990**, *11*, 279-290.

73. Seymour, L. W.; Ulbrich, K.; Steyger, P. S.; Brereton, M.; Subr, V.; Strohalm, J.; Duncan, R. Tumour tropism and anticancer efficacy of polymer-based doxorubicin prodrugs in the treatment of subcutaneous murine B16F10 melanoma. *Br. J. Cancer* **1994**, *70*, 636-641.

74. Seymour, L. W.; Duncan, R.; Strohalm, J.; Kopecek, J. Effect of molecular weight (MW) of N-(2-hydroxypropyl)methacrylamide copolymers on body distributions and rate of excretion after subcutaneous, intraperitoneal and intravenous administration to rats. *J. Biomed. Mater. Res.* **1987**, *21*, 1341-1358.

75. Ouchi, T.; Fujino, A.; Tanaka, K.; Banba, Y. Synthesis and antitumour activity of conjugates of poly(α-malic acid) and 5-fluorouracil bound *via* ester, amide or carbamoyl bonds. *J. Controlled Release* **1990**, *12*, 143-153.

76. Ouchi, T.; Hagihara, Y.; Takahashi, K.; Takano, Y.; Igarashi, I. Synthesis and anti-tumour activity of poly(ethyleneglycol)s linked to 5-fluorouracil *via* urethane or urea bonds. *Drug Des. & Discovery* **1992**, *9*, 93-105.

77. Bundgaard, H. The double prodrug concept and its application. *Adv. Drug Deliv. Rev.* **1989**, *3*, 39-65.

78. Kingsburry, W. D.; Boehm, J. C.; Mehta, R. J.; Grapel, S. F.; Gilvarg, C. H. A novel peptide delivery system involving peptidase activated prodrugs as antimicrobial agents. Synthesis and biological activity of peptidyl derivatives of 5-fluorouracil. *J. Med. Chem.* **1984**, *27*, 1447-1451.

79. Nichifo, M.; Schacht, E. H.; Seymour, L. W. Polymeric prodrugs of 5-fluorouracil. *J. Med Chem.* **1997**, *48*, 165-178.

80. Matsumoto, S.; Arase, Y.; Takakura, Y.; Hashida, M.; Sezaki, H. Plasma disposition and *in vivo* and *in vitro* antitumour activities of mitomycin C-dextran conjugate in relation to the mode of action. *Chem Pharm. Bull.* **1985**, *33*, 2941-2947.

81. Papsidero, L. D.; Wang, M. C.; Valenzuela, L. A.; Murphy, G. P.; Chu, T. M. A prostate antigen in sera of prostate cancer patients. *Cancer Res.* **1980**, *40*, 2428-2432.

82. Bruce, A. W.; Mahan, D. G.; Sullivan, L. D.; Goldenberg, L. The significance of prostate acid phosphatase in adenocarcinoma of the prostate. *J. Urol.* **1981**, *125*, 357-360.

83. Vihko, P.; Lukkarinen, O.; Konturri, M.; Vihko, R. Effectiveness of radioimmunoassay of human prostate-specific acid phosphatase in the diagnosis and follow-up of therapy on prostatic carcinoma. *Cancer Res.* **1981**, *41*, 1180-1183.

84. Lee, S.; Kim, H.; Yu, R.; Lee, K.; Gardner, T. A.; Jung, C.; Jeng, M.; Yeung, F.; Cheng, L.; Kao, C. Novel prostate-specific promoter derived from PSA and PSMA enhancers. *Mol. Ther.* **2002**, *6*, 415-421.

85. Su, S. L.; Huang, I. P.; Fair, W. R.; Powell, C. T.; Heston, W. D. alternatively spliced variants of prostate-specific membrane antigen RNA-ratio of expression as a potential measurement of progression. *Cancer Res.* **1995**, *55*, 1441-1443.

86. Pinto, J. T.; Suffoletto, B. P.; Berzin, T. M.; Qiao, C. H.; Lin, S.; Tong, W. P.; May, F.; Mukherjee, B.; Heston, W. D. Prostate-specific membrane antigen: a novel folate hydrolase in human prostatic carcinoma cells. *Clin. Cancer Res.* **1996**, *2*, 1445-1451.

87. Andra, J.; Berninghausen, O.; Wulfken, J.; Leippe, M. Shortened amoebapore analogues with enhanced antibacterial and cytolytic activity. *FEBS Lett.* **1996**, *385*, 96-100.

88. Warren, P.; Li, L.; Song, W.; Holle, E.; Wei, Y.; Wagner, T.; Yu, X. *In vitro* targeted killing of prostate tumour cells by a synthetic amoebapore helix 3 peptide modified with two gamma-linked glutamate residues at COOH terminus. *Cancer Res.* **2001**, *61*, 6783-6787.

89. Chang, S. S.; O'Keefe, D. S.; Bacich, D. J.; Reuter, V. E.; Heston, W.D.; Gaudin, P. B. Prostate-specific membrane antigen is produced in tumour-associated neovasculature. *Clin. Cancer Res.* **1999**, *5*, 2674-2681.

90. Hara, M.; Inorre, T.; Fukuyama, T. Some physico-chemical characteristics of gamma-seminoprotein, an antigenic component specific for human seminal plasma. *Jap. J. Legal Med.* **1971**, *25*, 322.

91. Li, T. S.; Beling, C. G. Isolation and characterization of two specific antigens of human seminal plasma. *Fertil. Steril.* **1973**, *24*, 134-144.

92. Sensabaugh, G. F. Isolation and characterization of semen-specific protein form human seminal plasma: a potential new marker for semen identification. *J. Forensic Sci.* **1978**, *23*, 106-115.

93. Graves, H. C. B.; Sensabaugh, G. F.; Blake, R. T. Postcoital detection of male-specific semen protein. Application to the investigation of rape. *New Engl. J. Med.* **1985**, *312*, 338-343.

94. Wang, M. C.; Valenzuela, L. A.; Murphy, G. P.; Chu, T. M. A simplified purification procedure for human prostate-specific antigen. *Oncology* **1982**, *39*, 1-5.

95. Villoutreix, B. O.; Getzoff, E. D.; Griffin, J. H. A structural model for the prostate disease marker, human prostate-specific antigen. *Protein Science* **1994**, *3*, 2033-2044.

96. Wang, M. C.; Valenzuela, L. A.; Murphy, G. P.; Chu, T. M. Purification of a human prostate-specific antigen. *Invest. Urol.* **1979**, *17*, 159-163.

97. Oesterling, J. E. Prostate-specific antigen: a critical assessment of the most useful tumour marker for adenocarcinoma of the prostate. *J. Urol.* **1991**, *145*, 907-923.

98. Ast, G. Drug-targeting strategies for prostate cancer. *Curr. Pharm. Des.* **2003**, *9*, 455-923.

99. Watt, K. W. K.; Lee, P.; M'Timkulu, T.; Chan, W.; Loor, R. Human prostate-specific antigen: structural and functional similarity with serine proteases. *Proc. Natl. Acad. Sci. USA* **1986**, *83*, 3166-3170.

100. Denmeade, S. R.; Sokoll, L. J.; Chan, D. W.; Khan, S. R.; Issacs, J. T. Concentration of enzymatically active prostate-specific antigen (PSA) in the extracellular fluid of primary human prostate cancers and human prostate cancer xenograft models. *The Prostate* **2001**, *48*, 1-6.

101. Garsky, V. M.; Lumma, P. K.; Feng, D. M.; Wai, J.; Ramjit, H. G.; Sardana, M. K.; Oliff, A.; Jones, R. E.; Jones, D. D.; Freidinger, R. M. The synthesis of a prodrug of doxorubicin designed to provide reduced systemic toxicity and greater target efficacy. *J. Med. Chem.* **2001**, *44*, 4216-4224.

102. Coombs, G. S.; Bergstrom, R. C.; Pellequer, J. L.; Baker, S. I.; Navre, M.; Smith, M. M.; Tainer, J. A.; Madison, E. L.; Corey, D, R. Substrate specificity of prostate-specific antigen (PSA). *Chem. and Biol.* **1998**, *5*, 475-488.

103. Denmeade, S. R.; Lou, W.; Lövgren, J.; Malm, J.; Lilja, H.; Issacs, J. T. Specific and efficient peptide substrates for assaying the proteolytic activity of prostate-specific antigen. *Cancer Res.* **1997**, *57*, 4924-4930.

104. Denmeade, S. R.; Nagy, A.; Gao, J.; Lilja, H.; Schally, A. V.; Issacs, J. T. Enzymic activation of a doxorubicin-peptide prodrug by prostate-specific antigen. *Cancer Res.* **1998**, *58*, 2537-2540.

105. Jakobsen, C. M.; Denmeade, S. R.; Issacs, J. T.; Gady, A.; Olsen, C. E.; Brogger Christensen, S. Design, synthesis and pharmacological evaluation of thapsigargin analogues for targeting apoptosis to prostatic cancer cells. *J. Med. Chem.* **2001**, *44*, 4696-4703.

106. Jones, D. D.; Garsky, V. M.; Wong, B. K.; Feng, D. M.; Bolyar, T.; Haskell, K.; Kiefer, D. M.; Leander, K.; McAvoy, E.; Lumma, P. Wai, J.; Senderak, E. T.; Motzel, S. L.; Keenan, K.; Zwieten, M. V.; Lin, J. H.; Freidinger, R.; Huff, J.; Oliff, A, Jones, R. E. A peptide-doxorubicin prodrug activated by prostate-specific antigen selectively kills prostate tumour cells positive for prostate-specific antigen *in vivo*. *Nature Medicine* **2000**, *6*, 1248-1252.

107. Thastrup, O.; Cullen, P. J.; Drobak, B. K.; Hanley, M. R.; Dawson, A. P. Thapsigargin, a tumour promoter, discharges intracellular Ca^{2+} stored by specific inhibition of the endoplasmic reticulum Ca^{2+}-ATPase. *Proc. Natl. Acad. Sci. USA* **1990**, *87*, 2466-2470.

108. Furuya, Y.; Berges, S. R.; Lundmo, P.; Issacs, J. T. Proliferation independent activation of programmed cell death as a novel therapy for prostate cancer, eds. Milhich, E.; Schimmke, R. T. Plenum Press, New York **1994**, pp 137-156.

109. Denmeade, S. R.; Jakobson, C. M.; Janssen, S.; Khan, S. R.; Garrett, E. S.; Lilja, H.; Brogger Christensen, S. B.; Issacs, J. T. Prostate-specific antigen-activated thapsigargin prodrug as targeted therapy for prostate cancer. *J. Natl. Cancer Inst.* **2003**, *95*, 990-1000.

110. Bodansky, M.; Bodansky, A. The practice of peptide synthesis 2nd Ed. **1984**, Springer-Verlag, Berlin. (ISBN 3540575057).

111. Bergmann, M.; Zervas, L. Über ein allgemeines verfahren der peptide synthese. *Ber. Dtsch. Chem. Ges.* **1932**, *65*, 1192-1201.

112. Tarbell, D. S.; Yamamoto, Y.; Pope, B. M. New method to prepare N-*t*-butoxycarbonyl derivatives and the corresponding sulfur analogs from di-*t*-butyl dicarbonate or di-*t*-butyl dithiol dicarbonates and amino acids. *Proc. Natl. Acad. Sci. USA* **1972**, *69*, 730-732.

113. Hu, W.; Hesse, M. Synthese der *p*-cumaroylspermidine. *Helv. Chim. Acta* **1996**, *79*, 548-559.

114. Carpino, L. A.; Sadat-Aalaee, D.; Chao, H. G.; DeSelms, R. H. ((9-Fluorenylmethyl)oxy)carbonyl (FMOC) amino acid fluorides. Convenient new peptide coupling reagent applicable to the FMOC/*tert*-buytl strategy for solution and solid-phase syntheses. *J. Am. Chem. Soc.* **1990**, *112*, 9651-9652.

115. Jones, J. The chemical synthesis of peptides. **1993**, Clarendon Press, London. (ISBN 0198558392).

116. Williams, D. H.; Fleming, I. Spectroscopic methods in organic chemistry 5th Ed. **1995**, McGraw-Hill.

117. Toki, B. E.; Cerveny, C. G.; Wahl, A. F.; Senter, P. D. Protease-mediated fragmentation of *p*-amidobenzyl ethers: a new strategy for the activation of anticancer prodrugs. *J. Org. Chem.* **2002**, *67*, 1866-1872.

118. Naylor, M. A.; Swann, E. Everett, S. A.; Jaffar, M.; Nolan, J.; Robertson, N. Indolequinone antitumour agents: reductive activation and elimination from (5-methoxy-1-methyl-4,7-dioxoindol-3-yl)methyl derivatives and hypoxia selective cytotoxicity in vitro. *J. Med. Chem.* **1998**, *41*, 2720-2731.

119. Hofmann, A.W. *Ber. Dtsch. Chem. Ges.* **1882**, *15*, 407.

120. Scobie, M.; Threadgill, M. D. Tumour-targetted boranes. 3. Synthesis of carbamate-linked nitroimidazolyl carboranes designed for boron neutron capture therapy of cancer. *J. Chem. Soc., Perkin Trans 1.* **1994**, 2059-2063.

121. Matthews, S. E.; Pouton, C. W.; Threadgill, M. D. Synthesis of porphyrin α,ω-bis(methylamino)peptide constructs. *New J. Chem.* **1999**, *23*, 1087-1096.

122. Kane, J. L.; Shea, M. K.; Crombie, A. L.; Danheiser, R. L. A ring expansion-annulation strategy for the synthesis of substituted azulenes. *Org. Lett.* **2001**, *3*, 1081-1084.

123. Strazzolini, P.; Giumanini, A. G.; Runcio, A. Scuccato, M. Experiment on the chaperon effect in the nitration of aromatics. *J. Org. Chem.* **1998**, *63*, 952-958.

124. Senokuchi, K.; Nakai, H.; Nagao, Y.; Sakai, Y.; Katsube, N.; Kawamura, M. New orally active enkephalinase inhibitors: their synthesis, biological activity, and analgesic properties. *Bioorg. Med. Chem.* **1998**, *6*, 441-463.

125. Brown, H. C.; Narasimhan, S.; Choi, Y. M. Improved procedure for borane-dimethyl sulfide reduction of primary amides to amines. *Synthesis* **1981**, 441-442.

126. Parveen, I.; Naughton, D. P.; Whish, W. J. D.; Threadgill, M. D. 2-Nitro-imidazol-5-ylmethyl as a potential bioreductively activated prodrug system: Reductively activated release of the PARP inhibitor 5-bromoisoquinolinone. *Bioorg. Med. Chem. Lett.* **1999**, *19*, 2031-2036.

127. Fox, D. J.; Reckless, J.; Warren, S. G.; Grainger, D. J. Design, synthesis, and preliminary pharmacological evaluation of N-acyl-3-aminoglutarimides as broad-spectrum chemokine inhibitors *in vitro* and anti-inflammatory agents *in vivo*. *J. Med. Chem.* **2002**, *45*, 360-370.

128. Dubowchik, G. M.; Mosure, K.; Knipe, K. O.; Firestone, R. A. CathepsinB-sensitive dipeptide prodrugs. 2. Models of anticancer drugs pactitaxel (Taxol), mitomycin C and doxorubicin. *Bioorg. Med. Chem. Lett.* **1998**, *8*, 3347-3352.

129. Dragovich, P. S.; Webber, S. E.; Babine, R. E.; Fuhrman, S. A.; Patick, A. K.; Matthews, D. A.; Reich, S. H.; Marakovits, J. T.; Prins, T. J.; Zhou, R.; Tikhe, J.; Littlefield, E. S.; Bleckman, T. M.; Wallace, M. B.; Little, T. L.; Ford, C. E.; Meador, J. W.; Ferre, R. A.; Brown, E. L.; Binford, S. L.; DeLisle, D. M.; Worland, S. T. Structure-based design, synthesis and biological evaluation of irreversible human rhinovirus 3C protease inhibitors. 2. Peptide structure-activity studies. *J. Med. Chem.* **1998**, *41*, 2819-2834.

130. Kisfaludy, L.; Schön, I. Preparation and applications of Pentafluorophenyl esters of 9-fluorenylmethyoxycarbonyl amino acids for peptide synthesis. *Synthesis* **1983**, 325-327.

131. Rai, R.; Katzenellenbogen, J. A. Guanidinophenyl-substituted enol lactones as selective, mechanism-based inhibitors of trypsin-like serine proteases. *J. Med. Chem.* **1992**, *35*, 4150-4159.

132. Sakaue, S.; Tsubakino, T.; Nishiyama, Y.; Ishii, Y. Oxidation of aromatic amines with hydrogen peroxide catalyzed by cetylpyridinium heteropolymetalates. *J. Org. Chem.* **1993**, *58*, 3633-3638.

133. Wada, S.; Urano, M.; Suzuki, H. The newborn surface of dull metals in organic synthesis. Bismuth-mediated solvent-free one-step conversion of nitroarenes to azoxy- and azoarenes. *J. Org. Chem.* **2002**, *67*, 8254-8257.

134. Corey, E. J.; Arai, Y.; Mioskowski, C. Total synthesis of (±)-5,6-oxido-7,9-*trans*,11,14-*cis*-eicosapentaenoic acid, a possible precursor of SRSA. *J. Am. Chem. Soc.* **1979**, *101*, 6748-6749.

135. Sonogashira, K.; Tohda, Y.; Hagihara, N. A convenient synthesis of acetylenes: catalytic substitutions of acetylenic hydrogen with bromoalkenes, iodoarenes and bromopyridines. *Tetrahedron Lett.* **1975**, *16*, 4467-4470.

136. Stephens, R. D.; Castro, C. E. The substitution of aryl iodides with cuprous acetylides. a synthesis of tolanes and heterocyclics. *J. Org. Chem.* **1963**, *28*, 3313-3315.

137. Castro, C. E.; Gaughan, E. J.; Owsley, D. C. Indoles, benzofurans, phthalides, and tolanes *via* copper(I) acetylides. *J. Org. Chem.* **1966**, *31*, 4071-4078.

138. Dieck, H. A.; Heck, R. F. Palladium catalyzed synthesis of aryl, heterocyclic and vinylic acetylene derivatives. *J. Organomet. Chem.* **1975**, *93*, 259-263.

139. Negishi, E.; King, A. O.; Okukado, N. Selective carbon-carbon bond formation via transition metal catalysis. 3. A highly selective synthesis of unsymmetrical biaryls and diarylmethanes by the nickel- or palladium-catalyzed reaction of aryl- and benzylzinc derivatives with aryl halides. *J. Org. Chem.* **1977**, *42*, 821-1823.

140. Sonogashira, K. In metal-catalysed cross-coupling reactions. Eds. Diederich, F.; Stang, P. J. **1998**, Wiley-VCH, Weinheim.

141. Laurenti, D.; Feuerstein, M.; Pèpe, G.; Doucet, H.; Santelli, M. A new tetratertiary phosphine ligand and its use in Pd-catalysed allylic substitution. *J. Org. Chem.* **2001**, *66*, 1633-1637.

142. Leonard, K. A.; Hall, Hall, J. P.; Nelen, M. I.; Davies, S. R.; Gollnick, S. O.; Camaco, S.; Oseroff, A. R.; Gibson, S. L.; Hilf, R.; Detty, M. R. A selenopyrylium photosensitiser for photodynamic therapy related in structure to the antitumor agent AA1 with potent *in vivo* activity and no long-term skin photosensitization. *J. Med. Chem.* **2000**, *43*, 4488-4498.

143. Moloney, G. P.; Martin, G. R.; Mathews, N.; Milne, A.; Hobbs, H.; Dodsworth, S.; Sang, P. H.; Knight, C.; Williams, M.; Maxwell, M.; Glen, R. C. Synthesis and serotonergic activity of substituted 2,N-benzylcarboxamido-5-(2-ethyl-1-dioxoimidazolinyl)-N,N-dimethyltryptamine derivatives: Novel anagonists for the vascular 5-HT_{1B}-like receptor. *J. Med. Chem.* **1999**, *42*, 2504-2526.

144. Stark, H.; Purand, K.; Ligneau, X.; Rouleau, A.; Arrang, J.-M.; Garbang, M.; Schwartz, J.-C.; Schunack, W. Novel carbamates as potent histamine H_3 receptor antagonists with high *in vitro* and oral *in vivo* activity. *J. Med. Chem.* **1996**, *39*, 1157-1163.

145. Van Betsbrugge, J.; Van Den Nest, W.; Verheyden, P.; Tourwé, D. New amino acids derived from L-pyroglutamic acid: synthesis of *trans*-4-benzyl-*cis*-5-phenyl-L-proline, L-α-(2-benzyl-3-phenylpropyl)-glycine and L-α-(3-phenylpropyl)-glycine. *Tetrahedron* **1998**, *54*, 1753-1762.

146. Provot, O.; Célérier, J. P.; Petit, H.; Lhommet, G. Synthesis of ant venom alkaloids from chiral β−enamino lactones: (3S,5R,8S)-3-heptyl-5-methylpyrrolizidine. *J. Org. Chem.* **1992**, *57*, 2163-2166.

147. Leschke, C.; Storm, R.; Breitweg-Lehmann, E.; Exner, T.; Nürnberg, B.; Schinack, W. Alkyl-substituted amino acid amides and analogous di- and triamines: new non-peptide protein G activators. *J. Med. Chem.* **1997**, *40* , 3130-3139.

148. Okumura, K.; Nakamura, Y.; Shin, C.-G. Total synthesis of a macrocyclic antibiotic, micrococcin P. *Bull Chem. Soc. Jpn.* **1999**, *72*, 1561-1569.

149. Supuran, C. T.; Scozzafava, A. Carbonic anhydrase activators: Amino acyl/dipeptidyl histamine derivatives bind with high affinity to isozymes I, II and IV and act as efficient activators. *Bioorg. Med. Chem.* **1999**, *7*, 2915-2923.

150. Van den Hoven, B.; Alper, H.; The first regioselective hydroformylation of acetylenic thiophenes catalyzed by a zwitterionic rhodium complex and triphenyl phosphite. *J. Org. Chem.* **1999**, *64*, 9640-9645.

151. Lin, Y. M.; Miller, M. J. Oxidation of primary amines to oxaziridines using molecular oxygen (O_2) as the ultimate oxidant. *J. Org. Chem.* **2001**, *66*, 8282-8285.

152. Hermetter, A.; Scholze, H.; Stütz, A. E.; Withers, S. G.; Wrodnigg, T. M. Powerful probes for glycoosidases: novel, fluorescently tagged glycosidase inhibitors. *Bioorg. Med. Chem. Lett.* **2001**, *11*, 1339-1342.

153. Ueda, M.; Wada, Y. Yamamura, S. Direct observation of the target cell for leaf-movement factor using novel fluorescence-labeled probe compounds: fluorescence studies nyctinasty in legumes. Part 1. *Tetrahedron Lett.* **2001**, *42*, 3869-3872.

154. Hanford, B. O.; Hylton, A. T.; Wang, K-T.; Weinatein, B. Amino acids and peptides. XVIII. synthesis of a tetrapeptide sequence (A1-A4) of glucagons. *J. Org. Chem.* **1968**, *33*, 4251-4255

155. Bernardi, F.; Garavelli, M.; Scatizzi, M.; Tomasini, C.; Trigari, V.; Crisma, M.; Formaggio, F.; Peggion, C.; Toniolo, C. Pseudopeptide foldamers: the homo-oligomers of pyroglutamic acid. *Chem. Eur. J.* **2002**, *8*, 2516-2524.

156. Luo, C.; Guldi, D. M.; Imahori, K.; Tamaki, K.; Sakata, Y. Sequential energy and electron transfer in an artificial reaction centre: formation of a long-lived charge-separated state. *J. Am. Chem. Soc.* **2000**, *122*, 6535-6551.

APPENDIX

(Figures 24 – 28)

A man who dares to waste one hour of time
- has not discovered the value of life.

- Charles Darwin

APPENDIX

Norethisterone *(a common progestogen)*

(17-Hydroxy-19-nor-17a-pregn-4-en-20-yn-3-one)

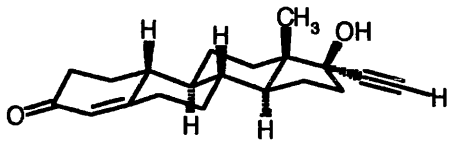

Diethylstilbestrol (Stilboestrol®)

(4-[4-(4-Hydroxyphenyl)hex-3-en-3-yl]phenol)

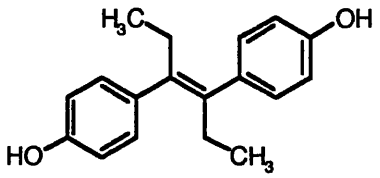

Figure 24. *A series of hormonal agonists used in hormone therapy in the treatment of prostate cancer*

Flutamide (Drogenil®)

(2-Methyl-N-[4-nitro-3-(trifluormethyl)-phenyl]propanamide)

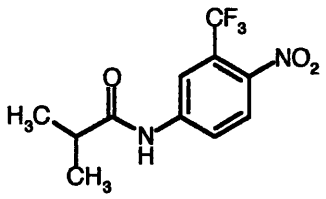

Figure 25. *A common hormone antagonist used in hormone therapy in the treatment of prostate cancer*

Vinblastine (23) ***(refer to Scheme 3, p30)***

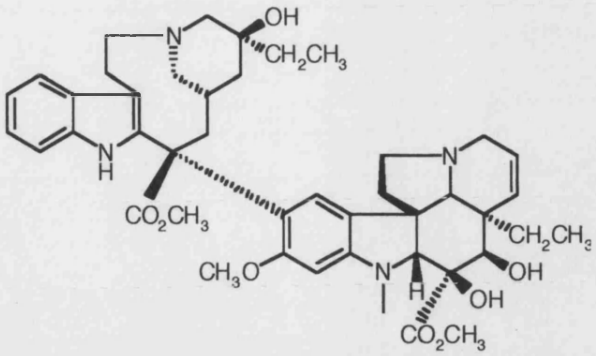

des-Acetyl-Vinblastine (**23**)
(the complete chemical structure)

Figure 26. *The complete chemical structure of vinblastine (**23**)*

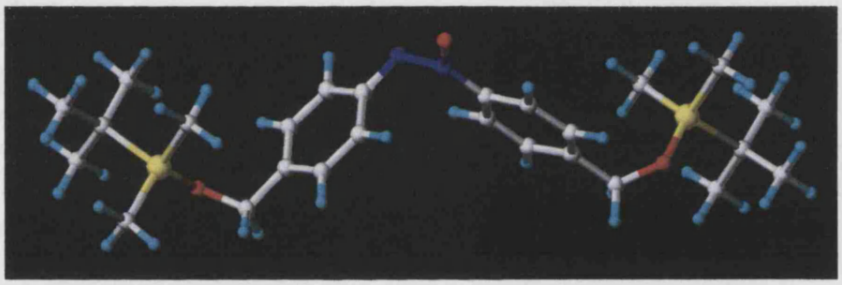

Figure 27. *A 3D model† of azoxy compound (**105**)*

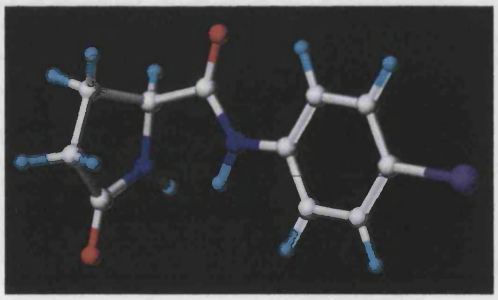

Figure 28. *A 3D model† of lactam (**156**)*

†The structures were created using Sybyl 7.1 Expert Molecular Modeling software and the structures where minimized using a conjugate gradient method as implemented within Sybyl 7.1.